

JOURNAL OF THE INDIAN ASSOCIATION OF SEDIMENTOLOGISTS

VOLUME 28

NUMBER 2

JULY - DEC. 2009

CONTENTS

| | | |
|---|--|-----|
| Physics and Mathematics of Transportation and Deposition of Clastic Sediments | <i>B.K.Sahu</i> | 1 |
| Characterisation of Depositional Processes and Identification of Shallow Drilling Hazards in a Growth Fault Setting using Seismic Data; a Study From Godavari Offshore, East Coast of India | <i>Satyabrata Nayak Rabi Bastia and Madhumita Das</i> | 7 |
| Cuddapah Basin: India's Emerging Uranium-Hub | <i>R. Dhana Raju</i> | 15 |
| Occurrence of Foraminifera and Pteropods Assemblages in Ganga Pro-Deltaic area of the Continental Shelf Region off West Bengal | <i>D.Bhattacharjee</i> | 25 |
| Hydrogeochemical Exploration for Uranium : A Case Study of Jabera Dome, Damoh and Jabalpur Districts, Madhya Pradesh | <i>Rahul Banerjee A.K. Verma M.K. Roy and P.B. Maithani</i> | 41 |
| Application of Multivariate Statistics - An Approach for Microenvironmental Zonation in a Tropical Tidal Flat of Chandipur, Orissa | <i>Swetalina Parhi</i> | 55 |
| Sedimentological Studies of Cores from a Well in Krishna-Godavari Basin, Offshore India | <i>Sunit K. Biswas Rajesh K. Patil and Rituraj K. Dubey</i> | 67 |
| Petrography and Textural Characteristics of the Barail and the Surma Sandstones of Tamenglong area, Western Manipur, in Relation to Depositional Processes and Orogeny | <i>Salam Ranjeeta Devi M.E.A.Mondal M Masroor Alam and Rabindra Nath Hota</i> | 77 |
| Provenance History of Kolhan Sediments from Chaibasa-Noamundi Basin | <i>Smita S. Swain and Sudarshan Gorana</i> | 87 |
| Mapping Seasonal Suspended Sediment Dynamics and Tidal Propagation in Coastal Waters of the Bay of Bengal using Oceansat- I Ocean Colour Monitor Data | <i>B. Veerananarayana P.N. Sridhar I.V. Ramana Rupert Leach K.S.N Reddy and M.Venkateswara Rao</i> | 101 |

Physics and Mathematics of Transportation and Deposition of Clastic Sediments

B.K.SAHU

Emeritus Professor, Dept. Earth Sciences, IIT Bombay, Mumbai-400076, India

Email: bksahu@iitb.ac.in; bas_sahu@yahoo.co.in

Abstract: Clastic sediments form at the earth's surface through various physical processes and mechanisms of transportation and deposition depending on textural characteristics; such as size (or its inverse specific surface), shape, roundness; of the constituting particles in that order of importance. Sedimentological transporting agents could operate in states such as: liquid water (fluvial; oceanic waves, currents, tides, turbidity flows; lacustrine processes), solid (glacial processes), and gas (aeolian processes), or gravity dominant processes, gravity operating in all three states. In liquids, clastic particles are dominantly transported/deposited by turbulent flows (assumed homogeneous Gaussian processes) having bedload, saltation, suspension and washload modes where deposition is effected during waning velocity conditions. The above modes and mechanisms of particle transportation are also present in wind and glacial processes. However, under gravity flows (such as landslides, tillites, conglomeratic turbidities, etc.), internal friction for the grains is the dominant factor and movement occurs if the downslope angle is greater than the friction angle.

A single homogeneous turbulent flow (assumed Gaussian turbulence) can transport and deposit the entire size, defined as nominal diameter of sphere having equal volume as the particle, (or its inverse the specific surface of grains) spectrum [10(E-6) to 10(E+5] mm.) of clastic sediments found in nature from coarse boulder-beds (with boulders, gravels, sands, etc) to fine shales (with silts, clays and colloids). Unfortunately, settling velocity is nonlinearly related to sphere (grain) sizes with different power functions that requires prior linearization before undertaking statistical analyses. At the maximum we can have five partitioned modes (polymodal size components) with respect to grain sizes with corresponding characteristic mean sizes and standard deviations. However, in nature due to lack of certain sized materials and/or to natural hydraulic processes a few velocity ranges/size modes may be absent in the sedimentary environment concerned, and often trimodal (alluvial fan sands, deltaic sands, distal-turbidite channel sands, etc.), bimodal (fluvial channel sands, tidalites, etc.), or unimodal (beach sands, aeolian dune sands, etc.) clastic sediments are deposited.

Mathematically, it is more convenient for analyses and inferences to transform nonlinear systems to equivalent linear systems and this linearisation is also required for statistical analyses and inferences. Hence, the power functions for size spectrum should be linearised by use of a logarithmic transformation (such as Krumbein's phi transform where phi-size is defined as the negative of log to base 2 of the grain diameter in millimeters; if specific surface is used instead of grain size, then the prefixed negative sign of this phi transform is deleted). Thus, the standard deviations of such fundamental phi-normal size distributions become 2 for suspension (size range 9.5 to 21.5 phi), 1 for saltation (size range from 3.5 to 9.5 phi), 1/2 for bedload-rolling sand and coarse silt grains (size range from 0.5 to 3.5 phi), 1 for sliding cum rolling bedload pebbles (size range from -5.5 to 0.5 phi), and 2 for sliding bedload boulders (size range from -17.5 to -5.5 phi), where each size mode is deterministically partitioned (using fuzzy logic with trapezoidal elements) on the phi scale and this procedure yields the required constant variance (or standard deviation) of velocities for the global cum causal homogeneous Gaussian turbulence. In nature, mixing in different proportions of some of these fundamental contiguous phi-normal size modes yields characteristic phi-size statistics of the clastic sediments which are useful for the required and desired two- and/or multi-group linear-discrimination of the different depositional mechanisms and environments using phi-size statistics as inputs. Thus, the sedimentary depositional environments can be fingerprinted through proper sampling, size analysis, and statistical analyses of above linearized and partitioned size distribution models.

Keywords: Clastic Sediments, Transportation and Deposition Processes.

INTRODUCTION

Clastic sediments form at the surface of Earth due to various external processes and mechanisms of particle transportation and deposition depending upon grain size (or its inverse the specific surface of grains), shape

and roundness of the particles in that order of importance (Sahu, 1987). Transporting agents include liquid water (fluvial, oceanic waves and currents, tides, turbidity currents); solid water (snow, glacier), gaseous medium (wind) or gravity dominated processes. Textural analysis such as size (sp. surface), shape and roundness of

deposited grains provide the necessary inputs for study of the processes and detailed mechanisms of transportation and deposition. The transportation process in any fluid medium can be modelled as the outcome of turbulent flows assumed to be homogeneous Gaussian velocity distributions about their mean velocity (excluding extreme chaotic flows having vertices, period doubling/tripling/quadrupling etc. resulting from extreme floods, cyclones (tempestites), tsunamis (tsunamites). Transportation loads are broadly classified as bedload, saltation and suspension loads, washloads. But detailed study of mechanisms of particle transport as bedload shows that they could move by rolling (ellipsoidal sands), sliding cum rolling (prismatic and ellipsoidal pebbles), or sliding (prismatic gravels and boulders). Saltation is found in fine sands and coarse silts as these are most vulnerable to erosion and suspensions occur in fine silts, clays and colloids with dominance of viscous drag forces. In larger sizes such as sands, pebbles, gravels, impact and frictional forces dominate over viscous forces which are neglected. The above principles of hydrodynamic transport also apply to wind, glacial and gravity transport, with different mean and variance of homogeneous turbulent velocities depending on the kinematic viscosity of the concerned medium. Thus size distribution of clastic sediments are seldom unimodal but often polymodal (maximum of five modes, Figure 1, for the above five mechanisms of particle transport) which may reduce to trimodal/bimodal size distributions depending on range of

velocities and/or grain sizes available at the site of deposition.

Textural studies date back to early 1900s (Udden, 1898, 1914) but progressed well during 1940s (Krumbein and Pettijohn, 1938, Twenhofel and Tyler, 1941). Due to availability of computers in the 1950s, univariate and multivariate statistical models as well as time series models were used (see, Krumbein and Graybill, 1965). Summary of collected information of sediments are available in Pettijohn (1974) and research has peaked around 1990s. The grain characteristics could be multivariate scalars, vectors or tensors that are independent for far away samples (statistical models) or dependent for near neighbors (time series models). Therefore, statistical analysis of data must be proper for realistic geological inference. However, measurements on zero, one, two or three dimensional spaces and on different frequency measures (number, length, area, volume/ weight) induce biases in the data and must be suitably transformed mathematically to give true statistical parameters and correct geological inference (these constraints have often missed the attention of many sedimentologists to obtain incorrect decisions). Polymodal distributions cannot be handled by usual statistical methods, and such size distributions need to be deterministically as well as optimally partitioned using Fuzzy logic into individual modes to obtain their characteristic means and standard deviations (variances) for each of these modes in order to make correct statistical inferences.

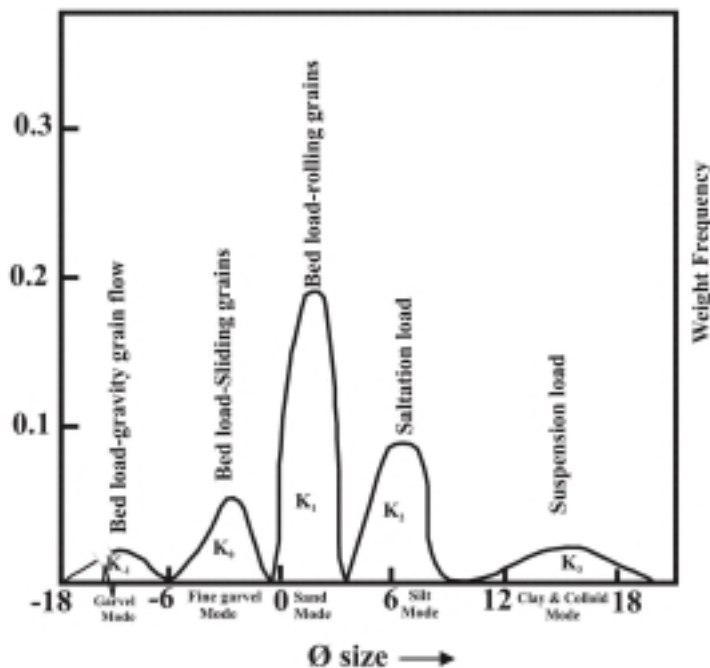


Fig. 1. Conceptual polymodal phi-normal size components of deposited clastic sediments with their mechanism (modes) of transport and deposition. Usually only 2 or 3 contiguous modes may be present in the sample showing NOTE: In Bedload Gravity, Grain Flow mode ($k(-1)$), grains move mostly by sliding on bed. In Bedload Sliding mode (K_0), grains move both by sliding (prismatic) and rolling. (see, Sahu, 2009).

Clastic sediment transportation and deposition relations of velocity versus size from hydrodynamic viewpoint have been established by Hjulstrom (1935) (Figure 2) for water transport and by Bagnold (1941) for wind transport. These results are based on homogeneous turbulent flow velocity field with a model of Gaussian distribution of velocities in spatial and/or temporal domains (Kolmogorov, 1941, 1962, Batchelor, 1953, Yaglom, 1987, Vallis, 1997).

PHYSICS OF TRANSPORTATION AND DEPOSITION PROCESSES

Consider a single unidirectional homogeneous turbulent flow with Gaussian distribution of velocities (river flow, turbidity current, glacial flow). The flow can transport and deposit the entire spectrum of sizes (or its inverse denoted as specific surface) from large boulders to fine clays as has been recorded in many coarse proximal turbidites that form a single sedimentation unit for field sampling, size analysis, and subsequent inferences on constant mean velocity, and constant variance (or std. deviation) of velocities of the causal linear Gaussian turbulent flow depositing the turbidite. However, turbulent velocities are nonlinearly related to grain size (or, sp. surface) as power functions (see, Lam, 1997, Vallis, 1997) for different size range partitions of the entire size range. For example, clays, fine silts are related through Stokes' Law as square of the grain size (sp. surface) since viscous forces dominate for their deposition (settling velocity), whereas for sands and granules impact forces dominate (viscous forces negligible) as per Newton's Impact Law and the settling velocity relation is square-root of the grain size (sp. surface). Since, Gaussian velocities are continuous

random variables in time/space, saltation mode of transport/deposition for fine sands and coarse silts would have the geometric mean of Stokes's and Newton's exponents of 2 and $\frac{1}{2}$. So velocity would be proportional to grain size as the square-root of $(2 \times \frac{1}{2})=1$. These power function relations are easily visualized (by constructing slopes to deposition curve at appropriate sizes) in Hjulstrom (1935) diagram (Figure 2), which can be extended using present theory to gravel and boulder sizes by utilizing the symmetry of Gaussian turbulent velocity distribution to higher velocity ranges of the mean flow velocity.

As sedimentation unit has a scale up to the formation dimensions, it is not localized but rather regional to basinwide. Hence, homogeneous turbulence Gaussian model would be useful for sedimentological inference as proposed by Kolmogorov (1941) and as was assumed in Sahu (1962, 1964, 1983, 1987). Although nonlinear turbulent theories of Kolmogorov (1962) and Vallis (1997) can explain vertices, periodic doubling/tripling/quadrupling of flows, and chaotic flows; etc., at higher Reynold's numbers but these more complex nonlinear turbulent flow models are not necessary nor useful for inference on deposition of clastic sediments.

Again, assuming continuous turbulent velocity fluctuations about velocity-mean due to homogeneous Gaussian model of velocity field and invoking symmetry on power function exponents on larger velocities for pebbles and boulders (because Gaussian distribution is symmetric about its mean), we get an exponent of 2 for boulders and gravels and 1 for fine pebbles, granules and coarse sands. Thus, at the maximum we get five different partitioned size modes (polymodal size distributions) with characteristic mean size and size variance (std. deviation) for each mode. In nature, a

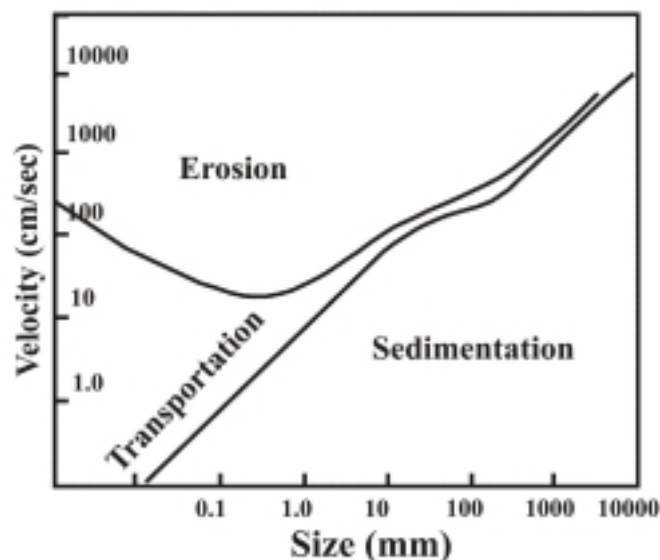


Fig. 2. Hjulstrom curves showing settling velocity vs sphere diameter (grain size) under processes of erosion, transportation and deposition of uniform sedimentary particles. (modified after Hjulstrom 1935 with extension to pebble and boulder sizes).

certain range of sizes may be missing or in the velocity range some part may be missing, so we can get 4, 3, 2 modes or be unimodal, as well. Trimodal deposits are often found in alluvial fans, deltas, distal turbidites, bimodal deposits are frequent in fluvial channels, tidalites, shallow marine/ lacustrine deposits, but unimodal size distributions are rare as often found in most beach sands due to constant range of wave velocities of ocean waves, or aeolian dunes due to rolling type bedload deposition of sand and silt grains.

The main reason for finding five distinct size modes is explained by detailed mechanisms of transport of coarse gravels by sliding, sliding cum rolling, rolling of grain at the bed surface and saltation and suspension loads for finer particles (sands, silts, clays). For boulders friction at bed surface is dominant resisting force and prismatic gravels move by sliding rather than rolling. For pebbles and coarse sands, friction is very important and particles move by sliding (prismatic grains) and also by rolling (ellipsoidal grains). For fine sands and coarse silts, there is no cohesive force, and they move by saltation mode within the medium but close to the bed surface and impact of grains on the bed becomes dominant force. On the other hand, viscous resistive forces dominant as specific surface is high for fine silts and clays which are transported and deposited by their settling velocity criteria (hydraulic value or the diameter of quartz sphere having same settling velocity as the particle; see, Sahu 1962, 1964).

However, under gravity induced flows such as landslides and conglomeratic turbidites, internal grain frictions become very important for gravels and movement occurs if downslope angle is greater than angle of friction. Hence, angular-prismatic grains with very high friction angles (say, 50 degrees or more) tend to move by sliding, rounded-prismatic and ellipsoidal grains with intermediate friction angles (say, 35 degrees) would move by sliding and rolling, respectively, whereas well-rounded prismatic and ellipsoidal sand or silt grains with low friction angles (say, about 10-15 degrees) would move by rolling rather than sliding. The above friction angles are for movement of grains in air medium but in water medium these angles should be reduced by 10-15 degrees for each category because of lubrication effect of water.

These generalizations hold for water, wind and glaciers as medium of normal transport/deposition. Exceptional conditions such as flash floods, cyclones, tsunamis, landfalls, earthquakes can produce complex chaotic flows (Vallis, 1997, p.323), where homogeneity is no longer valid and discontinuous size distributions can be common. Turbulent flows are known to be highly unpredictable and take the quasi-periodic route to reach chaotic flows (Vallis, 1997, p.323) as per following sequence:

Steady Flow > Periodic1Flow > Periodic2Flow > (Periodic3Flow) > Periodic4Flow > Strange Attractor with chaotic flows.

MATHEMATICS OF TRANSPORTATION AND DEPOSITION PROCESSES

Mathematically it is convenient, for analysis and inference, to transform nonlinear systems into linear systems through suitable nonlinear pre-transformation of data, and this also applies for statistical and stochastic analyses of sedimentological variables. This is because we know that superposition of linear systems remain closed (i.e., remain linear) which aids mathematical/statistical analyses and inferences. However, nonlinear systems do not possess such simple linear superposition law and hence need suitable prior linearization of inputs before analyses and inferences.

Thus standard deviation (positive square root of variance) of such linearized phi-normal(phi-Gaussian) partitioned size distributions becomes 2 for suspensions (Stokes' exponent) with phi ranges within 9.5 to 21.5, 1 for saltation with phi ranges within 3.5 to 9.5, 1/2 for rolling bedload sands (Newton's impact law exponent) with ranges within 0.5 to 3.5, 1 for sliding cum rolling bedload pebbles with phi ranges -5.5 to 0.5, and 2 for sliding bedload boulders with phi ranges -17.5 to -5.5. The corresponding mean phi sizes for these five modes are: 15.5, 6.5, 2.0, -2.5, and -11.5. Each of these phi size ranges are partitioned deterministically using Fuzzy logic trapezoidal elements and this procedure yields the desired Globally homogeneous Gaussian turbulence of velocities with a constant mean velocity and constant velocity variance (std. deviation) for the depositing flow. The five modes of transport/deposition as proposed here is verified by the existence and often observed in the field exposures of the presence of five item sequence (with bottom part ~ a ~ to the top part ~ e ~ of turbidite graded bed sedimentation unit) of Bouma (1962) complete turbidite sedimentation unit model. This seems more than a mere coincidence but the confirmation of the present theory with observations. Mathematically, the maximum phi standard deviation of size distribution could be about 6.0 and in nature it is seen to seldom exceed 4.5 for tillites and 3.8 for complete turbidites, which again proves the validity of present theory. Most glacial tills and turbidites are usually having polymodality with 2,3,4,5 size modes. The minimum phi standard deviation from theory is 0.5 for rolling bedload deposits and most beach sands possess an observed unimodal phi standard deviation around 0.5 which again confirms validity of present theory. As wind competency is less, the minimum unimodal phi standard deviation for stoss side of aeolian dunes would be less than that for water waves and this value is around $0.3 < 0.5$, which again shows consistency of present theory in case of different agents of transport/deposition. Bimodal sands belonging to fluvial channels would predictably have phi standard deviations around 0.8 and belonging to deltas would be around 1.0. Bimodal, trimodal, and quadrimodal turbidities would have a predictable phi

standard deviation from 1.3 to 3.3 and this range is often observed in real natural turbidities.

Thus mixing of these five fundamental phi normal size distributions in different proportions as is observed in naturally deposited sediments would yield characteristic mean, standard deviation, skewness and kurtosis in the polymodal clastic sediments and these statistics are shown to be useful for linear two-group or (preferably) linear multi-group discrimination of depositional environments (see, Sahu, 1962, 1964, 1983, 1987). Hence, finger printing of sedimentary depositional environments by proper size analyses and statistical processing has been well demonstrated by the author's above papers, in contrast to opinions of many western sedimentologists (see, for example, Twenhofel and Tyler, 1941, p.120; Pettijohn, 1974, p.50-53).

CONCLUSIONS

Physics and mathematics for homogeneous Gaussian turbulent flows responsible for clastic

sediment transportation and deposition induce polymodal (having five distinct modes) size distributions which have been validated by repeated field sampling of complete turbidite sedimentation units by many sedimentologists. This proves theory presented here to be correct.

As turbulent flows are unpredictable and have nonlinear exponents for different sizes (sp. surfaces) of particles, prior linearization by suitable log transform (Krumbein's phi transformation, negative of the logarithm to the base 2 of nominal diameter of the particle) is necessary for subsequent statistical analysis using multivariate statistical methodology.

Depositional mechanisms and depositional environments of clastic sediments are shown to be discriminable through use of various two-group or preferably multi-group linear discriminant functions as given in author's earlier papers (Sahu, 1962, 1964, 1983, 1987), in contradiction to the opinions of many western sedimentologists.

References

- Bagnold, R.A. (1941). The physics of blown sands and desert dunes., Methuen, London, 265p.
- Batchelor, G.K. (1953). An introduction to homogeneous turbulence., Cambridge Univ. Press., London.
- Bouma, A.H., (1962) Sedimentology of some flysch deposits. Elsevier, Amsterdam, 168p.
- Hjulstrom, F. (1935). Studies of the morphological activity of rivers as illustrated by the River Fyris, Bull.Geol.Inst.Uppsala, 25, 221-527.
- Kolmogorov, A.N., (1941) The local structure of turbulence on incompressible viscous flow for very large Reynold's numbers. C.R.Acad.Sci. USSR, 31(4), 538-540
- Kolmogorov, A.N. (1962). A refinement of previous hypothesis concerning local structure of turbulence in a viscous incompressible fluid. J. Fluid Mech 13, 82-85
- Krumbein, W.C., and Graybill, F.A. (1965). An introduction to statistical models in geology, Mc Graw Hill., New York.
- Krumbein, W.C., and Pettijohn, F.J. (1938). Manual of sedimentary petrography, Appleton, 549p. New York.
- Lam, L., (ed.). (1997). Introduction to nonlinear physics., Springer, Heidelberg, 417p.
- Otto, G.H. (1938). The sedimentation unit and its use in field sampling. J.Geol., 41, 519-582.
- Pettijohn, F.J. (1974). Sedimentary Rocks (3rd edn), Harper and Row, New York, 628p. (see, especially, p.50-53).
- Sahu, B.K. (1962). Environments of deposition from the size analysis of clastic sediments., Ph.D., Univ. Wisconsin (Madison), USA, 99p.
- Sahu, B.K. (1964). Depositional mechanisms from the size analysis of clastic sediments. J.Sed. Petrology, 34(1), 73-83.
- Sahu, B.K. (1983). Multigroup discrimination of sedimentary depositional environments using size distribution statistics. Ind. J. Earth Sci., 10, 20-29.
- Sahu, B.K. (1987). Stochastic approach in sedimentological analysis of Purana Basin. Memoir Geol. Soc. Ind., 6, 287-293.
- Sahu, B.K. (2009). in press, Inference on polymodal phi-size distribution component fractions of clastic rocks using corrected 3D size moments of thin-section 2D circle radii or 1D semi-intercepts, J. Indian Asso. Sedimentologists, (ms.21p.).
- Twenhofel, W.H., and Tyler, S.A. (1941). Methods of study of sediments., New York, MC.Graw Hill, 183p. New York.
- Udden, J.A. (1898). Mechanical composition of wind deposits. Augustana Univ. Library Publ., 1, 69p.
- Udden, J.A. (1914). Mechanical composition of clastic sediments. Bull. Geol. Soc. Am., 25, 655-744.
- Vallis, G.K. (1997). From laminar flow to turbulence. In: Lam, L., 1997, Introduction to nonlinear physics, Springer, 417p. (see p.308-358; esp. p.323.), New York.
- Yaglom, A.M. (1987). Correlation theory of stationary and related random functions, Springer, New York.

Characterisation of Depositional Processes and Identification of Shallow Drilling Hazards in A Growth Fault Setting using Seismic Data: A Study From Godavari Offshore, East Coast of India

SATYABRATA NAYAK¹, RABI BASTIA¹ and MADHUMITA DAS²

¹ Reliance Industries Ltd., Mumbai, ² Dept. of Geology, Utkal University, Bhubaneswar

E-mail: satyabrata.nayak@ril.com

Abstract: The study area represents a NE-SW trending growth fault setting In Godavari offshore. The principal fault trends of the above deformed zone divide the area into different blocks which act as sub basins within a basin. An attempt has been made to identify various depositional processes active in these fault blocks. The upthrown fault block is characterized by more of erosional processes while the downthrown part is more like a depositional low collecting ponded type of deposits. The study is further extended to recognize various possible geohazards such as gas seeps, gas chimneys, shallow water flow, unstable sliding strata etc. Shallow 3D seismic data which is quite useful has been used in this study to identify the above anomalies. The geohazard study in the sub basins could preempt the expected drilling related problems prior to exploratory drilling.

Keywords: Depositional processes, Shallow drilling hazards, Growth fault setting, Seismic data, Godavari offshore.

INTRODUCTION

This study is attempted to characterize depositional processes active in faults blocks in a growth fault setting and to identify various geohazards present in the area using 3D seismic data. The Study area is a part Krishna-Godavari basin, east coast of India. The area lies in the mouth of Godavari river with water bottom ranging from 40 to 400 m. Eastern continental margin of India is an Atlantic type passive margin. It is characterized by a relatively narrow continental shelf, which widens toward the inner part of the Bengal Bay and a relatively wide area comprising the continental slope and rise. Most of the sedimentation in the area can be contributed to Godavari river. The Godavari River is the third largest river in India, after the Ganges and Brahmaputra. While the Krishna River drains a basin about two thirds of that of the Godavari, it only has half of the sediment flux. For both rivers a significant part of the annual discharge and therefore the sediment flux occurs during the relatively short monsoonal period. Together the Godavari and Krishna rivers deliver an extensive sediment load (255 million tonnes per year Sharma 2002, Sarin et al. 2002) to this part of the eastern Indian continental margin.

The study area represents a growth fault regime with growth activities restricted to the Plio-Pleistocene section. A regional seismic section showing structural disposition is given in Fig. 2. NE-SW trending faults are

the major ones which are dissected by a number of cross trending faults (formed to accommodate higher sedimentation). Lithology, pressure regime (as observed from drilled wells) encountered in these wells are different. These faults merge on Paleocene, which act as a decollement surface. A number of wells have been drilled in different fault blocks. All these wells behave separately and hence it can be assumed that these fault blocks are independent of each other in regards to sedimentation process as well as hydrocarbon dynamics. Detailed description of hydrocarbon play in the area is out of defined objective of this study.

OBJECTIVE

This study aims at assessment of geohazards in the area, which are very important in planning any drilling campaign. Detailed interpretation of shallow 3D seismic data is done to define various depositional processes active in the area.

This kind of assessment of shallow hazards is done to avoid drilling problems, such as a gas blowout or subsidence of sediments (incase of a positioning of jack up rig), causing loss of equipment and, in the worst case, loss of the drilling rig and human lives. Another aspect of this study is to understand different depositional patterns and processes active in the area so that these can be characterized from hazard point of view.

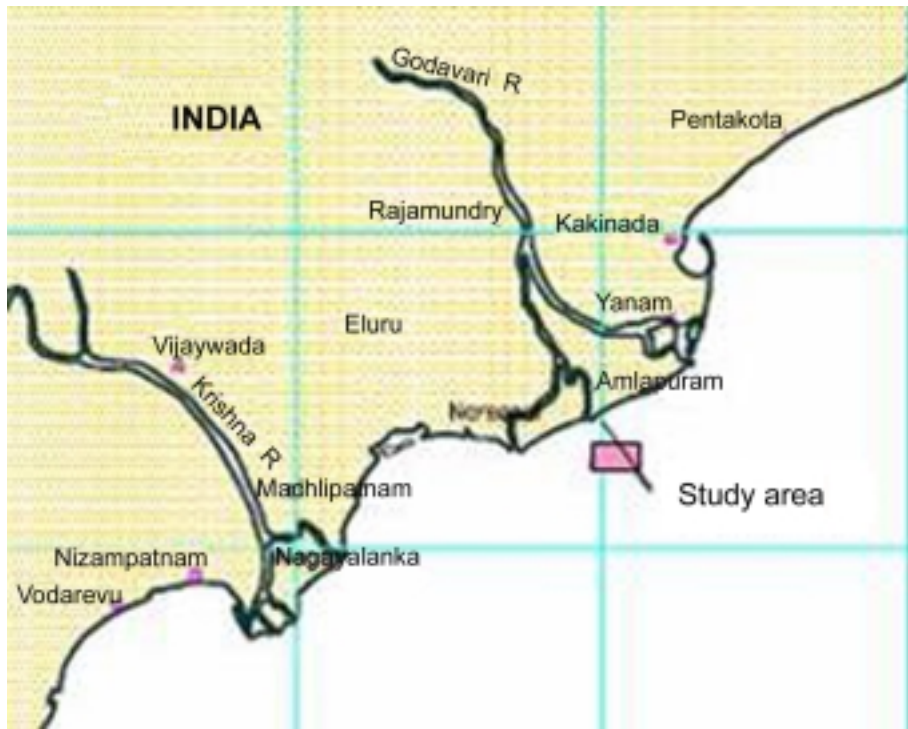


Fig. 1. Location Map showing study area.

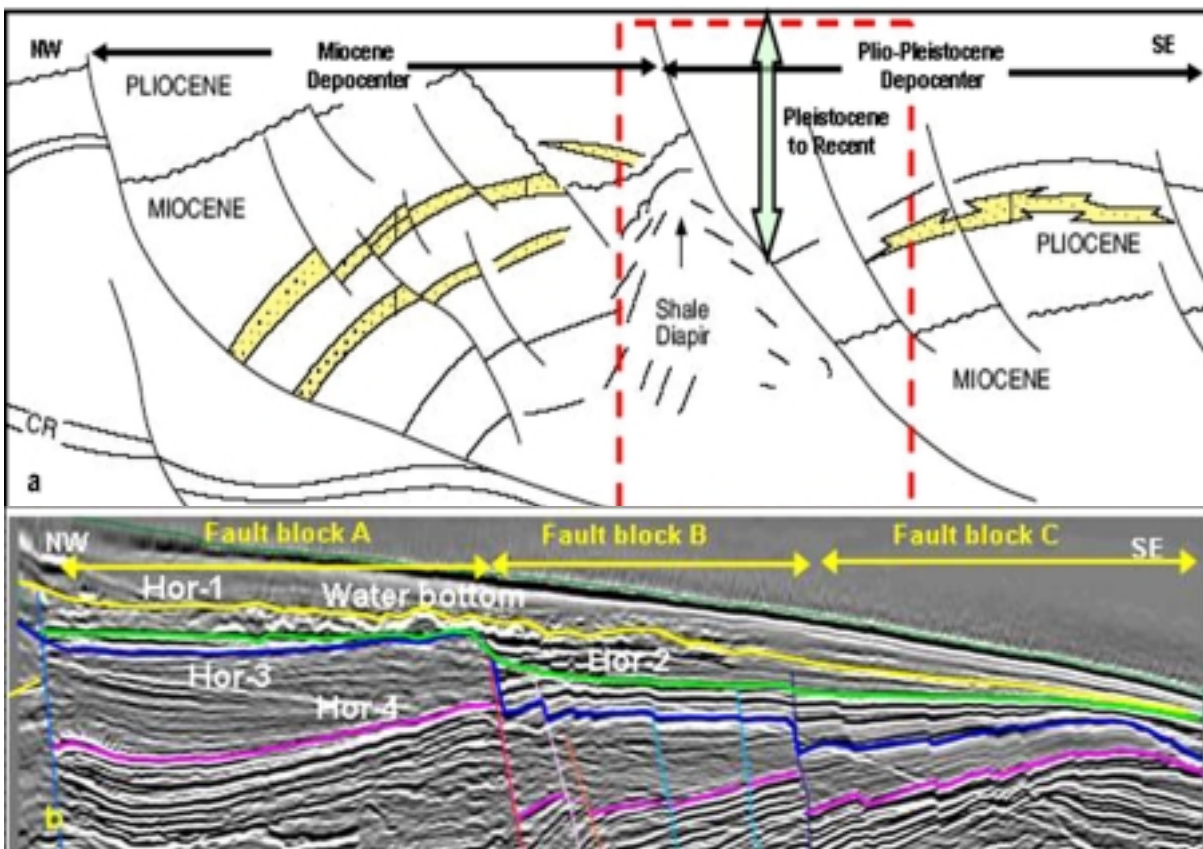


Fig. 2. A representative seismo-geological showing a number of growth faults (a). The red dotted polygon represents the area in which this study is being. Figure "b" represents a seismic section from the above red dotted area with different interpreted horizon.(location of section "a" is shown in Fig. 1. for scale of seismic section b please refer to Fig. 3).

METHODS

Exploration 3-D seismic data, covering an area of around 250 sq km. were used for the mapping of geohazards. The data were acquired and processed using standard exploration 3-D seismic parameters, with sample rate is 4 ms. Four horizons and seabed, were mapped using a standard seismic interpretation software. To highlight features of interest, different seismic attributes are generated and interpreted.

DEPOSITIONAL PATTERN

The area is characterized by a number of NE-SW trending growth faults. A dip seismic line is used to discuss evolution of growth fault as well as sedimentation process active in various fault blocks. Fig. 3 shows the attempted paleo reconstruction using horizon flattening method. Though this method has got inherent limitations, such reconstruction was

carried out to depict role of growth fault in formation of mini basins. The above seismic line running in NW-SE direction has been divided into three fault blocks namely A, B & C to discuss how sedimentation varies across the fault blocks. Water bottom and four horizons (Hor-1, 2, 3, 4) are used to show structural evolution with time. The sequence discussed here is of Pleistocene age. Fig. 3a represents present day structural configuration with interpreted horizons and faults. Sediments are seen to be prograding basin ward. Horizons are flattened to discuss the basin configuration at the time of deposition of the corresponding horizons. Few cases are described below:

Hor-3 Flattened (Fig. 3e)

Fault block ‘A’ showing prograding seismic reflector is seen to have more accommodation than Fault block B & C.

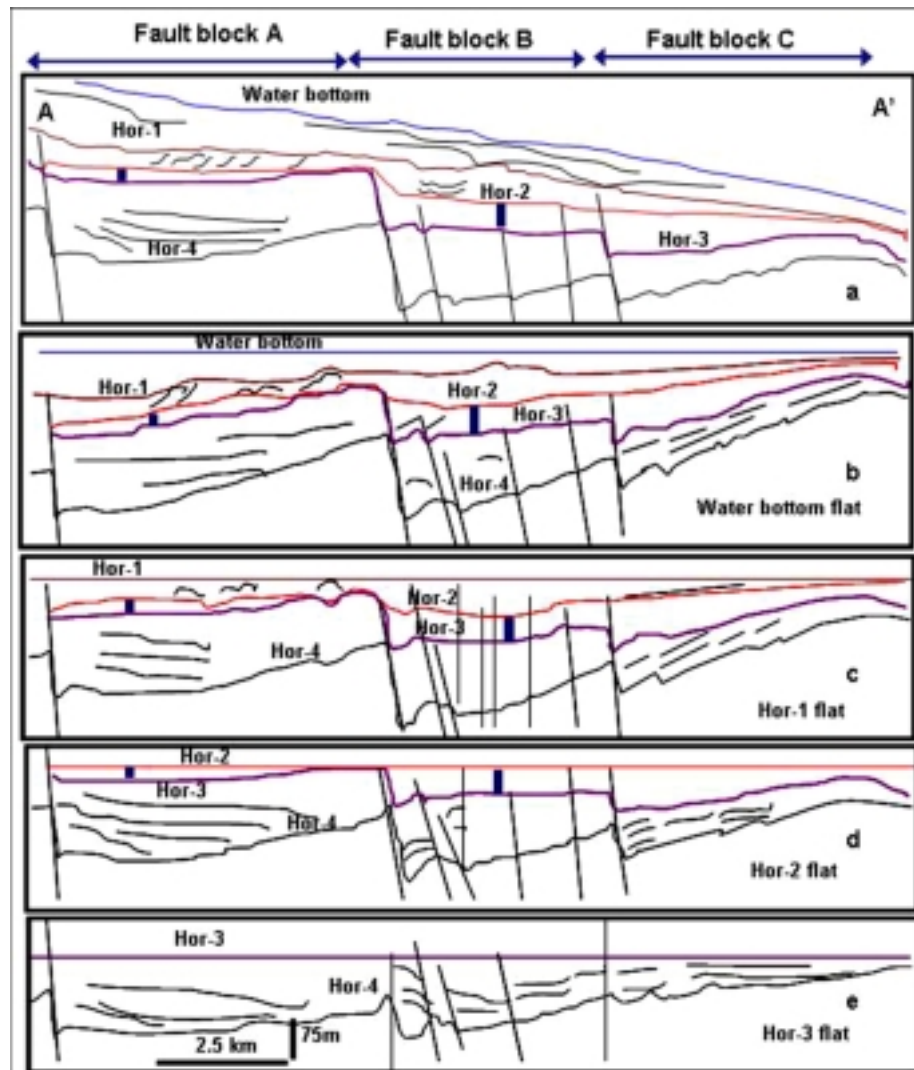


Fig. 3. Schematic diagrams showing evolution of different growth fault blocks with time. Horizon flattening method is used to discuss the structural disposition at different time. Change in depocentre from one fault block to other can be seen in the figures. Figure (a) represents present day structural configuration. (Location of the line is given in Fig. 5).

Hor-2 flattened (Fig. 3d)

This shows a lesser accommodation in the “A” block in comparison to B & C block, which suggests progradation more towards basinal part and hence depocentre is shifted from block A to B.

Hor-1 flattened (Fig. 3c)

This clearly shows a thick section of sediment between Hor-2 & Hor-3 in the fault block B. A number of slide block with development of small scale imbricate thrust are observed on top of Hor-2 suggesting mud flow (Moscardelli et al 2006).

Water bottom flattened (Fig. 3b)

The schematic diagram shows prograding reflectors on top of Hor-1 which are continuous across the block and have no fault Impression suggesting cessation of growth.

Fig. 3a shows present day condition. Sea bottom in this section is smooth, but at other part of the block a number of canyons, pock marks are observed (details in Fig. 5).

From the above discussion it can be assumed that in a growth fault regime each of the fault block behave like a mini basin each characterized by different sedimentation processes and sediment thickness. Amplitude extracted along Hor-2 is represented in Fig. 4 to show how sediment disposition changes in different fault blocks. The map shows presence of two well developed escarpments, of which one is generated due to presence of a fault (green dotted line) and other one (yellow dotted line) is because of erosion related to slide activity.

This area (less than 150 sq km) can be divided into three blocks for discussion. Block A is the shallowest one characterized by small scale imbricate thrust faults representing mud flow. Block B is having the maximum accommodation space where sediment ponding is taking place.

A narrow channel like feature (black dotted) is seen to be crossing across all the blocks. This may be one of the youngest one deposited once there is no growth activity and there is peneplanation. Block C is the youngest one representing a slide movement which erodes away a part of block B. A number of slope failures can be seen in the block C.

SHALLOW HAZARDS IDENTIFIED

A number of potential shallow geohazards identified in the 3-D data can be described as

- Risk of slope failure
- Possible gas charged unconsolidated deposits.
- Gas chimneys.

Few pock marks related to gas escape are also identified, but these are very small in size. Fig. 5 shows slope map extracted from water bottom, with identified hazard zones.

SLOPE FAILURE

A number of features believed to be slope-failure scars were revealed during mapping of the seabed and other shallow horizons (Fig. 7). Geometrical attributes like Edge detection, dip, azimuth, and slope are being used for better identification of scars. Slope attribute maps of sea bottom is used for slope failure discussion in this paper as the author feels the above attribute reveals horizon morphometry better. These attributes were applied on mapped time horizons to highlight steep dips, indicating escarpments and faults.

SEA FLOOR MORPHOLOGY

Fig. 5 shows slope attribute map of the seabed. A possible slope-failure scar is indicated on the map. This is the same slope-failure scar that is indicated in the seismic section in Fig. 6. Based on interpretation of various geometrical attributes four morphological zones have been recognized in the study area

- A channeled region
- An area with hummocky seafloor
- Areas with seafloor scours
- Smooth seafloor.

The scours are lineations that usually converge towards channel heads. The channeled area indicates active down slope transport. The hummocky sea bottom indicates mud flow impression. Out of the above four region the area with smooth sea bottom is of lowest risk and area with channelized is higher risk any drilling or engineering activity to be done on sea floor. These slope failure scars are also interpreted from other near sea bottom surfaces also. Fig. 4 shows slope failure interpreted from Hor1. A seismic line showing seismic impression of slope failure is given in Fig. 6.

A number of slide planes are interpreted from the figure. All the slope failure scars are seen to be retrograding. A similar development is well documented for the storegga slide, offshore Norway (Bryan et al, 2005). The slide scar has later been filled in with stratified, but more acoustically transparent sediments (position of seismic lines are given in Fig. 5). A zoomed slope attribute map showing development of a number of slope channels and escarpments are discussed in Fig. 7.

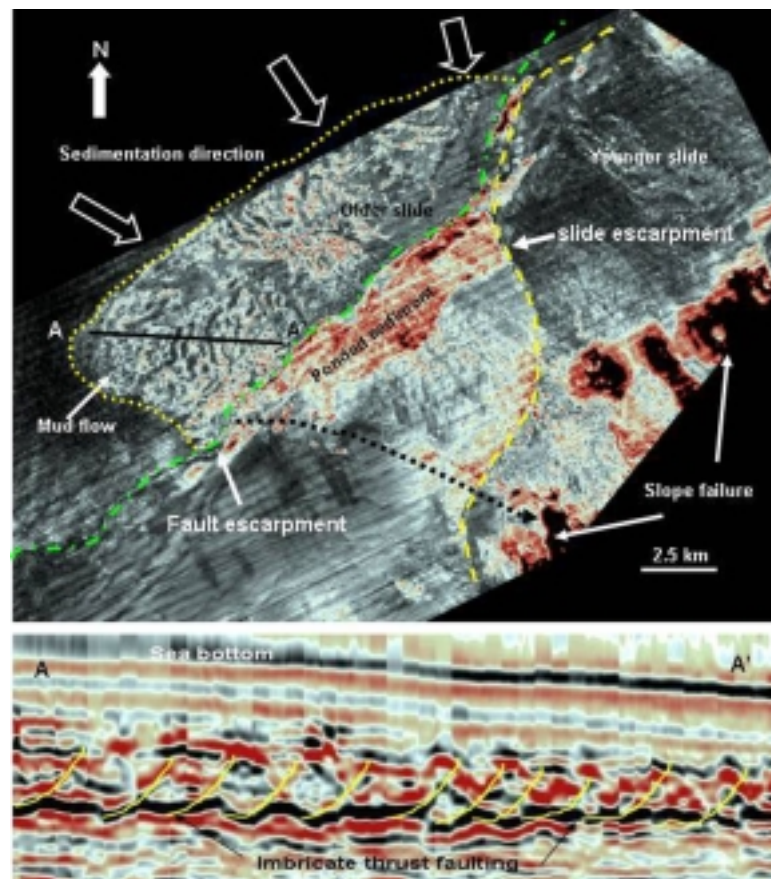


Fig. 4. Amplitude extracted along Hor-1 shows different identified morphologic features. Two prominent escarpments, one generated due to faulting and other due to sliding are clearly seen in the map. Small scale features generated by mud flow can be interpreted from the figure. Small scale imbricate thrust faulting characterizing mud flow is also shown in the seismic section.

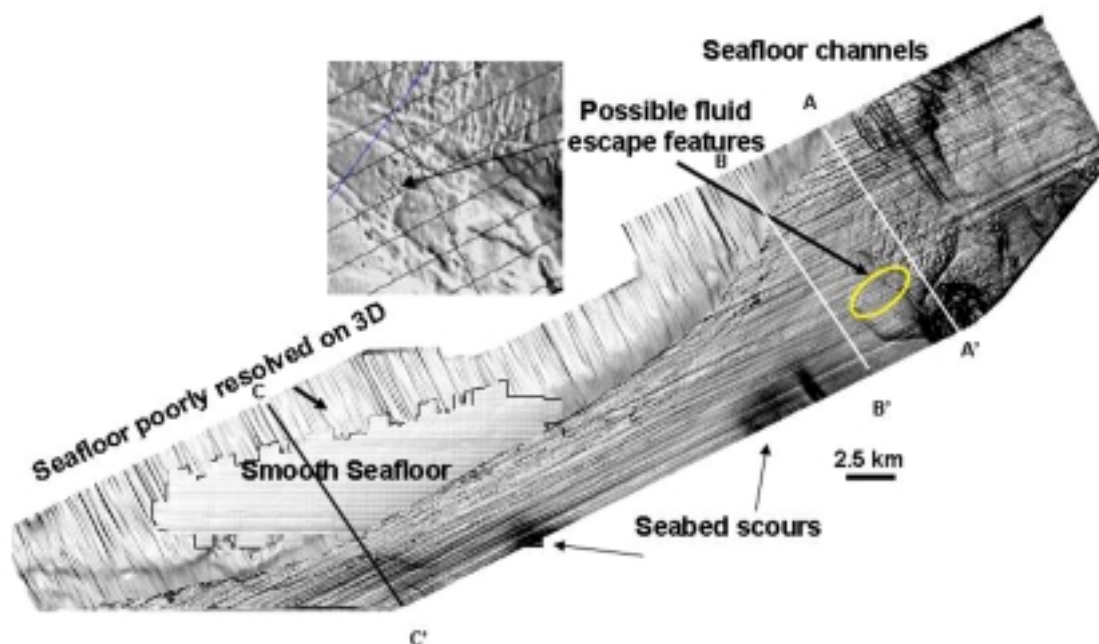


Fig. 5. Sea bottom map (slope attribute) showing various morphological classification. The central grey area is smooth, with no special features discernable on the seismic data. The possible fluid escape features are pockmark-like depressions. The inset is a magnification of the area with possible fluid escape features.

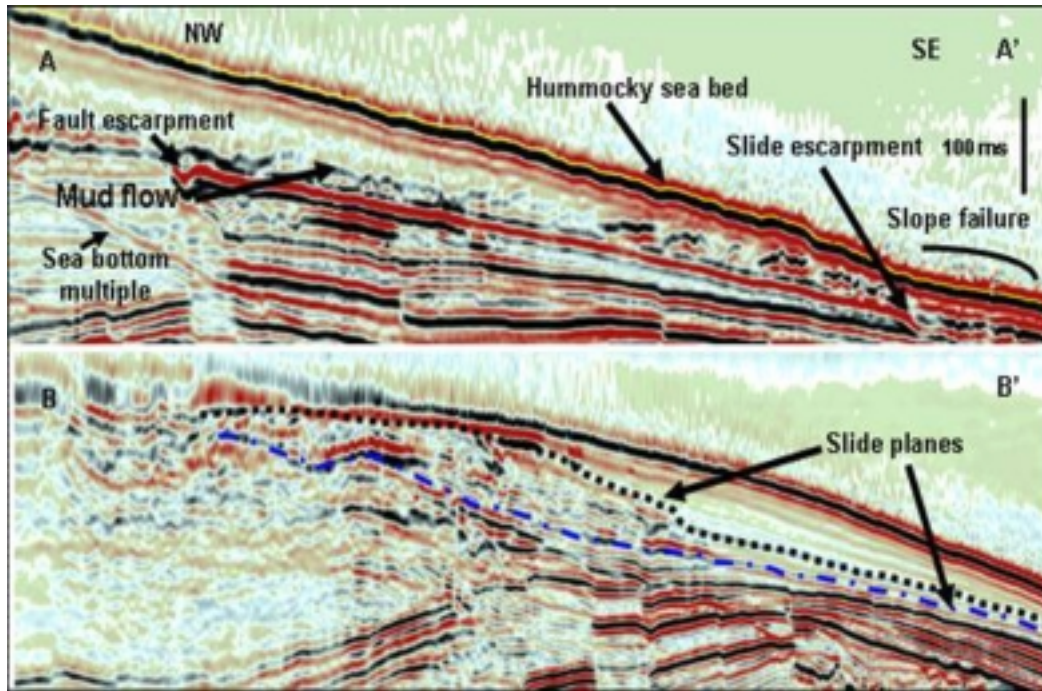


Fig. 6. Seismic line AA' and BB' showing seismic expression of geomorphologic features. (Position of lines are shown in Fig. 5).

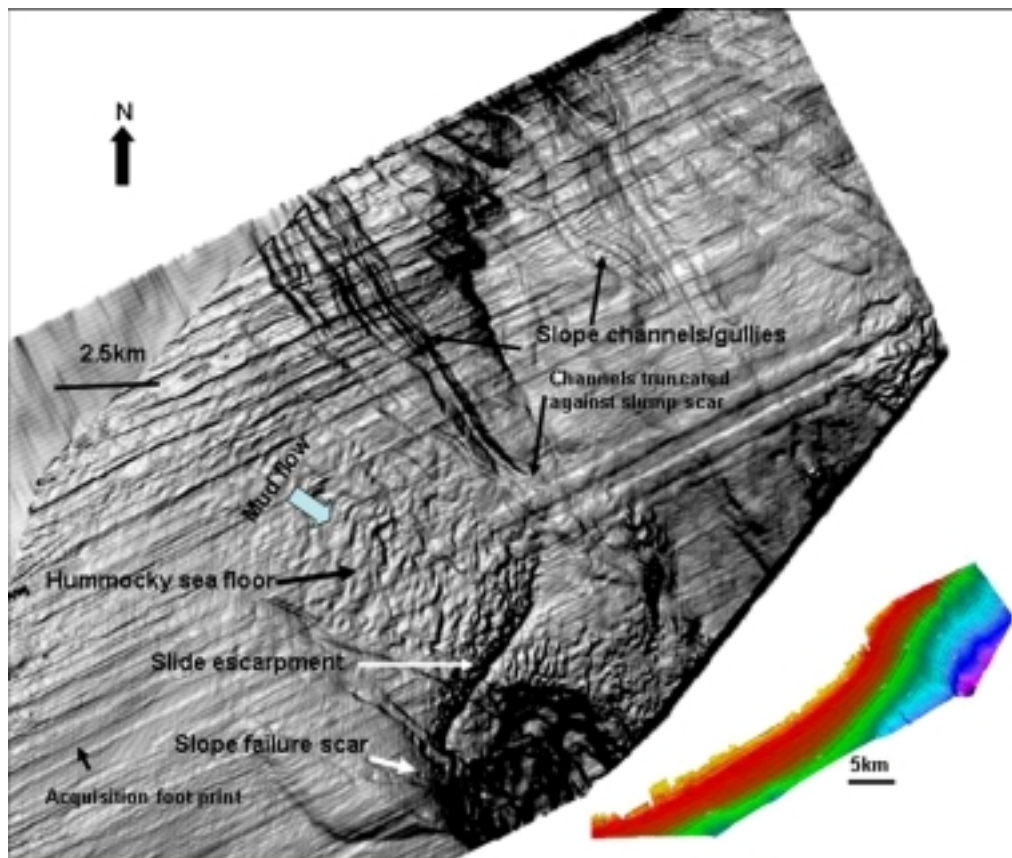


Fig. 7. Slope map on top of sea bottom showing various present day geomorphologic features. The colored map is a structure map of sea bottom. Slope channels are seen to be truncated by younger slides. Hummocky sea floor caused by mudflow is interpreted. The colored map represent the bathymetry of the area with yellow is the shallowest and pink is deepest water bottom.

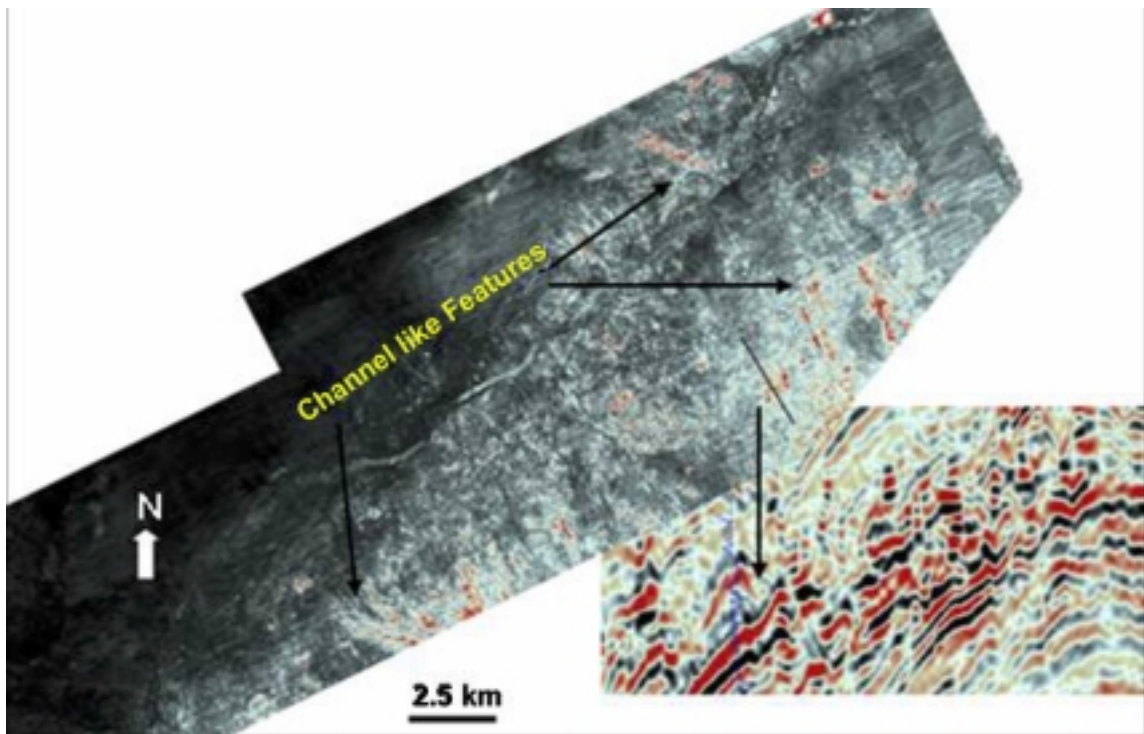


Fig. 8. Amplitude map showing channel like features. Inset shows the high amplitude pack along which the amplitude is extracted.

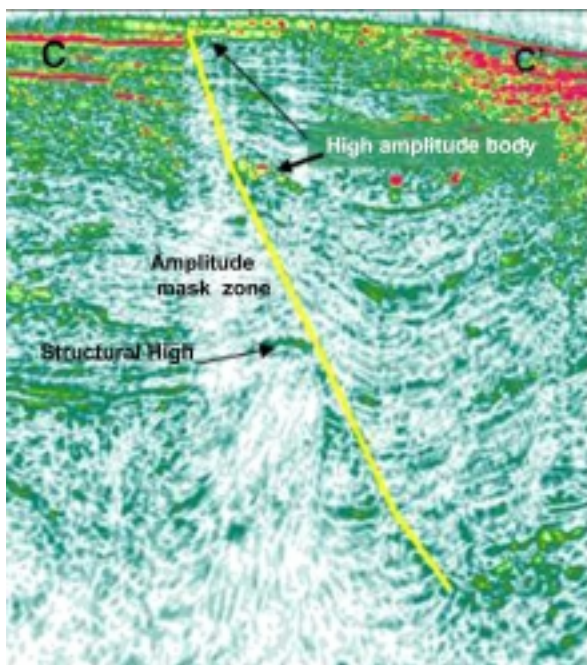


Fig. 9. Seismic section showing amplitude masking due to gas chimney effect. Few high amplitude anomalies can be seen against the yellow color fault. (Location of section is shown in Fig. 5).

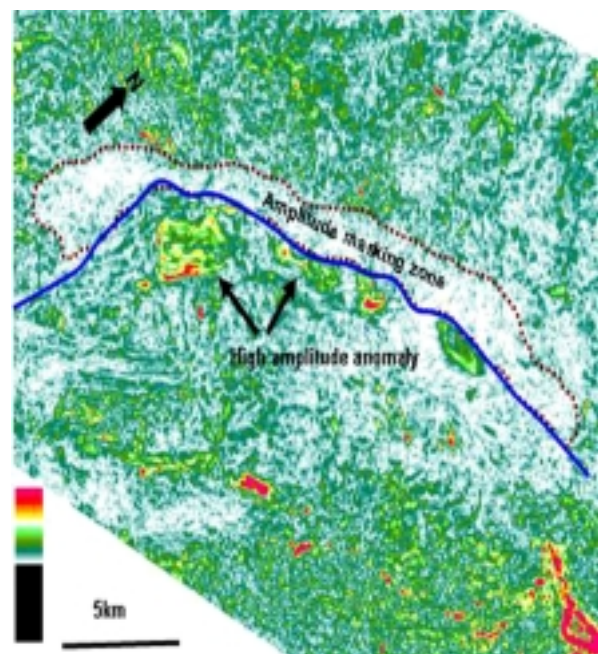


Fig. 10. Time slice through the shallow amplitude body showing an amplitude mask zone along the fault. Few high amplitude bodies are also identified against the fault. These amplitude bodies are shallow gas charged reservoirs.

GAS CHARGED UNCONSOLIDATED SANDBODY

During drilling of few wells in the above area shallow unconsolidated gas charged sands were encountered. These sands create problem of high pressure during drilling. Shallow channels interpreted from seismic are shown in Fig. 8.

GAS CHIMNEY

Chimneys indicate upward migration of gas from the deep to the shallow prospect (Heggland, 2004). These can cause problem of shallow gas during drilling. An interpreted gas chimney is being demonstrated in Fig. 9. The chimney is having an inverted cone type shape with low amplitude. Few high amplitude anomalies identified near to the gas chimney, indicate a risk of a gas accumulation in the shallow reservoir.

Amplitude maps are used to identify amplitude anomalies representative of shallow gas accumulations, as well as identify faults. A shallow bore hole drilled near to one of the anomaly encountered gas in the shallow section

suggesting shallow gas charge reservoir. A time slice (Fig.10) through the above high amplitude anomaly shows the probable lateral extent of the gas chimney zone.

CONCLUSIONS

The principal shallow hazards identified in this study were found to be a risk of slope failure and risk gas chimney. Geometrical attribute (slope etc.) maps were found to be useful for the study of slope failure. Various amplitude maps were used for the mapping of high-amplitude anomalies to predict shallow gas accumulations. Coherency and semblance volumes are used for detection of chimney. Understanding the depositional processes active in the area is helpful in defining shallow hazards. Closely spaced 3D seismic data is of much use in this type of study.

Acknowledgement: The authors are thankful to Reliance Industries Ltd for allowing publishing the paper.

References

- Bryn P, Berg K, Forsberg CF, Solheim A, Kvalstad TJ. (2005). Explaining the Storegga Slide. *Marine and Petroleum Geology* 22, 11-19
- Hartvelt, J. J. A. and Zwaag van der, G. L. (1993). Integrated geohazard study along the Krishna-Godavari Delta slope, east coast India. In: Ardu DA, Clare D, Hill A, Hobbs R, Jardine RJ and Squire JM. *Advances in Underwater Technology, Ocean Sciences and Offshore Engineering*. ISBN 0-7923-2363-7, Kluwer Academic Publishers. Offshore Site Investigation and Foundation Behaviour. 28, 333-346.
- Moscardelli L, Wood L, Mann P (2006). Mass-transport complexes and associated processes in the offshore area of Trinidad and Venezuela. *AAPG Bulletin* 90, 1059-1088.
- Sharma KP (2002). A study of sediment fluxes to the coastal zone in south Asia and their relationship to human activities. Project report on APN Project on a study of nutrient, sediment and carbon fluxes to the coastal zone in south Asia and their relationships to human activities, 20.
- Roar Heggland Definition of geohazards in exploration 3-D seismic data using attributes and neural-network analysis *AAPG Bulletin*, 88, (6) (June 2004), 857-868.

Cuddapah Basin: India's Emerging Uranium-Hub

R. DHANA RAJU

Atomic Minerals Directorate for Exploration and Research

Dept. of Atomic Energy, Govt. of India, 1-10-284/1, Begumpet, Hyderabad – 500 016

E-mail:rdhanaraju@hotmail.com

Abstract: The Mesoproterozoic Cuddapah Basin (CB), together with its inclusive Neoproterozoic Kurnool Basin, constitutes India's second largest Proterozoic (*Purana*) basin. It has an areal extent of ~ 44,500 sq km. Its potentiality for mineral resources is well-known and vast, as it hosts diverse metallic and non-metallic resources of lead, zinc, copper, iron, manganese, limestone, dolostone, barite, asbestos, phosphorite, dimensional stones, and diamonds; these are being exploited since long. To this list, uranium was added during the last decade. Thus, in spite of the earlier (late 1950s to early 1960s) exploration for atomic minerals in this basin showing it as mainly thoriferous, subsequent detailed exploration since late 1980s has demonstrated it as mostly uraniferous of diverse nature and types. Exploration by the Scientists of the Atomic Minerals Directorate (AMD) for Exploration and Research, Dept. of Atomic Energy, Govt. of India, has led to U-resources of 44,202 te of U_3O_8 in this basin, with continued exploration adding more.

The established deposits in CB are: (i) large-tonnage but low-grade stratabound, carbonate-hosted type in the Vempalle formation of the Cuddapah Supergroup in the Tummalapalle – Giddankipalle area of the Kadapa district in the SW part of CB, which is under exploitation by the Uranium Corporation of India Ltd. (UCIL) since November, 2007 and (ii) unconformity-proximal type, hosted mostly by the basement biotite granitoid and to a lesser extent by its overlying quartzite of the Srisailem formation of the Cuddapah Supergroup in the Lambapur – Peddagattu area in the Nalgonda district in the NE part of CB, which will be shortly exploited by UCIL. AMD is continuing exploration in the nearby areas of Chitrial in the Nalgonda district and Koppunuru (in the Palnadu basin) in the Guntur district to add further U-resources.

In addition, there are potential U-prospects in and around CB. These include: (i) Hydrothermal-type U-mineralization in the Gandhi and Giddankipalle areas in the Kadapa district in the SW part of CB; (ii) Fracture-controlled U-mineralization around Lakkireddipalle in the Kadapa district in the southern environs of CB; and (iii) Shear zone-hosted U-mineralization near the E-margin of CB near Somasila in the Nellore district. In this paper, an overview of the attributes of these U-deposits/prospects in CB is presented. All these deposits and prospects of U, together with the already-established substantial U-resources in the former, demonstrate that CB is India's emerging U-hub during the first-half of the 21st century and may meet, to a large extent, the requirement of indigenous U-fuel for the Country's civil and defense nuclear power/industry.

Keywords: Uranium deposits/prospects, Cuddapah basin, Andhra Pradesh, India.

INTRODUCTION

The Mesoproterozoic Cuddapah Basin (CB), including the Neoproterozoic Kurnool Basin within CB, constitutes India's second largest Proterozoic (*Purana*) basin. It has an areal extent of ~ 44,500 sq km. Its potentiality for mineral resources is well-known and vast, as it hosts diverse metallic and non-metallic mineral resources of lead, zinc, copper, iron, manganese, limestone, dolostone, barite, asbestos, phosphorite, dimensional stones and diamonds; these are being exploited since long (Geol. Surv. India, 1975; Kurien, 1980; Dutt, 1986; Nagaraja Rao *et al.*, 1987; Ramam, 1999). To this list, uranium was added during the last decade. It may be noted that earlier (late 1950s to early 1960s) exploration for atomic minerals in this basin, directed to the basal conglomerate and its overlying Gulhcheru quartzite of the Cuddapah Supergroup, led to the

discovery of mostly thoriferous activity, while subsequent exploration since late 1980s has demonstrated it as mostly uraniferous of diverse nature and types (Sundaram *et al.*, 1989; Vasudeva Rao *et al.*, 1989; Veerabhaskar *et al.*, 1991; Majumdar *et al.*, 1991; Sinha *et al.*, 1995; Jeyagopal *et al.*, 1996; Umamaheswar *et al.*, 2001a). Thus, exploration by the Scientists of the Atomic Minerals Directorate (AMD) for Exploration and Research, Dept. of Atomic Energy (DAE), Govt. of India, has led to U-resources of 44,202 te of U_3O_8 in Andhra Pradesh (as on January 1, 2009; AMD Newsletter, 2009), which are almost entirely in this basin. In CB, the established deposits are: (i) Stratabound, carbonate-hosted type in the Vempalle formation of the Cuddapah Supergroup in the Tummalapalle – Giddankipalle area, near Pulivendla, of the Kadapa district in the SW part of CB (Vasudeva Rao *et al.* 1989; Dhana Raju *et al.*, 1993; Roy and Dhana Raju, 1997; Jeyagopal and Dhana Raju,

1998) and (ii) Unconformity-proximal type, hosted by the basement biotite granitoid and its overlying Srisaïlam quartzite of the Cuddapah Supergroup in the Lambapur – Peddagattu area in the Nalgonda district in the NE part of CB (Sinha *et al.*, 1995) (Fig. 1). The Uranium Corporation of India Ltd. (UCIL), which is a Public Sector Undertaking of DAE for exploitation of U, is exploiting the Tummalapalle – Giddankipalle U-deposit since November 2007, with an estimated cost of Rs. 1106 crores for underground-mining and a mill to extract U, while it is planning to open up shortly the Lambapur – Peddagattu U-deposit with a project cost of Rs. 637 crores. AMD is continuing exploration in the contiguous areas of these deposits to add further U-resources. In addition, there are potential U-prospects in and around CB. These include: (i) Hydrothermal-type U-mineralization in the Gandhi (Umamaheswar *et al.*, 2001a

and 2001b) and Giddankipalle (Dhana Raju *et al.*, 1993) areas in the Kadapa district in the SW part of CB; (ii) Fracture-controlled U-mineralization around Rayachoti in the Kadapa district in the southern environs of CB (Dhana Raju *et al.*, 2002); and (iii) Shear zone-hosted U-mineralization near the E-margin of CB near Somasila in the Nellore district (Veerabhaskar *et al.*, 1991) (Fig. 1). In this paper, an overview of the attributes of these U-deposits and -prospects in CB is presented. All these deposits and prospects of U, together with the already-established substantial U-resources and potentiality for proving further resources in the former, demonstrate that CB is India's emerging U-hub during the first-half of the 21st century and may meet much of the requirement of indigenous U-fuel for the Country's civil and defense nuclear power and industry.

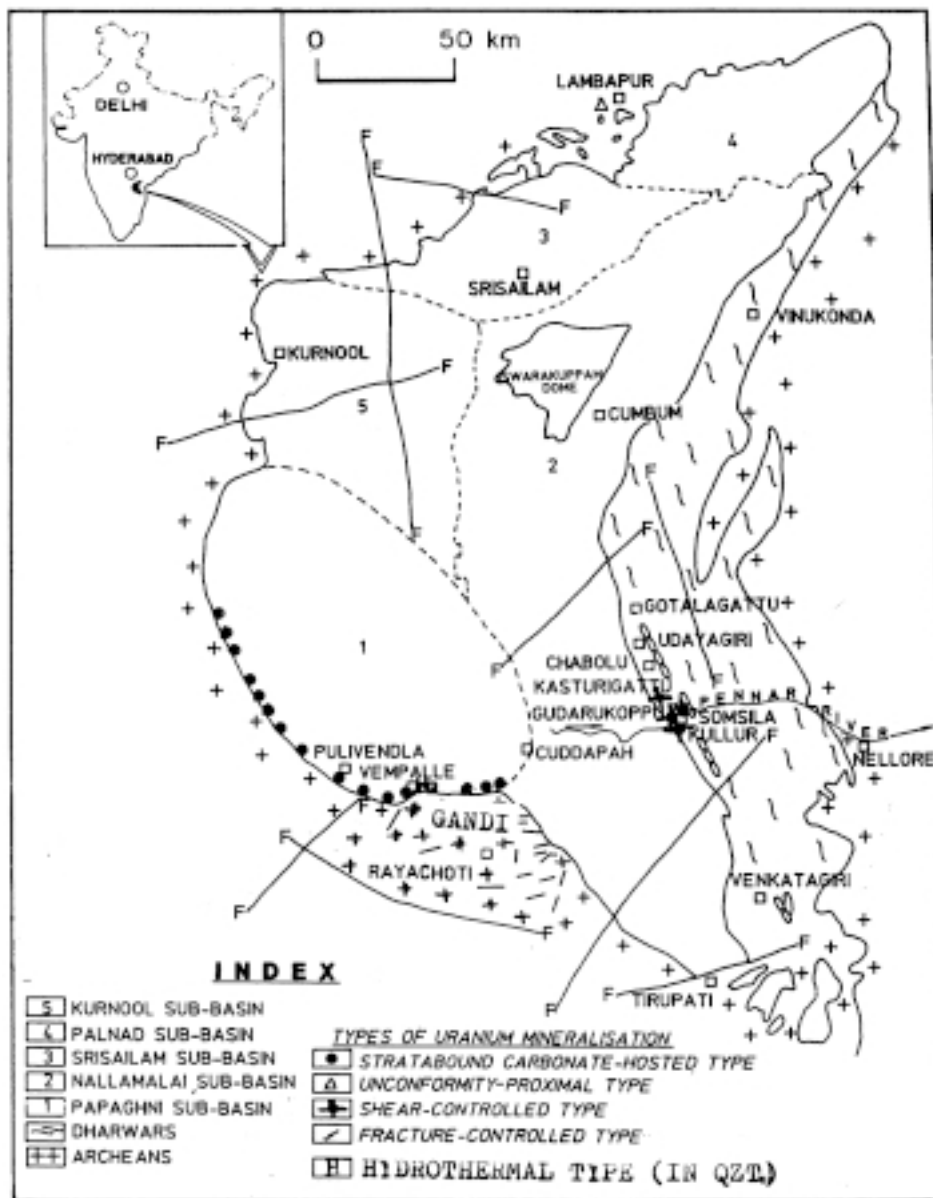


Fig. 1. Cuddapah basin and its sub-basins, with locations of different types of U-mineralization.

ESTABLISHED URANIUM DEPOSITS

Tummalapalle – Giddankipalle U-deposit

This is a low-grade (av. $\sim 0.045\%$ U_3O_8) but large-tonnage ($>30,000$ te U_3O_8) deposit, mostly in the Kadapa district and to a lesser extent in the Anantapur district. It is rather a rare deposit since carbonate rocks are considered as unfavourable hosts for U due to the soluble nature of uranyl bi-/tri-carbonate complex in which form U is usually transported. It is hosted by 'Phosphatic Siliceous Dolostone' (PSD) that is sandwiched between a massive dolostone below and red shale and cherty dolostone above, with intermittent intra-formational conglomerate below it. All these litho-units belong to the Vempalle formation of the Papaghni Group of the Cuddapah Supergroup. U-mineralization in PSD is homogeneous and is something like a coal seam, with a strike length of ~ 160 km, starting from Reddypalle in the Anantapur district in north to Maddimadugu in the Kadapa district in east, along the W/SW margins of CB, with a maximum width of $\sim 2-3$ km and better development in the central portion of the Tummalapalle – Rachakuntapalle – Giddankipalle sector, near Pulivendula (Fig. 2) (Vasudeva Rao *et al.*, 1989; Majumdar *et al.*, 1991; Jeyagopal and Dhana Raju, 1998).

AMD is exploring further in the extension areas of this sector to prove additional resources of U.

PSD exhibits primary sedimentary structures of ripple marks, mud-cracks and pelloids. Mineralogically, it comprises major minerals of ferroan dolomite ($\sim 50-70$ vol. %), silicates ($\sim 10-20$ vol. %) of detrital quartz, lesser microcline and Na-plagioclase, and collophane (francolite, $\sim 5-10$ vol. %), with minor minerals of calcite, clays, organic matter and opaque ores. Its U-mineralization is stratabound and essentially syn- and dia-genetic. U in it concentrates in the primary sedimentary structures and along bedding plane, interface between carbonate- and phosphate-rich layers, micro-stylolites, grain boundaries of clasts and within pelloids. The U-minerals are mainly pitchblende and coffinite, with occasional U-Ti complex (in quartz clasts), and $\sim 20\%$ U in PSD is present with collophane. The associated ore minerals are pyrite (including framboidal), organic matter, lesser chalcopyrite, bornite, digenite, covellite and molybdenite (Dhana Raju *et al.*, 1993; Roy and Dhana Raju, 1997; Jeyagopal and Dhana Raju, 1998). Geochemically, PSD contains, on an average, 28% CaO, 10% MgO, 21% SiO_2 , 7.9% P_2O_5 and 27% LOI (mostly CO_2), 250 ppm Pb, 200 ppm Mo, 200 ppm V, 45 ppm Cu (Vasudeva Rao *et al.*, 1989) and occasional Au ($<20-180$ ppb, with an average of 56 ppb; $n = 25$ samples) (Joshi

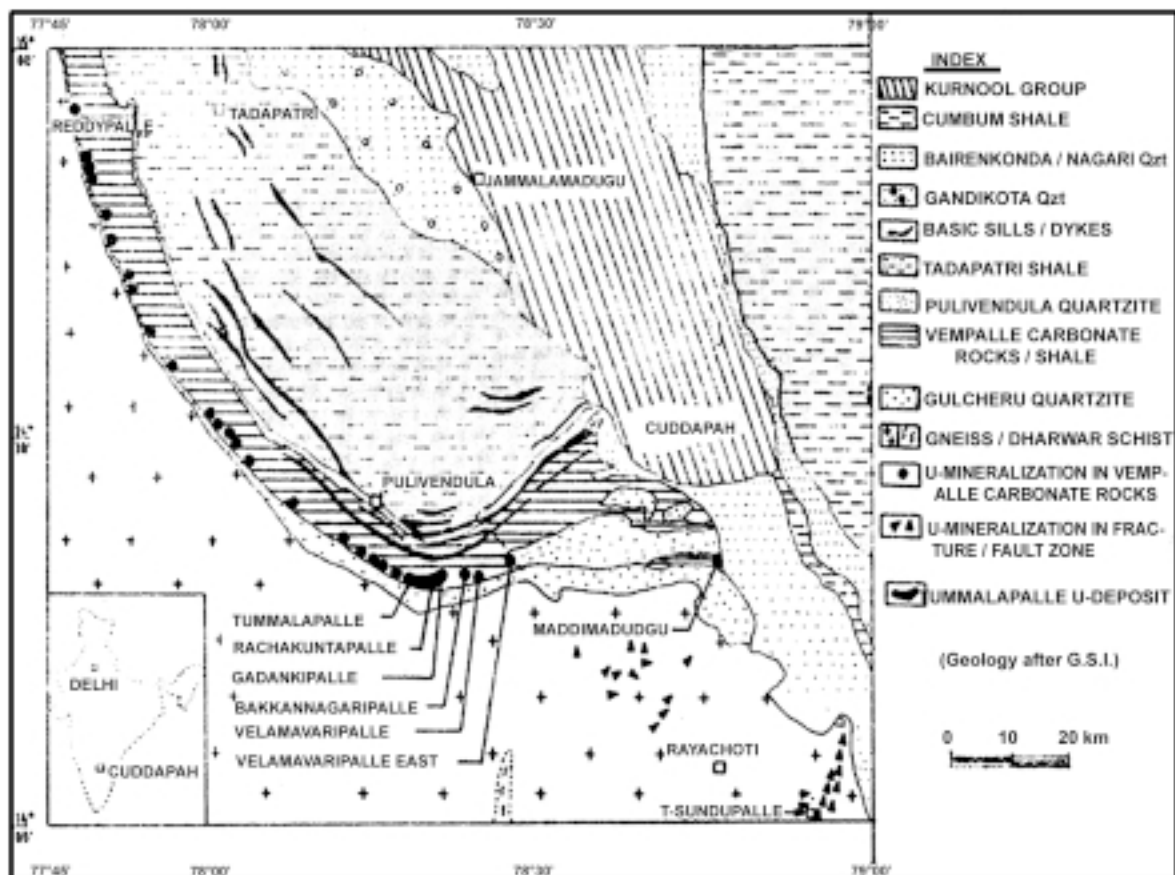


Fig. 2. Geological map of the SW part of the Cuddapah basin, showing locations of Stratabound, dolostone-hosted U-mineralization in the Vempalle formation of the the Cuddapah Supergroup.

et al., 1998). As regards the mineral-chemistry of essential ore minerals, pitchblende is almost Th-free with 77-87% U_3O_8 and 0.5% V_2O_5 , coffinite contains 63-81% U_3O_8 and 7-18.5% SiO_2 , and pyrite contains ~0.1% Ag and up to 0.12% Ag (Roy and Dhana Raju, 1999). Drilling-wise, U-mineralized PSD in the Tummalapalle – Rachakuntapalle – Giddankipalle sector has been explored by 264 boreholes, over 7.2 km along strike and ~1 km across. Two lodes, viz., hanging and footwall, are separated by a lean patch of 3 m, with the depth of the ore-body from surface being 30-270 m (Biswal, 2005). Leachability of U from mineralized PSD is 75-80% by alkaline pressure (8 kg/cm², 125°C) leaching, using $NaCO_3$ and $NaHCO_3$ as leachants, and industrial oxygen as oxidant (Dr. N.P.H. Padmanabhan, ODS, BARC, Hyderabad, *Personal Commn.*, Feb., 2006). Based on geological disposition of the ore body, the Tummalapalle U-deposit is proposed to be worked by underground method of mining, with decline as main entry. The production capacity of the mine will initially be 3000 TPD, with ROM grade of 0.042% eU_3O_8 . The mined ore will be treated in a process plant near mine using alkali route (Biswal, 2005; Gupta, 2007). As this U-deposit is of low-grade, any value-addition during extraction of its main product, namely, U will substantially reduce its cost of production. Since this ore contains ~0.02% V and ~0.02% Mo, their extraction, respectively, from pitchblende and pyrite will result in a recovery of ~5,000 te each of V and Mo, assuming a possible extraction of at least 2/3 of their total content. Besides, the ore contains on an average 56 ppb Au, with its pyrite analyzing ~0.1 Ag, and extraction of these high-value precious metals will further reduce the cost of production of U. Thus, V, Mo, Au and Ag could be the possible value-added by-products during extraction of U from this low-grade U-ore (Dhana Raju, 2009). Furthermore, the proposed mining, milling and processing of tens of millions of tonnes of this U-ore will result in accumulation of large tonnage of waste-products that comprise mainly U-leached/-free phosphatic siliceous carbonate material. As the P_2O_5 content of the ore is ~8 wt. %, the tailing and other waste (after extraction of U and the above-mentioned by-products from the ore) generated in this proposed project will contain more or less the same amount of phosphate. It appears plausible to use this P-rich waste as a low-cost substitute for more costly chemical phosphatic fertilizer in agricultural operations. Also, it appears feasible to use the powdered Ca- and Mg-rich waste, generated during the processing of this Ca-Mg-carbonate U-ore, as a low-cost de-fluoridation agent to reduce the high F contents of 2-7 ppm in drinking water to the permissible limit of ~1 ppm by simple contact of F-rich water with this waste for about 24 h (Dhana Raju, 2009).

Lambapur-Peddagattu-Chitrial-Koppunuru U-deposits

These deposits occur very near to the unconformity between the basement and overlying sedimentary rocks

of the Cuddapah basin and, hence, are designated as the unconformity-proximal type. These are located along the NE margin of the Cuddapah basin, with the first three in the Nalgonda district and the last one in the Guntur district (Fig. 3).

The Lambapur U-deposit occurs in the Lambapur outlier. Its U-mineralization (av. grade ~0.075% U_3O_8) is very close to the unconformity (associated with regolith or palaeosol) between its underlying basement biotite granite and its overlying Srisailam pebbly quartzite of the Cuddapah Supergroup, with ~85% mineralization in the former and rest in the latter. Besides these two, basic dykes and vein quartz within the basement granite are U-mineralized, with the latter also hosting lead and copper mineralization. U-mineralization has sharp outlines and shallow depth persistence, down to a maximum of 5 m below the unconformity. It occurs as linear pods at the intersection of the unconformity and two prominent sets of fractures, trending NNE-SSW and NW-SE, in the basement. The NNE-SSW-trending mineralization also closely follows the highly sheared margins of a basic dyke. The U-minerals are Th-poor uraninite, pitchblende and coffinite, associated with pyrite, chalcopyrite, galena, ilmenite, magnetite, goethite, kasolite and drusy quartz; this association points to the hydrothermal nature of mineralization. Close to the ore-zones, illite and kaolinite occur along the unconformity. Compared to the large-tonnage and high-grade unconformity-type U-deposits in the Athabasca basin of Canada and Pine Creek geosyncline in Australia (see Dahlkamp 1993, 137-168 and 168-191, respectively, for their characteristic features), the Lambapur U-deposit has the main similarities of (i) the age of the basement granite (2.2 to 2.48 Ga; Pandey *et al.*, 1988) that is fertile for U with an average of 27 ppm, (ii) the arenaceous Mesoproterozoic Srisailam formation, unconformably overlying the Palaeoproterozoic basement granite; (iii) elongate pod-shaped ore-bodies, with sharp outlines and trends, controlled by basement fractures; and (iv) primary U-minerals of pitchblende, uraninite and coffinite, whereas the most striking dissimilarity is the host rock for mineralization, which is a sheared/fractured granite at Lambapur, in contrast to the pelitic-carbonaceous schists in Canada and Australia (Sinha *et al.*, 1995). Subsequent exploration by AMD in the nearby areas of Lambapur in the Srisailam sub-basin in the Nalgonda district has led to the establishment of other unconformity-proximal U-deposits of Peddagattu and Chitrial with similar litho-structural setup as of Lambapur, whereas that in the nearby Palnad sub-basin in the Guntur district has led to the identification of similar mineralization in the Koppunuru area. The last differs from the rest in having the Neoproterozoic Banganapalle quartzite of the Kurnool Group, instead of the Srisailam formation, overlying the basement granite. These deposits are described below.

The Peddagattu U-deposit lies in the Peddagattu outlier that is one of the many dissected outliers of the

Srisailam formation in the NE margin of CB. U-mineralization in this deposit is mainly confined to the fractured, basement granite close to the unconformity. It occurs as elongate pods at the intersection of N-S, NNE-SSW and NW-SE-trending prominent sets of fractures and spreads along the unconformity between the basement fertile granite (with 10-116 ppm U) and the overlying sediments of the Srisailam formation. Pitchblende is the main primary U-mineral in this deposit and is closely associated with drusy quartz, galena, chalcopyrite and pyrite. Illitization and chloritization are the common alteration features, enveloping the mineralization (Mukundhan *et al.*, 2009).

In the Chitrial area in the Nalgonda district, the unconformity-proximal U-mineralization is hosted by basement biotite granite, intruded by large-scale N-S, NNW-SSE and NE-SW-trending dolerite and other basic dykes. The mineralization occurs along fractures, grain boundaries of gangue minerals and segregated close to altered feldspar. It is manifested by uraninite, pitchblende and coffinite. The ore zone is marked by alterations of illitization of feldspar and chloritization of biotite. Large scale intergranular fracturing, recrystallization and granulation quartz and feldspar allowed rich concentration of U, close to the unconformity contact. Presence of suitable reductants in the form of pyrite

and grey to black thinly limited shale of the Srisailam formation, besides recently identified organic matter (A. Latha, AMD, Hyderabad, *Personal Commn.*, 2009), helped in precipitation of U (Verma *et al.*, 2008).

The Koppunuru U-mineralization in the Guntur district (Jeyagopal *et al.*, 1996) is of the low-tonnage, unconformity-proximal and fracture-controlled type. It is hosted partly by the basement granitoid and partly by its overlying polymictic conglomerate and quartzite of the Banganapalle formation. The ore body is flat, dips 4-7° due north and west, and distributed in three lodes, designated as bands, A, B and C. The ore bands of A and B are hosted by the cover rock of the Banganapalle quartzite at 5-30 m above the non-conformity contact, whereas the bands B and C are sub-parallel to the non-conformity contact of grit/conglomerate and basement granitoid. The ore body has limited strike length of 700 m and stretches over a plan width of 1.2 km. Contour plan of the ore body shows inter-connectivity of ore bands, B and C, whereas ore bands, B and A are at very shallow depth. The U-mineralization occurs as stringers and veins, and also as fillings along cavities and grain boundaries. The mineralization is epigenetic in nature and is of low temperature. The U-minerals are pitchblende, coffinite and mixed phases of U, Ti, Si, Al, Ca, P and Pb. They are associated with pyrite,

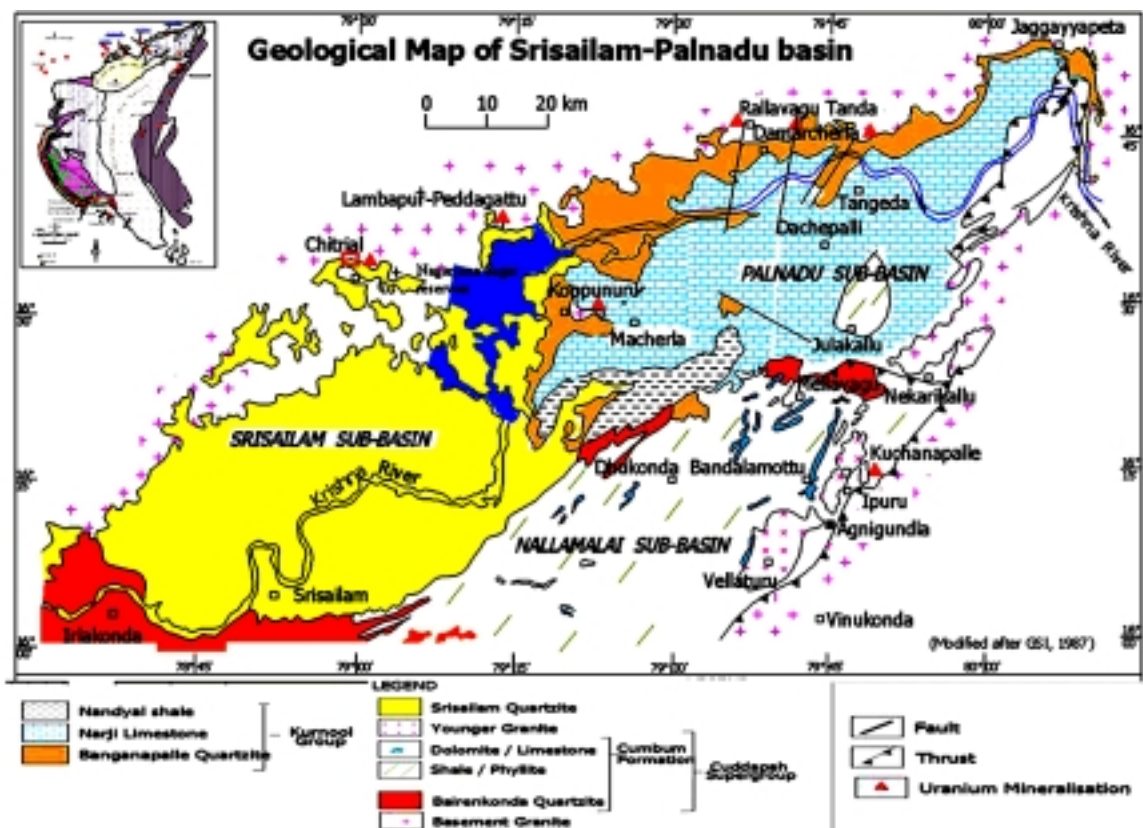


Fig. 3. Geological map of the Lambapur - Peddagattu - Chitrial (in Nalgonda district) and Koppunuru (in Guntur district), Andhra Pradesh, showing the location of the unconformity-proximal U-deposits in the Srisailam and Palnadu sub-basins of the Cuddapah basin.

chalcopyrite, bornite and carbonaceous material (in the Banganapalle quartzite) (Verma *et al.*, 2009; Jeyagopal *et al.*, 2009).

The above unconformity-proximal type U-deposits of Lambapur, Peddagattu and Chitrial in the Nalgonda district and Koppunuru in the Guntur district are of medium-tonnage (nearly 20,000 te of U_3O_8 , established hitherto) with a grade between 0.05 and 0.1% U_3O_8 . AMD is exploring further in the Chitrial area to add more resources. UCIL is planning to open up the Lambapur – Peddagattu U-deposit with a total project cost of Rs. 637 crores and got already the environmental and forest clearance (Gupta, 2007).

POTENTIAL URANIUM PROSPECTS

Hydrothermal-type U-mineralization in the Gandhi and Giddankipalle areas

This type, with a better grade (0.01 - 4.58% U_3O_8) as compared to the above two types of U-deposits, occurs in the structurally-weak zones of sulphide-bearing quartzite of the Gulcheru and Vempalle (?) Formations of CB, respectively, in the Gandhi and Giddankipalle areas in Kadapa district. Several U-occurrences were located by AMD in the Gulcheru quartzite, which have considerable extent and grade (0.01 - 4.58% U_3O_8). These occurrences spread along the E-W fault sections over 1 to 4 km length in the Gandhi area, at Gandhi, Gandhi west, Bolaguntacheruvu, Virannagattupalle and Rachakuntapalle (Fig. 4), all in the Kadapa district. The Gulcheru quartzite, hosting U and, at places Au and Ag, is grey-white/brown coloured, with abundant primary structures like cross-bedding, ripple marks and mud-cracks. Its framework clasts comprise monocrystalline quartz, polycrystalline quartz (chert) and rarely altered feldspar. These are corroded and infiltrated by authigenic, microcrystalline chlorite and authigenic quartz, interlocking with adjoining quartz clasts. The matrix (2-4 vol. %) is mainly composed of chlorite and clay minerals, whereas the authigenic quartz is the common cement. Uranium, ranging from 0.008 to 4.58% U_3O_8 (n=30; 22 surface samples + 8 drill-core samples), occurs in the form of fracture-fillings and veins, and also is interstitial along grain boundaries of quartz. U-mineralization occurs as lensoidal bodies in cross-bedded white/grey quartzite, spread over 4 km long E-W fault section in the Gandhi west area. The U-minerals are pitchblende, coffinite and uraninite, associated with sulphides like pyrite and galena. Significant U-values have also been recorded in the drill-core in the Gandhi area, with mineralized intercepts up to 1.04% U_3O_8 for 3.53 m. Apart from U, gold (<0.25-13 ppm) and Ag (<0.25-8 ppm), associated with sulphides, are generally high in the quartzite with high U values (~ 1 - 4.6% U_3O_8). Electron Probe Micro Analysis (EMPA) has shown Au up to 0.05% in galena, and Ag is up to 0.09% and 0.06%, respectively, in galena and pyrite. These data and

information confirm that potential hydrothermal type U-mineralization, associated with Au, Ag, Mo, Ni, Co, V, Cu and Pb in sulphides, occurs in the sulphide-bearing Gandhi quartzite along fault zones in the Gandhi and adjoining areas (Umamahaswar *et al.*, 2001 a, b). Similar hydrothermal-type U-mineralization in the form of pitchblende and coffinite, associated with pyrite, molybdenite and limonite, is recorded in the drill-core samples of brittle-deformed quartzite (Vempalle Formation ?) in the Giddankipalle area, near Pulivendla in Kadapa district. The U-minerals occur along pressure-dilation zones like fractures, microfractures, grain boundaries of quartz and pyrite (Dhana Raju *et al.*, 1993). These studies call for detailed exploration in the Gandhi, Giddankipalle and Rachakuntapalle areas to locate such sulphide-bearing quartzite in structurally weak zones like faults for the mineralization of U and, possibly Au and Ag.

Fracture-controlled U-mineralization around Rayachoti

The area around Rayachoti (Fig. 5) in the SW environs of CB, where the fracture-controlled U-mineralization occurs, is largely occupied by granitoids, criss-crossed by dolerite (and minor gabbro) dykes and fracture system that comprises 3 sets, viz., ENE-WSW, NNE-SSW and NW-SE. Most of these fractures are occupied by basic dykes. In a majority of these fractures, deformed variants of granitoids occur in the form of cataclasites, mylonites and phyllonites. Such deformed granitoids, mainly along the ENE-WSW fracture system within the Closepet equivalent pink granitoid, constitute the loci for U-mineralization, as recorded in over 50 fractures (750 to 2500 m in length) at Mulapalle, Chenchalapalle, Burjupalle, Payalapalle and Madireddigraipalle, all N/NE of Rayachoti. Besides, there is a 16 km-long N30°E-S30°W-trending fracture zone from T. Sundupalle (S of Rayachoti) to Sanipaya (bordering the margin of CB; E of Rayachoti), in which U-mineralization occurs intermittently. This fracture zone passes mainly through older granitoid (Peninsular Gneiss) and basic dykes, and less of younger Closepet equivalent granitoid. The deformed granitoids within these fractures exhibit large-scale metamorphic (greenschist facies) and metasomatic effects as well as a host of wall-rock alterations like hematitization, chloritization, sericitization and epidotization. Geochemically, they are marked by enrichment of Fe_2O_3 , Al_2O_3 , MgO and TiO_2 , with depletion of SiO_2 , FeO and Na_2O . In the U-mineralized fracture zones (200 to 450 m length, with a width of 1-7 m in the Mulapalle, Birjupalle and Chenchalapalle areas; ~3.5 km length, with 1-6 m width in the Sanipaya – T. Sundupalle area), radioactivity is of the order of 0.01- 0.53% eU_3O_8 with negligible Th and 15-40% disequilibrium in favour of parent U. The U-mineralization is manifested mainly by refractory minerals of brannerite and U-Ti complex, with traces to minor

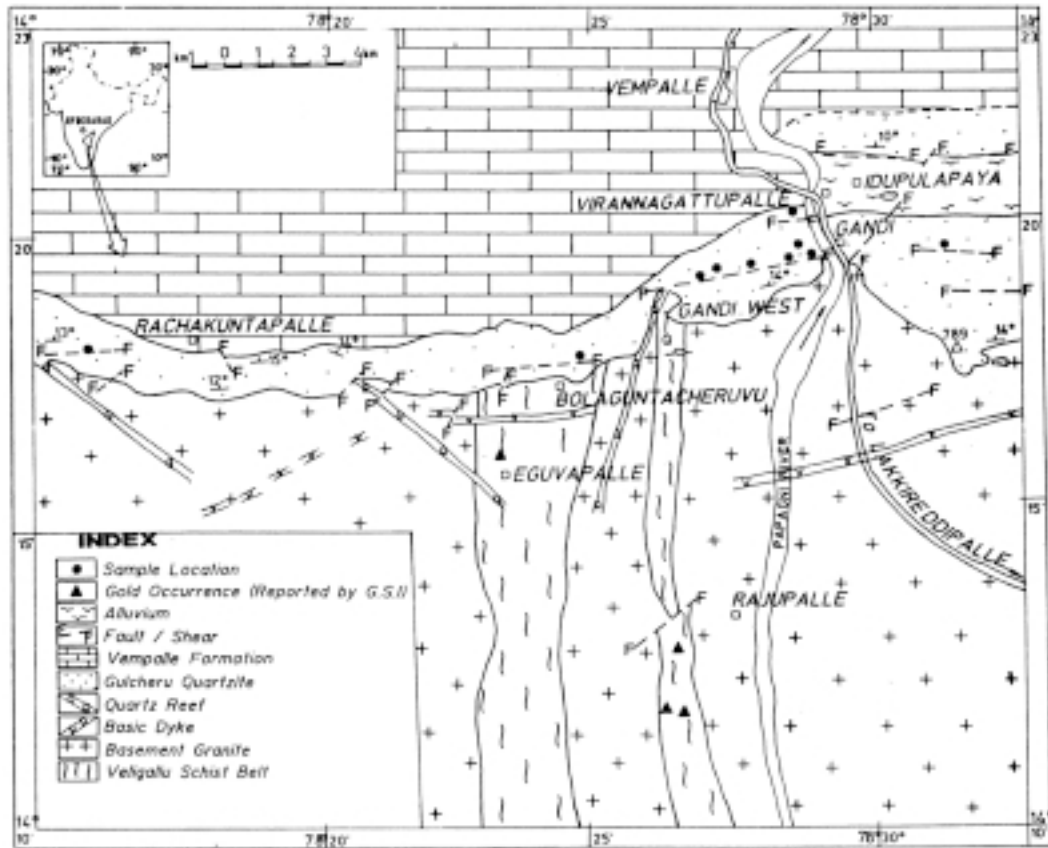


Fig. 4. Geological map of the area around Gandhi, Kadapa district, Andhra Pradesh, showing the sample locations of the hydrothermal-type U-mineralization (+ Au, Ag, at palces) in the Gulcheru quartzite.

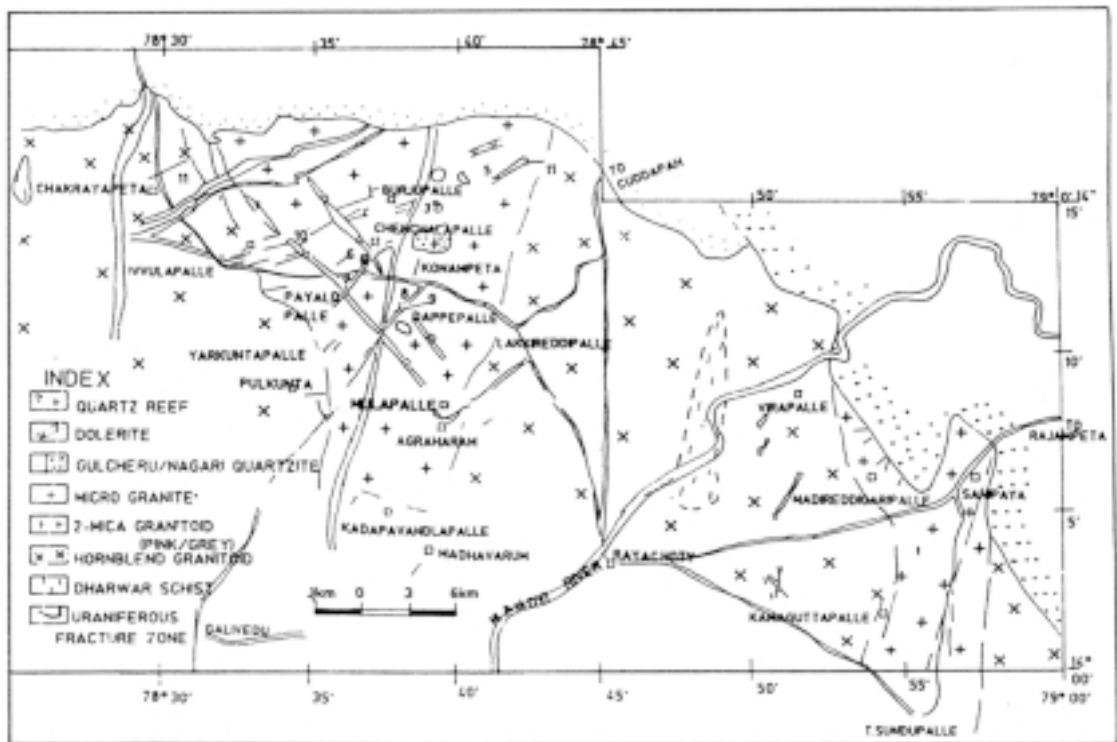


Fig. 5. Geological map of the area around Rayachoti, Kadapa district, Andhra Pradesh, showing the location of fracture-controlled U-mineralization in the deformed Granitoids.

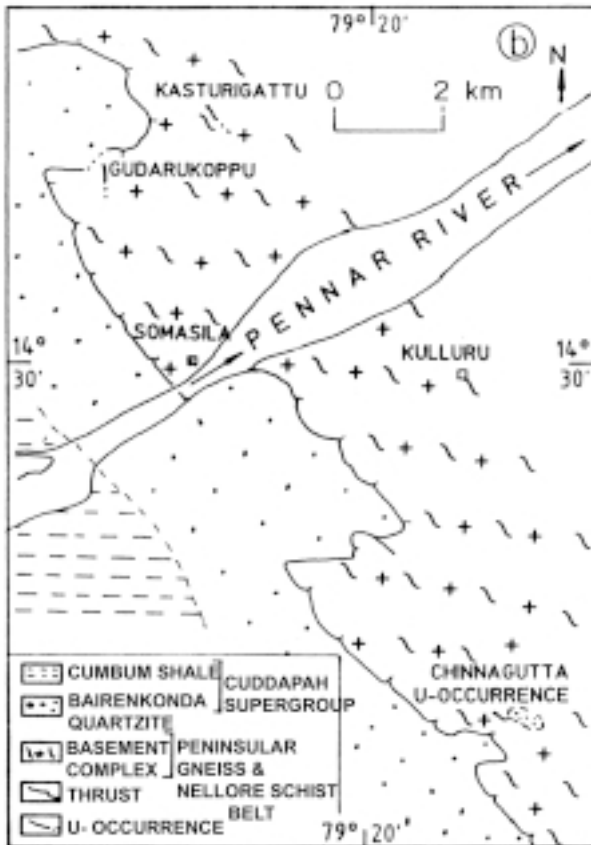


Fig. 6. Geological map of the area around Somasila, Nellore district, Andhra Pradesh, showing the location of the occurrences of shear zone-hosted U-mineralization (at Kasturigattu, Gudarukoppu and Kulluru) along the E-margin of the Cuddapah basin.

uraninite, pitchblende and coffinite; besides, a few uranyl minerals like mete-autunite, beta-uranophane and metauranocircite are recorded. The associated ore minerals include hematite, anatase, rutile, pyrite and chalcopyrite. As this fracture-controlled U-mineralization in the above-cited areas is mainly due to refractory U-Ti minerals, extraction of U requires high to very high acid consumption, viz., 90 to 180 kg/t of H_2SO_4 and 5 to 20 kg/t of MnO_2 for 70-80% leachability of U (Dhana Raju *et al.*, 2002). Therefore, this U-mineralization, though extensive, is presently cost-prohibitive for exploitation. To make it cost-effective, R & D work in mineral processing of this U-ore is required to reduce the high acid consumption, by examining other possibilities, including bacterial leaching.

Shear zone-hosted U-mineralization near Somasila along the E-margin of CB

In the area around Somasila, in close proximity to the eastern margin of CB, shear-zone hosted U-mineralization occurs at Kasturigattu, Gudarukoppu and Kulluru (Fig. 6). In this area, pre-Cuddapah basement rocks (Peninsular Gneiss and Nellore Schist belt) are

thrust over the Nallamalai Group of CB. Due to this thrust, parallel to subparallel shear zones occur close to the margin of CB. At Kasturigattu, schistose rocks occur at the base and are overlain unconformably by conglomerate, quartzite and phyllite, and the unconformity is marked by a thin band of regolith. The schists trend $N30^\circ W$ with steep (70° - 80°) dips toward NE, whereas the overlying metasedimentary rocks trend $N20^\circ W$ with 30° - 40° dips toward NE. All these formations are intensely sheared, with profuse injections of vein quartz along the shear. The granitoid in these areas was subjected to intense deformation, greenschist facies metamorphism and K-Fe-Mg-P metasomatism, resulting in schistose granite, mylonite/quartzofeldspathic schist, biotite-chlorite schist and biotite-chlorite-apatite schist. These rocks along the shear zones constitute the loci for structurally-controlled U-mineralization in these areas. Thus, U-mineralization at Kasturigattu occurs in the $N30^\circ E$ – $S30^\circ W$ -trending shear zone having a length of 1250 m, with the radioactive zone having a length 300 m and width of 1-5 m. At Gudarukoppu, the 750-m long shear zone trends in N-S, with radioactive zone having a length of 400 m and width of 1.5 to 8 m. At Kulluru, the 500-m long shear zone has a radioactive zone of 70 m length and 1-2 m width. These U-mineralized shear zones are occupied by schistose rocks containing biotite, chlorite, quartz, feldspar and apatite (the last mainly in the Gudarukoppu and Kulluru areas). In these, the radioactivity is of the order of 0.01 to 0.19% eU_3O_8 , with little Th and 10-35% disequilibrium in favour of parent U. This U-mineralization differs from that in the SW environs of CB around Rayachoti (see above) in aspects like shear-controlled against fracture-controlled, host rock being a schist, higher grade metamorphism (epidote amphibolite facies) and K-Fe-Mg-P metasomatic activity, manifested as biotitization and apatitization, and appreciable sulphides (pyrite, chalcopyrite, bornite, galena and pyrrhotite) as associated ore minerals. The U-minerals recorded are uraninite and pitchblende in the Kasturigattu area, uraninite, U-Ti complex and U with apatite in the Gudarukoppu area, and autunite and U with apatite in the Kulluru area. Besides, at Kasturigattu a high-temperature syn-magmatic U-mineralization in the form of inclusions of euhedral uraninite in gangue is recorded (Veerabhaskar *et al.*, 1991; Rai *et al.*, 1995). In these areas, very little drilling was carried out in the past. It is, therefore, necessary that an in-depth exploration, including extensive drilling, should be undertaken in these areas to examine the possibility of locating a deposit, especially at Kasturigattu, where the U-minerals are easily leachable, for cost-effective exploitation.

CONCLUSIONS

The Mesoproterozoic Cuddapah Basin (CB) in southern Andhra Pradesh, which hosts many metallic and non-metallic mineral resources that are exploited

since long, is emerging as the U-hub of India, due to establishment by AMD of diverse types of U-deposits/prospects. These occur mainly along the SW, NE, S, W and E margins/environs of CB. The deposits are: (i) large-tonnage (>30,000 te U₃O₈) and low-grade (~0.045% U₃O₈), stratabound, syn- and dia-genetic impure dolostone-hosted deposit in the Tummalapalle – Giddankipalle area (Papagghi sub-basin), near Pulivendla in the Kadapa district, along the SW margin; (ii) medium-tonnage (~15,000 te U₃O₈) and low-grade (~0.07% U₃O₈) unconformity-proximal type deposits, hosted mostly by basement granitoid and minor by overlying Srisailem/Banganapalle quartzite, as at Lambapur, Peddagattu and Chitrial (Srisailem sub-basin) in the Nalgonda district and Koppurnuru (Pakhal sub-basin) in the Guntur district. AMD is exploring in the contiguous areas of these deposits to add further resources. The promising U-prospects include: (i) hydrothermal-type mineralization in the Gandhi and

Giddankipalle areas in the Kadapa district; (ii) fracture-controlled mineralization around Rayachoti in the Kadapa district; and (iii) shear-zone hosted mineralization in the Somasila area in the Nellore district, along the E-margin of CB.

Acknowledgements: The author profusely thanks his former colleagues in the Atomic Minerals Directorate (AMD) for Exploration and Research, Dept. of Atomic Energy, for their support and encouragement during his service in AMD from April 1973 to December 2002. He also thanks Prof. D. Rajasekhara Reddy, Convener of the National Seminar on 'Deltas and Other Sedimentary Basins: Their Resource Potential' and XXVI Convention of the Indian Association of Sedimentologists, held during Dec. 16-18, 2009 at the Delta Institute, Andhra University, Visakhapatnam, for inviting him to present this paper. Reviewer of the Journal is sincerely thanked for his critical review of the manuscript.

References

- A.M.D. Newsletter (2009). A.M.D., D.A.E., Hyderabad, 16 (1), April 7.
- Biswal, D. (2005). Prospect of uranium mining in Andhra Pradesh. Souvenir Symp. on 'Technology Upgradation in Geology & Mining', Oct. 2-3, Mining Engineers' Assoc., India, Hyderabad Chapter, 239.
- Dahlkamp, F.J. (1993) Uranium ore deposits. *Springer-Verlag, Berlin*, 1-460.
- Dhana Rju, R. (2009). 'Value-addition' and 'Creation of wealth from waste' in mineral exploration/exploitation: Examples from uranium, mineral-sand and dimensional-stone industries. *In: Exploration Geology and Geoinformatics* (Eds. S. Anbazhagan, R. Venkatachalapathy and R. Neelakantan), Macmillan Publishers India Ltd., Delhi, 5-17.
- Dhana Raju, R., Roy, Minati, Roy, Madhuparna and Vasudeva, S.G. (1993). Uranium mineralisation in the south-western part of the Cuddapah Basin: A petromineralogical and geochemical study. *Jour. Geol. Soc. India*, 42, 135-149.
- Dhana Raju, R., Umamaheswar, K., Tripathi, B.K., Rai, A.K., Zakaulla, S., Thirupathi, P.V. and Nanda, L.K. (2002). Structurally-controlled and crystalline rock-hosted uranium mineralization in the southern environs of Cuddapah basin, Andhra Pradesh, India. *Expl. Res. At. Miner.*, 14, 95-108.
- Dutt, N.V.B.S. (1986). Geology and Mineral Resources of Andhra Pradesh. 3rd Ed. Natural Resources Development Co-op. Society (NRDC), Hyderabad, 1-434.
- Geological Survey of India (1975). Geology and Mineral Resources of Andhra Pradesh. Misc. Publ. No. 30, Pt. 8 – Andhra Pradesh, 1-51.
- Gupta, R. (2007). New uranium mining centers in Andhra Pradesh: A perspective. INSAC-2007, Nov. 21-24, Nuclear Fuel Complex, Hyderabad, Abstract, I-2.
- Jeyagopal, A.V. and Dhana Raju, R. (1998). Recognition criteria and sedimentology of the dolostone-hosted stratabound uranium mineralization in Vempalle formation, Cuddapah basin, Andhra Pradesh, India. *In: Recent Researches in Sedimentary basins*. (Ed. R.N. Tiwari), Proc. Nat. Symp., Indian Petroleum Publishers, Dehra Dun, 172-179.
- Jeyagopal, A.V., Kumar, Prakhar and Sinha, R.M. (1996). Uranium mineralization in the Palnad sub-basin, Cuddapah basin, Andhra Pradesh, India. *Curr. Sci.*, 71, 957-959.
- Jeyagopal, A.V., Deshpande, M.S.M., Gupta, S, Ramesh Babu, P.V., Umamaheswar, K. and Maithani, P.B. (2009). Uranium mineralization and association of carbonaceous matter in Koppunuru area, Palnadu sub-basin, Cuddapah basin, Andhra Pradesh. Natl. Symp. on 'Advances in Atomic Mineral Science in India during the 50 year period : 1959-2009', Aug. 26-28, A.M.D., Hyderabad, Abstract, 92-93.
- Joshi, G.B., Vasudeva Rao, M. and Satyanarayana, N. (1998). Gold content in uraniferous Mesoproterozoic dolostone of Tummalapalle, Cuddapah basin, Andhra Pradesh, India. *Jour. At. Miner. Sci.*, 6, 135-138.
- Kurien, T.K. (1980). Geology and Mineral Resources of Andhra Pradesh. Bull. Geol. Surv. India, Series A, Econ. Geol., No. 44, 1-242.
- Majumdar, A., Shrivastava, V.K., Agarwal, M., Banerjee, D.C. and Kaul, R. (1991). Uranium mineralization in the northern parts of Papagghi sub-basin of

- Cuddapah Supergroup, Andhra Pradesh, India, *Expl. Res. At. Miner.*, 4, 39-47.
- Mukundan, A.R., Saravanan, R., Reddy, S.V.S., Chavan, S.J. and Ramesh Babu, P.V. (2009). Geochemical characteristics of the mineralized granites of Peddagattu uranium deposit, Nalgonda district, Andhra Pradesh. Natl. Symp. on 'Advances in Atomic Mineral Science in India during the 50 year period : 1959-2009', Aug. 26-28, A.M.D., Hyderabad, Abstract, 8.
- Nagaraja Rao, B.K., Rajurkar, S.T., Ramalingaswamy, G. and Ravindra Babu, B. (1987). Stratigraphy, structure and evolution of the Cuddapah basin. *Geol. Soc. India. Mem.* 6, 33-86.
- Pandey, B.K., Prasad, R.N., Sastry, D.V.L.N., Kumar, B.R.M., Suryanarayana Rao, S. and Gupta, J.N. (1988). Rb-Sr whole rock ages for the granites from parts of Andhra Pradesh and Karnataka. In: 4th National Symposium on 'Mass Spectrometry' (Preprint vol.), Indian Institute of Science, Bangalore, EPS-3/1-5.
- Rai, A.K., Sharma, S.K., Umamaheswar, K., Nagabhushana, J.C. and Vasudeva Rao, M. (1995). Uranium mineralization in the eastern margin of Cuddapah basin. Abst. Vol., Geol. Soc. India Ann. Conv. and Seminar on 'Cuddapah basin', Tirupati '95, Sept. 9-12.
- Ramam, P.K. (1999). Mineral Resources of Andhra Pradesh. Economic Geology Series, Geol. Soc. India, 1-253.
- Roy, Minati and Dhana Raju, R. (1997). Petrology and depositional environment of the U-mineralised Phosphatic Siliceous Dolostone of Vempalle Formation in the Cuddapah basin, India. *Jour. Geol. Soc. India*, 50, 577-585.
- Roy, Minati and Dhana Raju, R. (1999). Mineragraphy and electron microprobe study of the U-phases and pyrite of the dolostone-hosted uranium deposit at Tummalapalle, Cuddapah district, Andhra Pradesh and its implication on genesis and exploitation. *Jour. Appl. Geochem.*, 1, 53-75.
- Sinha, R.M., Shrivastava, S.K., Sarma, G.V.G. and Parthasarathy, T.N. (1995). Geological favourability for unconformity related uranium deposits in northern parts of the Cuddapah Basin: Evidence from Lambapur uranium occurrence, Andhra Pradesh, India. *Expl. Res. At. Miner.*, 8, 111-126.
- Sundaram, S.M., Sinha, P.A., Ravindra Babu, B. and Muthu, V.T. (1989). Uranium mineralization in Vempalli Dolomite and Pulivendla conglomerate/quartzite of Cuddapah basin, A.P. *Indian Minerals*, 43 (2), 98-103.
- Umamaheswar, K., Basu, H., Patnaik, J.K., Ali, M.A. and Banerjee, D.C. (2001a). Uranium mineralization in the Mesoproterozoic quartzite of Cuddapah basin in Gandhi area, Cuddapah district, Andhra Pradesh : A new exploration target for uranium. *Jour. Geol. Soc. India*, 57 (5), 405-409.
- Umamaheswar, K., Sharma, U.P., Zakaulla, S., Basu, H., Thomas, A.M. and Ali, M.A. (2001b). Occurrence of gold in association with uranium in Gulcheru quartzite of Cuddapah basin, Gandhi—Rachakuntapalle area, Cuddapah district, Andhra Pradesh. *Curr. Sci.*, 81 (7), 754-756.
- Vasudeva Rao, M., Nagabhushana, J.C. and Jeyagopal, A.V. (1989). Uranium mineralization in the Middle Proterozoic carbonate rock of the Cuddapah Supergroup, Southern Peninsular India. *Expl. Res. At. Miner.*, 2, 29-38.
- Veerabhaskar, D., Sarkar, M., Thimmaiah, M., Sharma, M. and Dhana Raju, R. (1991). Uranium mineralization at Kasturigattua, Nellore district, A.P., India: An example of shear-controlled syngenetic remobilized type in the Proterozoic granitic and low grade metamorphic rocks. *Expl. Res. At. Miner.*, 4, 27-37.
- Verma, M.B., Gupta, S., Singh, R.V., Latha, A., Maithani, P.B. and Chaki, A. (2009). Ore body characterisation of Koppunuru uranium deposit in Palnadu sub-basin, Guntur district, Andhra Pradesh. Natl. Symp. on 'Advances in Atomic Mineral Science in India during the 50 year period : 1959-2009', Aug. 26-28, A.M.D., Hyderabad, Abstract, 51-52.
- Verma, M.B., Som, A., Latha, A., Umamaheswar, K. and Maithani, P.B. (2008). Geochemistry of host granitoids of uranium deposit at Chitrial area, Srisailem Sub-basin, Nalgonda district, Andhra Pradesh. In: Golden Jubilee Volume – Contributions to Geochemistry, (Eds. A. Chaki and K. Shivakumar), *Geol. Soc. India Mem.* 73, 37-54.

Occurrence of Foraminifera and Pteropods Assemblages in Ganga Pro-Deltaic area of the Continental Shelf Region off West Bengal

D.BHATTACHARJEE

OPEC-II, Marine Wing, GSI, Samudrika, Visakhapatnam-530018

E mail: debajyoti1955@yahoo.com

Abstract: The Ganga delta is an important tide dominated delta located in the southern part of West Bengal with several distributaries, channels and creeks. Good number of foraminifera with some pteropods, gastropods and bivalves occur in the prodeltaic region of continental shelf and they act as proxy indicator of the environment, in the northern parts of Bay of Bengal. Occurrence of the foraminiferal assemblages in the surface seabed sediments of 735 sq. km area between 14 m and 85 m isobaths indicates the presence of three benthic foraminiferal biofacies (Ammonia-Quinqueloculina, Ammonia- Astrorotalia and Astrorotalia- Nonion) in the continental shelf region. The sediment column of two gravity cores of 2.08 m and 2.17 m length has been divided into three subdivisions on the basis of the quantitative analysis of the benthic foraminiferal assemblage in this region. The lower part of the sediment column extends from bottom to 1.55 m b.s.f(average), the middle part from 1.55 m to 1.0 m b.s.f and the upper part from 1.00 m b.s.f to the top of the gravity core.

The faunal assemblage of the sediment column indicates a change in the depositional environment of the above sediment subdivisions. The upper and lower parts of the sub zones reveal the deposition in the near shore while the middle subzone in the inner shelf environment respectively. Higher abundance of planktonic foraminifera and pteropods in the middle subzone reveal an acme faunal zone and further suggests a transgressive phase of the Holocene time.

Keywords: Foraminifera, Pteropods, Ganga Pro-Deltaic area.

INTRODUCTION

The Ganga prodeltaic region collects a huge sediment flux (440.10 tone/ year, Milliman *et al.*1989) from Ganga River and subsequently contributes for the evolution of the subaqueous delta. The continental shelf region of Bengal covers a large area (about 18000 sq. km) with an average shelf width of 100 km and length of 180 km in the northern part of Bay of Bengal. The huge load of sediments and fresh water discharge from the Ganga-Brahmaputra River system continuously modify the subaqueous geological set up and ecological parameters of this fluvio- marine environment. The modern delta of this region grades into more extensive subaqueous delta and grows rapidly with the development of prograding depositional sequences (Lindsay *et al.*1991). The significance of foraminifera and associated biogenic components in the seabed sediments, from the proximal region of delta and prodeltaic region, indicated the usefulness for better understanding the Quaternary environment since last few decades. A good amount of work has been carried out on the modern delta in the onshore region of the east coast of India but data available from the offshore region is limited (Nageswar Rao *et al.*2003). The area is subjected to intense littoral current, wide variation of salinity, temperature, nutrient and suspended particles which influences the biological regime as well as

foraminiferal assemblages. River discharges affects the water chemistry, oceanographic factors and influences the local habitats which in turns affects the characteristic epifaunal and infaunal assemblages of microorganisms. The occurrence of foraminiferal and pteropod assemblages in the prodeltaic region reveals important ecological set up of the region and depositional history of sediment sequences. It is important to note that this type of environmental study is useful to understand the sea level changes with the help of faunal record.

Seabed survey is being systematically carried out by the Operation East Coast-I, Marine Wing, Geological Survey Of India (GSI) in the Territorial water off West Bengal and Orissa for the preparation of geological map of the ocean floor sediments in the Bay of Bengal for the last twenty five years with the help of its research vessels (*R.V. Samudra Manthan* and *R.V.Samudra Kaustubh*). Good amount of foraminifera, radiolarian, ostracods, pteropods, gastropods, bivalves, bryozoans, coral fragments occurs in the seabed sediments of this area. Microorganisms play a significant role to understand the depositional history and evolution of the prodeltaic domain during the late Quaternary time.

PREVIOUS WORK

The benthic foraminifera are always used as an important environmental proxy in Bengal Basin. Bhalla

(1968) studied the recent foraminifera from beach sands of Puri. Cullen (1981) examined the effect of changing salinity on microorganism in the Bay of Bengal. Foraminiferal presence in the seabed sediments had been used as a tool for examining sea level fluctuations (Banerjee & Sen, 1987). Banerjee and Sengupta (1992) reported the presence of relict sediments in the inner shelf region and considered it as one of the principal criteria for delineation of low sea stand of the sea in this region. The occurrence of benthic foraminifera at different isobaths and sediment textures has been discussed in the light of similar studies by earlier researchers (Corliss, 1983, Naidu, 1992 & 2005 and Scott *et al.* 2001). Majumdar *et al.* (1999) studied the ecological conditions of benthic foraminifera from the near shore to inner shelf region of the Digha coast. Mallick *et al.* (2002) examined the foraminiferal and sedimentological aspects of the Ganga delta between Krishananagar and Sagar Island in West Bengal and interpreted their environmental significance. Bhattacharjee (2002, 2007 and 2009) examined the depth diagnostic benthic foraminiferal taxa from the continental shelf, slope and abyssal plain in the Bay of Bengal and compared them with the adjoining basin within the Exclusive Economic Zone (EEZ) of India for environmental interpretation.

The present work discusses mainly on the foraminiferal assemblages with some brief account of pteropod taxa in the ocean floor sediments collected during the GSI cruise ST:182 of the FSP: 2006-07 from the Ganga prodeltaic region off West Bengal. The author has endeavored to present the difference of depositional environment in the sediment column and the distribution pattern of benthic taxa and textural analysis in the surface and subsurface seabed sediments on the strength of eighty eight seabed samples.

MATERIALS AND METHODOLOGY

Seabed sampling was carried out in the continental shelf region, within an area of 735 sq km, lying between the latitudes 20° 40' N and 21° 00' N and longitudes from 87° 57' E to 88° 14' E, NHO Chart No.351 (Fig.1, Location map). Sixty three seabed samples were collected with the help of Van Veen type of medium grab and gravity core samplers, between 14 m and 85 m water depths at 4 km x 4 km (approximately) grid interval (Fig.2, Sample location map) during the month of November, 2006. Sixty three surface seabed samples and twenty five subsurface samples of the two gravity cores were selectively subjected for micropalaeontological studies. About 10

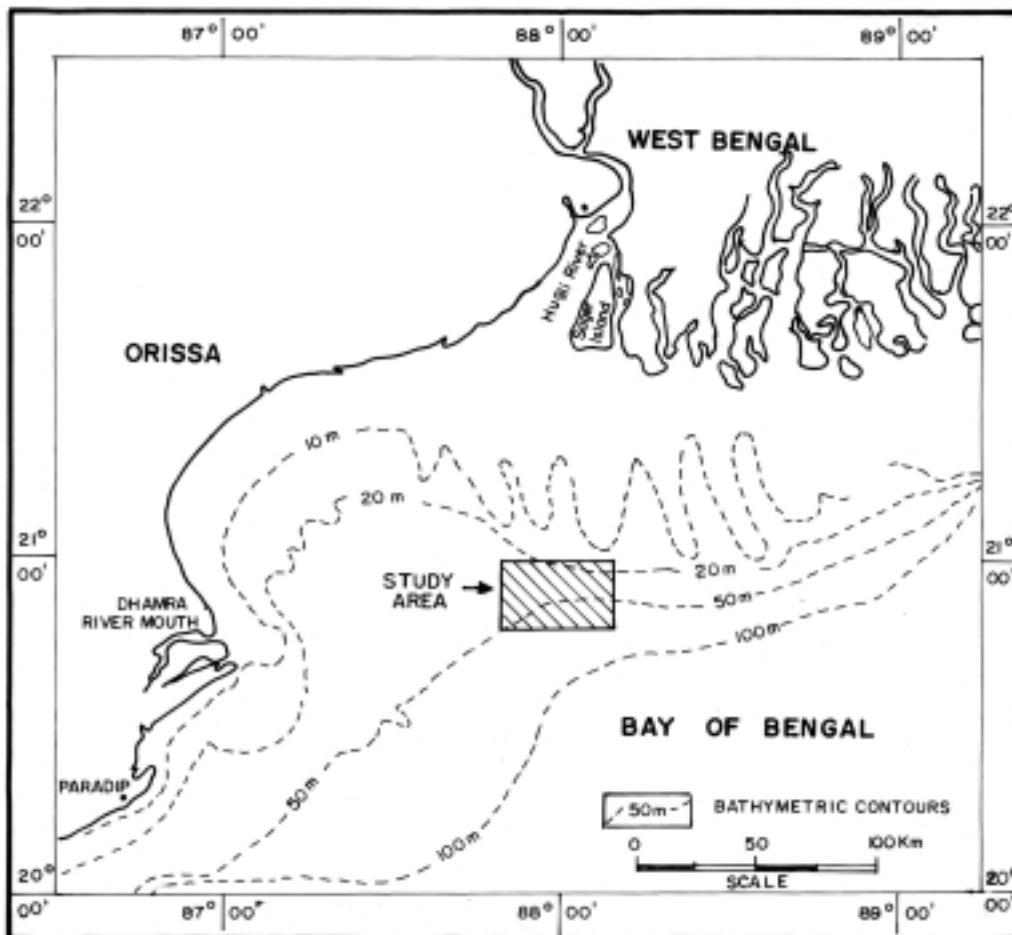


Fig.1. Location map of the working area.

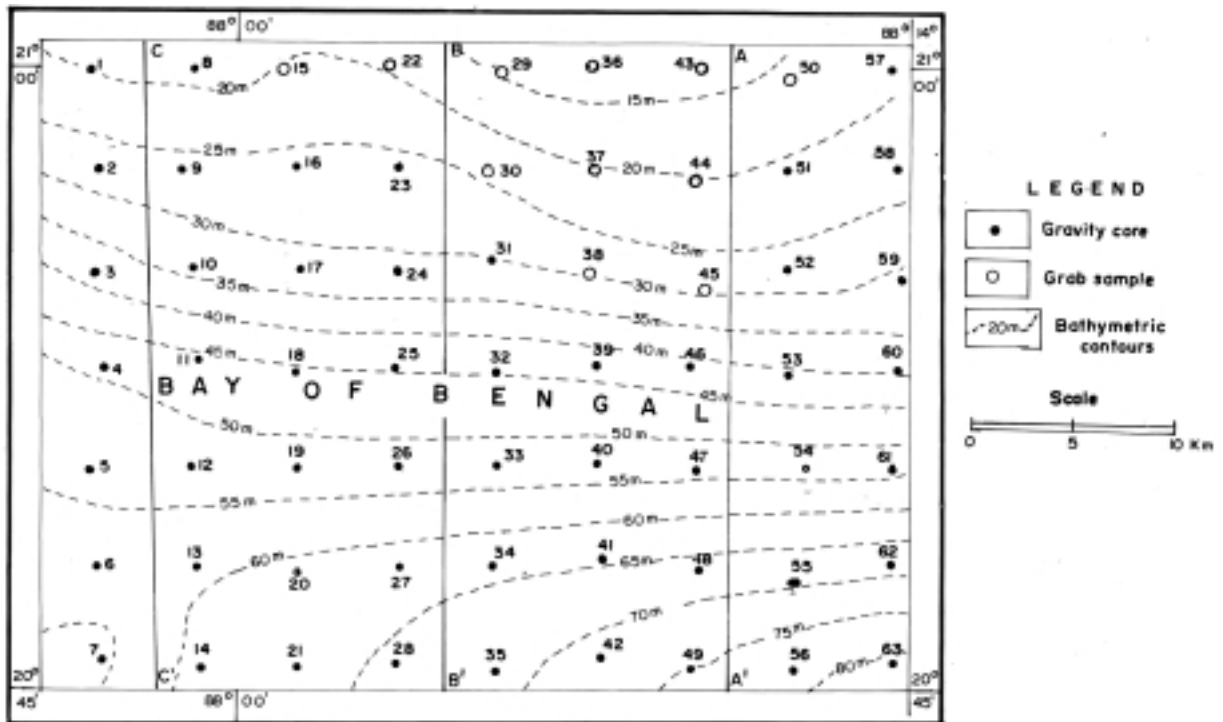


Fig.2. Sample location and bathymetric map of working area in the Bay of Bengal.

gram representative seabed sediment was selected from the bulk sample by coning and quartering with the help of an autosplitter. The sea bed sediments are air dried and treated with 30% H_2O_2 to remove the organic materials for size analysis. The coarser fractions (sand) are separated with the help of running water over a 63 micron sieve. Pipetting is then carried out to obtain the percentage of silt and clay in the sediments. Different sediment types are classified on the basis of sand, silt and clay percentage as per Shepard's (1954) classification and sea bed sediment distribution was prepared on the basis of size analysis data. The gravity cores collected during the cruise were split into two halves and one half was generally sampled from 20 to 30 cm interval, as per lithological variation of the sediment column, with each sub sample length being 5 cm. Some cores were sampled at lesser interval (20 cm) following the variation in sediment texture in the sediment sequence. Sediment columns were megascopically logged and down core variation of different parameters are recorded with the description of colour, composition, compactness and relative proportion of biogenic and terrigenous constituents.

Seabed samples are systematically processed following standard method of Boltovskoy and Wright, 1976 for systematic palaeontological studies. The weight percentage of the coarser fraction, Terrigenous (T): Biogenic (B) ratio, nonagglutinated (NA): agglutinated (A) and Benthonic (B): Planktonic (P) ratio of the sediments has been calculated (Table.1). The percentage

of different microorganisms (planktonic and benthic foraminifera, microgastropods, bivalves, pteropods, ostracode and bryozoa) was noted in order to their decreasing abundance. Foraminiferal specimens were thoroughly picked up from suitable aliquot of the processed samples with the help of stereoscopic binocular microscope. The classification by Leoblich and Tappan (1988) and Eliss and Messina (1968) work was followed for foraminifera in most of the generic level identification. A total of about 9000 specimens of foraminifera were hand picked and mounted them on micropalaeontological trays for taxonomic identification and quantitative analysis from 88 seabed samples. 48 benthic foraminiferal taxa, 14 planktonic taxa and eleven pteropod taxa were identified from the total faunal assemblage. Specific level identification is done as per Kennett and Srinivasan (1976), Barker (1960), Ingle *et al.*(1980), Bolli *et al.*(1987) and Gupta (1994). Their ecological significance was discussed with respect to Holocene environmental set up as per the earlier work of Scott *et al.*(2001) and Fiorini (2004). The number of benthic specimens and their percentage in three major suborders (Rotaliina-Miliolina-Textulariina) was calculated (Table 2, 3 & 4) and their relative abundance was plotted in the triangular diagram as per the procedure followed by Murry (1991 72003) and Armstrong & Brazier (2005). Diversity index of benthic foraminifera in different seabed samples was determined as per the number of various species divided by the logarithm of the number of total specimens in each and every sample (Margaef, 1967). Taxonomic work of Be and Gilmer (1977) has been

gradient is 1: 450 from 20 to 32 m, 1: 350 from 32 to 48 m and 1: 440 from 48 to 66 m isobaths respectively. The overall profiles reveal a very gentle slope towards the south.

SEDIMENT DISTRIBUTION

Four sediment types are observed on the basis of their megascopic and textural characteristics in the surface seabed of the survey area. They are silty sand, sandy silt, clayey silt and silt. The sediments blanketing the seafloor are mainly made up of silt (50 to 55%). The rest three types viz. sandy silt, clayey silt and silty sand contributes for 18%, 17% and 10% approximately. The seabed sediment reveals that northern side of the seafloor is generally covered by silty sand and sandy silt but the southern side by silt (Fig. 3). The seafloor is covered by yellowish brown to pale brown silty sand in the shallower region between 15 m and 22 m isobaths as elongated patch. The silty sand sediment grades into sandy silt and silt towards the deeper part of the sea. Sandy silt and clayey silt occur as elongated patches in between 22 m and 50 m isobaths. These two units are nearly parallel alignment with the coast (Fig. 3). Surface sediments are generally slushy in nature but clayey silt to sticky clay layers is present with varying degree of compactness at different places.

The terrigenous to biogenic ratio of these sediments varies between 25:1 and 15:1 which is characteristic of the prodeltaic sediments. The terrigenous materials are made of quartz, feldspar and mica with some amount of

pyroxene, amphibole and opaque minerals. The proportion of quartz and mica varies from place to place. Muscovite and biotite are two important varieties of mica in this region. The accessory black minerals are generally made of ilmenite, magnetite, tourmaline, hornblende, pyroxene, garnet and zircon. Carbonaceous materials occur as small patches and thin layers in the southern side of area, especially in the clayey silt. The biogenic materials of the coarser fraction(>63 micron) are mainly comprise of benthic and planktonic foraminifera with some amount of pteropods, gastropods, bivalve, ostracods, bryozoa fragments, echinoid spines as well as a few crinoids stems, worm tubes, fish otolith, burrows and coral fragments in their decreasing abundance. It is observed that the biogenic component gradually increases with depth.

Size analysis result of twenty five subsurface samples of two gravity cores (GC:31 and GC:52) along with the total foraminiferal number from top to bottom of the sediment column has been presented in Tables 3 and 4 for textural analysis of sediment columns. Lithologically, both the gravity cores are mainly made up of clayey silt to silty sediments with a few thin layers of silty sand at places. Upper part (top to 1.55 m b.s.f level) of the gravity core GC: 31 are made of clayey silt but the lower part of the same core samples represent silt. In gravity core GC: 52, the upper part (top to 0.95 m b.s.f level) is made up of clayey silt, middle part (from 0.95 to 1.54 m b.s.f level) is comprised of silt while lower portion (1.54 to 2.17 m b.s.f level) is consists of clayey silt. It is observed that foraminiferal number is more in

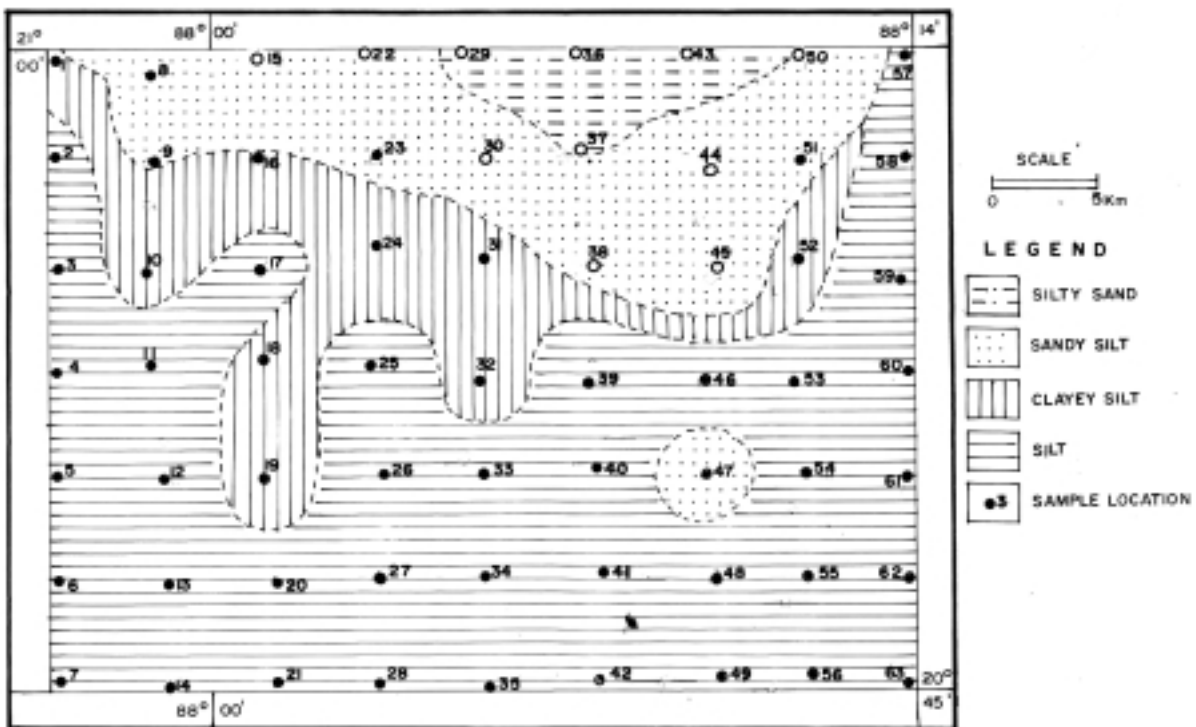


Fig.3. Surface sediment distribution map off Ganga prodeltaic region, Bay of Bengal.

the silt in different subsurface levels of the gravity cores.

MICROPALAEONTOLOGICAL OBSERVATION

The present study was mainly based on the examination of the coarser fraction of the bulk samples. Weight% of the fraction of the sediment varies between 65% and 3%. This value increases from south to north direction. The coarser fraction is made up of biogenic and terrigenous materials and the distribution pattern of these two components varies widely in the survey area.

Foraminifera

The processed samples with good amount of foraminifera were split with an Otto micro-splitter in order to obtain a suitable aliquot that contains about 200 to 250 specimens. All the specimens were hand picked and kept in separate assemblage trays for their identification up to the generic and species level as far as possible. The benthic foraminifera contain 50 to 60% of the total biota present in the seabed sediments. Important benthic foraminiferal species of the study area are *Ammonia beccarii*, *A. gaimerdii*, *A. tepida*, *Astrorotalia trispinosa*, *Elphidium articulatum*, *E. crispum*, *E. magellanicum*, *Trochammina inflata*, *T. compacta*, *T. irregularis*, *Ammobaculites exiguus*, *Textularia earlandi*, *T. agglutinans*, *T. saggitula*, *Bolivina spathulata*, *Haplophrogmoides sp.*, *Miliammina fusca*, *Protoelphidium anglicum*, *Discorbis*

rosacea, *D. chasteri*, *Rosalina floridana*, *Nonion scaphum*, *N. asterizans*, *N. boueanum*, *Noniondes auricularis*, *Quinqueloculina venusta*, *Q. seminulum*, *Spiroloquolina communis* and *Pseudononion atlanticum*. Faunal assemblage reveals a clear cut dominance of the suborder Rotaliina over suborder Miliolina and Textulariina and they prefer clayey silt and silty bottom sediments.

Foraminiferal biofacies

Distribution pattern of dominant benthic taxa in seabed sediments and their relation to the bottom texture and water depth is shown in Table 1. The benthic assemblage is dominated by five families (Rotaliidae, Boliviniidae, Elphidiidae, Haurinidae and Nonionidae) followed by another five important families (Buliminidae, Bagginiidae, Spiroloculinidae, Textulariniidae and Cassidulinidae). Besides these other seven families (Calcarinidae, Cibicides, Eponoidae, Harmosonidae, Trochomonidae, Buliminellidae and Vagnulinidae) are commonly observed.

The foraminiferal biofacies has been prepared after the method adopted by Walton (1964), Patterson and Cameroon (1991) as well as Patterson (1993). Utilising this distribution pattern of total benthic taxa, three foraminiferal biofacies (*Ammonia-Quinqueloculina*, *Ammonia-Astrorotalia* and *Nonion-Astrorotalia*) are delineated in the surface seabed sediments for this area (Fig. 4). The number of benthic specimens and their percentage in three major suborders (Rotalina – Textularina- Miliolina) was calculated (Table: 2) and their

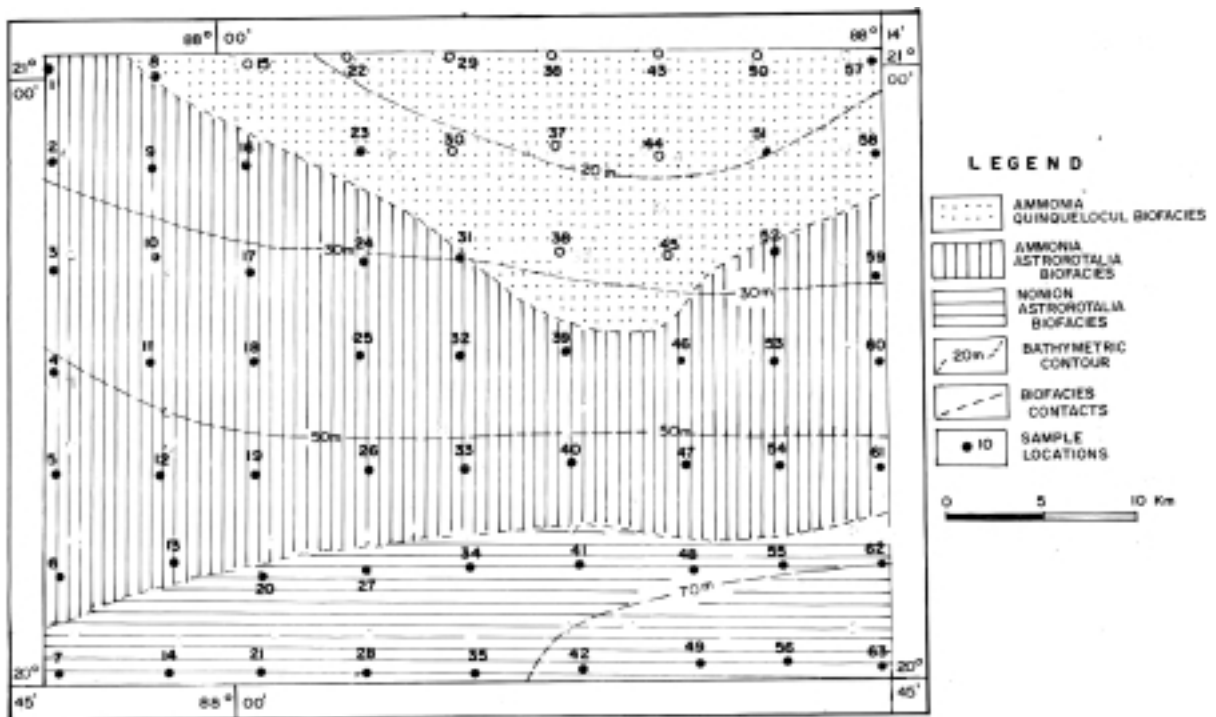


Fig.4. Foraminiferal biofacies map off Ganga prodeltaic region, Bay of Bengal.

percentage was plotted in the triangular diagram Fig: 5 for environmental interpretation. A brief description of the biofacies is given below.

Ammonia- Quinqueloculina biofacies

Ammonia- Quinqueloculina biofacies occurs in the northern part of the area as a East-West trending elongated patch within the water depths of 18 m to 36 m. Bottom sediments of this unit is sandy silt and silty sand. *Ammonia beccardii* and *Quinqueloculina sp.* are the dominant taxa of this facies and their total percentage varies from 48 to 64 of the total foraminiferal population. Other important taxa of this unit are *Ammonia tepida*, *A. gaimerda*, *Quinqueloculina parkari*, *Q. reticulata*, *Q. lamarkana*, *Q. seminulum*, *Trochommia inflata*, *Cibicides lobatulus*, *E. crispum*, *Eponoides rependus*, *T. agglutinans*, *M. subrotunda*, *Triloculina trigonula*, *Pseudorotalia sp.*. Benthic (B): Planktonic (P) ratio varies between 10:1 and 15:1 while the Non-agglutinated (NA): agglutinated ratio ranging from 8:1 to 10:1 respectively. Diversity index of benthic foraminifera is low (3.3 to 5.4) and Total foraminiferal number (TFN) per gram of sample varies from 5 to 8.

Ammonia-Astrorotalia biofacies:

Ammonia-Astrorotalia biofacies occurs in the central part of the area between 40 m and 55 m water depth as an elongated strip (Fig.4). Bottom sediments of this facies are mainly made of silt and clayey silt. *Astrorotalia trispinosa* and *Ammonia beccardii* is the major constituent (60 to 65%) of this facies. The former taxon dominates the latter in abundance and shows

better mode of preservation. Other important taxa of this unit are *Astrorotalia dentata*, *A. inflata*, *Calcarina calcer*, *Lenticulina sp.* *Planulina sp.* *Bolivina robusta*, *Spiroloculina communis*, *Textularia saggitula*, *T. agglutinans*, *Trochommia irregularis* and *Triloculina tricarinata*. The NA: A ratio increases (10:1 to 12:1) but B: P ratio decreases (9:1 to 5:1) in this biofacies. Diversity index of benthic taxa increases (5.4 to 8.1) and TFN value changes from 8 to 13 per gram of sample.

Astrorotalia- Nonion biofacies

Nonion-Astrorotalia biofacies occurs to the southern side of the area in the deeper water (50.0 to 85.0 m) within the clayey silt to silty sediments. The dominant species of this biofacies are *Nonion asterizan* plus *N.scaphum* (28 to 34%) and *Astrorotalia trispinosa* (16 to 19%). It is important to note that the size of the *A. beccardii* is relatively small in this biofacies. Important taxa of this unit are *Bolivina robusta*, *B. alata*, *B. spathulata*, *Nonionella turgida*, *N. depressula*, *Fissurina orbigney*, *F. kerguelenus*, *Cibicides bradii*, *Lenticulina sp.* *Spiroloculina depressa*, *Sigmoilopsis suchlumbergeri*, *Eponoides rependus*, *Reophax sp.*, *Textularia sp.* Some amount of planktonic foraminifera is observed in this unit which is represented by *Globigerinoides ruber*. *Gs. immatures*, *Gs. sacculifer*, *Globorotalia menardii*, *Globigerinata sp.* *Neogloboquadrina duterteii*, *Globigerina sp.* and *Pulleniatina obliquileata*. The B: P and NA: A values ranges from 3:1 to 1:1 and 14:1 to 16:1 respectively. The assemblage mostly belongs to asymmetrical-angular morpho group. This group embodies elongated, rectilinear, cylindrical forms which are flattened, tapering

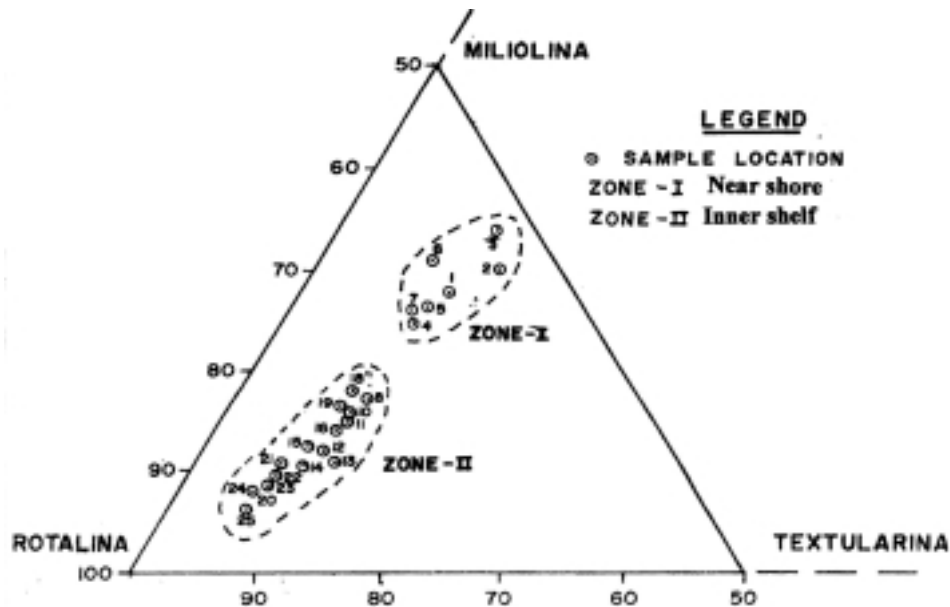


Fig.5. Grouping of surface samples shown in the triangular graph consisting Rotalina- Textularina- Miliolina suborders of Ganga prodeltaic region in the Bay of Bengal.

bluntly and appears oval to compressed aperture. These taxa generally possess less resistant shell, thin test, roughly parallel to sub parallel ornamented and show more pore surface density. Diversity index of benthic foraminifera ranges from 8.0 to 12.5 and TFN value for per gram of sample varies from 13 to 17.

Distribution of foraminifera in the sediment sequences

Twenty five subsamples from top to bottom of two gravity cores (GC:31 and 52), having a core lengths of 2.08 m and 2.17 m respectively, were systematically analysed for examining the microfaunal variation of the sediment columns. Clay constituted the 20% of the sediment while sand is considerably less having a percentage of only 5 to 10. Benthic foraminifera are the dominant member along with some amount of planktonic foraminifera, pteropods and a few ostracods. Total number of foraminifera (TNF) in 10 gram of dry sample varies from 20 to 450 as shown in the frequency diagram Table: 3 and 4.

The distribution pattern of the depth diagnostic benthic taxa from top to bottom of the two gravity core in different subsurface levels has been noted and shown in Table: 5 and Table: 6. The foraminiferal record is also illustrated by the frequency distribution curves in Fig.6 and Fig.7, for attribution of the ecological significance to various faunal assemblages at different b.s.f the ecological interpretation are also mentioned in the above diagrams. The entire sediment column of the gravity cores has been subdivided into three subdivisions on

the basis of the above foraminiferal record as *Ammonia*, *Nonion-Astrorotalia* and *Ammonia- Astrorotalia* sub zones in ascending order (Fig:6 and Fig:7). The *Ammonia* sub zone occurs in the lower part of the core from bottom to 1.75 m bsf level in GC: 31 and bottom to 1.40 m bsf level in GC:52. The dominant taxa of this sub zone are *Ammonia beccarii* and *A. tepida*. Other important members of this sub zone are *Quinqueloculina venusta*, *Q. seminulam*, *Elphidium crispum* and *psudorotalia rotandata*. The B: P ratio is high (10:1 to 15:1) due to low presence of planktonic foraminifera.

Nonion-Astrorotalia subzone occurs in the middle part of the core in between 1.75 m to 0.95 m b.s.f level in GC:31 and 1.40 m to 1.00 m b.s.f level in GC:52. The dominant taxa of the middle subzone are *Nonion asterizan*, *N. scaphum* and *Astrorotalia trispinosa*. Common taxa of this sub zone are *Bolivina spahutata*, *B. robusta*, *Bulimina marginata*, *Cibicides bradyi*, *A. beccarii* and *Quinqueloculina sp.* Some planktonic foraminifera (*Globigerina sp.*, *Globigerinata glutinata*, *Globigerinoides immatures*) are commonly present in the subzone. The B: P ratio of the foraminifera decreases (3:1 to 1:1) due to the increase of planktonic population. A few pteropods (*Limacina inflata*, *Crecesis acicula*, *C. virgula*, *Clio pyramidata*, *C. inflexa*, *Diacria quadridentata* and *Peraclise sp.*) are also noted from this unit. The faunal assemblage of this biozone indicates the inner shelf zone.

Ammonia- Astrorotalia sub zone occurs in the upper part of the gravity cores from top to 0.95 m bsf level in GC: 31 and top to 1.00 m bsf level in GC: 52

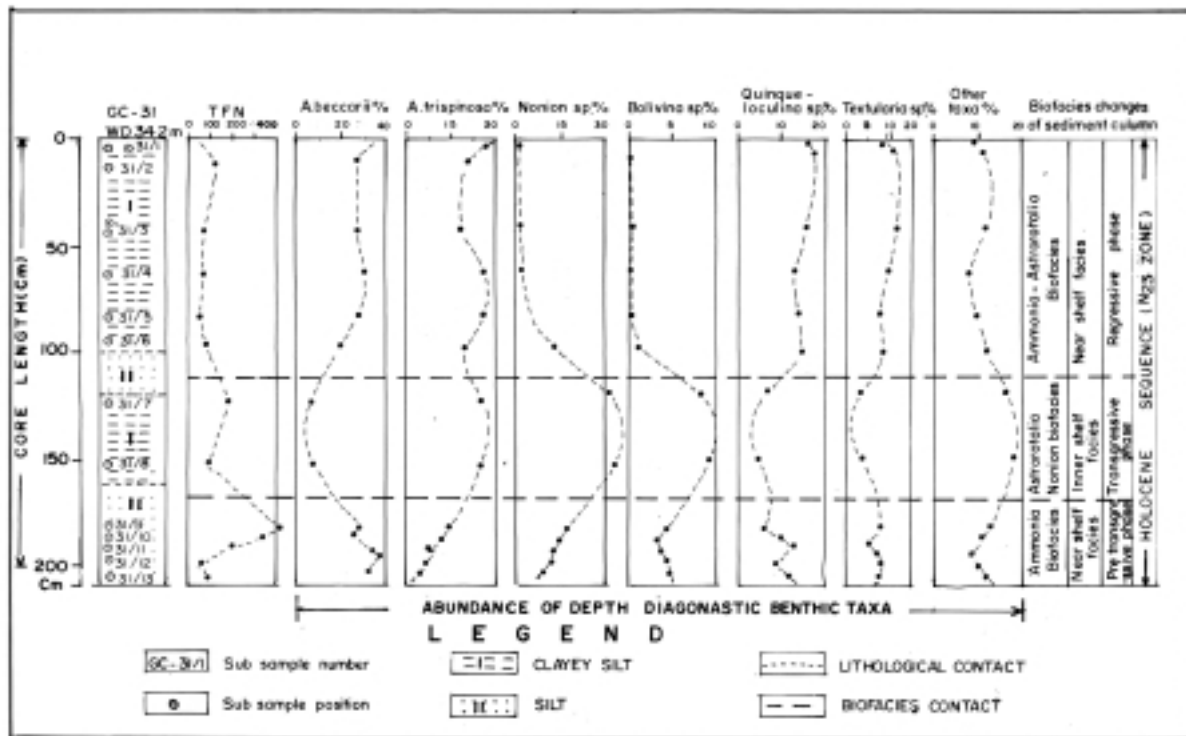


Fig.6. Frequency distribution curves of the depth diagnostic benthic taxa in the gravity core (GC: 31).

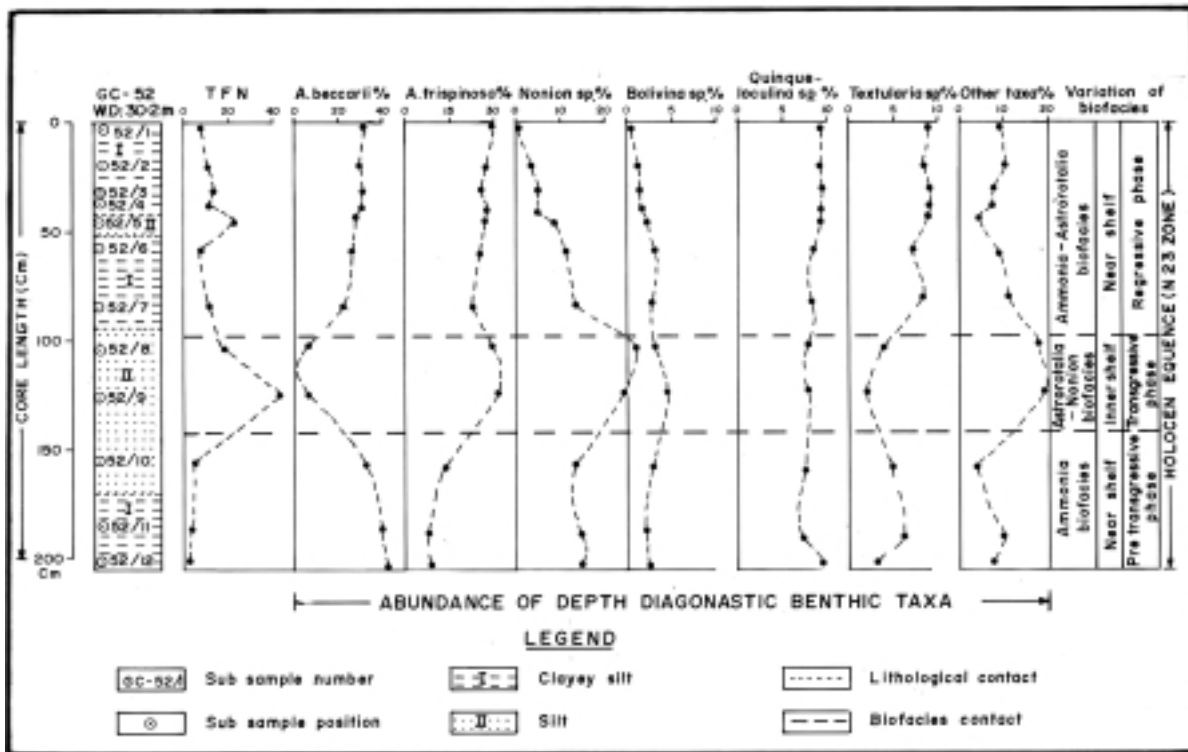


Fig.7. Frequency distribution curves of the depth diagnostic benthic taxa in the gravity core (GC: 52).

respectively. The dominant taxa of this subzone are *Ammonia beccarii*, *A. tepida* and *Astrorotalia trispinosa*. Other important species are *E. crispum*, *Q. seminulam*, *Q. lamarkana*, *Calcarina hispida*, *Bolivina spatulata* and *Textularia agglutinans*. The increase of B: P ratio (8:1 to 12:1) is observed in this subzone because of the increase of shallow water benthic epifaunal taxa. The total number of taxa of the Rotalina, Textularina and Miliolina suborders in the above three subdivisions of the two gravity cores have been calculated and their relative percentage is shown in Table: 7. The number indicated against different suborder represents their actual count from 10 gram (approximately) seabed samples and the bracketed number indicates their percentage.

The faunal assemblage of the *Nonion-Astrorotalia* subzone indicates a relatively deeper water environment of deposition with respect to its underlying and overlying sub zones. The above three subzones belong to the N23 Zone (Blow, 1979) of Holocene time. The frequency distribution of depth diagnostic benthic taxa from top to bottom of gravity cores indicates that middle part contain comparatively deeper water taxa and some planktonic foraminifera indicating a transgressive phase. This transgression could be correlated with the standard Holocene curve of Bengal basin, established by various researchers (Banerjee, 2000 & 2003; Neheluddin and Abdullah, 2003 and Islam, 2004). It is important to note that the sediment sequences of these gravity cores can be correlated with the prodeltaic sediments, off Matla

River, to the northern side of the present survey area. The above three subzones of the present area matches well with the foraminiferal record preserved in the adjoining West Bengal and Orissa coast for the late Quaternary time in the Bay of Bengal (Bhattacharjee et al, 2004, 2007 and 2008).

Pteropods

Pelagic gastropods (pteropods) are accessory biota in the study area and they are occasionally observed in the silt and clayey silt sediments within the depth range from 42m to 85m in surface sediments. Their presence is generally restricted within the certain depth due to its highly fragile (aragonite) tests. Preservation of the pteropod tests depends upon the wave action, salinity, turbidity, littoral current, suspended particles and long shore current condition of the shelf region. Bhattacharjee (2005) examined the pteropod preservation profile in the seabed sediments and its environmental significance for better understanding of the geological set up of the Holocene sequences in the Andaman Sea. The pteropod record has its importance due to its more susceptible nature than calcite skeletal remains of foraminifera for environmental analysis. Bhattacharjee (2008a) carried out environmental analysis of Quaternary sediments off Krishna- Godavary delta region in the Bay of Bengal with the help of pteropods and foraminifera. The mode of preservation of the pteropod tests in the seabed sediment is moderate to poor in this region. Mechanical

Table 5. Frequency distribution of diagnostic benthic taxa in the Gravity Core GC/31.

| S. No | Sub-sample No. | Sub sample level (m) | A. beccarii % | E. crispum % | A. trispinosa % | N. scaphum % |
|-------|----------------|----------------------|---------------|--------------|-----------------|--------------|
| 1 | GC-31/1 | 0.00-0.05 | 31.00 | 3.00 | 26.00 | 0.00 |
| 2 | GC-31/2 | 0.10-0.15 | 28.00 | 4.00 | 22.00 | 0.00 |
| 3 | GC-31/3 | 0.29-0.34 | 26.00 | 3.00 | 24.00 | 0.00 |
| 4 | GC-31/4 | 0.62-0.67 | 30.00 | 5.00 | 26.00 | 1.00 |
| 5 | GC-31/5 | 0.80-0.85 | 28.00 | 3.00 | 26.00 | 3.00 |
| 6 | GC-31/6 | 0.90-0.95 | 20.00 | 3.00 | 19.00 | 6.00 |
| 7 | GC-31/7 | 1.20-1.25 | 6.00 | 1.00 | 26.00 | 17.00 |
| 8 | GC-31/8 | 1.50-1.55 | 6.00 | 2.00 | 25.00 | 14.00 |
| 9 | GC-31/9 | 1.77-1.82 | 29.00 | 6.00 | 13.00 | 9.00 |
| 10 | GC-31/10 | 1.82-1.87 | 30.00 | 8.00 | 12.00 | 9.00 |
| 11 | GC-31/11 | 1.87-1.91 | 34.00 | 5.00 | 11.00 | 6.00 |
| 12 | GC-31/12 | 1.99-2.04 | 36.00 | 6.00 | 10.00 | 6.00 |
| 13 | GC-31/13 | 2.04-2.06 | 33.00 | 3.00 | 9.00 | 5.00 |

Table 6. Frequency distribution of depth diagnostic benthic taxa of the gravity core GC/52.

| Sl. No | Sub-sample No | Sub sample level bsf (m) | A. Beccarii % | A. trispinosa % | E. Crispum % | N. Scaphum % | B. Spathulata % | Q. seminulum % | Q. venusta % | S. Communis % | Agg |
|--------|---------------|--------------------------|---------------|-----------------|--------------|--------------|-----------------|----------------|--------------|---------------|-----|
| 1 | GC-52/1 | 0-0.05 | 32 | 30 | 6 | 0 | 1 | 5 | 4 | 4 | |
| 2 | GC-52/2 | 0.98-0.23 | 30 | 28 | 7 | 1 | 3 | 4 | 5 | 3 | |
| 3 | GC-52/3 | 0.31-0.35 | 32 | 26 | 8 | 2 | 3 | 5 | 4 | 5 | |
| 4 | GC-52/4 | 0.35-0.40 | 31 | 28 | 7 | 3 | 3 | 6 | 3 | 4 | |
| 5 | GC-52/5 | 0.43-0.48 | 29 | 27 | 6 | 4 | 5 | 5 | 4 | 3 | |
| 6 | GC-52/6 | 0.58-0.62 | 28 | 24 | 7 | 6 | 7 | 3 | 4 | 2 | |
| 7 | GC-52/7 | 0.90-0.95 | 24 | 22 | 6 | 7 | 7 | 4 | 3 | 3 | |
| 8 | GC-52/8 | 1.00-1.05 | 8 | 30 | 6 | 7 | 7 | 3 | 3 | 2 | |
| 9 | GC-52/9 | 1.20-1.25 | 7 | 32 | 2 | 11 | 9 | 4 | 2 | 1 | |
| 10 | GC-52/10 | 1.50-1.54 | 33 | 12 | 8 | 6 | 6 | 3 | 2 | 2 | |
| 11 | GC-52/11 | 1.80-1.82 | 41 | 8 | 7 | 7 | 5 | 3 | 2 | 3 | |
| 12 | GC-52/12 | 2.12-2.17 | 42 | 9 | 6 | 5 | 5 | 2 | 1 | 1 | |

Table 7. Absolute number and percentage of Textularina, Rotalina and Miliolina suborders in sediment columns of two gravity cores of Ganga prodeltaic region in the Bay of Bengal

| Sample No. | Depth (m) | Sample length (cm) | Textularina number and % | Rotalina number and % | Miliolina number and % | TFN (Benthic) in 10 gm | Foraminiferal biofacies |
|--------------|-----------|--------------------|--------------------------|-----------------------|------------------------|------------------------|-------------------------------|
| 182/GC-31/1 | 34.30 | 0-5 | 8 (12) | 42 (60) | 20 (28) | 70 | <i>Ammonia - Astrorotalia</i> |
| 182/GC-31/2 | | 10-15 | 18 (15) | 66 (55) | 36 (30) | 120 | do |
| 182/GC-31/3 | | 29-34 | 8 (13) | 35 (53) | 22 (34) | 90 | do |
| 182/GC-31/4 | | 62-67 | 9 (11) | 52 (65) | 19 (24) | 80 | do |
| 182/GC-31/5 | | 80-85 | 6 (11) | 32 (63) | 13 (26) | 50 | do |
| 182/GC-31/6 | | 90-95 | 6 (9) | 42 (60) | 22 (31) | 70 | do |
| 182/GC-31/7 | | 120-125 | 5 (3) | 113 (64) | 47 (26) | 175 | <i>Nonion - Astrorotalia</i> |
| 182/GC-31/8 | | 150-155 | 3 (4) | 64 (72) | 17 (19) | 85 | do |
| 182/GC-31/9 | | 177-182 | 34 (8) | 344 (80) | 47 (12) | 425 | <i>Ammonia</i> |
| 182/GC-31/10 | | 182-187 | 35 (10) | 259 (74) | 56 (16) | 350 | do |
| 182/GC-31/11 | | 187-191 | 20(10) | 144(72) | 36(18) | 200 | do |
| 182/GC-31/12 | | 199-204 | 16 (10) | 127(79) | 18 (11) | 160 | do |
| 182/GC-31/13 | | 204-206 | 3 (10) | 23 (75) | 5 (15) | 31 | do |
| 182/GC-52/1 | 30.20 | 0-5 | 8 (9) | 69 (78) | 14 (18) | 90 | <i>Ammonia - Astrorotalia</i> |
| 182/GC-52/2 | | 18-23 | 10 (8) | 95 (80) | 15 (12) | 120 | do |
| 182/GC-52/3 | | 31-35 | 12(9) | 103(76) | 20(15) | 135 | do |
| 182/GC-52/4 | | 35-40 | 10 (9) | 87 (79) | 14 (12) | 110 | do |
| 182/GC-52/5 | | 43-48 | 23 (10) | 174 (76) | 27 (14) | 225 | do |
| 182/GC-52/6 | | 58-62 | 6 (7) | 76 (82) | 8 (10) | 90 | do |
| 182/GC-52/7 | | 90-95 | 8 (7) | 111 (83) | 15 (11) | 134 | do |
| 182/GC-52/8 | | 100-105 | 8 (4) | 161(85) | 21 (11) | 190 | <i>Nonion - Astrorotalia</i> |
| 182/GC-52/9 | | 120-125 | 13 (3) | 365 (83) | 44 (14) | 425 | do |
| 182/GC-52/10 | | 150-155 | 6(13) | 39(83) | 2(4) | 45 | <i>Ammonia</i> |
| 182/GC-52/11 | | 180-185 | 4(12) | 29(82) | 2(6) | 35 | do |
| 182/GC-52/12 | | 212-217 | 3 (11) | 11(85) | 1(4) | 15 | do |

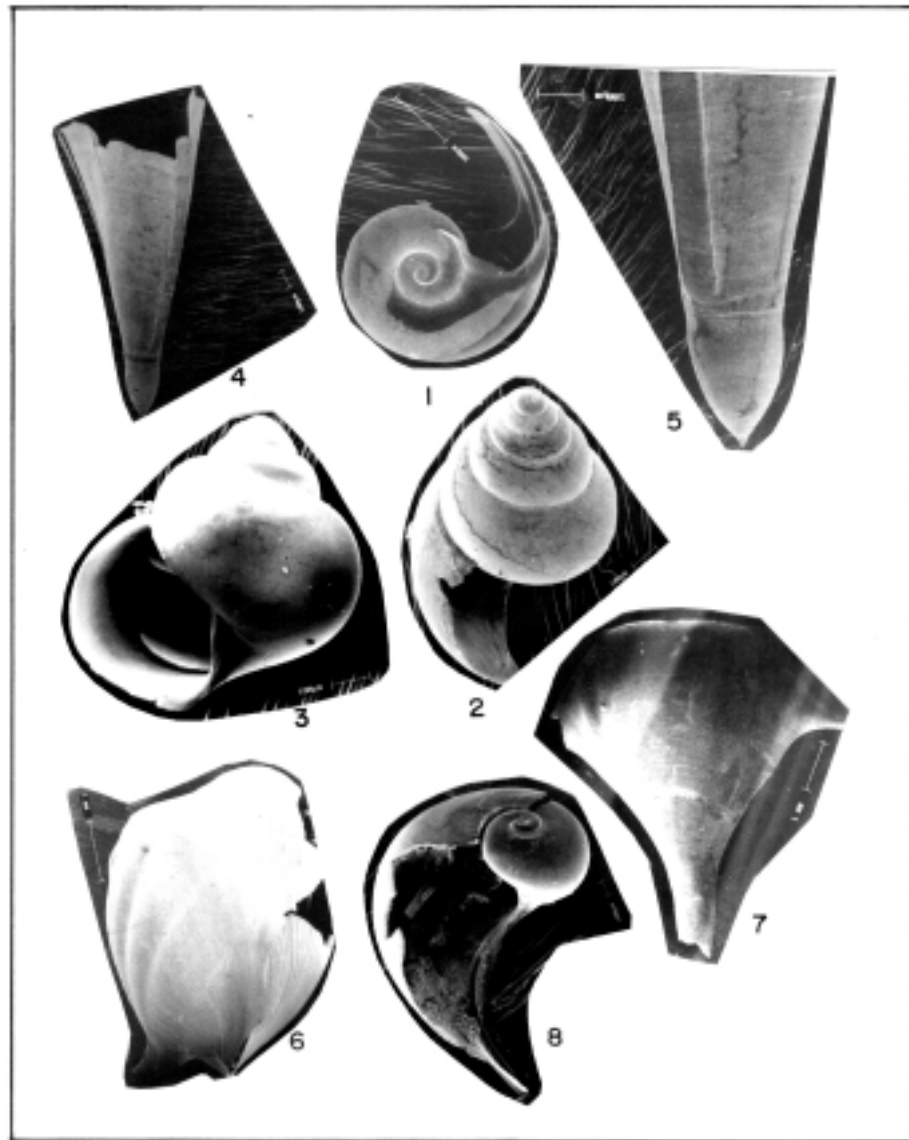
breakdown is very common due to their fragile tests. Occurrences of pteropods are noticed mainly to the southern part of the area (GC: 14, 20,34,48,49 and 63) in relatively low energy environment.

Three families (Limaceniidae, Peraclididae and Cavolinidae) of two suborder Euthecosomata and Pseudothecosomata of the pelagic gastropod are noticed in this region. Only eleven species of pteropods have been identified and they are represented by *Limacina inflata*, *L. trociformis*, *L. bulloides*, *Cresis acicula*, *C. virgule*, *Clio convexa*, *C. pyramidata*, *Cavolina globulosa*, *Peraclis reticulate*, *Diacria trispinosa* and *Cresis acicula virgula*. Eight of the species has been illustrated with the help of SEM photographs in Fig: 8 (Photographs. 1 to 8). On the basis of the shell strength of different pteropod taxa, it is noticed that the *Limacina sp.* and *Diacria sp.* show moderate preservation, *Clio sp.* and *Cresises sp.* show moderate to poor and *Peraclise sp.* and *Cavilina sp.* show poor mode of preservation respectively. Occurrence of these taxa indicates a low salinity tropical faunal assemblage. Quantitative study of pteropods was not carried out due the low frequency of different taxa in sediment samples; however, qualitative analysis of pteropods reveals that their presence is more in middle part of the sediment column of the two gravity cores (GC:31 and GC:52) samples than the upper and lower part of the cores. The presence of pteropods in the two cores

suggests a comparatively low salinity condition during the deposition of the sediments deposited in the middle part of the gravity cores than the underlying and overlying parts.

SUMMARY AND CONCLUSIONS

The population density of the biota as well as their species diversity are comparatively less in the northern part when compared to the southern part of the area, indicating a higher rate of sedimentation in the former domain than the latter. The biogenic components of the sediments varies from 15 % to 25 % and the biogenic (B): terrigenous (T) ratio increases systematically with water depth. The observed foraminiferal and pteropod assemblages are found to be of Indo-pacific geographical province representing a warm water tropical environment. The benthic faunal assemblage reveals a euryhaline and eurythermal population which can withstand the ecological inhospitality due to changing salinity, temperature, wave action and turbidity. Three foraminiferal biofacies namely *Ammonia-Quinqueloculina*, *Ammonia-Astrorotalia* and *Nonion-Astrorotalia* had been identified as elongated east-west trending stripes. These benthic biofacies are nearly parallel to the coast and their occurrence reveals a relation to the increasing depth of the prodeltaic region. The variation of the biofacies in the sediment columns



1. *Limacina inflata* (d'Orbigny, 1836) apical view, 2. *L. bullimoides* (d'Orbigny, 1836) side view, 3. *L. trochiformis* (d'Orbigny, 1836) apertural view, 4. *Clio convexa* (Bose, 1886) side view, 5. *C. pyramidata* (Bose, 1886) side view, 6. *Cavofina globulosa* Gay, 1865, marginal view, 7. *Diceria trispinosa* (de Blainville, 1827) and 8. *Peraclype reticulata* (d'Orbigny, 1836) apertural view.

Fig. 8. SEM photographs of some pteropod taxa with scale bars.

of the gravity core samples also indicates a deeper environment of deposition for the middle part of the core in comparison to their upper and lower parts. The increase of the P:B ratio and B:T ratio in the middle part of the core also corroborates the above fact.

The study suggests that Holocene sea level change is observed on the basis of the foraminiferal record and the result of such analysis shows the estimation of paleo-depth change which is in turn unravels the Holocene transgression around the study area. The whole sediment column of the gravity cores is deposited during the Holocene time as per the occurrence of N23 Zone planktonic faunal assemblage (Blow, 1979). The upper and lower parts are characterized

by the presence of shallower benthic taxa representing a regressive phase while the middle part represents an acme foraminiferal zone of the transgressive phase.

Acknowledgements: Author express his sincere gratitude to Sri U. K. Roy, Senior Deputy Director General, Marine Wing, GSI for his kind permission for submitting the paper in the seminar and necessary help for completing the work. Thanks are due to Dr. S. Madabhushi, Director, OPEC-II, MW, GSI for his constant encouragement during the work. Author is also thankful to the reviewers, Prof. S. Banerjee and Prof. T.Y.Naidu for their valuable comments/suggestions and improving the manuscript.

References

- Armstrong, H and Brasier, M. D. (2005). *Foraminifera*. In: *Microfossils*, Second edition, Blackwell publisher, Oxford, UK, 142-187.
- Banerjee, A and Sengupta, R, (1987). Evidence of low stands on the continental shelf on the East coast of India; Recent geoscientific studies in the Bengal and Andaman Sea. GSI, Spl. Pub.no.29,163-170.
- Banerjee, M and Sen, P.K. (1987). Paleobiology in understanding the change of sealevel and coastline in Bengal basin during Holocene period. *Ind. Jour. Sci. Spl. no, Modern trend in Quaternary Geology*, 14(3-4), 307-320.
- Banerjee, M. (2000). Paleobiological evidence on biogeotatmospheric changes during Himalayan upheaval with particular reference to Eastern Indian subcontinent in the Neogene period. Invited paper for spl. Vol. on *Himalayan Science & Culture*. 66,(1&2), 57-66.
- Banerjee, M. (2003). Evolution of biosphere and related climatic geographic changes in the Eastern Indian subcontinents period, *Proc of GEOSAS-IV, Geo. Sur. India*, New Delhi, 239-254.
- Barker, R.W.(1960).Taxonomic notes on the species figured by H.B.Brady in his report on the foraminifera during the year 1873-1875 *Soc.Eco.Pal.Min.Spl.Pub.9*, Pt.X-XXIV,1-238.
- Bhalla, S.N.(1968). Recent foraminifera from beach sands and its relation to the known foramegeographical province of the Indian Ocean, In: *Symp. Indian Ocean, Bull. Nat. Int. Sci. India*, 38(1),376-392.
- Be, A.W.H and Gilmer, W.R.(1977): A zoogeographic and taxonomic review of Euthecasomatus pteropod. In: Ramsay, A.T.S (Eds), *Oceanic Micropalaeontology*, Academic press, 733-808.
- Bhattacharjee, D, Ghosh, S. K, Bandyopadhyay, A, and Bandyopadhyay, R. R. (2002). Foraminiferal biofacies in the northern parts of Bay of Bengal and their environmental implications. Four decades of marine geosciences in India – A retrospect, *Proceedings National Seminar on four decades of Marine Geosciences*: GSI Spl. Pub. No.74, 80-85
- Bhattacharjee, D., Ghosh, S. K. and Roy Chowdury, S.(2004). Quarternary sedimentary environment in Ganga prodeltaic region, Northern part of Bay of Bengal. *Jour. Geological Society of India*, 67, 585-593.
- Bhattacharjee, D. (2005). Pteropod preservation profiles in the sediments off Middle Andaman Islands In Andaman Sea, *Indian Journal of Marine Science*, 34(3),259-266.
- Bhattacharjee, D. (2007). Quaternary sediments off Hoogly and Subarnarekha rivers in Bay of Bengal- An environmental appraisal. *National seminar on coastal zone development vis-a-vis marine environment: The recent trends*. Organized by Earth & Planetary Science Section, WAST, 4-6.
- Bhattacharjee, D., Ghosh, S. K., Nagandran, G; Katari, A and Panda, P.K.(2007). Foraminiferal evidence of Holocene transgression in the sediment column from territorial water off Behuda river mouth of Orissa, East coast of India, *News Letter, Marine Wing, GSI*, 21(1&2), 23-25.
- Bhattacharjee, D., Ghosh, S. K. and Panda, P.K. (2008). Foraminiferal record in the Holocene sediments off Sagar Island and its implication on sea level changes in Bay of Bengal, Proc. Vol. workshop IGCP-464,103-115.
- Bhattacharjee, D. (2008a): Quaternary sediments off Krishna- Godavari delta and their environmental implication: Foraminiferal evidence, *MGMI Transaction*, 104 (1 & 2), 111-134.
- Bhattacharjee, D. (2009). Benthic foraminiferal distribution in the Holocene sediments off Matla River in the continental shelf region, Bay of Bengal. *Indian Journal of geosciences*, 63(1), 53-66.
- Blow, W.H.(1979). The Cainozoic Globigerinoida, Part-I & II, Section I, *A study of the morphology, taxonomy, evolutionary relationship and stratigraphical distribution of some Globigerinada*, E.J. Brill, Leiden, Netherlands,63-66.
- Bolli, H.N; Saunder, J.B and Nielsen, K.P. (1987). *Planktonic stratigraphy*, Cambridge University Press, Cambridge, 158-265.
- Boltovoskoy, B and Wright, R. (1976): *Recent foraminifera*, (Ed:W. Junk), B.V. Publisher, The Haquye, 515 p
- Corliss, B.H.(1983). Distribution of Holocene deep-sea benthic foraminifera in the southwest Indian Ocean, *Deep-sea Research*. 3092, 95-117.
- Cullen, J.L.(1981). Microfossil evidences for changing salinity pattern in the Bay of Bengal over the last 20,000 years, *Paleogeography Paleoclimatology, Paleoecology*., 35, 315-356.
- Ellis, B.F and Messina, A.R.(1968). *Catalogue of foraminifera*, Spl. Pub.American Museum Natural History. New York, 1,2 & 3.
- Fiorini, F. (2004). Benthic foraminiferal association from upper Quaternary deposits of southeastern Po plan, Italy, *Micropaleontology*, 40(1), 45-58.
- Gupta, A.K. (1994). Taxonomy and bathymetric distribution of Holocene deep –sea benthic foraminifera in the Indian Ocean and Red sea, *Micropaleontology*, 40(4), 351-367.
- Ingle, J.C, Keller, G and Kalpack, R.L.(1980). Benthic foraminiferal biofacies , sediments and water masses of the southern Peru-Chiletrench area, *Micropaleontology*, 26(2),113-150.
- Islam, M, S.(2004). Sequences of differential siltation in the Bengal basin and proxies of regional monsoon climate variability during Holocene, *Geo. Soci., India*, Abs., 20.

- Kennett, J. P. and Srinivasan, M. S. (1976). *Neogene Planktonic foraminifera. A Phylogenetic Atlas*. Hutchinson Ross Pub., USA, 163p.
- Leoblich, A.R and Tappan, H.(1988): *Foraminiferal genera and their classification*, Van Nostrand Reinhold Co.,New york,1-970.
- Lindsay, J.F, Holiday, D.W and Hulberd, A.G.(1991). Sequence stratigraphy and the evolution of the Ganga-Brahmaputra Delta complex, *Ame. Asso. Per. Geo. Bull.*, 75(1),1233-1254.
- Majumdar, S, Choudhury, A and Naidu, T.Y. (1999). Recent benthic foraminifera from the near shore to inner shelf of Digha, North-east Coast of India, *V.U ,Jour. Biological Science*, 5,1-8.
- Margaef, R. (1967). Some concepts relative to the organization of plankton, *Marine biological annul review*, 5, 257-289.
- Mallick, T. K, Bhattacharjee, D. and Mukherjee, P.K.(2002). Depositional environments in the lower reaches of Ganga delta, some clues from micropaleontological studies, *Proce. XVIII Indian Collu. Micro. Strati*, Nagpur. 39-44.
- Milliman, J.D., Broadus, J.M and Gable, F.(1989). Environmental and economic implications of rising sea level and subsiding deltas, The Nile and Bengal examples, *Ambio*, 18(6), 340-345.
- Murry, J.W.(1991): *Ecology and paleoecology of benthic foraminifera*, Longman, Harlow, Essex, 15-145.
- Murry, J.W. (2003): Foraminiferal assemblage formation in depositional sinks on the continental shelf west of Scotland. *Journal of Foraminiferal Research*, 33(2), 101-121.
- Nageshwar Rao, K; Sadakata, N, Hemamalini, B; Sarma, V.V.LI.N and Kasima, K.(2003). Reconstruction of the stage in Holocene evolution of Godavari Delta, India. *Transactions, Japanese Geomorphological Union, Chikei*, 24, 295-309.
- Naidu, T.Y. (1992). Distribution of foraminifera in the sediments of the Kalingapatnam shelf, east coast of India, *Studies in the benthic foraminifera BENTHOS '90*, Sendai 1990, Tokai University press, 159-165.
- Naidu, T.Y, Kamalakaram, S and Kaladhar, R. (2005). Recent Benthic foraminiferal biofacies and its environmental significance in the Goguleru creek, coastal Andhra Pradesh, *Jour. Geolo, Soci. India*, 66, 223-228.
- Nehaluddin, M and Abdulla, S.K.M. (2003). Quaternary geology and aquifer systems in Ganga-Brahmaputra- Meghna deltacomplex, Bangladesh, *Procdeing Vol. GEOSAS-IV, Geo.Sur. India*, New Delhi, 400-416.
- Patterson, R.T and Cameron, B.E.B. (1991). Paleo-environmental significance of the foraminiferal biofacies succession in the Late Quaternary sediments of the Fraser river delta, British Columbia, *Journal of Foraminiferal Research*, 21, 228-243.
- Patterson, R.T. (1993). Late quaternary benthic foraminiferal biofacies and paleoceanography of Queen Charlotte sound and southern-hecate strait, British Columbia, *Journal of Foraminiferal Research*, 23(1), 1-18.
- Scott, D. B., Medioli, F. S. and Schafer, C. T. (2001). *Monitoring in coastal environments using foraminifera and Thecamoebians as indicators*, Cambridge University Press, Cambridge, 50-90.
- Shepard, F.P.(1954). Nomenclature based on sand-silt-clay ratios: *Jour. Sed. Petro.* No.24, 1-30.
- Walton, W.R.(1964). Recent foraminiferal ecology and paleoecology .In; J. Imbri & D. Newell (Eds.).*Approaches to Paleoecology*, Wiley, New York.,151-171.

Hydrogeochemical Exploration for Uranium : A Case Study of Jabera Dome, Damoh and Jabalpur Districts, Madhya Pradesh

RAHUL BANERJEE¹, A.K. VERMA², M.K. ROY² AND P.B. MAITHANI¹

Atomic Minerals Directorate for Exploration and Research

¹ 1-10-153/156, AMD Complex, Begumpet, Hyderabad-500 629

² AMD Complex, Central Region, Civil Lines, Nagpur-440 001

Email: rahulbnrg@gmail.com

Abstract: Application of hydrogeochemical techniques, an important tool in uranium exploration program, has been successfully utilised to delineate potential target zones in Jabera dome and its environs exposing Neoproterozoic Rewa and Bhandar Group of rocks (Upper Vindhyan) in predominantly soil covered area. Hydrogeochemical data of 215 groundwater samples has indicated 0.25–330ppb U, 0.35–2.67mmhos/cm conductivity, 10–500 ppm SO₄, 50–700 ppm HCO₃, 0.5–23 ppm PO₄, 0.5–3.8 ppm F while pH ranges from 5.2 to 8.2. Other elements such as Na, K, Ca and Mg analysed upto 575 ppm, 99 ppm, 425 ppm and 130 ppm, respectively. Statistical evaluation of processed data (without nugget values) shows 1.7 ppb U as mean value with 1.33 ppb standard deviation giving rise to 39 anomalous uranium values above threshold (Mean+2SD) value of 4.36 ppb. Similarly, U/Conductivity ratio data has indicated 1.45, 0.95 and 3.35 as mean, SD and threshold, respectively and recorded 45 anomalies after neutralization of effect of total dissolved salts (TDS). This has resulted in delineation of two anomalous uranium zones confined within Upper Bhandar Sandstones at the northeastern (Bakal–Jharauli–Ramnagar sector) and northwestern (Bamhori–Kalhara–Tejgarh sector) fringes of Jabera dome. The radioelement distribution pattern in rock samples have also indicated comparatively higher uranium content in Sirbu Shale (upto 8ppm) and Upper Bhandar Sandstone (upto 10ppm) than the general abundance (sandstone– 0.45ppm; Shale– 3.7ppm). In view of favourable lithostructural setup viz., deposition of Upper Vindhyan sediments in rift related basin in an extensional tectonic environment, multiple reactivation cycles with influx of juvenile material including post–Vindhyan diapiiric emplacement of felsic plutons beneath Jabera dome, vis-à-vis presence of fertile provenance, gas shows (ONGC well Jabera#1) and hydrouanium anomalies points towards the possibility of sandstone-hosted/fracture controlled uranium mineralisation in the area.

Keywords: Hydrogeochemical exploration, uranium mineralisation, Neoproterozoic Upper Vindhyan, Jabera dome, Damoh district, Madhya Pradesh

INTRODUCTION

Proterozoic basins are considered to be highly potential for uranium mineralisation world wide after the discovery of world's largest uranium bearing multi-metal (Olympic Dam, Australia; Hitzman, 2000; Hitzman and Valenta, 2005; Williams et al., 2005) and richest uranium (Mc-Arthur River, Canada; Jefferson et al., 2007) deposits associated with these horizons. These deposits are hosted in Proterozoic rocks close to the Archaean–Proterozoic boundary and located at comparatively deeper levels with scanty surface expressions. Hence, uranium exploration in such type of terrain requires an integrated approach including various geophysical and geochemical techniques. In Indian context, intense prospecting and exploration efforts by Atomic Minerals Directorate (AMD) targeting Proterozoic terrain during last two decades have resulted in discovery of several uranium occurrences of unconformity/vein/palaeoplacer types in Andhra Pradesh, Karnataka, Rajasthan,

Chhattisgarh and Madhya Pradesh (Mahadevan, 1986, 1995; Sinha et al., 1995; Rai et al., 2002; Chaki et al., 2004; Khandelwal et al., 2008). Meso- to Neoproterozoic Vindhyan sediments have also come into prominence after the discovery of uranium anomalies associated with Semri sediments and younger intrusives in basement granite gneisses (Chhotanagpur Granite Gneissic Complex; CGGC) in parts of Sidhi district, Madhya Pradesh (Sesha Rao et al., 2004; Saxena et al., 2005; Bhattacharjee et al., 2008). Oxyatmoversion during this period has changed the reducing environment due to the heavy influx of oxygen in the system, which had played a vital role in mobilisation and concentration of uranium, a strong oxyphile element, in near surface conditions. The remobilized uranium was subsequently fixed at suitable horizons in the presence of reductant, such as, pyrite, carbonaceous matter, methane gas, ferric minerals etc. Uranium solution mineral equilibria at low temperature have been discussed in detail by Miller (1958), Hostetler and Garrels

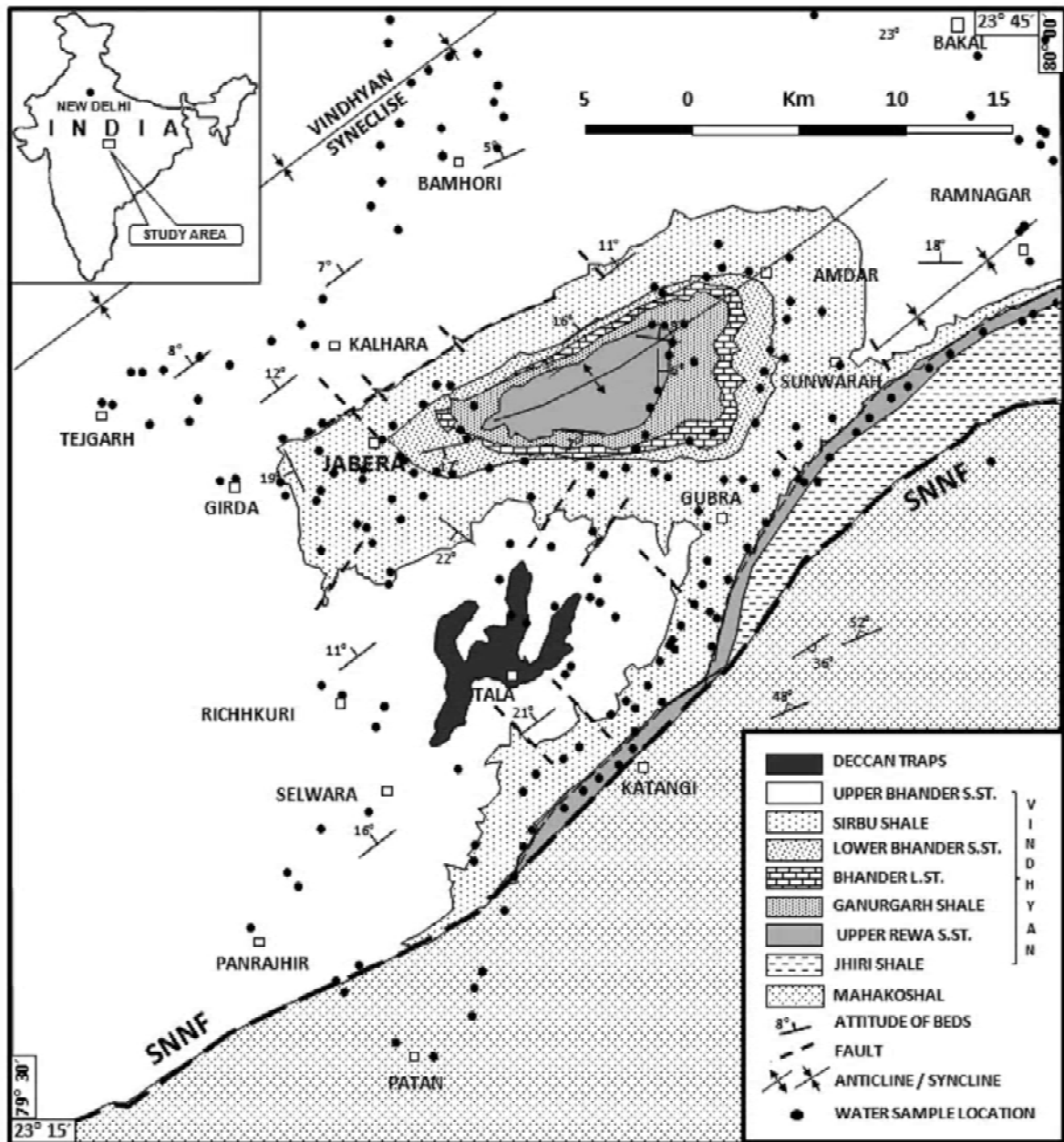


Fig. 1. Geological map (after GSI, 1994, 2001) of Jabera dome area, Damoh and Jabalpur districts, M.P. showing water sample locations.

area is based on Oil and Natural Gas Commission (ONGC) well data (Jabera#1).

Upper Vindhyan sequence comprising Rewa and Bhandar Group of rocks constitutes major part of the study area and exhibit ENE–WSW to NE–SW trending faulted contact with underlying Palaeoproterozoic Mahakoshal metasediments (Fig. 1). The most striking feature in this part is NE–SW fault bounded oval shaped Jabera dome (~35 x 15 km). Its emergence as an inlier with outward radiating dips is attributed to diapiric emplacement of post-Vindhyan pluton. At Jabera dome, upper part of Rewa Group and lower part of Bhandar Group are surrounded by Sirbu shales and Upper Bhandar sandstones. The study area exhibits ENE–

WSW to NE–SW trending major structural grain, sympathetic to the Son–Narmada mega lineament. This major structural trend is intersected by another prominent lineament showing NNW–SSE trend and inferred as the site of magmatic activity. Besides, signatures of multiple tectonic reactivation and juvenile magmatism are quite apparent and exhibited by intense faulting/fracturing, drags, diapiric activity, silicification and ferruginisation.

The oldest Vindhyan sediment in the study area is Jhiri Shale of Rewa Group. These are represented by yellowish grey to white coloured shales underlying hard, compact and pinkish to greyish white coloured massive Upper Rewa Sandstones. These sandstones form a NE–

Table 3. Hydrogeochemical data of Jabera dome area

| S. No. | U (ppb) | pH | Cond. | U/Cond. | Na | K | Ca | Mg | HCO ₃ | Cl | SO ₄ | PO ₄ | F |
|--------|---------|-----|-------|---------|--------------------|----|-----|-----|------------------|-----|-----------------|-----------------|-----|
| | | | | | All values in mg/l | | | | | | | | |
| 1 | 0.25 | 6.9 | 0.37 | 0.68 | 4 | 1 | 70 | 25 | 55 | 10 | <20 | <1 | <1 |
| 2 | 0.25 | 7.5 | 0.88 | 0.28 | 152 | 5 | 60 | 25 | 355 | 20 | 20 | 2 | <1 |
| 3 | 3.50 | 7.0 | 1.50 | 2.33 | 32 | 6 | 245 | 55 | 405 | 105 | 40 | 1 | <1 |
| 4 | 1.20 | 7.3 | 0.79 | 1.52 | 28 | 3 | 80 | 25 | 275 | 40 | <20 | <1 | <1 |
| 5 | 0.25 | 7.0 | 0.69 | 0.36 | 61 | 3 | 70 | 25 | 290 | 15 | <20 | <1 | <1 |
| 6 | 0.60 | 7.3 | 0.68 | 0.88 | 13 | <1 | 95 | 35 | 290 | 10 | <20 | <1 | <1 |
| 7 | 0.50 | 7.1 | 0.75 | 0.67 | 18 | 1 | 80 | 45 | 275 | 10 | <20 | <1 | <1 |
| 8 | 4.70 | 6.9 | 1.63 | 2.88 | 81 | 4 | 150 | 85 | 555 | 100 | 40 | <1 | <1 |
| 9 | 1.00 | 7.5 | 0.75 | 1.33 | 13 | 1 | 160 | 15 | 315 | 10 | <20 | 1 | <1 |
| 10 | 2.30 | 7.1 | 2.43 | 0.95 | 390 | 19 | 160 | 125 | 225 | 45 | 500 | <1 | <1 |
| 11 | 0.25 | 7.0 | 0.70 | 0.36 | 20 | 1 | 80 | 20 | 275 | 15 | <20 | 1 | <1 |
| 12 | 0.60 | 7.1 | 0.94 | 0.64 | 65 | 1 | 80 | 15 | 450 | 15 | <20 | 1 | <1 |
| 13 | 0.25 | 6.5 | 1.03 | 0.24 | 62 | 4 | 80 | 35 | 330 | 100 | <20 | 1 | <1 |
| 14 | 0.25 | 6.9 | 0.44 | 0.57 | 7 | 2 | 70 | 20 | 130 | 10 | <20 | <1 | <1 |
| 15 | 0.60 | 7.0 | 0.85 | 0.71 | 35 | 4 | 60 | 55 | 305 | 40 | 20 | 1 | <1 |
| 16 | 0.60 | 7.1 | 0.83 | 0.72 | 12 | 1 | 80 | 5 | 410 | 15 | <20 | 1 | <1 |
| 17 | 1.00 | 7.0 | 0.96 | 1.04 | 25 | 2 | 70 | 40 | 475 | 15 | <20 | <1 | <1 |
| 18 | 1.10 | 6.6 | 0.84 | 1.31 | 11 | 2 | 60 | 40 | 420 | 15 | <20 | 1 | <1 |
| 19 | 2.30 | 6.8 | 1.69 | 1.36 | 71 | 6 | 210 | 50 | 380 | 15 | 250 | 1 | <1 |
| 20 | 0.25 | 6.9 | 0.54 | 0.46 | 24 | 1 | 45 | 5 | 235 | 10 | <20 | 1 | <1 |
| 21 | 5.10 | 7.0 | 1.54 | 3.31 | 129 | 3 | 105 | 75 | 645 | 65 | <20 | 1 | <1 |
| 22 | 2.70 | 7.0 | 1.65 | 1.64 | 24 | 4 | 115 | 50 | 435 | 85 | <20 | 1 | <1 |
| 23 | 2.30 | 7.2 | 0.97 | 2.37 | 27 | 2 | 60 | 40 | 450 | 15 | <20 | 1 | <1 |
| 24 | 3.10 | 6.9 | 1.19 | 2.61 | 95 | 3 | 105 | 20 | 460 | 70 | <20 | 1 | 1.7 |
| 25 | 0.90 | 7.0 | 0.77 | 1.17 | 26 | 1 | 60 | 40 | 515 | 15 | <20 | <1 | <1 |
| 26 | 0.50 | 7.3 | 0.83 | 0.60 | 5 | 1 | 80 | 30 | 410 | 10 | <20 | 1 | <1 |
| 27 | 1.40 | 7.8 | 0.85 | 1.65 | 22 | 2 | 95 | 20 | 370 | 15 | <20 | 1 | <1 |
| 28 | 1.40 | 7.5 | 0.76 | 1.84 | 15 | 1 | 70 | 50 | 330 | 15 | <20 | <1 | <1 |
| 29 | 0.25 | 7.3 | 0.75 | 0.33 | 60 | 2 | 80 | 35 | 290 | 15 | <20 | <1 | <1 |
| 30 | 0.25 | 8.1 | 0.54 | 0.46 | 16 | 2 | 35 | 15 | 170 | 15 | <20 | 1 | <1 |
| 31 | 0.25 | 6.7 | 0.41 | 0.61 | 4 | 1 | 95 | 35 | 105 | 10 | <20 | <1 | <1 |
| 32 | 2.10 | 7.7 | 0.77 | 2.73 | 7 | 4 | 70 | 55 | 330 | 10 | <20 | <1 | <1 |
| 33 | 0.25 | 6.2 | 0.35 | 0.71 | 5 | 4 | 45 | 5 | 65 | 10 | <20 | 1 | <1 |
| 34 | 0.80 | 7.5 | 0.91 | 0.88 | 21 | 2 | 70 | 85 | 355 | 25 | <20 | 1 | <1 |
| 35 | 1.60 | 7.1 | 1.03 | 1.55 | 72 | 3 | 80 | 55 | 330 | 45 | 40 | 1 | <1 |
| 36 | 0.25 | 7.2 | 0.91 | 0.27 | 13 | 1 | 95 | 65 | 380 | 15 | 20 | 2 | <1 |
| 37 | 1.20 | 7.3 | 1.07 | 1.12 | 51 | 6 | 60 | 55 | 410 | 15 | 90 | 1 | <1 |
| 38 | 0.80 | 7.2 | 1.06 | 0.75 | 38 | 5 | 130 | 40 | 355 | 15 | 80 | 2 | <1 |
| 39 | 1.30 | 7.0 | 0.97 | 1.34 | 23 | 4 | 70 | 55 | 450 | 20 | 20 | 1 | <1 |
| 40 | 1.30 | 7.0 | 0.89 | 1.46 | 35 | 10 | 60 | 75 | 275 | 40 | 20 | <1 | <1 |
| 41 | 2.90 | 7.4 | 1.12 | 2.59 | 40 | 9 | 80 | 65 | 435 | 50 | <20 | 3 | <1 |
| 42 | 0.25 | 7.5 | 0.80 | 0.31 | 102 | 5 | 60 | 15 | 345 | 10 | <20 | <1 | <1 |
| 43 | 0.70 | 6.8 | 1.05 | 0.67 | 17 | 1 | 70 | 55 | 490 | 25 | <20 | 1 | <1 |
| 44 | 0.70 | 6.9 | 1.03 | 0.68 | 8 | 2 | 80 | 50 | 460 | 10 | <20 | 1 | <1 |
| 45 | 0.25 | 6.0 | 0.35 | 0.71 | 3 | 2 | 25 | 30 | 90 | 15 | <20 | 2 | <1 |
| 46 | 0.25 | 5.6 | 0.39 | 0.64 | 5 | 8 | 35 | 15 | 65 | 15 | <20 | <1 | <1 |
| 47 | 0.25 | 6.9 | 0.50 | 0.50 | 28 | 4 | 70 | 15 | 100 | 15 | <20 | 1 | <1 |
| 48 | 0.25 | 6.7 | 0.43 | 0.58 | 9 | 3 | 60 | 5 | 90 | 15 | <20 | 1 | <1 |
| 49 | 0.25 | 6.5 | 0.54 | 0.46 | 11 | 3 | 60 | 5 | 160 | 15 | <20 | 1 | <1 |
| 50 | 1.80 | 7.0 | 1.38 | 1.30 | 40 | 99 | 80 | 15 | 305 | 95 | 40 | 4 | <1 |
| 51 | 7.30 | 7.1 | 2.23 | 3.27 | 88 | 67 | 160 | 65 | 460 | 225 | 50 | 2 | <1 |
| 52 | 1.30 | 7.2 | 0.86 | 1.51 | 13 | 2 | 80 | 30 | 345 | 15 | 20 | <1 | <1 |
| 53 | 1.20 | 7.1 | 1.06 | 1.13 | 26 | 3 | 90 | 40 | 395 | 35 | 20 | 3 | <1 |

Contd..

Table 3 contd...

| S. No. | U (ppb) | pH | Cond. | U/Cond. | Na | K | Ca | Mg | HCO ₃ | Cl | SO ₄ | PO ₄ | F |
|--------|---------|-----|-------|---------|--------------------|-----|-----|----|------------------|-----|-----------------|-----------------|-----|
| | | | | | All values in mg/l | | | | | | | | |
| 108 | 2.00 | 7.2 | 0.80 | 2.50 | 18 | <1 | 20 | 15 | 345 | 30 | <20 | <1 | <1 |
| 109 | 0.25 | 6.0 | 0.60 | 0.42 | 19 | 1.6 | 30 | 10 | 165 | 20 | <20 | <1 | <1 |
| 110 | 0.25 | 6.5 | 0.70 | 0.36 | 19 | 7.3 | 35 | 10 | 125 | 15 | <20 | 2 | <1 |
| 111 | 0.25 | 6.8 | 0.50 | 0.50 | 5 | <1 | 30 | 5 | 355 | 25 | <20 | <1 | <1 |
| 112 | 1.00 | 7.2 | 0.90 | 1.11 | 31 | 32 | 50 | 25 | 125 | 25 | 20 | <1 | <1 |
| 113 | 0.25 | 6.2 | 0.50 | 0.50 | 7 | 3 | 25 | 5 | 330 | 55 | 20 | <1 | <1 |
| 114 | 1.00 | 7.0 | 0.90 | 1.11 | 21 | 2 | 45 | 20 | 140 | 50 | 20 | <1 | <1 |
| 115 | 2.10 | 7.6 | 1.25 | 1.68 | 143 | 1 | 35 | 20 | 335 | 140 | <25 | 4 | <1 |
| 116 | 2.30 | 7.3 | 1.19 | 1.93 | 73 | 1 | 70 | 40 | 490 | 85 | <25 | 1 | <1 |
| 117 | 3.50 | 7.2 | 1.22 | 2.87 | 57 | 1 | 80 | 30 | 555 | 55 | <25 | 3 | <1 |
| 118 | 1.30 | 7.4 | 1.82 | 0.71 | 233 | 2 | 30 | 25 | 570 | 55 | <25 | 1 | <1 |
| 119 | 2.60 | 7.1 | 1.21 | 2.15 | 125 | 1 | 45 | 30 | 555 | 55 | <25 | 3 | <1 |
| 120 | 5.00 | 7.4 | 1.14 | 4.39 | 50 | 1 | 70 | 15 | 525 | 55 | <25 | 4 | <1 |
| 121 | 1.00 | 7.3 | 0.52 | 1.92 | 20 | 1 | 10 | 10 | 140 | 55 | <25 | 3 | <1 |
| 122 | 9.50 | 7.1 | 1.89 | 5.03 | 67 | 1 | 160 | 60 | 445 | 160 | <25 | 10 | <1 |
| 123 | 0.50 | 6.8 | 0.65 | 0.77 | 9 | 1 | 45 | 45 | 190 | 55 | <25 | 3 | <1 |
| 124 | 1.00 | 6.8 | 0.70 | 1.43 | 13 | 11 | 35 | 20 | 235 | 70 | <25 | 5 | <1 |
| 125 | 0.50 | 6.5 | 0.46 | 1.09 | 6 | 2 | 20 | 15 | 80 | 35 | <25 | 2 | <1 |
| 126 | 0.50 | 6.4 | 0.43 | 1.16 | 4 | 1 | 25 | 15 | 110 | 55 | <25 | 2 | <1 |
| 127 | 1.80 | 7.3 | 0.81 | 2.22 | 31 | 1 | 75 | 10 | 335 | 70 | <25 | 3 | <1 |
| 128 | 1.00 | 6.9 | 0.75 | 1.33 | 21 | 1 | 90 | 25 | 225 | 70 | <25 | 2 | <1 |
| 129 | 1.10 | 7.2 | 0.87 | 1.26 | 17 | 1 | 75 | 25 | 335 | 55 | <25 | 5 | <1 |
| 130 | 1.00 | 7.3 | 0.63 | 1.59 | 13 | 2 | 55 | 10 | 175 | 55 | <25 | 2 | <1 |
| 131 | 1.00 | 7.5 | 0.74 | 1.35 | 10 | 1 | 70 | 15 | 235 | 70 | <25 | 3 | <1 |
| 132 | 1.60 | 7.1 | 0.88 | 1.82 | 19 | 1 | 70 | 30 | 300 | 70 | <25 | 5 | <1 |
| 133 | 1.90 | 7.3 | 1.20 | 1.58 | 10 | 12 | 110 | 40 | 445 | 90 | <25 | 3 | <1 |
| 134 | 2.90 | 7.5 | 1.05 | 2.76 | 14 | 1 | 90 | 30 | 490 | 70 | <25 | 3 | <1 |
| 135 | 1.90 | 7.1 | 0.91 | 2.09 | 17 | 1 | 100 | 20 | 365 | 55 | <25 | 3 | <1 |
| 136 | 3.00 | 7.3 | 1.04 | 2.88 | 42 | 1 | 95 | 25 | 490 | 90 | <25 | 2 | <1 |
| 137 | 2.00 | 6.9 | 1.10 | 1.82 | 10 | 3 | 80 | 20 | 435 | 45 | 20 | 3 | <1 |
| 138 | 0.50 | 6.8 | 0.60 | 0.83 | 11 | 12 | 95 | 10 | 130 | 35 | <20 | 4 | <1 |
| 139 | 3.00 | 6.9 | 1.30 | 2.31 | 27 | 15 | 105 | 35 | 485 | 80 | 20 | 3 | 1 |
| 140 | 2.00 | 6.9 | 1.00 | 2.00 | 18 | 2 | 90 | 20 | 453 | 30 | <20 | 1 | 1 |
| 141 | 3.00 | 6.8 | 1.50 | 2.00 | 33 | 2 | 75 | 40 | 502 | 125 | <20 | <1 | <1 |
| 142 | 1.00 | 7.0 | 0.90 | 1.11 | 3 | 1 | 40 | 10 | 395 | 15 | <20 | <1 | <1 |
| 143 | 1.00 | 6.9 | 0.90 | 1.11 | 8 | 2 | 95 | 15 | 390 | 35 | <20 | <1 | <1 |
| 144 | 0.50 | 5.2 | 0.60 | 0.83 | 7 | 2 | 25 | 10 | 50 | 50 | 20 | 3 | <1 |
| 145 | 1.00 | 6.9 | 0.90 | 1.11 | 16 | <1 | 95 | 30 | 470 | 20 | <20 | 5 | 2 |
| 146 | 0.50 | 7.7 | 0.70 | 0.71 | 16 | 2 | 75 | 30 | 315 | 15 | <20 | 6 | <1 |
| 147 | 3.00 | 6.8 | 0.80 | 3.75 | 30 | 1 | 50 | 20 | 345 | 25 | <20 | 3 | <1 |
| 148 | 6.00 | 6.8 | 0.60 | 10.00 | 16 | 2 | 60 | 15 | 150 | 25 | <20 | 2 | <1 |
| 149 | 0.50 | 6.1 | 0.40 | 1.25 | 5 | <1 | 30 | 10 | 65 | 30 | <20 | 1 | <1 |
| 150 | 0.50 | 6.4 | 0.40 | 1.25 | 3 | 3 | 15 | 10 | 65 | 20 | <20 | 2 | <1 |
| 151 | 0.50 | 5.9 | 0.40 | 1.25 | 6 | 2 | 15 | 10 | 75 | 30 | <20 | 2 | <1 |
| 152 | 1.00 | 6.8 | 0.80 | 1.25 | 44 | <1 | 15 | 10 | 370 | 25 | <20 | 4 | 1 |
| 153 | 0.50 | 7.0 | 0.70 | 0.71 | 16 | 3 | 55 | 20 | 205 | 30 | <20 | <1 | <1 |
| 154 | 0.50 | 6.9 | 0.80 | 0.63 | 36 | 4 | 30 | 20 | 255 | 30 | 38 | 3 | <1 |
| 155 | 0.50 | 7.0 | 0.70 | 0.71 | 23 | 3 | 35 | 20 | 265 | 30 | 20 | 3 | <1 |
| 156 | 0.50 | 7.2 | 0.90 | 0.56 | 131 | 3 | 35 | 15 | 395 | 25 | <20 | 3 | <1 |
| 157 | 1.00 | 7.2 | 0.80 | 1.25 | 26 | 1 | 10 | 15 | 345 | 30 | <20 | 4 | 1 |
| 158 | 0.50 | 8.1 | 1.30 | 0.38 | 266 | 2 | 55 | 25 | 502 | 95 | <20 | 2 | 3 |
| 159 | 4.00 | 7.5 | 0.98 | 4.08 | 43 | 4 | 60 | 40 | 400 | 65 | <20 | <1 | 3.8 |
| 160 | 1.00 | 7.2 | 0.96 | 1.04 | 27 | 2 | 90 | 35 | 355 | 80 | <20 | <1 | 1 |
| 161 | 2.00 | 7.0 | 0.86 | 2.33 | 12 | 4 | 90 | 30 | 345 | 75 | 20 | <1 | <1 |

Contd..

study area is concerned, it is observed that groundwater is practically unaffected by chemical fertilizers and hence, uranium signature is not influenced by the same. The groundwater of the area is neutral to marginally alkaline while average content of various ions and radicals (Table 4), barring sporadic high F values, are well below the prescribed limits for safe drinking water by WHO (1984) and ISI (1991).

The hydrogeochemical data pertaining to different lithounits showing various depositional environments indicate heterogeneity and skewed distribution. Hence, normalizing transformation was applied to these data sets to obtain meaningful output. Uranium values in present water samples have indicated lognormal distribution and therefore subjected to a log transformation during statistical evaluation of data. Apart from intrinsic uranium content of various lithounits, the evapotranspiration also plays significant role in enhancing the hydrouranium content, especially in those waters which are undersaturated in respect of certain uranium compounds (Dekkers et al., 1989). Seasonal fluctuations in uranium concentration are apparent in groundwater depending upon variation in water discharge pattern. To overcome these limitations, a few repeat samples were collected with an interval of

nearly three months vis-à-vis uranium/ conductivity ratio was preferred for various interpretation purposes.

Anomalous values were obtained by calculating threshold for uranium and uranium/conductivity ratio in water samples on the basis of geometric mean and standard deviation as shown in Table 5. Frequency distribution pattern of uranium indicates that majority of samples (184 nos.) range between 1 to 6 ppb while 6–10 ppb, 10–50 ppb and >50 ppb values were shown by 11, 8 and 12 samples, respectively. Statistical evaluation of raw uranium data has resulted in higher standard deviation (43.2 ppb) as compared to mean value of 11.5 ppb due to the nugget effect of samples with higher values (>50 ppb). These results lead to a higher estimate of threshold which masks most of the anomalies i.e., values higher than threshold. Hence, processed uranium data (without nugget values) were considered for all statistical evaluation and interpretations, which shows 1.7 ppb, 1.33 ppb and 4.36 ppb as mean, SD and threshold (Mean+2SD), respectively (Table 5). Similarly, U/Conductivity ratio of processed data indicated 1.45, 0.95 and 3.35 as mean, SD and threshold, respectively. A total of 39 anomalous uranium values above threshold (including samples with nugget values as they fall in the anomalous zone of processed data) have been

Table 4. General statistics of hydrogeochemical data.

| | U (ppb) | pH | Cond. (mmhos /cm) | Na | K | Ca | Mg | HCO ₃ | Cl | SO ₄ | PO ₄ | F |
|------|---------|------|-------------------|--------------------|-------|-------|-------|------------------|-------|-----------------|-----------------|-------|
| | | | | All values in mg/l | | | | | | | | |
| Max. | 330 | 8.2 | 2.67 | 575 | 99 | 425 | 130 | 700 | 290 | 500 | 23 | 3.8 |
| Min. | 0.25 | 5.2 | 0.35 | 3 | 0.5 | 5 | 5 | 50 | 10 | 10 | 0.5 | 0.5 |
| Mean | 11.5 | 7.13 | 0.96 | 56.46 | 4.66 | 72.95 | 33.4 | 333.7 | 56.12 | 21.08 | 2.28 | 0.6 |
| SD | 43.2 | 0.41 | 0.364 | 72.06 | 9.257 | 43.86 | 23.46 | 131.9 | 49.25 | 42.84 | 3 | 0.405 |

Table 5. Uranium statistics of Jabera dome area.

| | Uranium | U/Conductivity |
|------------------|---------|----------------|
| n | 184 | 179 |
| Mean | 1.7 | 1.45 |
| Std. Dev. | 1.33 | 0.95 |
| Threshold | 4.36 | 3.35 |
| No. of anomalies | 39 | 45 |

No. of samples in different class

| U (ppb) Class | No. of samples |
|---------------|----------------|
| 1-6 | 184 |
| 6-10 | 11 |
| 10-50 | 8 |
| 50-300 | 12 |

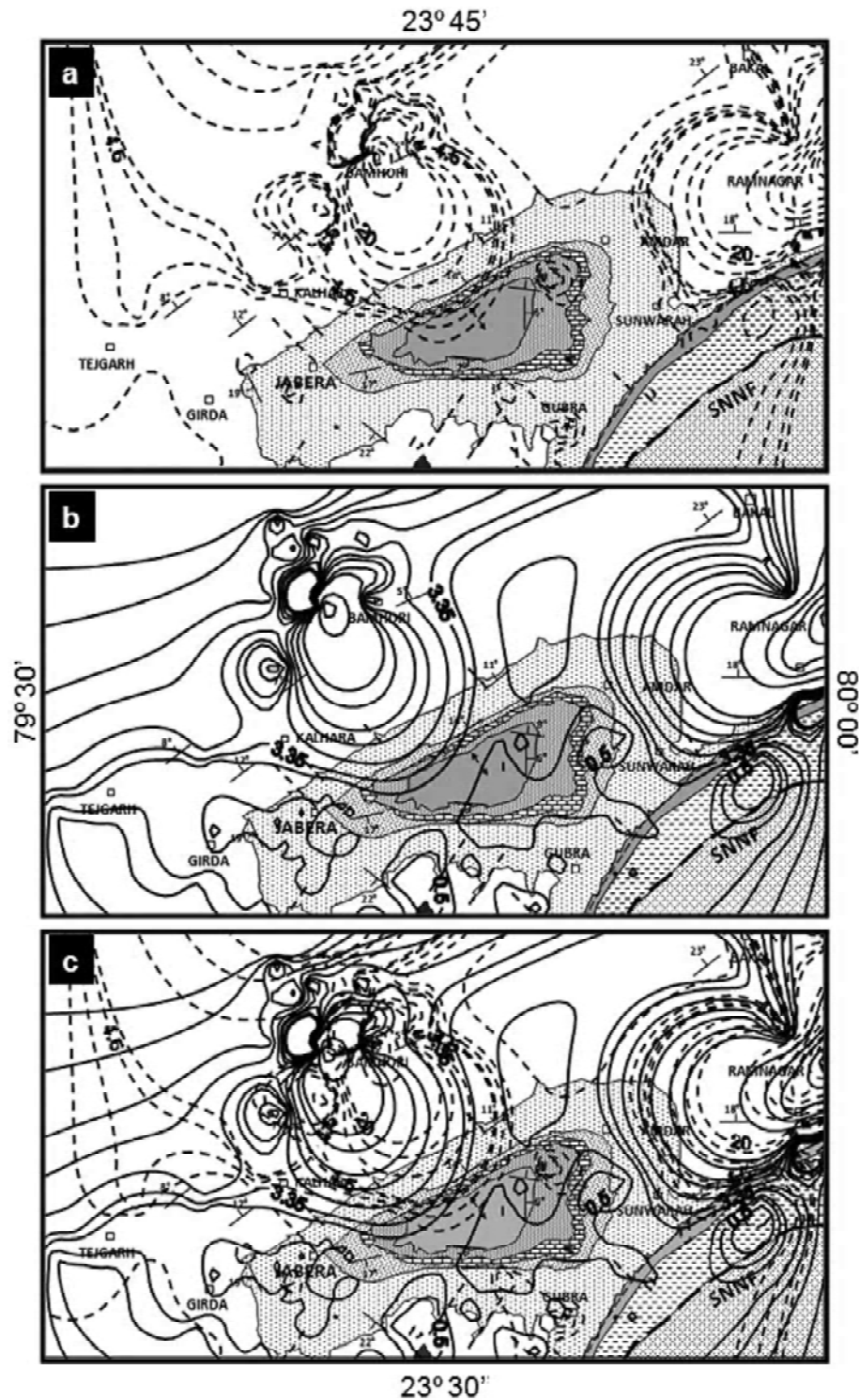


Fig. 2. Isoconcentration contours for Uranium (a), U/Conductivity (b) and superimposed U and U/Conductivity (c) in water, Jabera dome area.

DISCUSSION AND CONCLUSIONS

The application of hydrogeochemical survey as a tool for uranium exploration in a virgin area around Jabera dome has helped in narrowing down the target from 1000 km² to nearly 250 km² in two different segments.

These two zones namely, Bakal–Jharuli–Ramnagar and Patna–Bamhori–Teigarh sectors are confined within Upper Bhandar Sandstone Formation and located adjacent to northeastern and west-northwestern fringes of Jabera dome. In addition, ENE–WSW trending linear anomalous uranium cluster along Vindhyan–

- G.S.I. (1994). Geological Map of Jabalpur quadrangle, Madhya Pradesh (55M). Geol. Surv. India, Calcutta.
- G.S.I. (2001). District Resource Map (DRM) of Damoh district, Madhya Pradesh. Geol. Surv. India, Calcutta.
- Hitzman, M.W. (2000). Iron oxide-Cu-Au deposits: What, where, when, and why. In: Porter, T.M. (ed.), Hydrothermal iron oxide-copper-gold and related deposits: A global perspective. Adelaide, Australia, Australian Mineral Foundation, 9–25.
- Hitzman, M.W. and Valenta, R.K. (2005). Uranium in iron oxide-copper-gold (IOCG) systems. *Economic Geology*, 100, 1657–1661.
- Hostetler, P.B. and Garrels, R.M. (1962). Transportation and precipitation of uranium and vanadium at low temperatures, with special reference to sandstone type uranium deposits. *Economic Geology*, 57, 137–167.
- ISI (1991). Indian standard specification for drinking water. IS:10500, Indian Standard Institution, 1–5.
- Jain, S.C., Nair, K.K.K. and Yedekar, D.B. (1995). Geology of the Son–Narmada–Tapi lineament zone in Central India. *Geol. Surv. India, Spl. Pub.*, 10, 1–154.
- Jain, S.C., Nair, K.K.K. and Yedekar, D.B. (1995). Tectonic evolution of the Son–Narmada–Tapi lineament zone in Central India. *Geol. Surv. India, Spl. Pub.*, 10, 333–371.
- Jefferson, C.W., Thoma, D.J., Gandhi, S.S., Ramaekers, P., Delaney, G., Brisbin, D., Cutts, C., Portella, P. and Olson, R.A. (2007). Unconformity associated uranium deposits. In: Mineral Resources of Canada: a synthesis of major deposit types, district metallogeny, the evaluation of geological provinces, and exploration methods. *Geol. Soc. Canada*, 1–33.
- Khandelwal, M.K., Bisht, B.S., Tiwari, A., Dash, S.K., Mundra, K.L., Padhi, A.K., Nanda, L.K. and Maithani, P.B. (2008). Uranium–copper–molybdenum association in the Rohil deposit, North Delhi Fold Belt, Rajasthan. *Mem. Geol. Soc. India*, 73, 117–130.
- Langmuir, D. (1978). Uranium solution–mineral equilibria at low temperatures with applications to sedimentary ore deposits. *Geochim. Cosmochim. Acta*, 42, 547–569.
- Lisitsin, A.K. (1962). Form and occurrence of uranium in groundwaters and conditions of its precipitation as UO_2 . *Geokhimiya*, 9, 763–769.
- Lisitsin, A.K. (1971). Ratio of the redox equilibria of uranium and iron in stratiform aquifers. *Intl. Geol. Rev.*, 13, 744–751.
- Mahadevan, T.M. (1986). Space–time controls in Precambrian uranium mineralisation in India. *Jour. Geol. Soc. India*, 27(1), 47–62.
- Mahadevan, T.M. (1995). Identifying high-grade uranium deposits in the Proterozoic basins of India: A challenge to exploration. *Expl. Res. At. Min. (EARFAM)*, 8, 49–60.
- Maithani, P.B., Banerjee, Rahul, Panchal, P.K., Verughe, S.K., Ramachandran, S. and Singh, R. (1998a). Exploration for sandstone type uranium mineralisation in Mesozoic basins of Gujarat: a hydrogeochemical approach. *Jour. Indian Assoc. Sediment.*, 17(2), 263–270.
- Maithani, P.B., Gurjar, R., Banerjee, Rahul, Balaji, B.K., Ramachandran, S. and Singh, R. (1998b). Anomalous fluoride in groundwater from western part of Sirohi district, Rajasthan and its crippling effect on human health. *Current Science*, 74(9), 773–777.
- Maithani, P.B., Gurjar, R. and Banerjee, Rahul (2000). Application of hydro-geochemical technique as a guide for uranium exploration in Palri–Andor area, Sirohi district, Rajasthan. *Jour. Appl. Geochem.*, 2(2), 91–105.
- Miller, L.J. (1958). The chemical environment of pitchblende. *Economic Geology*, 53, 521–545.
- Malone, S.J., Meert, J.G., Banerjee, D.M., Pandit, M.K., Temrat, E., Kamenov, G.D., Pradhan, V.R. and Sohl, L.E. (2008). Paleomagnetism and Detrital Zircon Geochronology of the Upper Vindhyan sequence, Son Valley and Rajasthan, India: A ca. 1000 Ma closure age for the Purana Basins? *Precambrian Research*, 164, 137–159.
- Muto, T., Hirono, S. and Kurata, H. (1968). Some aspects of fixation of uranium from natural waters. *Japan Atomic Energy Research Institute Report, NSJ Translation No. 91.*, *Mining Geology (Japan)*, 15, 287–298.
- Nichols, C.E. (1984). Uranium exploration techniques. In: Uranium Geochemistry, Mineralogy, Geology, Exploration and Resources. *The Inst. Min. Met.*, 23–42.
- Pandey, D., Verma, A.K., Srinivasan, S., Bangroo, P.N., Kumar, M. and Singh, D. (1998). Hydrogeochemical exploration for uranium in parts of Bhiwani district, Haryana, India – a preliminary study. *Expl. Res. At. Min. (EARFAM)*, 11, 99–108.
- Rai, A.K., Zakaulla, S., Jaygopal, A.V., Vasudev Rao, M., Nagabhushana, J.C. and Vardaraju, H.N. (2002). Uranium mineralisation in the south-western part of the Cuddapah basin, Andhra Pradesh. *Expl. Res. At. Min. (EARFAM)*, 14, 79–94.
- Ramakrishnan, M. and Vaidyanadhan, R. (2008). *Geology of India (Vol. 1)*. *Geol. Soc. India*, 556p.
- Ray, J.S., Veizer, J. and Davis, W.J. (2003). C, O, Sr and Pb isotope systematics of carbonate sequences of the Vindhyan Supergroup, India: age, diagenesis, correlations and implications for global events. *Precambrian Research*, 121, 103–140.
- Ray, J.S. (2006). Age of the Vindhyan Supergroup: A review of recent findings. *Jour. Earth Syst. Sci.*, 115(1), 149–160.
- Samal, J.K. and Mitra, D.S. (2006). Field study of shear fractures – Its tectonic significance and application in hydrocarbon exploration – An example from Vindhyan basin. In: 6th International conference and Exposition on Exploration Geophysics, Kolkata 2006, 35–42.

Application of Multivariate Statistics - An Approach for Microenvironmental Zonation in a Tropical Tidal Flat of Chandipur, Orissa

SWETALINA PARHI

Department of Geology and Geophysics, I.I.T Kharagpur, West Bengal - 721302

E-mail: sweta.parhi@gmail.com

Abstract: The micro-zonation discrimination in a tidal flat environment only from grain size parameters has been done through multivariate statistics. It is observed that within a tidal flat setting, there is a tendency for the mean grain size to show randomness. With transport both off and onshore, the coarser and finer sediments are selectively removed. The coarser fractions are buried below the advancing sediments and the finer ones are transported further along and offshore while the intermediate size fraction takes active part in the distribution pattern. The finer admixture give rise to the fining-upward sequence and overlie a carpet of coarser materials. This leads to the generation of unimodality in the sediment distribution. The selective segregation of bed materials are the results of increase in energy conditions.

This mechanism provides a clue to the process of grain sorting in the studied tidal flat environment and the particle distribution is log-normal. In order to distinguish between environments having closely similar energy condition several discrimination function with their level of significance are established by multivariate analysis. Inference about the environment has been drawn from concordant relation between variation in sample statistics through space and/or time and environment of deposition. In this work, I have tried to discriminate among the four environments (i.e. coastal dune, beach face, Inter tidal bar and barred flat) on the basis of multivariate analysis.

Key words: Tidal flat, Size parameter, Multivariate statistics, Environment zonation

INTRODUCTION

Studies of sediment texture have been used to understand the depositional environment with an assumption that the size distribution of coarse clastic sediments is related to the fluidity (viscosity) factor of depositing medium and the energy factor of the environment (site) of deposition. There are a number of defects in the uses of the popular and commonly discussed bivariate plots for finding out the depositional environment (B.K. Sahu, 1983). Hence an attempt is made here to apply the method of multigroup discrimination to discriminate among the four environments i.e. coastal dune, beach face, inter tidal bar and barred flat region in Chandipur tidal flat, Orissa.

SIGNIFICANT PARAMETERS

For environment discrimination, parameter of significance must (a) be quantitative (b) discriminate among environments (to varying degrees) (c) be constant through time (not subject to diagenetic changes) (d) perfectly universal (measurable in all sediments both recent and ancient) (B. Greenwood, 1969).

The objective of this study is to obtain a number of sediment parameter (r) from a set of samples (n) on the basis of information available in ($r \times n$) matrix, solution to

the problem of discrimination of depositional environment is done.

STUDY AREA AND DEPOSITIONAL ENVIRONMENT

The area under investigation is Chandipur (21° 26'31" N 81° 1' 40" E), Orissa forms a part of the arcuate coastal stretch on the east coast of India, which is bounded between the deltaic bulges of the river Subarnarekha in the northeast and the compound delta of the rivers Baitarani and Brahmani in the southwest (Fig. 1).

The coastal region under study can be broadly divided into two morphozones: namely zone A and zone B.

Zone A is the land ward most zone characterised by a monotonous low level mainly modified by fluvial processes of the river Burahbalang resulting in formation of point bars, natural levees, channel islands etc.

Zone B is the sea ward zone comprising marine terraces, coastal dune belt, tidal creeks and tidal flat with inter-tidal bars.

COASTAL DUNE

The coastal dune system is continuous and co-extensive with the coastal trend. This dune belt like most of the coastal dunes of California (W.S. Cooper, 1967)

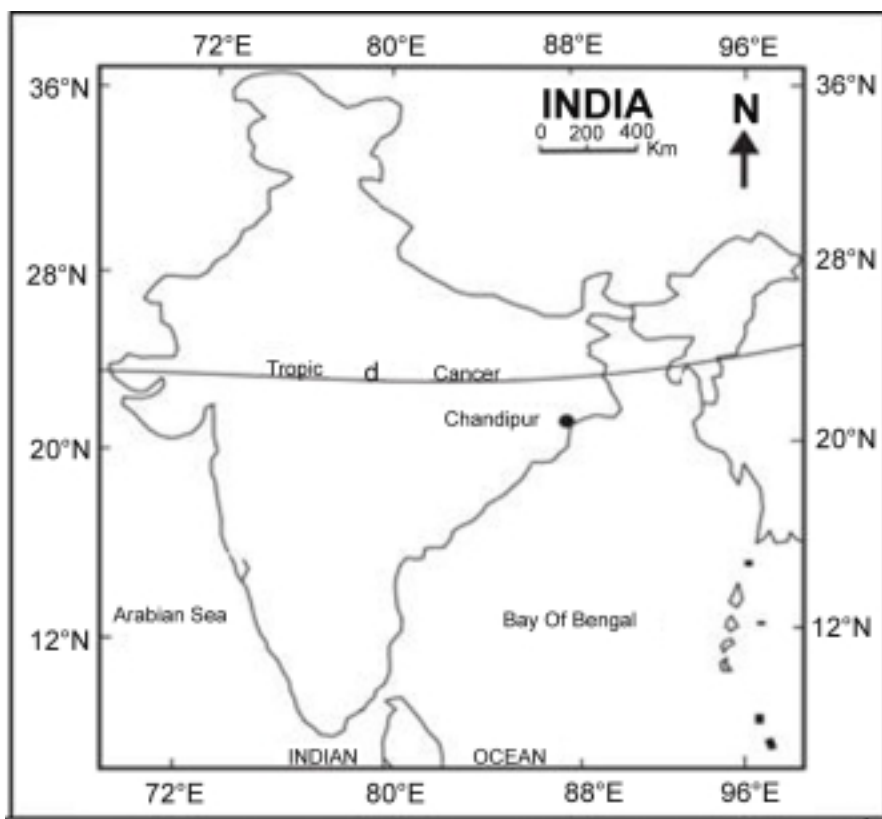


Fig. 1. Area of Investigation in Indian map.

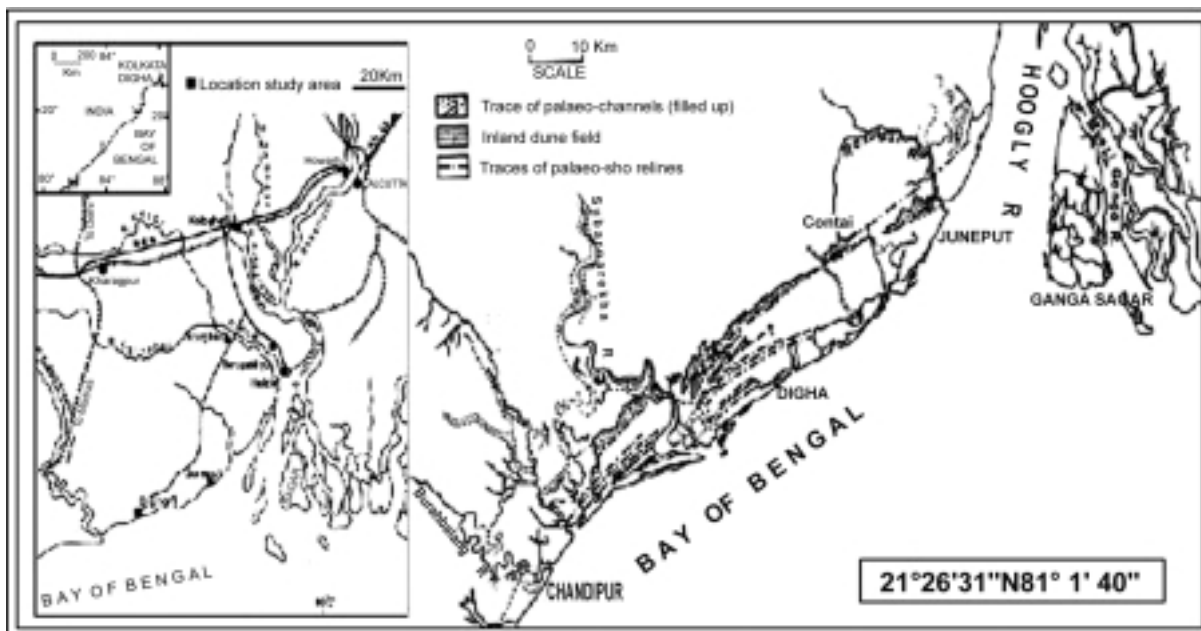


Fig. 2. Geology of the area.



Fig. 3. Satellite image of the study area (Source: Google Earth, Date: 11.08.2007).

belongs to parallel wavy dunes (E.D. McKee, 1980). The land ward margins of these dune ridges are marked by irregular tongues and lobes. Dune heights vary from place to place. The maximum height recorded is about 15 meters.

TIDAL FLAT

Consist of two sub-environments i.e., beach face zone and planar flat zone.

Beach face zone

Flanked by the coastal dune and fronted by a wide near horizontal platform, the beach face is characterized by a sandy texture. The beach face slope varies between 4° and 6° and direction of the slope is towards east.

In spite of the homogeneous appearance, this zone exhibits considerable variation in sediment texture. There is a distinct difference in the sediment texture between the upper and the lower beach faces. The fine sand content in the sediment of the upper beach face is more in contrast to that of the lower beach face.

Planar flat zone

This zone has been laterally subdivided into (a) non-barred planar flat (b) planar flat ornamented with inter-tidal bars.

Non-barred planar flat

These are monotonous plane surfaces. Two tidal channels of moderate width (avg. 45 m during low tide

time) and low depth (avg 0.50 m), one close to the beach face running parallel to the shore, and the other restricted to the mid flat of the region and running oblique to the shore. Transverse furrows (runnels) of low depth related to rainwater draining are also seen to be developed in the mid flat region, during the monsoon months.

Barred planar flat and inter-tidal bar

The smoothness of planar flat is virtually lost due to the presence of inter tidal sand bodies clustered near the river. Except the triangular sand body located at the mouth of the main channel, these bars are aligned parallel to the shore and are cusped or tadpole shaped. They are mostly necked out towards the river Burahbalanag.

BI-VARIATE PLOTS

From the graph it is evident that the various combinations of textural parameters, neither brings out any co-relation between them, nor they are effective in discriminating the beach face and the barred environment of tidal flat. Even the negative relation between the mean size and the standard deviation is not visible for the beach face (Fig-7) sediments though such a relation is faintly observed in the barred flat environments (Fig-13).

LINEAR DISCRIMINATE ANALYSIS

Although the barred planar flat encompasses a wide range of energy condition, discriminant analysis has been done for the environments coastal dune, beach face, inter tidal bar and barred flat together.

Coastal Dune

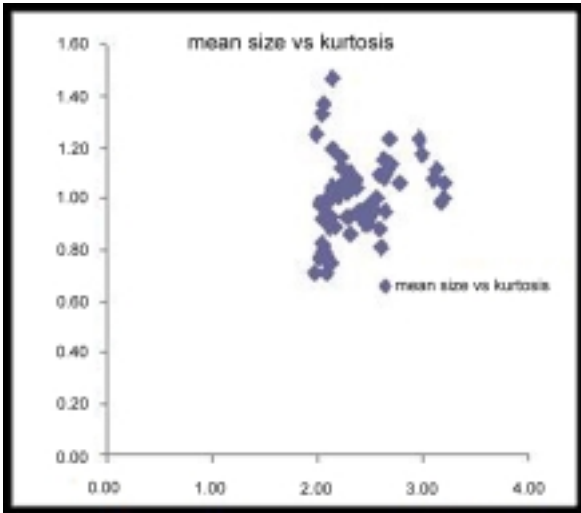


Fig. 4. Bi-Variate Plot of Mean Size vs. Kurtosis.

Beach Face

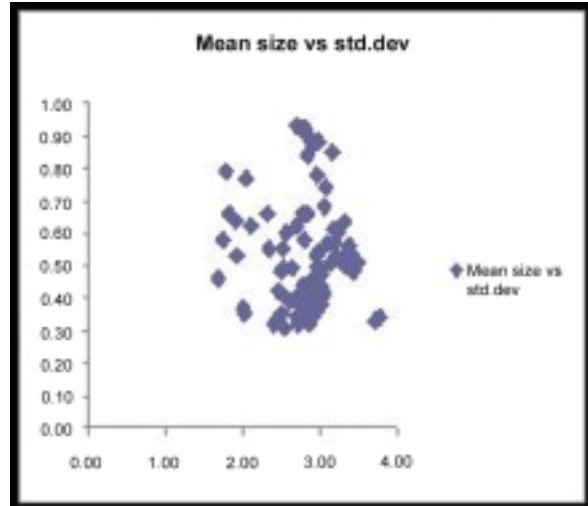


Fig. 7. Bi-Variate Plot of Mean Size vs. Std. Deviation.

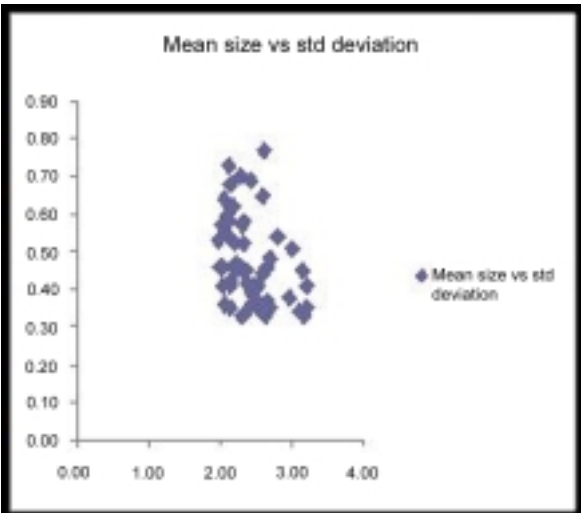


Fig. 5. Bi-Variate Plot of Mean Size vs. Std. Deviation.

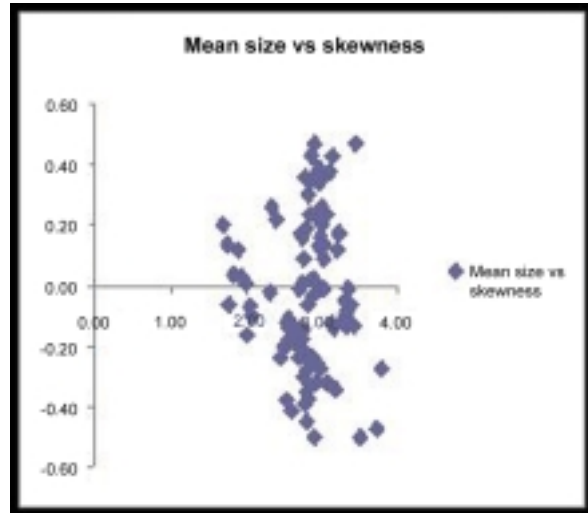


Fig. 8. Bi-Variate Plot of Mean Size vs. Skewness.

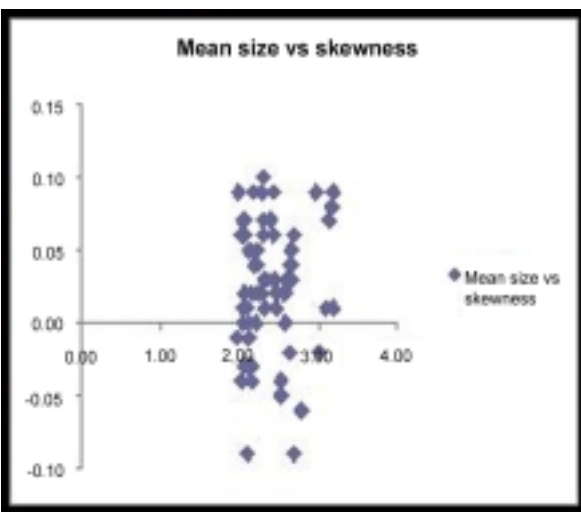


Fig. 6. Bi-Variate Plot of Mean Size vs. Skewness.

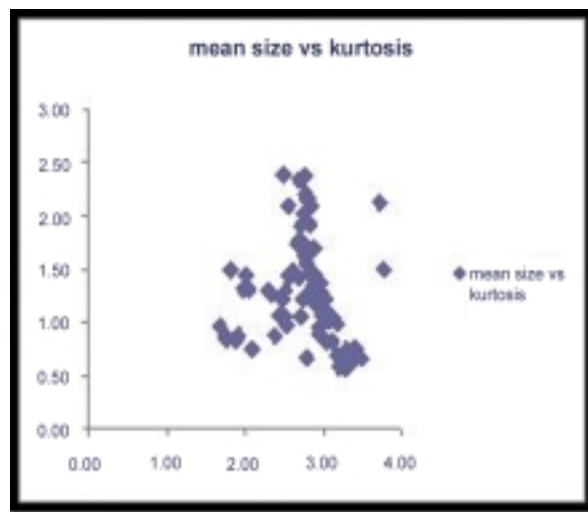


Fig. 9. Bi-Variate Plot of Mean Size vs. Kurtosis.

Inter Tidal Bar

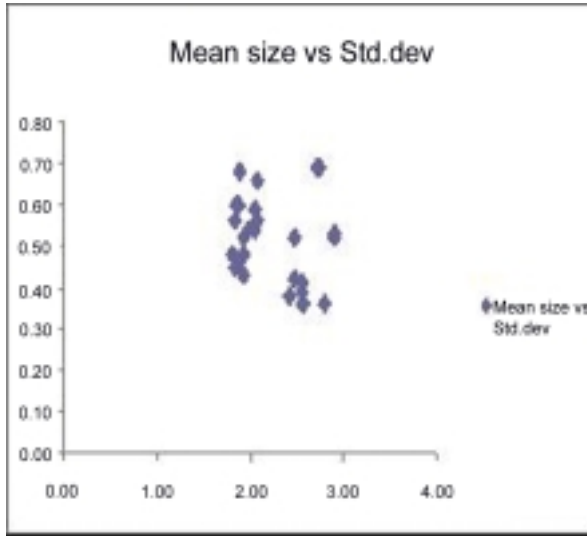


Fig.10. Bi-Variate Plot of Mean Size vs. Std. Deviation.

Barred Flat

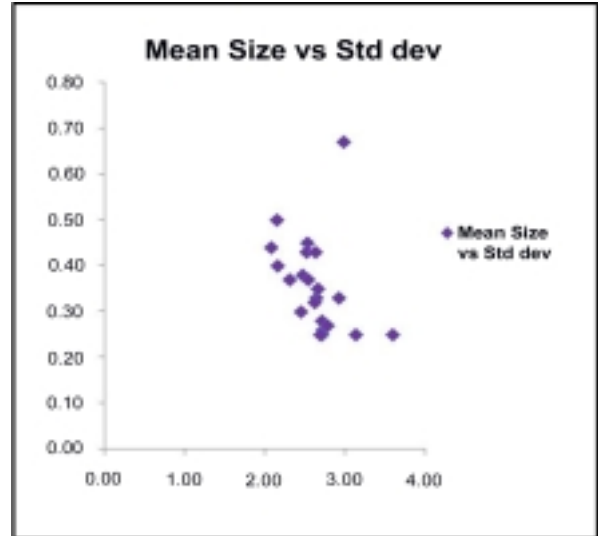


Fig. 13. Bi-Variate Plot of Mean Size vs. Std. Deviation.

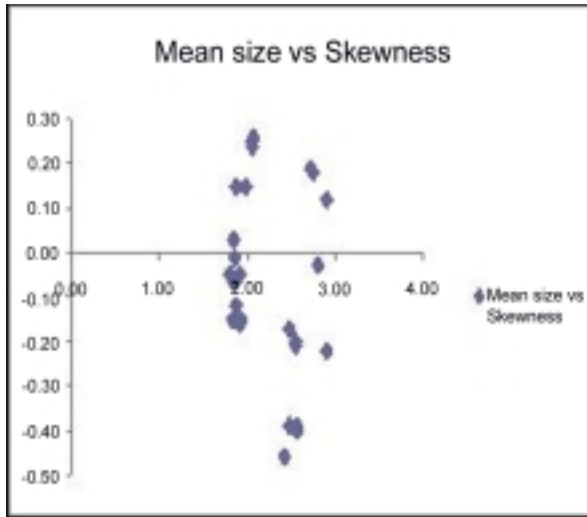


Fig. 11. Bi-Variate Plot of Mean Size vs. Skewness.

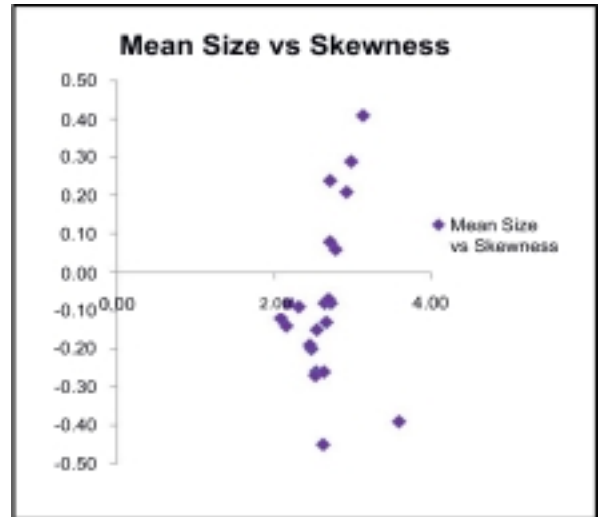


Fig. 14. Bi-Variate Plot of Mean Size vs. Skewness.

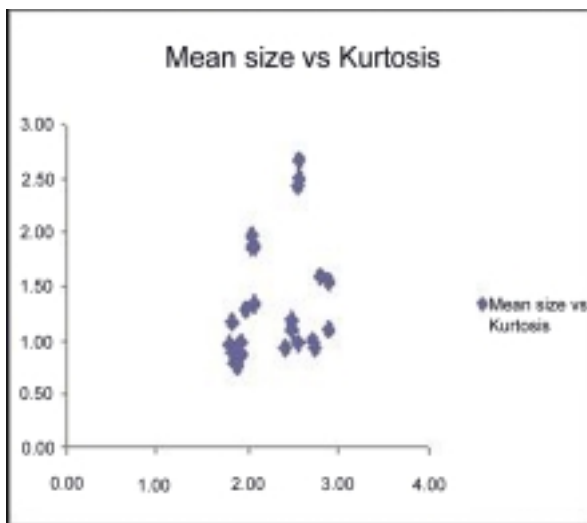


Fig. 12. Bi-Variate Plot of Mean Size vs. Kurtosis.

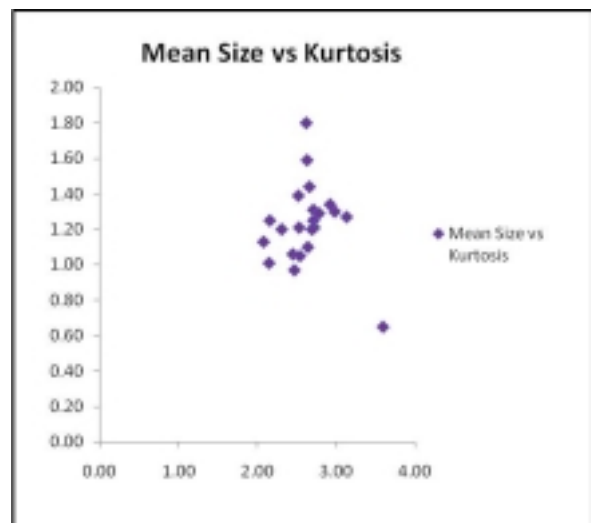


Fig. 15. Bi-Variate Plot of Mean Size vs. Kurtosis.

RESULTS AND DISCUSSION

Using SAS software, the discriminant analysis for the micro environmental zonation has been done. The SAS program and partial output of the data which includes the values of discriminate indices, Mahalanobis distance (D²) (P.C. Mahalanobis 1927, 1930) and the frequency distribution of overlapped observation and many more contextual statistics have been shown below.

SAS program:

Table 1. SAS Code for the Analysis.

```
proc discrim data=envdata wcov pcov
method=normal
           pool=test simple distance
           canonical anova listerr;
class env;
priors prop;
var mean sd skew krts;
run;
```

In this program (Table 1) wcov and pcov option provides within and pooled covariance matrices assuming homogeneity in variance among the class. The "priors as prop" options are included to emphasize the proportional sample size. The "listerr" option provides the list of misclassification.

From the first snapshot of the output (Table 2), we

can see that, there are 207 sample observations present. We can also see that four variables (viz. mean, standard deviation, skewness and kurtosis) are playing their role to being a most significant variable to discriminate among four classes/environments (viz. coastal dune, inter tidal bar, beach face and barred flat). The degree of freedom indicates the number of independent observations to estimate the variables respectively. For example, there are three linearly independent equations exist to estimate the four classes.

In the class level information, we can see that basic statistics of the four classes whereas from the simple statistics of the total sample we can get the basic statistics of the four variables.

In this snapshot of the output (Table 3) we are concentrating in within class and pooled covariance matrices. This is because of the fact that the values of these matrices indicate the well-sorted (small variance) behaviours of the samples. Within the class covariance matrices of each of the classes, if we go through the diagonal which is actually the variance of the respective variables, we can say that the values are very small which in turn indicates that the samples of the corresponding classes are very much well-sorted (Fig. 16). But from the within class covariance matrices we cannot say that whether the classes as a whole closely/widely distributed or not. Whereas, pooled covariance matrix can solve this confusion. The small values of diagonal of the pooled covariance matrix indicate that as a whole the classes are also closely distributed. So, from this discussion we have an idea of overlapped distribution of the environments (Fig. 17).

Table 2. SAS Output (partial). Descriptive Statistics for all four Environments.

Table 3. Within-Class Covariance Matrices for all four Environments.

The DISCRIM Procedure

Within-Class Covariance Matrices

env = barred_flat, DF = 21

| Variable | Label | mean | sd | skew | krt5 |
|----------|-------|--------------|--------------|--------------|--------------|
| mean | mean | 0.1128538961 | -.0118220779 | 0.0171841991 | -.0111363636 |
| sd | sd | -.0118220779 | 0.0105774892 | -.0002636364 | 0.0022632035 |
| skew | skew | 0.0171841991 | -.0002636364 | 0.0467396104 | 0.0029173160 |
| krt5 | krt5 | -.0111363636 | 0.0022632035 | 0.0029173160 | 0.052251082 |

env = beachface, DF = 92

| Variable | Label | mean | sd | skew | krt5 |
|----------|-------|--------------|--------------|--------------|--------------|
| mean | mean | 0.09902275 | 0.01402810 | 0.0460892857 | -.010103621 |
| sd | sd | 0.0790380952 | -.0231783069 | -.0109386243 | 0.3118804233 |
| skew | skew | 0.0003462678 | -.0045604212 | 0.0398711336 | -.0090571517 |
| krt5 | krt5 | 0.0003462678 | -.0045604212 | -.0090571517 | 0.1505521574 |

Fig. 16. Non-overlapped clustered sample.

Fig. 17. Overlapped clustered sample.

Pooled Within-Class Covariance Matrix, DF = 203

| Variable | Label | mean | sd | skew | krt5 |
|----------|-------|--------------|--------------|--------------|--------------|
| mean | mean | 0.1453553920 | -.0092404147 | -.0016867186 | 0.0003462678 |
| sd | sd | -.0092404147 | 0.0196380646 | 0.0039767851 | -.0045604212 |
| skew | skew | -.0016867186 | 0.0039767851 | 0.0398711336 | -.0090571517 |
| krt5 | krt5 | 0.0003462678 | -.0045604212 | -.0090571517 | 0.1505521574 |

Table 4. Homogeneity Test of Within Class Covariance Matrices.**Table 5.** Homogeneity Test of Within Class Covariance Matrices Contd...

In this output (Table 4&5) we have tested the homogeneity assumption upon within the class covariance matrices. The typical chi-square test indicates that there is no harm if we use within class covariance matrices in our further analysis.

Here (Table 6) we are getting the squared distance between the groups which indicates the distance from one group to other. In the first matrix, we can see that all the diagonals are zero which is very obvious according to the formula. But in the generalised square distance, we can see that the diagonals are having some significant values which are nothing but the distance which we can infer through our prior knowledge (probability, which depends on the sample size). In the virtue of relativity, we can infer that except coastal dune the other three environments are positioned (overlapped) very close to each other.

In this output (Table 7) we are trying to identify the

most significant variable among the four variables (viz. mean, standard deviation, skewness and kurtosis). From the F-values of the four variables we can say that except skewness the other three can able to discriminate among the four environments (B.K. Sahu, 1983). But, we cannot say among these three variables which is the most significant one.

In this output (Table 8) we can see the result of canonical discriminant analysis where we trying to make some variables by linear combinations of three variables mean, standard deviation and kurtosis which are highly correlated. The idea of this analysis is that when a set of discriminating variables are highly correlated, we are trying to make some variables out of those original variables as linear function such that the first one will explain the maximum correlation and so on. Among these new variables, any one may alone discriminate the classes. But from the lower half of the output, we can

Table 6. Mahalanobis Distances for all four Environments.

| Pairwise Squared Distances Between Groups | | | | | | | | | |
|---|-------------|--------------------|-------------------|--------------------|--------------------|-----------|--------------------|---------|--------|
| F2Statistics, _Num DF=3,1 Den DF=203 | | | | | | | | | |
| D (i j) = (X - X)' COV (X - X) | | | | | | | | | |
| Total j | | | | | | | | | |
| Variable | Label | Standard Deviation | Squared Deviation | Standard Deviation | Standard Deviation | R-Square | R-Square / (1-RSq) | F Value | Pr > F |
| | | From env | flat | beachface | cstl_dune | intdl_bar | | | |
| mean | mean | 0.4392 | 0.3813 | 0.2567 | 0.2575 | 0.3468 | 23.47 | <.0001 | |
| sd | barred_flat | 0.1471 | 0.1401 | 1.11445 | 8.05075 | 0.1176 | 8.86654 | <.0001 | |
| skew | beachface | 0.2010 | 3.59047 | 0.1997 | 0.0381 | 0.0278 | 2.82235 | 0.1341 | |
| krts | cstl_dune | 0.4059 | 3.36441 | 0.3880 | 1.60094 | 0.0995 | 2.72781 | <.0001 | |
| | intdl_bar | | 2.92565 | 1.89140 | 9.09248 | | 0 | | |
| Pairwise Generalized Squared Distances Between Groups | | | | | | | | | |
| Average R-Square | | | | | | | | | |
| D (i j) = (X - X) Unweighted COV (X - X) + In COV - 2 In PRI OR | | | | | | | | | |
| Weighted by Variance | | | | | | | | | |
| Generalized Squared Distance to env | | | | | | | | | |
| | | From env | flat | beachface | cstl_dune | intdl_bar | | | |
| | barred_flat | | -8.48318 | -6.95490 | -6.67224 | 0.79993 | | | |
| | beachface | | -4.89271 | -8.06935 | -4.62232 | -5.24426 | | | |
| | cstl_dune | | -5.11877 | -6.46841 | -14.72299 | -5.33880 | | | |
| | intdl_bar | | -5.55753 | -6.17795 | -5.63051 | -8.06661 | | | |

Table 7. Uni-Variate test Statistics Table for all four measures.

Table 8. Canonical Discriminant Analysis.

Table 9. Table of Misclassified sample with probability of being classified in any of the four environments.

Table 10. Cross Table of frequency of sample for classified sample.

| Number of Observations and Percent Classified into env | | | | |
|--|--------------|-----------|-----------|-----------|
| From env | barred_ flat | beachface | cstl_dune | intdl_bar |
| barred_ flat | 13 | 6 | 4 | 0 |
| beachface | 4 | 10 | 9 | 0 |
| cstl_dune | 0 | 0 | 21 | 0 |
| intdl_bar | 0 | 0 | 0 | 5 |
| Total | 17 | 16 | 21 | 5 |
| Priors | 0.1063 | 0.4493 | 0.3092 | 0.1353 |
| Rate | 0.8636 | 0.1505 | 0.2031 | 0.8929 |
| Priors | 0.1063 | 0.4493 | 0.3092 | 0.1353 |

have the following observations like, (i) all the three eigen vectors are significant, (ii) From the cumulative proportion of the correlation, we can say that first two eigen vectors can explain almost 90% of the total correlation and (iii) there is no significant difference between the second and third eigen vectors in terms of explaining the correlation. Since the explaining power of the eigen vector in terms of total correlation is not decreasing drastically we have to consider all of them as a discriminant function. So, even from canonical analysis we cannot able to find out a single discriminant function.

In this typical snapshot (Table 9) of the output we are trying to predict the probability of each of sample being classified correctly or not. It is sample level output where for each of the sample we are calculating the probability of being classified in each of the environments. For example, the first observation collected from the coastal dune has a probability of being classified into barred flat, beach face, inter tidal bar and coastal dune itself are 0.2277, 0.3967, 0.0879 and 0.2877 respectively.

In this result (Table 10) we are demonstrating the number of observations and the percentage of the sample

classified/misclassified into four environments collected from a particular environment. For example, out of 22 samples collected from barred flat environment, classified into barred flat, beach face, coastal dune and inter tidal bar are 3, 10, 9 and 0 respectively. So, if we go through the diagonal of this typical arrangement we will get the statistics correctly classified samples. From this output we can infer that though most of the samples collected from beach face and coastal dune are rightly classified we cannot rule out our initial inference of overlapping distribution of environments.

The Mahalanobis distance is a measure of separation between two discriminant indices expressed in units of the pooled variance. The near sameness of the values of discriminant indices and low values of D2 which are significant even at 1% level of confidence are indicative of a strong overlap.

Finally we can say that, although the data show strong overlapping, through the result of discriminant analysis as shown above, it can be concluded that mean, standard deviation and kurtosis are the fairly significant parameters for micro-environmental discrimination within a tidal flat environment which is not the case for skewness.

CONCLUSION

There is a wide range of overlap in the size parameters of sediments in different sub environments in the Chandipur tidal flat. These sub environments cannot be totally differentiated through discriminant analysis using sediment size parameters as variables because of constant winnowing and remixing of sediments by physical

process, frequent addition of river borne mud and dune sediments through cliff erosion. The reason behind this partial failure provides a clue to the process of grain sorting in the studied tidal flat environment and as the particle distribution is log-normal. In order to distinguish between environments having closely similar energy condition therefore multiple discrimination functional analysis has to be repeatedly used.

References

- Cooper, W.S. (1967): Coastal Dunes of California: Geol. Soc. Amer. Mem. 104, 131c.
- Greenwood, B. (1969): Sediment parameter and environment discrimination: An application of multivariate statistics; Can. Jour. Earth sciences, 6, 1347-1358.
- Mahalanobis, P.C. (1927): Analysis of race mixtures in Bengal: Jour and Proc. Asiatic Soc. Bengal, 23, 301-333.
- Mahalanobis, P.C. (1930): On tests and measures of group divergent: Jour. Asiatic Soc. Bengal, 24, 541-588.
- Mckee, E. D. (1980): Global sand seas: U.S. Geol. Survey. Process. Pap, 1052, 429c.
- Sahu, B. K. (1983) Multigroup discrimination of dispositional environments using size distribution statistics. Indian Journal of Earth Science, 10(1), 22-29.

Sedimentological Studies of Cores from a Well in Krishna-Godavari Basin, Offshore India

SUNIT K. BISWAS, RAJESH K. PATIL and RITURAJ K. DUBEY

Gujarat State Petroleum Corporation Ltd., GSPC Bhavan, Gandhinagar, Gujarat 382010

E-mail: sbiswas@gujaratpetro.com

Abstract: Krishna-Godavari Basin, offshore India, has become one of the foremost exploration targets after major oil and gas discoveries were made in the sedimentary successions, spanning in age from Mesozoic to Cenozoic era in various depositional set-ups. Understanding of these sedimentary depositional settings enables to resolve the reservoir heterogeneities and to reconstruct the depositional environment. The conventional cores provide an opportunity to directly investigate the litho-facies, micro structural controls and heterogeneities in the sedimentary characteristics. The present study aims to produce an integrated sedimentology and an interpretation of the core data from a well in the Krishna-Godavari Basin, offshore India.

Detailed sedimentological work was carried out on the cored succession and major recurring litho-facies associations were identified. The lower and middle core sections are characterized by a series of fluvial channel lithofacies association, varying from a moderate sinuosity, anastomosing fluvial system to a lower sinuosity braided system. The upper core section largely comprises stacked muddy and sandy hetero-lithics, suggesting its deposition within a delta front setting. This is corroborated with the notable lack of bioturbation, extensive soft-sediment deformation and dominance of bed-forms indicating wave and storm activity.

Keywords: Conventional cores, Delta, Fluvial system, Mesozoic depositional environment, Krishna-Godavari basin.

INTRODUCTION

The offshore segment of the Krishna Godavari (KG) basin records the presence of huge sedimentary succession, spanning in age from Mesozoic to Cenozoic eras in various depositional set-ups. These sedimentary depositional settings are needed to be studied thoroughly, in order to resolve the reservoir heterogeneities and to reconstruct the depositional environment. Owing to this, the conventional cores from a well in the Krishna-Godavari Basin have been taken up in the present study to investigate the litho-facies, micro structural controls and heterogeneities in the sedimentary characteristics.

KRISHNA GODAVARI BASIN

The KG-Basin, wherein, the study area (Fig. 1) is a part, was a major intra-cratonic rift within Gondwanaland until Early Jurassic (Rao, 2001). It records the history of the breakup of east Gondwana in the Mesozoic (Curry and Murre, 1971, Subrahmanyam and Chand, 2006) and the northerly drift of India from the early Cretaceous (Gordon et al., 1990) to its Eocene collision with Eurasia (Srivastava and Chowhan, 1987) and contains thick sequences of sediments with several cycles of deposition ranging in age from Late Carboniferous to Holocene (Rao, 2001). Tectonically, KG basin has been studied by many workers (Rao et al., 1993, Rao, 2001, Gupta, 2006). It is an ENE-WSW trending peri-cratonic, passive margin basin which is juxtaposed orthogonally on the south eastern extension of NNW-SSE trending Pranhita-Godavari

basin, containing Gondwana sediments. The KG basin extends from land to the shelf-slope and adjacent deep sea area along the eastern passive continental margin of India. It includes the deltaic plains of the Krishna and Godavari rivers and the inter-deltaic regions. Archaean crystalline basement and late Cretaceous sedimentary outcrops demarcate the northwestern basin margin.

METHODOLOGY

A total of 136.80m of cores from one of the several drilled wells, within the study area, were viewed and logged. Features were recorded at 1:50 scale from the slabbed cores as well as their photographs. The features documented, comprised the following observations: lithology; bed boundaries and measured bed thickness; grain shape and size; sedimentary structures, including type and scale; sorting; clay content; matrix cementation or relative indurations, composition, morphology (e.g. nodular, beds etc). Logged biogenic and sedimentological features are grouped into lithofacies, and are described and interpreted in terms of depositional processes and environments, based on their stacking patterns.

LITHOFACIES

A lithofacies coding scheme has been used for this study and five major recurring lithofacies, along with associated sub-lithofacies, have been identified (Table 1), which are described in detail in the following paragraphs.

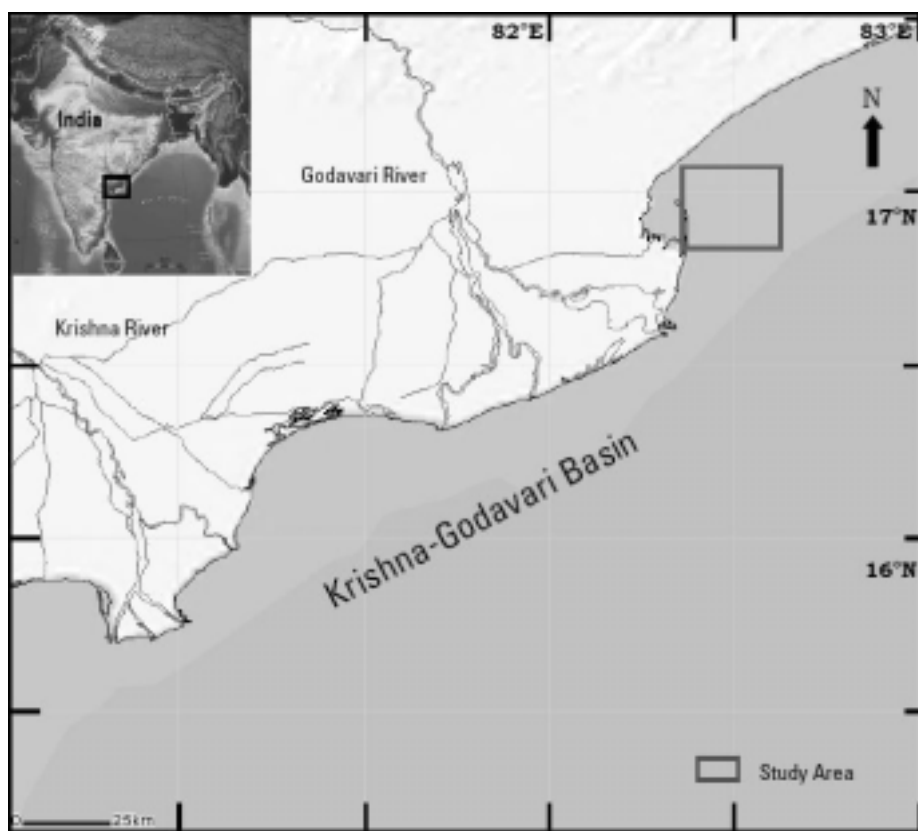


Fig 1. Location map of the study area.

Table 1. Lithofacies along with coding scheme for the study.

| Litho-Facies | Symbol | Sub-Lithofacies |
|------------------------|--------|-------------------------------|
| Conglomerate | CO | ---- |
| Cross Bedded Sandstone | Sp | Planar Cross Bedded Sandstone |
| | St | Trough Cross Bedded Sandstone |
| Sandstone | Slm | Laminated Sandstone |
| | pedSm | Pedogenic Massive sandstone |
| Siltstone | Zlm | Laminated Siltstone |
| Claystone | Clm | Laminated Claystone |

Lithofacies CO-Conglomerate

This lithofacies is characterized by pebble sized and cobble-sized, sub-rounded to sub-angular, clasts in a coarse sandy matrix (Figure 2A). Clasts comprise quartzite and sandstone intraclasts, cemented siltstone clasts with occasional lithic fragments. The lithofacies typically displays horizontal or high-angle stratification.

Lithofacies Sp-Planar cross-bedded sandstone

This lithofacies is characterized by coarse to medium sized, moderately sorted, angular to sub-rounded sandstone. This unit is medium to thickly bedded with steeply dipping fore-sets (Figure 2B). Bed boundaries are also highly inclined. Some of the bed bases contain granule- to pebble size lags. Varying amounts of mudstone rip-up clasts, wood fragments and carbonaceous fragments are also observed.

Lithofacies St-Trough cross-bedded sandstone

This lithofacies is characterized by thinly to thickly bedded, fine to coarse, moderately to well sorted, sub-angular to sub-rounded sandstones with small and large scale trough cross-beds (Figure 2C). Lags occur at places

and contain carbonaceous detritus. Micaceous, rip-up clasts and plant detritus are also commonly observed. Trough cross-bedding is formed by migrating dunes in shallow water settings reflecting subaqueous to sub-aerial environments. Soft sediment deformation suggests rapid sedimentation.

Lithofacies Slm-Laminated sandstone

This lithofacies is a rare lithofacies in the study, comprising very thinly bedded, well to very well sorted, fine to medium, sub-angular to sub-rounded, parallel laminated to low-angle cross-laminated sandstones (Figure 3A). Minor carbonaceous flecks are common throughout. At places, the laminae appear wavy, associated with slight soft sediment deformation. These laminated sandstones seem to be deposited via weak traction currents.

Lithofacies pedSm-Pedogenic massive sandstones

This lithofacies comprises massive sandstones with loss of primary bedding fabric associated with pedogenesis (Figure 3B). Remnant rootlets are also common within these sandstones. The rootlets suggest emergence or near emergence from zones just above these sandstones.

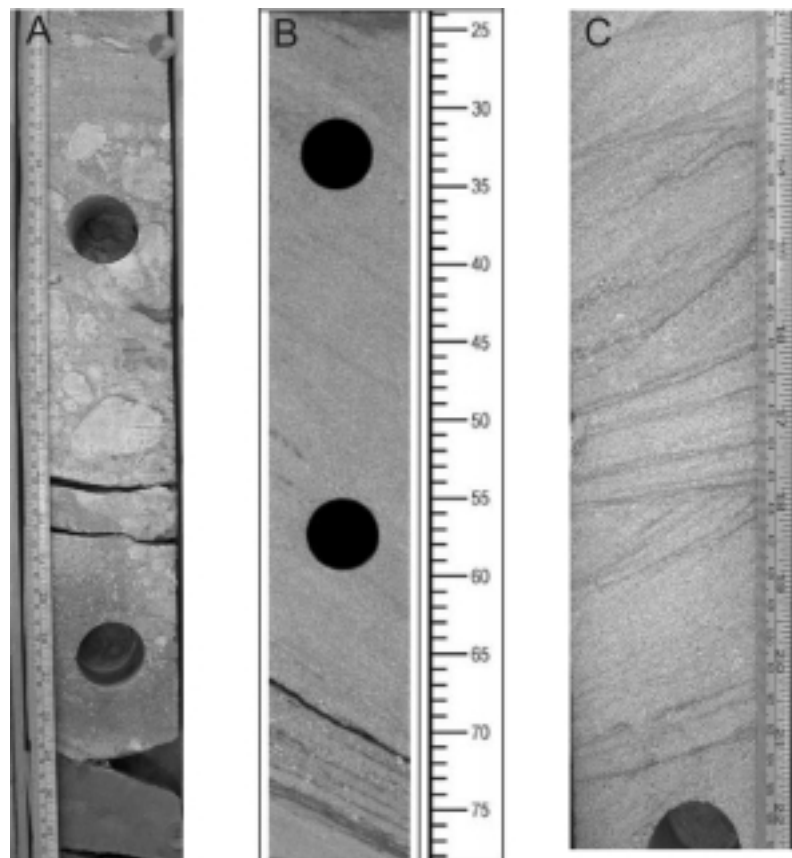


Fig 2 A. Conglomerate, **B.** Planar-, granules are abundant towards the base, and **C.** Trough Cross-bedded lithofacies in core.

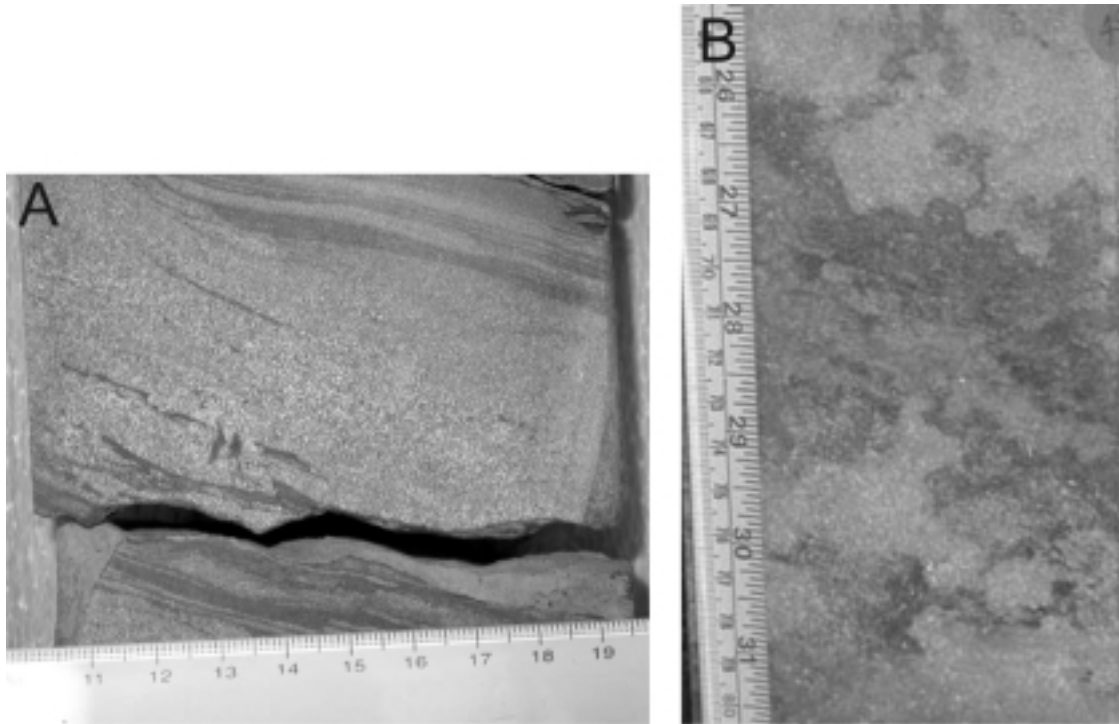


Fig 3 A. Fine-grained sandstone with low-angle lamination, **B.** Massive sandstone associated with Pedogenesis.

Lithofacies Zlm-Laminated siltstones

This lithofacies (Figure 4A) comprises carbonaceous laminated dark grey siltstones, often with high sand content and at places; remnant rootlets are also visible (Figure 4B). The siltstones, interlaminated with claystones, represent deposition dominantly by suspension in a low-energy setting. The presence of rootlets locally suggests emergent or near emergent conditions and the development of a palaeosol.

Lithofacies Clm-laminated claystones

Finely laminated, dark grey claystones characterize this lithofacies (Figure 4C). This lithofacies is rare in the section. The dominance of mud indicates low energy conditions, where sediment settles out of suspension.

LITHOFACIES ASSOCIATIONS

The lithofacies can be grouped into six different lithofacies associations. These lithofacies associations have been defined in the following paragraphs.

Delta front lithofacies association

This facies association comprises dominantly siltstones and claystones with thin parallel- and ripple laminated sandstone units and thin mm-scale stringers, at base (distal delta front), grading upward into a series of stacked, parallel-laminated sandstones alternating with

laminated mudstones at the top (proximal delta front). The sandstone units represent the bed boundaries of relatively high energy condition, whereas, silts and clays represent accumulation from suspension during fair weather periods. The lack of bioturbation in the system suggests a substantial freshwater influx, a feature which is common at the delta front. The upward coarsening and thickening succession of sandstone beds further corroborates the delta front setting. This association is only seen in upper Core-section (Figure 5).

Unconfined fluvial channel fill

This lithofacies association is characterized by dominantly medium to coarse trough and planar cross-bedded and horizontally stratified sandstones and matrix-supported conglomerates (Figure 6). Many of the sandstones are highly granular and pebbly throughout, with numerous granule- and pebbly-rich lags (Figure 6). Trough cross-bedding is the most common structure, with thicknesses of sets decreasing upwards, from 30-100cm thick, to 3-10cm thick. These deposits are characterized by a lower erosive surface, often overlain by a conglomerate or conglomeratic lag, and overlain by a fining-upward unit of medium to coarse sandstones. This lithofacies association occurs only in lower core-section. These deposits are thought to represent the deposits of an unconfined braided-type fluvial system, wherein, the coarse grain sizes, such as gravels and coarse sand, form the dominant load and they are typically overlain by thickly bedded trough cross-bedded

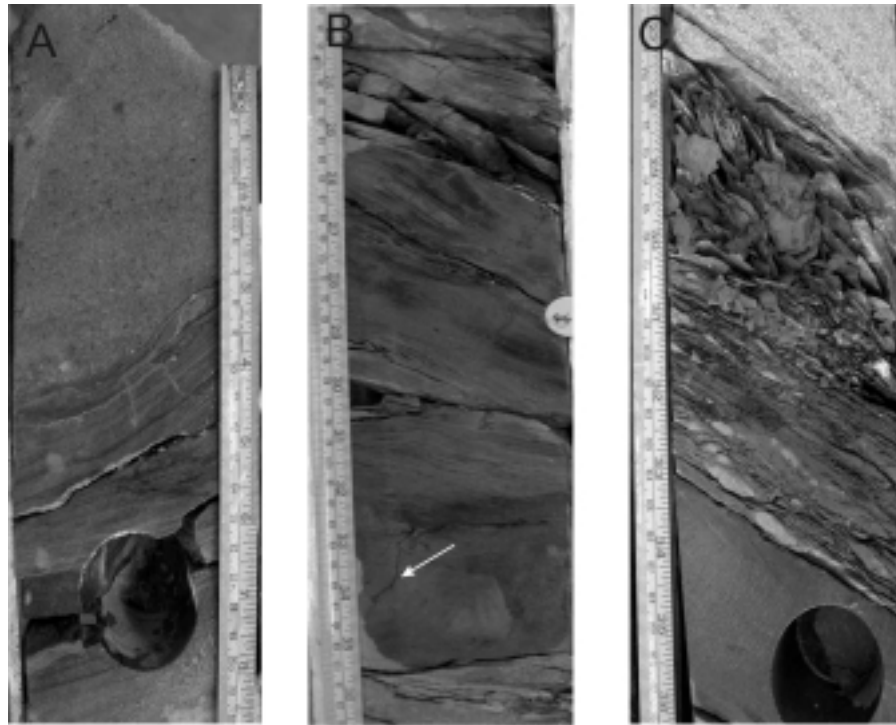


Fig 4A. Laminated siltstone, B. with rootlets, indicated with an arrow, and C. Laminated claystone.

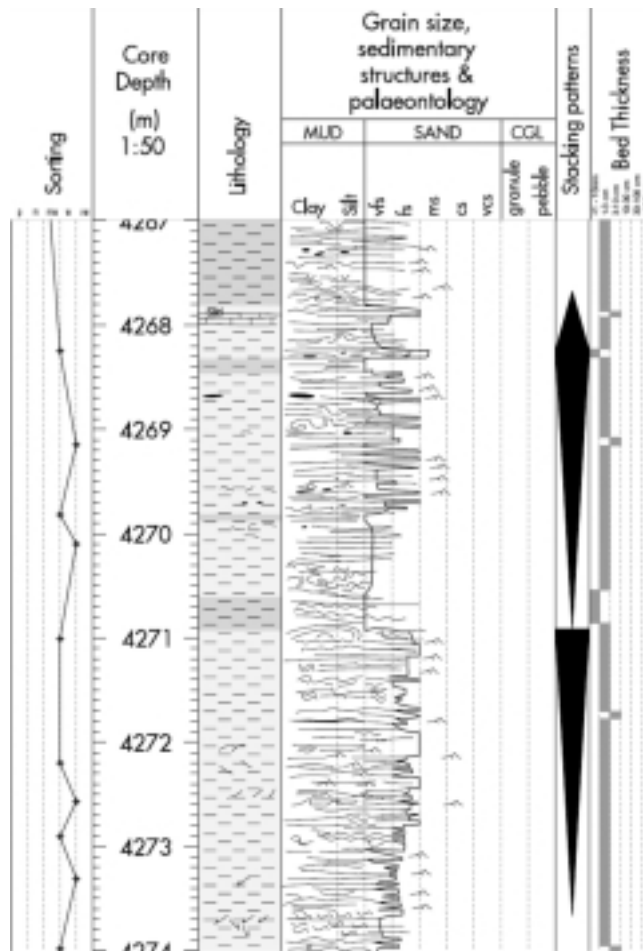


Fig 5. Sedimentary Log of proximal to distal delta front, in upper core-section.

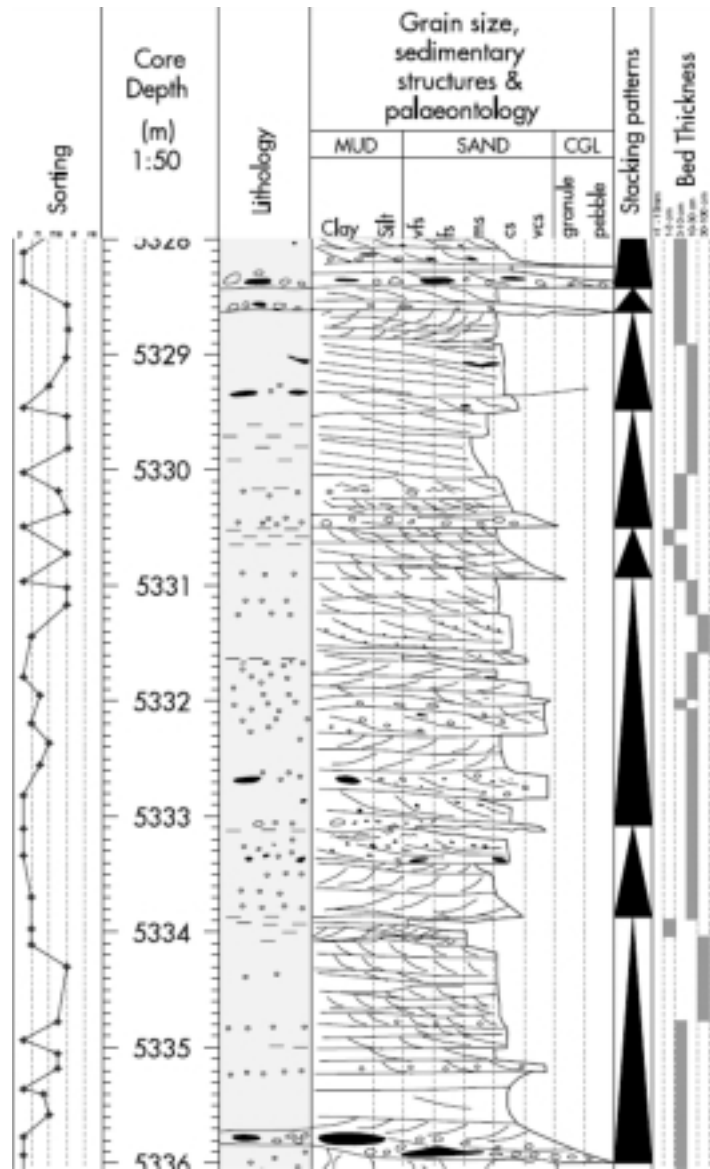


Fig 6. Sedimentary Log of proximal to distal delta front, in upper core-section.

sandstones a few meters thick to tens to hundreds of meters wide (Cant and Walker, 1978). They may be cut by broad shallow scours, giving rise to conglomeratic lags. Smaller scale trough cross-bedding at the tops of individual packages occur in the shallow areas of the channel fill, and are associated with falling-water stages (Miall, 1996).

Confined fluvial channel fill

This lithofacies association is characterized by medium to thickly bedded trough cross-bedded and horizontally stratified fine to medium sandstones (usually bimodal), alternating with thinly bedded laminated very fine to fine sandstones (Figure 7). Individual packages display fining-upward trends with increasing horizontally stratified and parallel laminated sandstones dominant towards the top. This lithofacies association is the most common, occurring within middle and lower Core-

sections. They typically alternate with thin and very thick suspension deposits, many highly mottled. These deposits are thought to represent the deposits of a more confined fluvial system than that described previously, likely to be an anastomosing fluvial system (Miall, 1996). The stacked channel successions represent repeated cut and fill within the channel. The main depositional element is the point bar, which builds laterally and downstream across the floodplain. Upward fining grain-size profiles, combined with corresponding upward decreases in the scale of trough cross bedding, reflect a decrease in flow velocities through time. This can result from either lateral migration of the point bar, or more commonly, from channel abandonment. The notable lack of thick well-developed floodplain fines with mature palaeosol development indicates that the system is not a high sinuosity meander system, but perhaps a moderate sinuosity, anastomosing one.

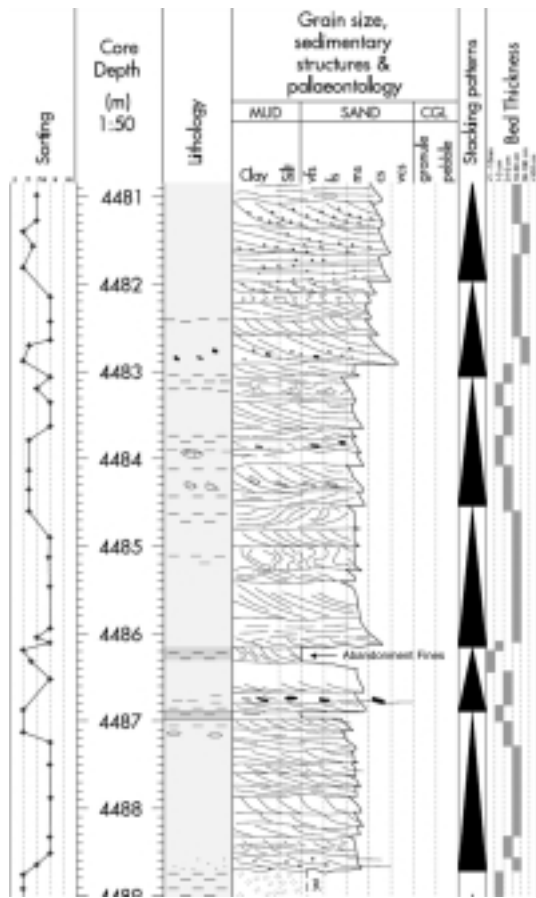


Fig 7. Sedimentary Log of confined fluvial channel fill and thin abandonment fines (see arrow).

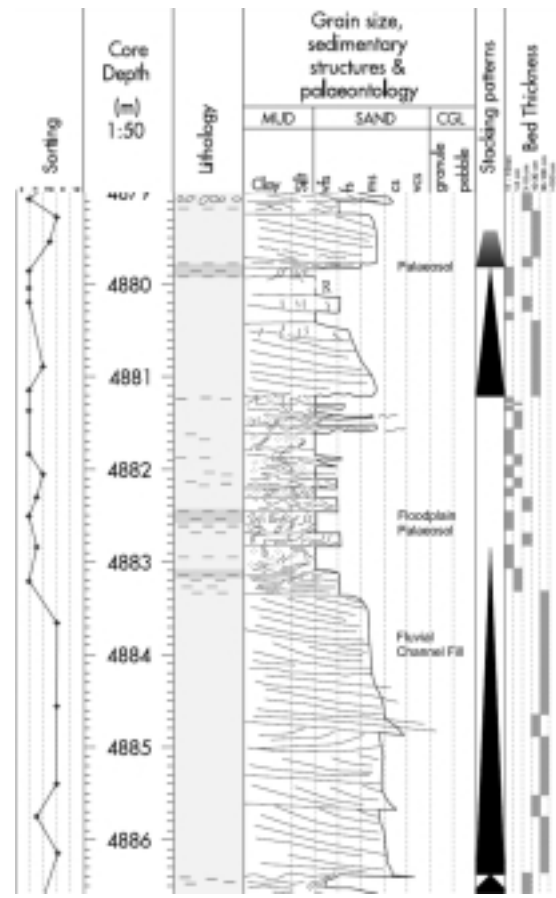


Fig 8. Sedimentary Log of floodplain palaeosol overlying confined fluvial channel fill.

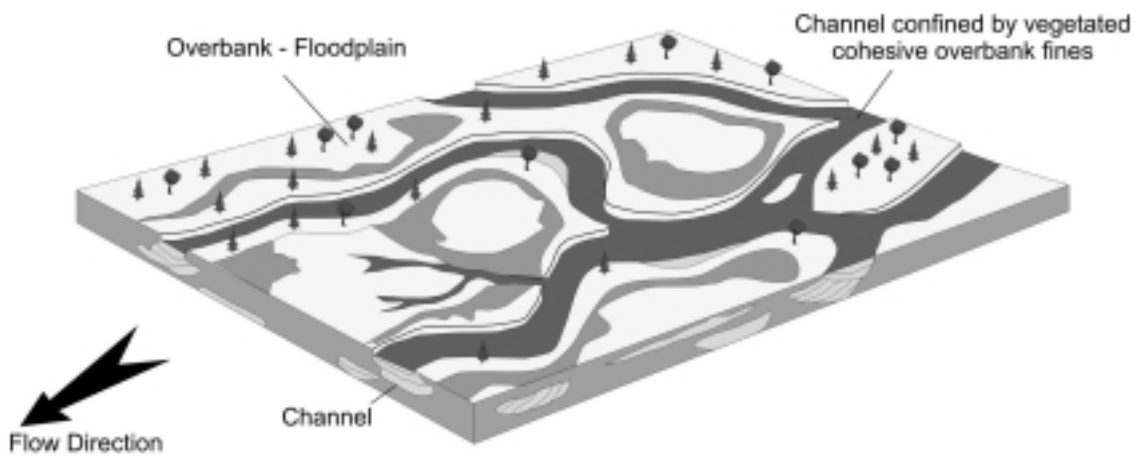


Fig 9. Block diagram of an anastomosing fluvial system illustrating the lithofacies associations, channel belts and floodplain fines (modified from Galloway, 1981; Miall, 1992; Richards 1996).

Abandonment fines

Alternating laminated siltstones and claystones, often highly carbonaceous, characterize this facies association (Figure 7). They form packages from 5cm to 15cm thick, sometimes with sandstone stringers. Locally they are carbonate cemented. They often comprise numerous laths of carbonaceous material. They represent waning flow and subsequent temporary abandonment of the point bar. They therefore are not characterized by palaeosols and not cross-cut by splays.

Floodplain fines

Floodplain fines are characterized by alternating laminated siltstones, claystones and carbonaceous mudstones with associated palaeosol development (Figure 8). The floodplain fines occur towards the top of a fluvial channel fill, and represent filling and subsequent abandonment of the system. This can be due to simple channel filling and abandonment, or channel avulsion.

Floodplain-palaeosol

Palaeosols are characterized by alternating laminated and massive siltstones, and some laminated claystones with thin sandstone stringers or units (Figure 8). Rootlets tend to occur throughout these units. They commonly display reddened zones, and are often highly mottled and fractured due to pervasive cementation (pyrite and carbonate cements). This facies association represents low-energy subaqueous deposition within inter-channel areas. In-situ rootlets reflect emergence or near emergence in these areas, also suggested by the reddening which is also characteristic. Deposition is

attributed primarily to suspension deposition, with minor laminated sandstones introduced via distal splays. Units which are very highly cemented, displaying abundant pyrite concretions and pervasive carbonate cements are interpreted to indicate the presence of a more mature palaeosol.

DISCUSSION AND CONCLUSIONS

Based on the seismic interpretation of the study area, the core section comprises sediments belonging to Lower Cretaceous age. The deposits represented in middle and lower Core-section are thought to represent a series of fluvial channels deposited within a system, which varies from a confined, moderate sinuosity anastomosing channel belt system to a lower sinuosity, braided river system (Figure 9). In contrast, the deposits represented in upper Core-sections are thought to represent deposition within a proximal to distal, tidally influenced deltaic system, with a strong freshwater influx, as indicated by the lack of bioturbation. The soft sediment deformation suggests rapid sedimentation, which is typical of deltas. However, with such limited core coverage, and without intersecting a channelized part of the system, it is difficult to speculate on the system in more detail. A study, with the conjunction of all the core data from several other wells, within the study area, warrants attention.

Acknowledgements: Authors are thankful to the Managing Director, GSPCL for his kind approval for this technical presentation. They also acknowledge Dr. Bijay K. Behera, DGM for his support and guidance. They are thankful to the anonymous reviewer who has critically gone through the manuscript and helped to present the article in more significant manner.

References

- Cant, D.J. and Walker, R.G. (1978). Fluvial processes and facies sequences in the sandy braided South Saskatchewan River, Canada, *Sedimentology*, 25, 625-648.
- Curray, J. R., and Moore, D. G. (1971). Growth of the Bengal Deep-Sea Fan and denudation of the Himalayas. *Geol. Soc. Am. Bull.*, 82, 563-572.
- Galloway, W. E. (1981). Depositional architecture of Cenozoic Gulf Coastal Plain fluvial systems: *Soc. of Economic Paleontologists and Mineralogists Spec. Pub. No. 31*, 127-155.
- Gordon, R. G., DeMets, C. and Argus, D. F. (1990). Kinematic constraints on distributed lithospheric deformation in the equatorial Indian Ocean from present plate motion between the Australian and Indian plates: *Tectonics*, 9(3), 409-422.
- Gupta, S. K. (2006) Basin architecture and petroleum system of Krishna Godavari Basin, east coast of India: *The Leading Edge*, 25, 830-837.
- Miall, A.D. (1992). Alluvial deposits, in R.G. Walker and N.P. James, eds., *Facies Models: Response to Sea Level Change*: Geological Association of Canada, 119-142.
- Miall, A.D. (1996). *The geology of fluvial deposits, Sedimentary Lithofacies, Basin Analysis and Petroleum Geology*. Springer-Verlag. 582p.
- Rao, G.N., Satyanarayana, K. and Mani, K. S. (1993). Seismo-stratigraphic analysis of Lower Gondwana (pre-Cretaceous) hydrocarbon producing horizons of Mandapeta area of Krishna Godavari basin: *Jour. AEG*, 14(4), 165-172.

- Rao, G.N. (2001). Sedimentation, Stratigraphy, and Petroleum Potential of Krishna-Godavari Basin, East Coast of India, AAPG Bulletin, 85 (9), 1623-1643.
- Richards, M.T., (1996). Fluvial Systems, In: Emery, D. and Myers, K.J., 1996, Sequence Stratigraphy, Blackwell Science, 111-133.
- Srivastava, V. K. and Chowhan, R. K. S. (1987). Study of focal mechanism solutions of events distributed in and around the Indian lithospheric plate: New Delhi, Oxford and IBH Publishing, 139-156.
- Subrahmanyam, C., and Chand, S. (2006). Evolution of the passive continental margins of India-a geophysical appraisal: Gondwana Research, 10, 167-178.
- Internal Core Reports on KG Wells, GSPC.

Petrography and Textural Characteristics of the Barail and the Surma Sandstones of Tamenglong area, Western Manipur, in Relation to Depositional Processes and Orogeny

SALAM RANJEETA DEVI¹, M.E.A.MONDAL¹, M MASROOR ALAM² and RABINDRA NATH HOTA³

¹Dept. of Geology, ²Dept. of Civil Engineering, Aligarh Muslim University, Aligarh - 20202

³P.G. Department of Geology, Utkal University, Bhubaneswar, Orissa - 751004

E-mail: ranjeeta_27@rediffmail.com

Abstract: The Barail and the Surma sandstones of Tamenglong area in western part of Manipur have been examined to establish the relationship between depositional environment process and orogeny using petrographic result and applicable depositional environmental analysis techniques based on grain size frequency distribution. These sandstones were derived from dominantly quartzose to lithic recycled sedimentary and metasedimentary rocks distributed in an orogenic highland that formed during fold-thrust processes at collisional Indo-Myanmar suture. Statistical analysis of grain-size parameters suggests that the Barail sandstones are fine to medium grained ($Mz = 1.616$ to 2.56ϕ), poorly to moderately sorted ($\sigma_1 = 0.49$ to 1.07), positively skewed and mesokurtic to very platykurtic whereas, the Surma sandstones are very fine to medium grained ($Mz = 1.766$ to 3.6ϕ), very poorly to moderately sorted ($\sigma_1 = 0.592$ to 1.08ϕ), positively skewed and very leptokurtic to platykurtic. Bivariate plots of different statistical parameters grain size suggest the fluvial nature, predominance of river process and channel sub-environment in transportation and deposition. This study reaffirms that the major river system from orogenic highland transported the recycled orogenic sediments to this basin.

Keywords: Barail Sandstone, Surma Sandstone, Depositional Process, Orogeny, Grain Size Frequency Distribution.

INTRODUCTION

The study area (Fig.1), located in the Western part of Manipur is bounded by two well known collisional belts- the Himalayas at the distant north and the Indo-Myanmar ranges in the east. Materials eroded from the orogenic belts and deposited in the associated basin can provide insight into the evolution and unroofing history of the orogens through time. Devi and Mondal (2008) have carried out the petrological studies to workout the provenance and tectonic setting of the Barail and the Surma sandstones the study area (Fig. 2). The purpose of the present study is to examine the petrography and textural characteristics of the Barail and the Surma sandstones to establish the relationship between depositional processes and orogeny in the regional tectonic perspective using easily available and applicable techniques of depositional-environment analysis based on grain size frequency distribution. The grain size parameters of sediments have been successfully used to distinguish different depositional processes, understanding the mechanism of environments and sub-environments of deposition (Stewart, 1961; Friedman, 1961; Sahu, 1964; Visser, 1969; Royse, 1970).

GEOLOGICAL SETTING

The Indo-Myanmar ranges (IMR), comprising the Naga Hills, the Chin Hills and the Arakan-Yoma fold

belt, were formed during the Cenozoic as a result of subduction of the Indian plate under the Asian plate. The tectonic evolution of the Indo-Myanmar region has been interpreted as an accretionary prism obducted upon the Indian plate and hence the prism as a whole youngs towards the west (Hutchinson, 1989). The bulk of these ranges consist mainly of Cretaceous to Eocene pelagic sediments and a thick succession of Eocene to Oligocene flysch, overlain by upper Miocene to Pleistocene molasse (Brunnschweiler, 1966; Ni et al., 1989). Folded and faulted thick deposits of monotonous flysch sediments known as Disang (Early Cretaceous to Eocene) and sandy subflysch Barail (Eocene to Oligocene) occupies the Naga Hills. Folded belt of the Surma valley, Tripura, Mizoram, western Manipur, Chittagong tracts and coastal Myanmar is collectively called as the Surma basin (Dasgupta, 1984), comprising Neogene molasse sediments and exposed to the west of Naga-Chin Hills. The Surma Group is well exposed in these areas and divided into a lower Bhuban Formation and an upper Bokabil Formation. The lower Bhuban Formation, the lower Formation of the Surma Group is exposed largely in the Barak basin (Fig. 3) and is characterized mainly by cross laminated, grey micaceous sandstones, silty shale, conglomerate and thin coal streaks at places. Ripple marks have been observed at many places. The Bokabil Formation consists of mudstone, shale, silty shale, sandy shale with massive and coarse-grained sandstones. The Surma Group in the study area is underlain by Barail Group, which

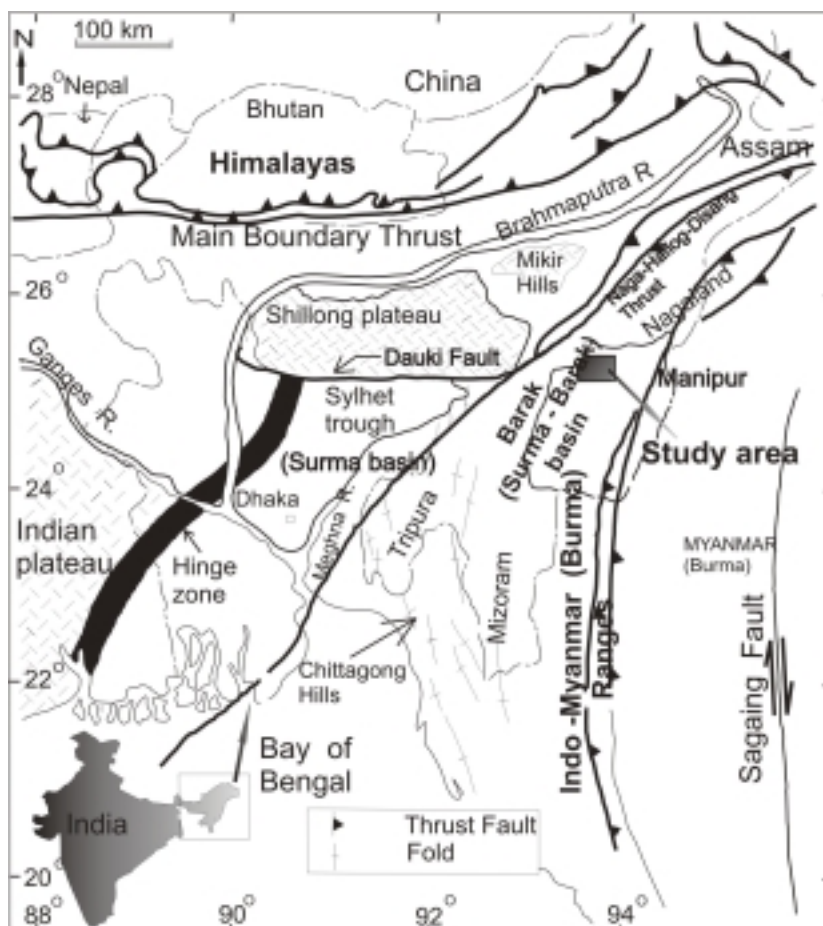


Fig. 1. Regional tectonic map of the study area and adjoining areas (after Uddin and Lundberg, 1998 a, b).

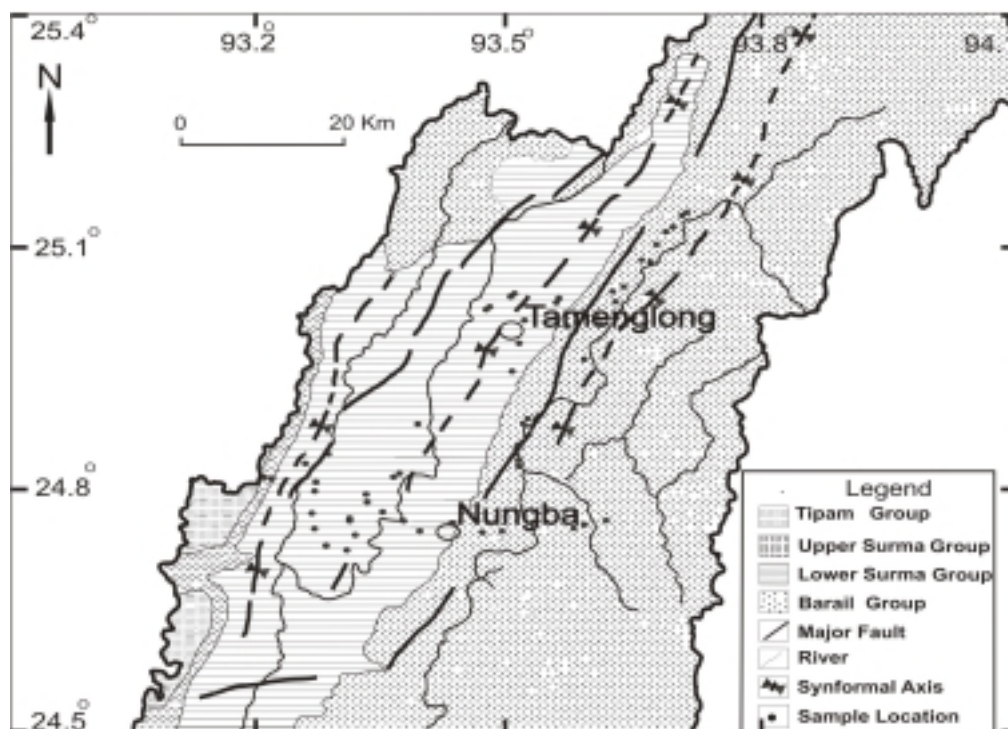


Fig. 2. Simplified geological map of the study area, Barak (Surma-Barak) basin (Chingkei, 2002), showing the important sample locations.

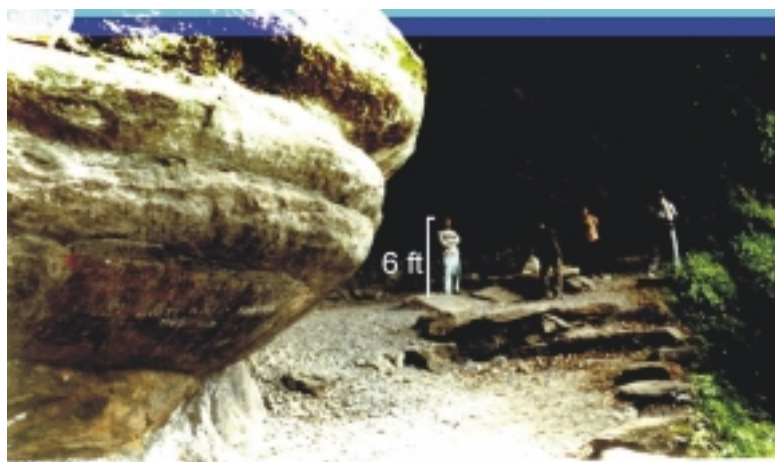


Fig. 3 . Photograph of sandstone of the Surma group of rock exposed at Tamenglong, Barak basin.

consists dominantly of massive to thickly bedded sandstone with siltstone and minor dark grey to khaki green thinly bedded shale with locally exposed coal streaks, twigs and plant impressions. The Tipam Formation consisting of massive to thick-bedded sandstone with shale overlies the Surma Group.

METHODS OF STUDY

Fresh rock samples consisting of sandstone, siltstone, shale and conglomerate were collected from outcrops exposed in stream cuts, road cuts and small quarries from the area in and around Tamenglong, western part of Manipur (Fig. 2). Thin sections of selected sandstone samples were prepared to investigate mineralogical and textural properties of these sandstones. Petrological modal analysis of samples was carried out in order to determine the quantitative mineralogical aspects of sandstone samples. About 500 points of 20 sandstone samples were counted using the Gazzi-Dickinson point counting methods (Dickinson, 1970; Gazzi et al., 1973). The granulometric analyses of the rocks from the thin sections have been carried out following standard methods (Folk and Ward, 1957; Friedman, 1961, 1967; Friedman and Sanders, 1978, and Pettijohn, 2004). Statistical variants were determined following methods of Passega (1964), Sahu (1964, 1983), Sevon (1966) and Davis (2002).

Grain size distribution curves were drawn and formulae suggested by Folk and Ward (1957) and Folk (1968) were used in order to determine statistical parameters of grain size distribution. The depositional processes and environments of the Barail and Surma sandstones were found out from the bivariate plots of Friedman (1961), Stewart (1958), Royse (1970) and Passega (1964) and discriminant function proposed by Sahu (1964). A linear discriminant function (D_{BS}) was worked out to discriminate between Barail and Surma

sandstones of the area. Further, comparison of multivariate vector means and variance-covariance matrices of the major constituents (quartz, feldspar and rock fragments) of the Barail and Surma sandstones were done by the methods outlined by Davis (2002).

PETROGRAPHY AND TEXTURAL CHARACTERISTICS

Results of modal and grain size analysis of the sandstones are given in Table 1 and 2. According to the Folk's classification (1980), the Barail sandstones are sublitharenites, litharenites and quartzarenites, whereas, the Surma sandstones are sublitharenites and litharenites (Devi and Mondal, 2008). QtFL, QmFLt and QpLvLs (Fig. 4) ternary provenance diagrams (Dickinson, 1985) suggest that the Barail and the Surma sandstones were derived dominantly from quartzose to lithic recycled sedimentary rocks with minor contribution from the igneous plutonic and volcanic rocks distributed in an orogenic highland that was formed during fold-thrust processes at a collisional zone.

Statistical analysis of thin sections revealed that the Barail sandstones are fine to medium grained with mean grain size ranging from 2.56 to 1.616 ϕ (0.170 - 0.326 mm). These sandstones are poorly to moderately well sorted with standard deviation ranging from 0.49 to 1.07. The skewness values of these sandstones are positive and vary from 0.725 to 1.248, which suggest excess of the fine admixture over coarse fraction i.e. the sediments are very fine to finely skewed. The grain size distribution curves of the most of the sandstones are meso- kurtic to very platykurtic.

In case of the Surma sandstones, mean size values range from 3.6 to 1.766 ϕ (0.082 - 0.326 mm) indicating a very fine to medium grained nature of sandstones (Table 2). The standard deviation varies from 0.592 to 1.08. ϕ indicating that these sandstones are poorly to

Table 1. Petrographic data (in percent) of the Barail and the Surma sandstones of the Barak basin.

| | Quartz | | Feldspar | Lithic fragments | | | Traces | Matrix |
|-----------------------------|-----------------|-----------------|----------|------------------|-------------|----------|--------|--------|
| | Monocrystalline | Polycrystalline | | Sedimentary | Metamorphic | Volcanic | | |
| (a) Surma Formation | | | | | | | | |
| Sample No. | | | | | | | | |
| Nb-2 | 81.07 | 1.44 | 1.08 | 7.44 | 3.14 | 0.00 | 0.00 | 3.41 |
| Kj-3 | 37.49 | 4.11 | 1.14 | 41.83 | 7.43 | 0.00 | 2.51 | 2.40 |
| Kj-4 | 74.84 | 3.51 | 1.29 | 4.09 | 1.51 | 0.00 | 12.19 | 0.00 |
| Kj-6 | 67.85 | 2.43 | 2.06 | 15.89 | 0.56 | 0.00 | 10.84 | 0.00 |
| Kh-8a | 72.09 | 3.64 | 1.64 | 16.91 | 5.00 | 0.00 | 0.00 | 0.00 |
| Kh-11 | 73.39 | 3.87 | 0.58 | 15.85 | 2.32 | 0.00 | 3.09 | 0.71 |
| Kb-9 | 82.35 | 3.51 | 0.55 | 5.59 | 2.08 | 0.00 | 0.00 | 1.10 |
| Kb-11 | 54.87 | 6.02 | 2.83 | 16.81 | 1.59 | 0.00 | 12.74 | 1.24 |
| Sb-12 | 63.77 | 3.20 | 1.98 | 12.79 | 4.72 | 0.61 | 6.70 | 1.98 |
| Nk-13 | 69.78 | 1.82 | 3.31 | 10.76 | 3.81 | 0.00 | 1.24 | 4.14 |
| Nk-14 | 69.25 | 1.66 | 2.77 | 4.43 | 4.16 | 0.00 | 14.40 | 0.00 |
| Km-15 | 70.63 | 1.96 | 1.88 | 6.43 | 9.29 | 0.00 | 1.16 | 4.64 |
| On-18 | 64.91 | 2.11 | 1.20 | 20.03 | 3.61 | 0.45 | 0.00 | 3.16 |
| Nk-19 | 66.94 | 3.79 | 2.61 | 15.28 | 3.55 | 0.36 | 1.07 | 3.55 |
| Kd-2 | 66.03 | 2.61 | 0.89 | 23.73 | 3.94 | 0.00 | 0.00 | 0.45 |
| Kd-6 | 53.24 | 5.07 | 0.58 | 33.24 | 3.91 | 0.00 | 0.76 | 1.57 |
| (b) Barail Formation | | | | | | | | |
| Kjr-1 | 77.95 | 0.69 | 0.23 | 12.32 | 2.32 | 0.00 | 0.00 | 3.10 |
| Kjr-2 | 73.31 | 7.97 | 0.40 | 6.27 | 8.27 | 0.00 | 0.60 | 0.00 |
| Kjr-4 | 72.17 | 2.61 | 0.65 | 12.22 | 5.38 | 0.16 | 0.00 | 2.25 |
| Bh-2 | 88.58 | 6.41 | 0.39 | 3.42 | 0.48 | 0.00 | 0.19 | 0.00 |
| Bh-3 | 88.75 | 3.20 | 0.00 | 4.29 | 1.87 | 0.00 | 0.12 | 0.42 |
| Bh-4 | 75.05 | 8.41 | 0.00 | 6.48 | 4.93 | 0.00 | 0.00 | 0.00 |
| Bl-8 | 59.75 | 8.36 | 1.00 | 20.18 | 3.23 | 0.00 | 2.12 | 3.46 |
| Bl3-8 | 55.72 | 10.83 | 3.79 | 17.69 | 3.17 | 0.00 | 1.06 | 1.58 |
| 28c | 91.67 | 4.03 | 0.00 | 2.89 | 0.44 | 0.00 | 0.53 | 0.00 |
| 29c | 87.70 | 0.27 | 0.61 | 5.95 | 2.34 | 0.00 | 0.00 | 0.68 |
| Akh-1 | 61.59 | 5.97 | 0.80 | 25.77 | 3.78 | 0.00 | 0.00 | 0.60 |
| Akh-3 | 58.78 | 3.16 | 1.12 | 27.55 | 3.37 | 0.00 | 0.00 | 3.37 |
| Kei-12 | 49.50 | 8.47 | 0.00 | 35.15 | 2.65 | 0.00 | 1.06 | 1.06 |

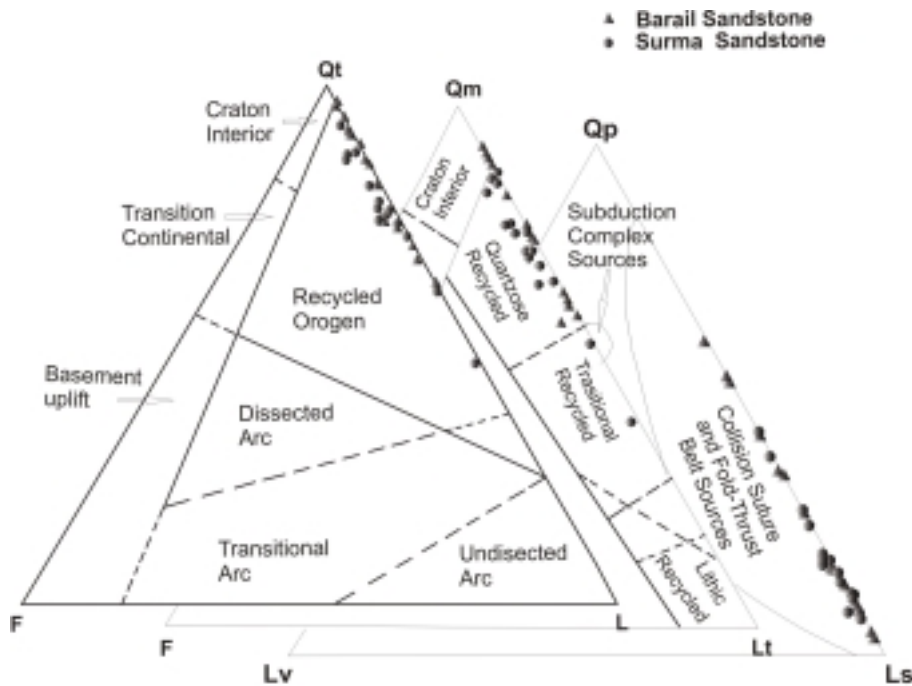


Fig. 4. Provenance field ternary diagrams of QtFL, QmFLt and QpLvLs (after Dickinson, 1985; Dickinson and Suczek, 1979; Dickinson et al., 1983). Qt, Total quartz; F, Total Feldspar; L, Total lithic fragments; Qp, Total Polycrystalline quartz; Lv, Total volcanic and metavolcanic lithic fragments; Ls, Total sedimentary and metasedimentary lithic fragments.

Table 2. Grain size parameters of the Barail and the Surma sandstones of the Barak basin.

| Sandstone Sample No. | Mean (M_z) | Standard Deviation (σ_i) | Skewness (S_{ki}) | Kurtosis (K_G) |
|-----------------------------|----------------|-----------------------------------|-----------------------|--------------------|
| (a) Surma Formation | | | | |
| Nb-2 | 1.91 | 0.87 | 0.92 | 0.749 |
| Kj-3 | 3.43 | 0.72 | 0.21 | 0.89 |
| Kj-4 | 3.26 | 0.72 | 0.60 | 1.13 |
| Kj-6 | 3.43 | 0.72 | 0.21 | 0.89 |
| Kh-8a | 3.51 | 0.71 | 1.2 | 0.99 |
| Kh-11 | 3.5 | 0.712 | 1.2 | 0.9 |
| Kb-9 | 3.4 | 0.723 | 0.93 | 2.19 |
| Kb-11 | 3.38 | 0.726 | 0.9 | 2.02 |
| Sb-12 | 3.05 | 1.08 | 1.023 | 1.2 |
| Nk-13 | 3.36 | 0.86 | 1.03 | 0.89 |
| Nk-14 | 1.983 | 0.658 | 0.963 | 1.004 |
| Km-15 | 3.6 | 0.86 | 0.49 | 0.77 |
| On-18 | 2.45 | 0.723 | 0.942 | 0.942 |
| Nk-19 | 1.766 | 0.592 | 1.042 | 0.947 |
| Kd-2 | 1.91 | 0.87 | 0.92 | 0.749 |
| Kd-6 | 2.65 | 0.81 | 0.94 | 0.85 |
| (b) Barail Formation | | | | |
| Kjr-1 | 1.8 | 1 | 1.248 | 0.945 |
| Kjr-2 | 2.56 | 1.07 | 0.95 | 1.05 |
| Kjr-4 | 1.866 | 1.052 | 1.038 | 0.86 |
| Bh-2 | 1.866 | 1.052 | 1.038 | 0.860 |
| Bh-3 | 2 | 0.87 | 1.05 | 1.04 |
| Bh-4 | 1.916 | 0.964 | 0.925 | 0.743 |
| Bl-8 | 2.283 | 0.702 | 0.999 | 1.027 |
| Bl3-8 | 2 | 1.021 | 0.981 | 0.637 |
| 28c | 1.616 | 0.828 | 1.04 | 0.819 |
| 29c | 1.98 | 0.49 | 0.983 | 0.846 |
| Akh-1 | 2.01 | 0.68 | 0.86 | 0.80 |
| Akh-3 | 2.43 | 0.69 | 0.995 | 1.176 |
| Kei-12 | 2.05 | 0.72 | 0.725 | 0.90 |

moderately sorted. The Surma sandstones are positively skewed with skewness value ranging from 0.21 to 1.2, which suggest the dominance of fine sediment over the coarse fraction. The kurtosis values ranging from 0.75 to 0.2.19 suggest that the grain size distribution curves are platykurtic (five samples), mesokurtic (five samples), leptokurtic (two samples) and very leptokurtic (two samples).

INTERPRETATION OF MECHANISMS AND ENVIRONMENTS OF DEPOSITION

Utilising the grain size parameters, Passega (1957), Stewart (1958), Friedman (1961), Sahu (1964), Visher (1969) and Royse (1970) have proposed different discrimination models to differentiate and deduce the depositional processes, mechanism of sedimentation and energy condition of the transporting medium. These have been used to discriminate the depositional environments of the Barail and the Surma sandstones of the Barak basin in the present work.

Friedman (1961, 1967) proposed that beach and river sediments can be discriminated by standard deviation vs. skewness plot while the dune and river sediments

can be discriminated by standard deviation vs. mean size plot. In the present work, these models were used to establish the environment of deposition of Surma and Barail sediments. Fig. 5 shows the plot of skewness vs. standard deviation in which all the 29 data plot in the river field. The Mean size vs. standard deviation of the Surma and Barail sandstones have been plotted in Fig. 6. In this case also all the

plots fall in river field confirming the deposition of Surma and Barail sandstones in fluvial environment.

Stewart (1958) has shown that the river process, wave process and slow deposition from quite water could be effectively discriminated by plotting the median vs. standard deviation of the sediments, Fig. 7. shows the plotting of these values of the Barail and Surma sandstones. Clustering of the plots in and around river processes field and in between river process and wave processes field suggest deposition of these sandstones mostly by river process.

Royse (1970) used skewness vs. median plot (Fig.8) to differentiate sub-environments of river, like channel, flood plain and back swamp. The Surma and Barail sandstones plot within and around channel field in this diagram, suggesting the deposition of these

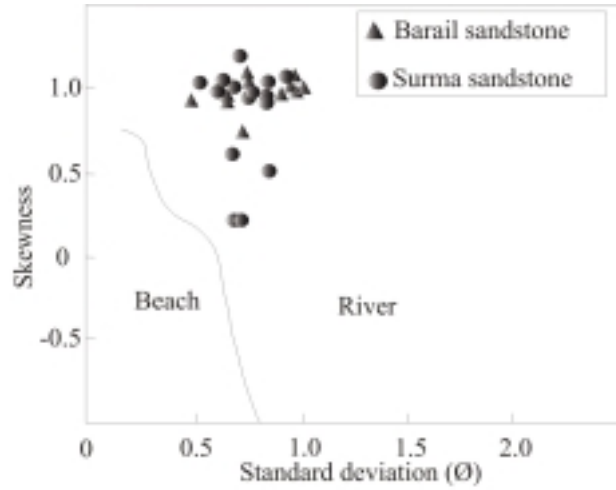


Fig. 5. Bivariate discriminant plot showing dominant depositional environments and/ or processes (after Friedman, 1961) of the Barail and the Surma sandstones.

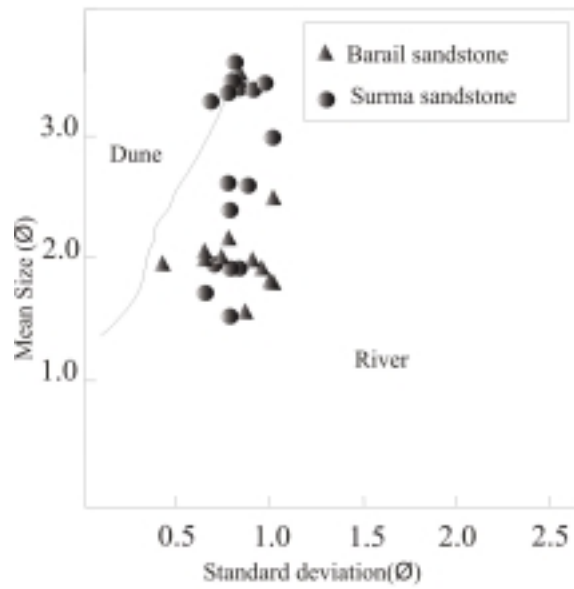


Fig. 6. Bivariate plot of mean vs. standard deviation of the Barail and the Surma sandstones.

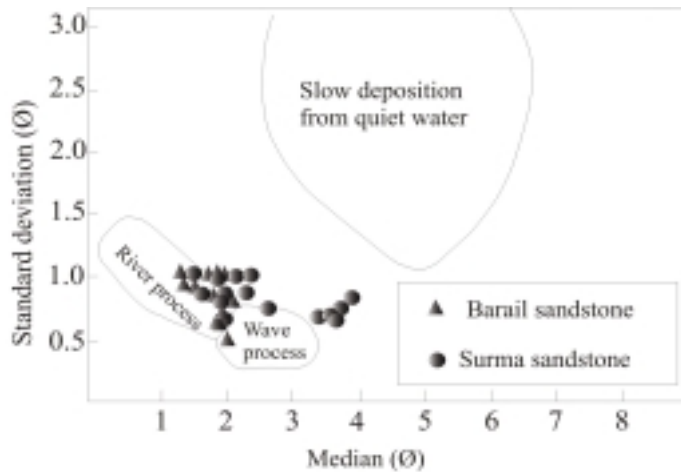


Fig. 7. Bivariate discriminant plot of median vs. standard deviation (Stewart, 1958) of the Barail and the Surma sandstones.

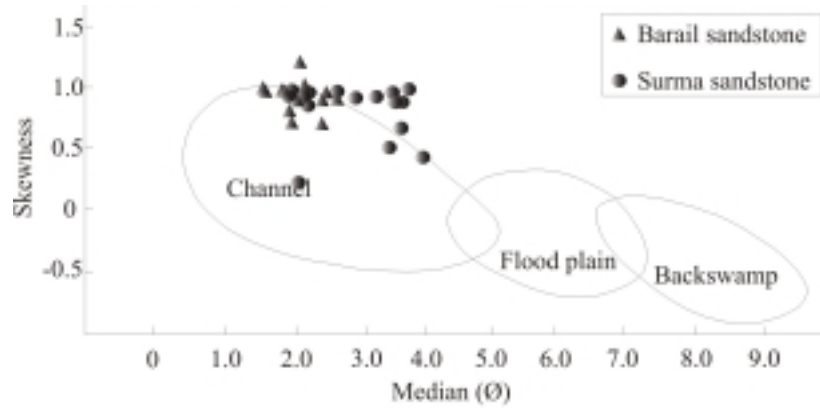


Fig. 8. Bivariate discriminant plot of skewness vs. median (Roys, 1970) of the Barail and the Surma sandstones.

Table 3. Results of the discriminatory analysis (Sahu, 1964, Equation 13) of Barail and the Surma sandstones of the Barak basin.

| Barail Formation | | | | Surma Formation | | | |
|----------------------|-------------|----------------------|-------------|----------------------|-------------|----------------------|-------------|
| Sandstone Sample No. | \bar{Y}_u |
| Kjr-1 | -14.3082 | B13-8 | -13.1435 | Nb-2 | -11.5425 | Sb-12 | -13.5393 |
| Kjr-2 | -13.2414 | 28c | -11.8422 | Kj-3 | -6.31393 | Nk-13 | -11.5728 |
| Kjr-4 | -13.7214 | 29c | -8.49714 | Kj-4 | -8.25919 | Nk-14 | -9.86255 |
| Bh-2 | -13.7214 | Akh-1 | -5.76608 | Kj-6 | -6.31393 | Km-15 | -8.86778 |
| Bh-3 | -12.1389 | Akh-3 | -10.1637 | Kh-8a | -11.043 | On-18 | -10.199 |
| Bh-4 | -12.389 | Kei-12 | -9.22702 | Kh-11 | -11.0677 | Nk-19 | -9.73556 |
| B1-8 | -10.3375 | | | Kb-9 | -9.80921 | Kd-2 | -11.5425 |
| | | | | Kb-11 | -9.70259 | Kd-6 | -10.898 |

sandstones in channel sub-environment of the fluvial regime.

Sahu (1964) established a number of discriminant functions based on the graphical parameters of the sediments to distinguish different mechanisms and environments of deposition. The discriminant function to discriminate between shallow marine and the fluvial process is given below:

$$= 0.2852 M_z - 8.7604 \sigma_1^2 - 4.8932 Sk_1 + 0.0482$$

K_G , where

M_z = mean size

σ_1^2 = variance

Sk_1 = skewness

K_G = kurtosis

Values of \bar{Y}_u less than -7.4190 indicate fluvial environment while values greater than -7.4190 indicate shallow marine deposit. Most of the values of the Barail and the Surma sandstones are less than -7.4190 (except two samples, one from each formation), which indicate that these sandstones were deposited in fluvial environment (Table 3).

DISCRIMINATION BETWEEN BARAIL AND SURMA SANDSTONES

Utilizing the grain size parameters of the sandstones of the Barak basin, a linear discriminant function was

found out to distinguish between Barail and Surma sandstones. The function is given below:

$$D_{BS} = 3.387 M_z - 4.457 \sigma_1 + 1.193 Sk_1 - 0.754 K_G$$

Where

M_z = Mean size (in ϕ), σ_1 = Standard deviation (in ϕ), Sk_1 = Skewness and K_G = kurtosis

The centres of the Barail and Surma sandstones calculated from the linear discriminant function are 3.48 and 6.62 respectively. The discriminant index ($R_0 = 5.16$) is the point located about half way between these two centres (Davis, 2002). The centres of the Barail and Surma sandstones are projected onto the discriminant function line (Fig. 9). The significance of the difference between Barail and Surma groups was tested by F-test. The computed value of 'F' is 5.00 that exceed the critical value (2.78) at 0.05 significance level with 4 and 24 degrees of freedom (Table 4). This leads to the rejection of the null hypothesis (H_0) that the two multivariate means are equal and the distance between them is zero. In other words, the linear discriminant function worked out in the present case is statistically significant. Values of D_{BS} less than 5.16 indicate Barail sandstone whereas values greater than 5.16 denote Surma sandstone. The values of the linear discriminant function corresponding to 13 Barail and 16 Surma sandstones have been plotted on the line (Fig. 9). These are the raw discriminant scores. It is seen that one (8%) Barail and four (25%) Surma

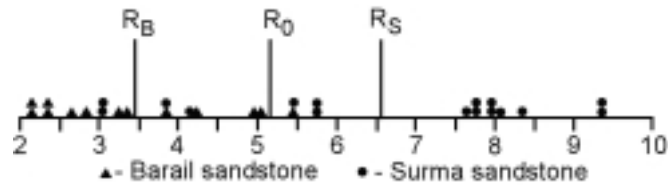


Fig. 9. Projection of Barail and Surma sandstones of the Barak basin onto the discriminant function line. R_B and R_S are the projections of the multivariate means of Barail and Surma sandstones respectively. R_0 is the discriminant index.

Table 4. Statistical data of test of significance of discriminant function (F-test) and equality of variance and covariance matrices (χ^2 - test) of the Barail and Surma sandstones.

| Number of Sandstones Studied (or number of data) | | F-test | | | | χ^2 - test | | | |
|--|------------------|-------------------------|--------------------|-------------------------|-----------------------|--------------------|--------------------|----------------------------------|--------------------------------|
| Barail Sandstones | Surma Sandstones | Degrees of Freedom | Significance Level | Calculated Value of 'F' | Critical Value of 'F' | Degrees of Freedom | Significance Level | Calculated Value of ' χ^2 ' | Critical Value of ' χ^2 ' |
| 13 | 16 | $v_1 = 4$ $v_2 = 24$ | 0.05 | 5.00 | 2.78 | 24 | 0.05 | 41.76 | 36.42 |

sandstones are misclassified by the discriminant function, which indicate the discriminatory power of the function. The mean size values of the four misclassified Surma sandstones are less than 2ϕ , which may be due to sampling and / or experimental errors.

DICUSSION

The ternary provenance discrimination diagrams suggest that the Barail and the Surma sandstones of the present study area are derived from the recycled orogenic highland that was formed during fold-thrust processes at a collisional suture. The Barail sandstones were derived from the Himalayas and the Indo-Burman range with minor contribution from Indian craton while the Surma sandstones were derived mostly from the Himalayas and the Indo-Burma range (Devi and Mondal, 2008). This has been tested by the equality of the multivariate vector means of the major lithologic constituents like quartz, feldspar and rock fragments. The computed value of 'F' is equal to 5.00 that exceeds the critical value (2.78) at 0.05 significance level with 4 and 24 degrees of freedom. This leads to the rejection of the null hypothesis (H_0) that the mean vector of the parent population of the Surma sandstones is the same as the parent population of the Barail sandstones. The equality of the Barail and Surma sandstone population parameters was further investigated by equality of variance-covariance matrices of the petrography data. In this case also the computed χ^2 value (41.76) exceeds the critical value (36.42) for 24 degrees of freedom at 0.05 significance level (Table 4), which leads to the rejection of the null hypothesis (H_0 = the population variance-covariance matrices are the same). These

statistical analyses confirm the difference of the petrography data of the Barail and the Surma formations, which may be due to some difference in provenance lithology. The present study suggests that the major river system originating from these orogenic highlands might have transported recycled orogenic sediment to the basin. The Barail Group in Naga Hills consists of the deltaic and prodeltaic deposit (Rangarao, 1983) and occupied a position in the more subsiding, proximal part of a foreland basin. Johnson and Alam (1991) also suggested that the Barail Group of Oligocene age is fluvial but probably passed abruptly into delta and prodelta deposits in a rapidly subsiding trough on the west flank of the Indo-Myanmar ranges. Imam and Shaw (1985) suggested that sedimentation of the Surma Group was in fluvial, deltaic and open-shelf environment in the shallow areas and in submarine fans in deeper parts of the basin (Alam, 1989), followed mainly by fluvial deposition of the Mio-Pliocene Tipam Group. According to Uddin and Lundberg (2004) major river system (paleo-Brahmaputra, paleo-Meghna, paleo-Karnafuli) delivered detritus from the Indo-Myanmar ranges and the eastern Himalayas straight to the Bengal fan through the Sylhet trough and the northern Chittagong Hill tract forming a major delta complex at the northeastern part of Bangladesh. During Miocene, major drainage system transported orogenic sediments to the early Bengal fan. The present study also suggests that lithic fragment rich sublitharenite and litharenite sandstones from the study area, which lies between the orogenic belts and the Bengal fan, were transported by a palaeoriver system. Litharenites are not only deposited in frontal basins but also in proximal alluvial fan and in other fluvial environments (Boggs, 1995).

CONCLUSIONS

The present study suggest that the Barail sandstones are fine to medium grained poorly to moderately sorted, positively skewed and mesokurtic to very platykurtic, whereas the Surma sandstones are very fine to medium grained, very poorly to moderately sorted, positively skewed and very leptokurtic to platykurtic. Statistical analysis of grain size parameters of the Barail and the Surma sandstones suggests the fluvial nature, predominance of river process and channel sub-environment in transportation and deposition. The Barail and Surma sandstones can be effectively differentiated by the linear discriminant

function ($D_{BS} = 3.387 M_z - 4.457 \sigma_1 + 1.193 Sk_1 - 0.754 K_G$). It is inferred from this study that the major river system from this orogenic highland transported the recycled orogenic sediments to this basin. Minor difference in the provenance setting of Barail and Surma sandstones as revealed by ternary plots is also statistically significant.

Acknowledgements: Authors are thankful to Chairman, Department of Geology, Aligarh Muslim University, for providing certain necessary facilities. The authors thanked the two anonymous reviewers for their critical review and suggestions which have substantially improved the final version of the manuscript.

References

- Alam, M., (1989). Geology and depositional history of Cenozoic sediments of the Bengal Basin of Bangladesh. *Palaeogeography, Palaeoclimatology, Palaeoecology*, 69, 125-139.
- Boggs, Jr. S. (1995). *Principles of sedimentology and stratigraphy*. Upper Saddle River, New Jersey, 774 pp.
- Brunnschweiler, R.O. (1966). On the geology of the Indo-Burma ranges. *Geol. Soc. Austral., Bull.*, 13, 137-194.
- Chingkhei, R., (2002). Application of GIS Techniques in evaluation and monitoring of vegetation in Barak basin. Unpublished Ph.D. Manipur University, Manipur, India.
- Dasgupta, S. (1984). Tectonic Trends in Surma Basin and possible genesis of the folded Belt. *Geol. Surv. India, Mem.*, 113 (IV), 58-61.
- Davis, J.C. (2002). *Statistics and data analysis in Geology*. John Wiley and Sons, 638pp.
- Devi, S.R. and Mondal, M.E.A. (2008). Provenance and tectonic setting of Barail (Oligocene) and Surma (Miocene) Group of Surma-Barak Basin, Manipur, India: Petrographic Constraints. *Jour. Geol. Soc. India*, 71, 459-467.
- Dickinson, W.R., (1970). Interpreting detrital modes greywacke and arkose. *Jour. Sed. Petrol.*, 40, 695-707.
- Dickinson, W.R., (1985). Interpreting provenance relations from detrital modes of sandstone. In: Zuffa, G.G. (ed.), *Reading provenance from arenites*, 333-361. Dordrecht, The Netherlands, Riedel.
- Dickinson, W.R. and Suczek, C.A., (1979). Plate tectonics and sandstone compositions. *Amer. Assoc. Petrol. Geol. Bull.*, 63, 2164-2182.
- Dickinson, W.R., Beard, S.L., Brakenridge, G.R., Erjavec, J.L., Fergusson, R.C., Inman, K.F., Knepp, R.A., Linberg, F.A. and Ryberg, P.T., (1983). Provenance of North American Phanerozoic sandstones in relation to tectonic setting. *Geol. Soc. Amer. Bull.*, 94, 222-235.
- Folk, R.L. (1980). *Petrology of Sedimentary Rocks*. Hemphill Austin, Texas.
- Folk, R.L. and Ward, W. C. (1975). Brazos river bar, a study in significance of grain-size parameters. *Jour. Sed. Petrol.*, 3-27.
- Friedman, G.M (1961). Distinction between dune, beach and river sands from their textural characteristics. *Jour. Sed. Pet.* 31, 87-97.
- Friedman, G.M. (1967). Dynamic processes and statistical parameters compared for size frequency distributions of beach and river sands. *Jour. Sed. Pet.*, 37, 327-354.
- Friedman, G.M. and Sanders, J.E., (1978). *Principles of Sedimentology*. John Wiley and Sons, N. Y., 792.
- Hutchinson, C.S. (1989). *Geological evolution of South-East Asia*. Press, London, 368 pp.
- Imam, M.B. and Shaw, H.F. (1985). The diagenesis of Neogene clastic sediments from the Bengal basin, Bangladesh. *Jour. Sed. Petrol.*, 55, 665-671.
- Johnson, S.Y. and Nur Alam, A.M. (1991). Sedimentation and tectonics of the Sylhet trough, Bangladesh. *Geol. Soc. Amer. Bull.*, 103, 1513-1527.
- Ni, J.F., Guzman-Speziale, M., Bevis, M., Holt, W.E., Wallace, T.C. and Searger, W.R. (1989). Accretionary Tectonics of Burma and Three-dimensional Geometry of the Burma Subduction Zone. *Geology*, 17, 68-71.
- Passega, R. (1964). Grain size representation by CM patterns as a geological tool. *Jour. Sed. Petrol.*, 34, 830-847.
- Pettijohn, F.J., 2004. *Sedimentary Rocks (3rd Edn)*. CBS Publishers and Distributors, New Delhi, India, 628.
- Rangarao, A. (1983). Geological and Hydrocarbon potential of a part Assam- Arakan Basin and adjacent regions. In: L.L. Bandari et al., (eds), *Petroliferous Basin of India, Oil and Natural Gas Comm.*, pp.127-158, India, Dehra Dun.
- Royse, F.J.Jr. (1968). Recognition of fluvial environments particle size characteristics. *Jour. Sed. Petrol.*, 38, 1177-1178.

- Royse, C.F.Jr. (1970). A sedimentologic analysis of the Tongue river Sentinel butte interval (Paleocene) of the Williston basin, Western South Dakota. *Sed. Geol.* 4, 19-80.
- Sahu, B.K. (1964). Depositional mechanisms from the size analysis of clastic sediments. *Jour. Sed. Petrol.*, 34, 73-83.
- Sahu, B.K. (1983). Multigroup discrimination of depositional environments using size distribution statistics. *Indian Jour. Earth Sci.*, 10, 20-29.
- Schlee, J.S., Uchupi, Elazar and Trumball, J.V.A. (1964). Statistical parameters of Cape Cd beach and eolian sands. U.S. Geol. Surv. Prof. Paper, 501-D, D118-D122.
- Sevon, W.D. (1966). Distinction of New Zealand beach, dune and river sands by their grain size distribution characteristics, New Zealand. *Jour. Geol. and Geophysics*, 9, 212-223.
- Shepard, F. P. and Young, Ruth (1961). Distinction between beach and dune sands. *Jour. Sed. Petrol.*, 31, 196-214.
- Stewart, H, B.Jr. (1958). Sedimentary reflections on depositional environments in Migue lagoon, Baja, California. *Bull. Amer. Asso. Petrol. Geol.*, 42, 2567-2618.
- Uddin, A. and Lundberg, N., (1998a). Cenozoic history of the Himalayan-Bengal System. Sand composition in the Bengal basin, Bangladesh. *Geol. Soc. Amer. Bull.*, 110, 497-511.
- Uddin, A. and Lungberg N., (1998b). Unroofing history of the eastern Himalaya and the Indo-Burma ranges: heavy mineral study of the Cenozoic sediments from the Bengal basin, Bangladesh. *Jour. Sed. Res.*, 68, 465-472.
- Visher, G.S. (1969). Grain size distribution and deposition processes. *Jour. Sed. Petrol.*, 39, 1075-1106.

Provenance History of Kolhan Sediments from Chaibasa-Noamundi Basin

SMITA S. SWAIN and SUDARSHAN GORANA

Department of Geology and Geophysics, IIT Kharagpur, West Bengal-721302

Email: smitaswarupaswain@gmail.com

Abstract: The Kolhan Group of rocks from Chaibasa-Noamundi basin towards the east of Singhbhum Granite is a shale-dominated succession deposited in continental rift setting. The basin comprises a thin layer of conglomerate and sandstone at the base grading upward to very thick layer of shale with patches of limestone, which exhibits an asymmetry in the vertical basin fill architecture. Petrography and major element concentration from geochemical analysis have integrated together to infer the source rock lithology, climatic condition and paleoweathering. Petrography grades the sandstones into quartz arenite and sub arkosic type, which suggests the granitic source terrain. Intracratonic setting of the basin is inferred from the QFL plot as well as from the major element composition of shale. The bivariate plot between K_2O/Na_2O vs. SiO_2 and ternary plot of $CaO-K_2O-Na_2O$ reveals the stable craton or passive margin setting for the basin. CIA values and A-CN-K compositional trend of the shale samples indicate a moderate to high degree of chemical weathering in a humid tropical climatic condition.

Keywords: Kolhan, Petrography, Geochemistry, Paleoweathering, Provenance.

INTRODUCTION

The 2100-2200 Ma Kolhan Group (Saha et al., 1988; Mukhopadhyay, 2001) of rocks represents one of the youngest Precambrian stratigraphic unit in Singhbhum geology (Saha, 1994), which was first recognized by Dunn (1940). The low dipping ($5-10^\circ$) Kolhan Group lie unconformably over Singhbhum granite along the northeastern side, the Jagannathpur lavas on the SE and S and the Iron Ore Supergroup at the eastern margin of the Noamundi Syncline on the west. The Kolhan Group is represented by four detached isolated outliers, exposed in the Chaibasa-Noamundi basin, Chamakpur-Keonjhar basin, Mankarchua basin and Sarapalli-Kamakhyanagar basin. The present investigation is focused on the Chaibasa-Noamundi basin.

Earlier studies reported the detailed stratigraphy, lithology and structure of the Chaibasa-Noamundi basin (Ray and Bose, 1959, 1964; Saha, 1948a, 1948b; Chatterjee and Bhattacharya, 1969; Mukhopadhyay et al. 2006; Bandopadhyay and Sengupta, 2004; Bhattacharya and Chatterjee, 1964). The provenance history of the Chaibasa-Noamundi basin has not been worked out. This paper deals with an integrated approach of petrographical and geochemical analysis of clastic sediments to infer the provenance and tectonic setting of the basin. Provenance study includes the identification of source rocks, relief and climate in the source area and tectonic setting. Petrographical analysis of sedimentary rocks is widely employed as a tool for characterizing source of sediments (Dickison, 1970; Basu et al., 1975; Folk, 1980) and tectonic setting of the area.

As the Chaibasa-Noamundi basin is dominated by the shale lithounit with very thin units of sandstone, petrographical analysis has to be supported by the geochemical analysis of shale. Shales are best suited for provenance studies of clastic sediments because of (i) their relatively homogeneity (ii) their post-depositional impermeability (iii) they dominate the sedimentary mass balance. Geochemical composition of sedimentary rocks is widely used to (i) determine the composition of source area (McLennan et al., 1979) (ii) evaluate weathering processes and paleoclimate by application of chemical indexes based on major elements (Nesbitt and Young, 1982; Fedo et al., 1995) (iii) reconstruct tectonic setting of depositional basin by use of SiO_2 and K_2O/Na_2O ratio (Roser and Korsch, 1986), $CaO-Na_2O-K_2O$ plot (Bhatia, 1983) (iv) evaluate the composition and evolution of continental crust (Condie, 1967; McLennan and Taylor, 1980). In the present work we integrate petrographic and geochemical techniques, which provide the information on the tectonic setting, source rock, weathering paleoweathering trend and climatic conditions.

GEOLOGY OF CHAIBASA-NOAMUNDI BASIN

Towards the western and northwestern parts of the Singhbhum granite craton, the Kolhan Group of sediments is preserved as a linear belt in the Chaibasa-Noamundi region of Jharkhand (Dunn, 1940, Saha, 1948a). It covers an area around 800 km² along the western margin of Singhbhum granite. The main basin extends in NNE-SSW direction for about 60 km from

Chaibasa (85° 48' – 22° 33') in the north to Noamundi (85° 28' – 22° 09') in the south with a maximum width of about 12 km (Mahadevan, 2002). The geological map (Fig. 1) shows the basin resting unconformably on the Singhbhum Granite and showing facies variation from basal sandstone conglomerate to phyllitic shale through sandstone and impersistent limestone in thickness of only a few tens of meters (Chatterjee and Bhattacharya, 1969; Bhattacharya and Chatterjee, 1964). The western contact of the basin is faulted against the Iron Ore Supergroup (Saha, 1948b).

The geological section along the river Gumuagara near village Rajanka (22° 26', 85° 44') seems to be the best exposure among all the sections studied and may be taken as the reference section for the Kolhan Group (Chatterjee and Bhattacharya, 1969). The stratigraphy of the area is as follows.

| | | |
|-------------|--|-------|
| Proterozoic | Newer Dolerite | |
| | Kolhan shale (slightly phyllitic) | |
| | Kolhan limestone (phyllitic in upper part) | 22 m |
| | Kolhan sandstone..... | 8 m |
| | Kolhan conglomerate | 0.3 m |
| ----- | Unconformity | ----- |
| Archaean | Singhbhum granite (3.0 Ga) | |

On the basis of different sedimentary structures, grain size, textural maturity of sandstone, six facies have been interpreted as Granular-lag sandstone facies (GLA), Granular sandstone facies (GSD), Sheet sandstone facies (SSD), Ripple laminated sandstone facies (RSD), Plane laminated sandstone facies (PLSD) and Thinly laminated sandstone facies (TLSD).

METHOD OF STUDY

Thin section petrography and modal analysis of fifty one thin sections of sandstones, collected from Matgamburu, Gumua gara river section-Kudduhatu, Rajanbasa, Bistampur, ITI Chaibasa, Kondwa, Lisyra, Baramirglindi, Gangabasa and Pungsiya were done following standard procedure (Gazzi-Dickinson point counting method, Dickinson, 1985). On average 300 grains were counted per slide and their mineralogical compositions have been calculated. The recalculated values were plotted in standard triangular plots of Folk, (1980), Dickinson, (1985) (Figs.6, 7). Heavy mineral analyses were done by point counting method and ZTR index values were calculated (Fig. 9).

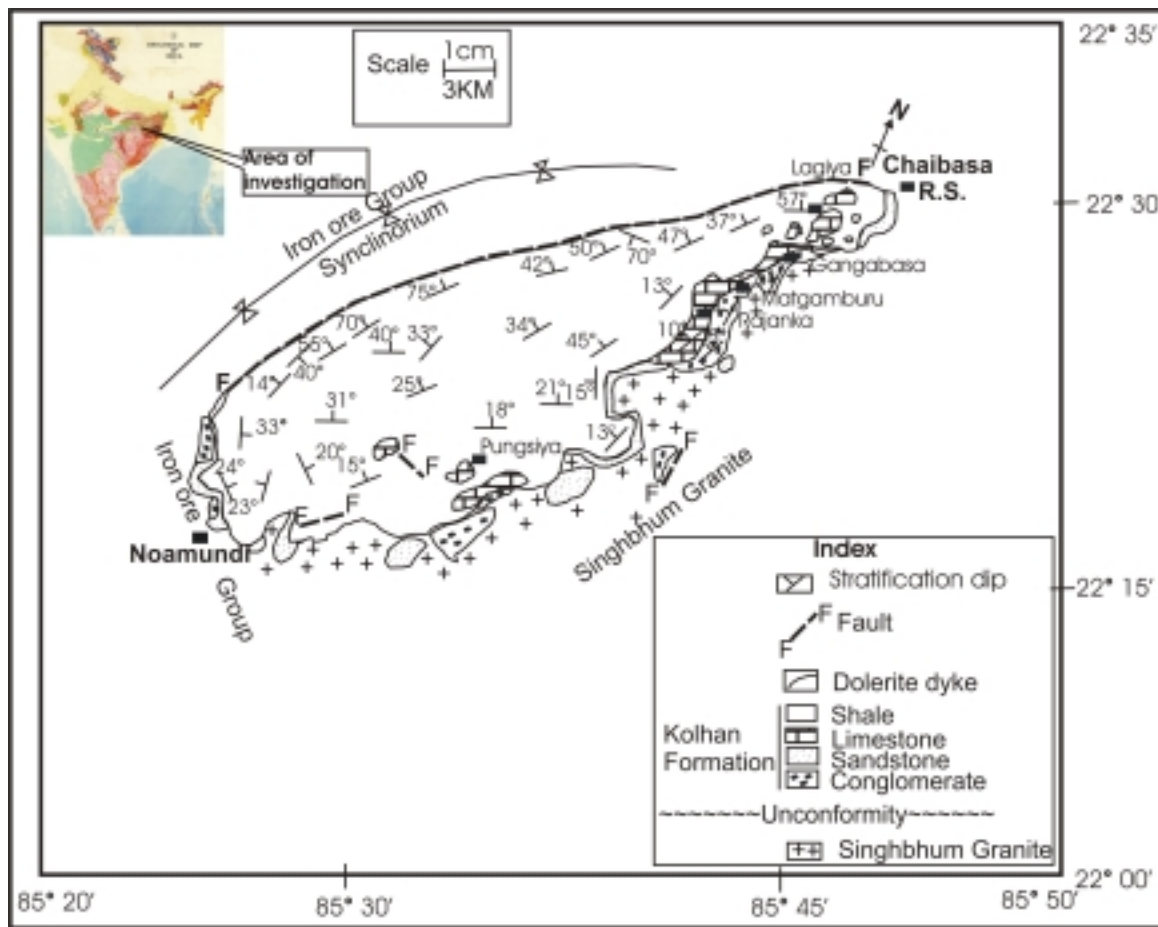


Fig.1. Geological map of the Chaibasa-Noamundi basin (Chatterjee and Bhattacharya, 1969).

For geochemical analysis, shale samples were crushed to finer size in an agate planetary ball mill. In this ball mill, 10-12 g of the sample powder together with 7-8 big and small agate balls are put in a metallic cup and rigorously rotated. After grinding, the sample and agate balls were taken out of the sample cups and balls were cleaned by ethanol thoroughly before the next round of use. The powder samples were analyzed for major oxides by using XRF SRS 3400 at NML Jamshedpur. XRF SRS 3400 is a general purpose sequential X-ray spectrometer for qualitative and quantitative analyses of elements from atomic no. 5 onwards.

RESULTS AND DISCUSSION

Petrography

The Kolhan sandstones are composed mainly of an aggregate of subangular to subrounded quartz

embedded in siliceous matrix, with subordinate amounts of feldspar, jasper, muscovite and rock fragments like granite, BHJ, chert, recycled pebbles of quartzite and conglomerate. Zircon, tourmaline, sphene, rutile are the common heavy minerals. Biotite is rare (Table 1, Fig. 2). Quartz is the dominant detrital mineral constituent with a modal variation from 60.3 % - 89.2 %. The grains are mostly subangular - subrounded with grain size varying from 0.06 - 1 mm. The quartz type is dominantly monocrystalline non-undulatory type, which suggests the provenance to be plutonic igneous rock (Fig. 3). Polycrystalline and also undulose quartz grains are uncommon. The grains are frequently coated with iron oxide and exhibit authigenic overgrowths which produce euhedral out line in some cases (Fig. 4a). Feldspar is the next dominant mineral, which varies in modal proportions from practically 1.4 to about 13.5 %. The grain size varies from 0.09 to 1 mm and the grains are mostly sub angular and coated with hematite. They are usually altered and show all stages from nearly fresh to almost completely

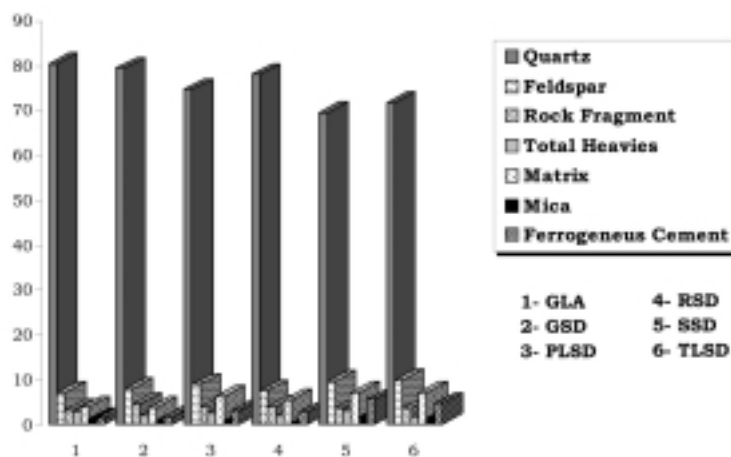


Fig. 2. Percentages of different constituents obtained from sandstone samples taken from six different lithofacies.

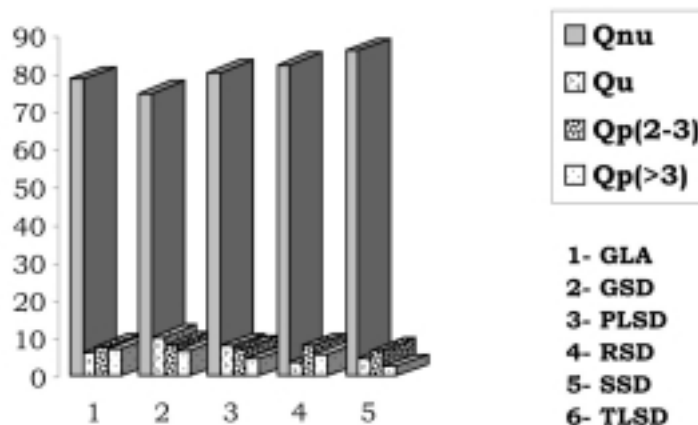


Fig. 3. Quartz type percentage for six lithofacies showing the dominance of non-undulatory quartz percentage indicate the provenance to be plutonic igneous rocks.

Table 1. Modal percentage of Kolhan sandstone from different facies with average.

| Facies | Sample no. | Q | F | RF | H | AMX | FCT | M |
|--------|-------------|-------------|------------|------------|------------|------------|------------|------------|
| GLA | SD 1 | 79.0 | 6.2 | 4.7 | 3.6 | 3.0 | 1.2 | 1.7 |
| | SD 2 | 81.3 | 7.8 | 1.6 | 2.1 | 4.5 | 1.5 | 0.5 |
| | Avg. | 80.2 | 7.0 | 3.2 | 2.8 | 3.8 | 1.4 | 1.1 |
| GSD | SD 3 | 73.2 | 9.9 | 4.9 | 2.7 | 3.8 | 2.6 | 2.0 |
| | SD 4 | 76.4 | 11.8 | 2.0 | 2.7 | 4.4 | 1.8 | 0.8 |
| | SD 5 | 88.8 | 1.4 | 2.0 | 3.7 | 1.6 | 1.2 | 0.0 |
| | SD 6 | 77.7 | 7.6 | 4.4 | 1.6 | 5.3 | 2.0 | 0.4 |
| | SD 7 | 89.2 | 2.2 | 1.6 | 2.3 | 1.5 | 1.8 | 0.6 |
| | SD 8 | 79.7 | 6.5 | 4.9 | 3.2 | 3.8 | 0.2 | 1.2 |
| | SD 9 | 72.9 | 9.3 | 4.7 | 0.6 | 4.4 | 2.7 | 1.2 |
| | SD 10 | 71.4 | 10.6 | 7.8 | 2.6 | 5.6 | 0.4 | 1.0 |
| | SD 11 | 79.0 | 8.9 | 5.8 | 1.4 | 2.2 | 1.5 | 0.6 |
| | SD 12 | 74.1 | 9.4 | 6.7 | 2.2 | 5.5 | 0.8 | 0.0 |
| | SD 13 | 73.6 | 11.8 | 7.0 | 1.2 | 2.7 | 1.2 | 0.5 |
| | SD 14 | 83.3 | 5.6 | 2.2 | 0.7 | 4.4 | 3.2 | 0.0 |
| | SD 15 | 81.1 | 6.3 | 5.2 | 0.2 | 2.2 | 2.4 | 2.1 |
| | SD 16 | 80.6 | 7.9 | 4.1 | 2.2 | 3.5 | 2.0 | 0.0 |
| | SD 17 | 81.3 | 6.7 | 4.8 | 1.0 | 2.6 | 1.8 | 1.3 |
| | Avg. | 78.8 | 7.7 | 4.5 | 1.9 | 3.6 | 1.7 | 0.8 |
| PLSD | SD 18 | 76.2 | 4.2 | 1.9 | 2.1 | 8.4 | 5.5 | 0.0 |
| | SD 19 | 67.9 | 12.6 | 1.6 | 5.3 | 8.9 | 2.2 | 0.6 |
| | SD 20 | 82.9 | 2.4 | 1.2 | 2.1 | 6.2 | 4.6 | 0.0 |
| | SD 21 | 75.2 | 11.3 | 4.2 | 3.8 | 3.9 | 2.1 | 0.0 |
| | SD 22 | 67.3 | 13.5 | 3.4 | 2.5 | 7.9 | 3.6 | 1.0 |
| | SD 23 | 76.7 | 7.0 | 5.2 | 2.1 | 4.7 | 0.0 | 3.3 |
| | SD 24 | 73.6 | 9.0 | 5.3 | 0.0 | 7.1 | 4.2 | 0.0 |
| | SD 25 | 73.3 | 10.6 | 7.2 | 1.0 | 1.6 | 2.0 | 2.1 |
| | Avg. | 74.1 | 8.8 | 3.8 | 2.4 | 6.1 | 3.0 | 0.9 |
| RSD | SD 26 | 70.7 | 12.2 | 7.6 | 1.2 | 4.1 | 3.6 | 0.0 |
| | SD 27 | 77.0 | 10.7 | 3.4 | 2.6 | 3.7 | 2.2 | 0.0 |
| | SD 28 | 79.2 | 7.0 | 3.1 | 1.2 | 4.1 | 3.7 | 0.9 |
| | SD 29 | 74.4 | 8.5 | 3.8 | 3.7 | 8.0 | 1.2 | 0.6 |
| | SD 30 | 80.8 | 2.5 | 1.1 | 0.5 | 9.5 | 4.2 | 0.8 |
| | SD 31 | 77.0 | 7.6 | 3.6 | 3.0 | 4.8 | 3.8 | 0.4 |
| | SD 32 | 82.0 | 7.7 | 4.3 | 1.96 | 3.4 | 0.0 | 0.3 |
| | SD 33 | 81.1 | 7.5 | 6.3 | 0.6 | 1.4 | 1.0 | 0.1 |
| | SD 34 | 81.6 | 2.7 | 1.9 | 1.8 | 6.5 | 4.8 | 0.0 |
| | SD 35 | 78.5 | 5.1 | 3.4 | 2.4 | 6.6 | 2.4 | 0.9 |
| | SD 36 | 75.9 | 7.9 | 4.5 | 2.1 | 4.2 | 3.3 | 0.9 |
| | SD 37 | 78.9 | 8.3 | 0.4 | 1.4 | 6.7 | 3.9 | 0.0 |
| | SD 38 | 74.5 | 10.2 | 6.2 | 1.6 | 6.4 | 0.6 | 0.0 |
| SD 39 | 76.2 | 5.8 | 6.3 | 2.5 | 5.6 | 2.3 | 0.6 | |
| | Avg. | 77.7 | 7.4 | 4.0 | 1.9 | 5.4 | 2.6 | 0.4 |
| SSD | SD 40 | 77.8 | 9.1 | 2.2 | 3.4 | 5.6 | 2.7 | 0.0 |
| | SD 41 | 60.3 | 11.1 | 4.4 | 5.8 | 10.2 | 5.6 | 1.9 |
| | SD 42 | 68.4 | 10.3 | 2.6 | 4.3 | 6.6 | 7.9 | 0.6 |
| | SD 43 | 72.1 | 8.3 | 4.1 | 2.7 | 3.9 | 5.1 | 2.8 |
| | SD 44 | 72.0 | 10.9 | 2.6 | 1.3 | 8.0 | 4.0 | 0.0 |
| | SD 45 | 68.6 | 8.9 | 5.8 | 2.3 | 8.5 | 5.5 | 0.0 |
| | SD 46 | 67.5 | 7.8 | 4.2 | 0.8 | 6.2 | 7.7 | 6.5 |
| | Avg. | 69.5 | 9.5 | 3.7 | 2.9 | 7.0 | 5.5 | 1.7 |
| TLSD | SD 47 | 73.6 | 10.2 | 1.7 | 0.7 | 7.8 | 4.0 | 0.2 |
| | SD 48 | 70.6 | 7.6 | 4.4 | 2.2 | 8.0 | 3.0 | 3.4 |
| | SD 49 | 72.8 | 11.5 | 2.5 | 2.6 | 6.1 | 5.1 | 0.0 |
| | SD 50 | 69.1 | 13.0 | 4.9 | 0.6 | 4.4 | 6.3 | 0.7 |
| | SD 51 | 70.5 | 6.5 | 4.2 | 1.5 | 8.8 | 4.9 | 2.2 |
| | Avg. | 71.3 | 9.7 | 3.5 | 1.5 | 7.0 | 4.7 | 1.3 |

Q=Total quartz, F=Total feldspar, RF=Rock fragment, H=Heavy minerals, AMX=Argillaceous matrix, FCT=Ferruginous cement, M-mica

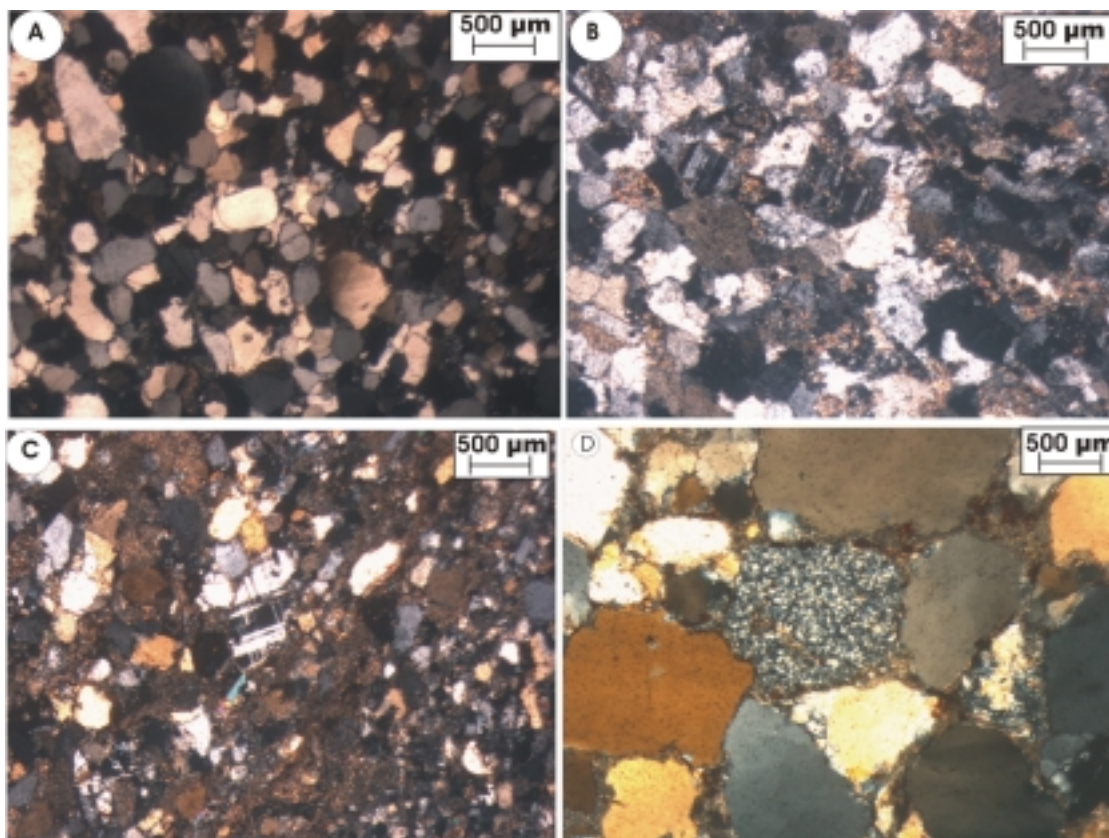


Fig. 4. Photomicrographs of sandstone samples showing **A.** sub-rounded to well rounded quartz grains with overgrowth, **B-C.** sub-arkose showing the presence of plagioclase feldspar and microcline, with high percentage of matrix, **D.** rounded sedimentary rock fragment at the centre indicate recycling of sediments.

seriticized with few fresh relics. The feldspar is dominantly detrital and includes sodic plagioclase and microcline. The photomicrographs (Fig. 4b, 4c) show the sub-arkose type of sandstone with very high percentage of matrix. Rock fragments vary in modal analysis from 0.4 to 7.0 % and exhibit a size variation in sand grade. They are mostly sub rounded to well rounded meta-quartzite, micro-granite, shale and phyllite and quartz schist. The rounded rock fragments indicate the recycling nature of sediments (Fig. 4d).

Muscovite percentage shows a maximum value up to 2.8 %; which often shows locally replaced by illite-clay matrix. The primary matrix varies between 1.4 to 10.2 % in general. Cement is mainly ferruginous which constitutes nil to 6.6 % of the detrital minerals. Diagenetic replacement of quartz and clayey matrix by iron oxide is frequently observed. Fig. 5a shows a quartz arenite with the dominance of angular to well rounded quartz (Q_m and Q_p) and very low matrix percentage, indicating the recycling of sediments. Fig. 5b shows a strong bimodality, polycrystalline quartz with wide range of angularity of grains. Chatterjee and Bhattacharya, (1969) have suggested a source area with complex lithology and more than one provenance type presumably a granitic in the east and northeast and an Iron-ore Formation type to the southwest and northwest of the

basin. A detrital mode of sandstone plots on a QFL diagram of Dickinson, 1985 not only depicts the tectonic setting of the source area but also the prevailing climate (Basu, 1985). In particular, sandstones derived from low to moderate relief source areas under humid climatic conditions are depleted in feldspars, rock fragments and enriched in quartz (Potter, 1978; Basu, 1985). The recalculated values of Q-F-L percentage and standard ternary plots (Folk, 1980) (Table 2, Fig. 6) show that most of the samples plot in quartz-arenite - subarkose field suggesting the source terrain to be dominated by granitic rocks weathered in a humid climatic condition. Tectonic setting of the basin as inferred from the Q-F-L plot of Dickinson, 1985 is passive margin i.e. stable craton (Fig. 7).

Heavy minerals

The Kolhan Sandstones in general are poor in non-opaque heavy minerals tourmaline, zircon, rutile, garnet and sphene in decreasing order of abundance (Table 3, Fig. 8). The opaque heavies are hematite, illmenite and magnetite. The mineralogical maturity of the heavy mineral assemblages of sandstones is quantitatively defined by zircon-tourmaline-rutile (ZTR) index which is the percentage of the combined zircon, tourmaline,

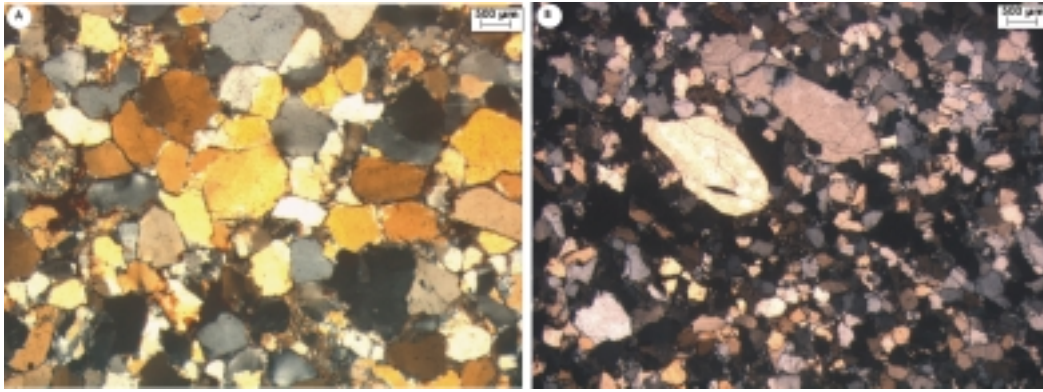


Fig. 5 A. Quartz arenite showing the matrix percentage is very low, B. strong bimodality of the rock samples.

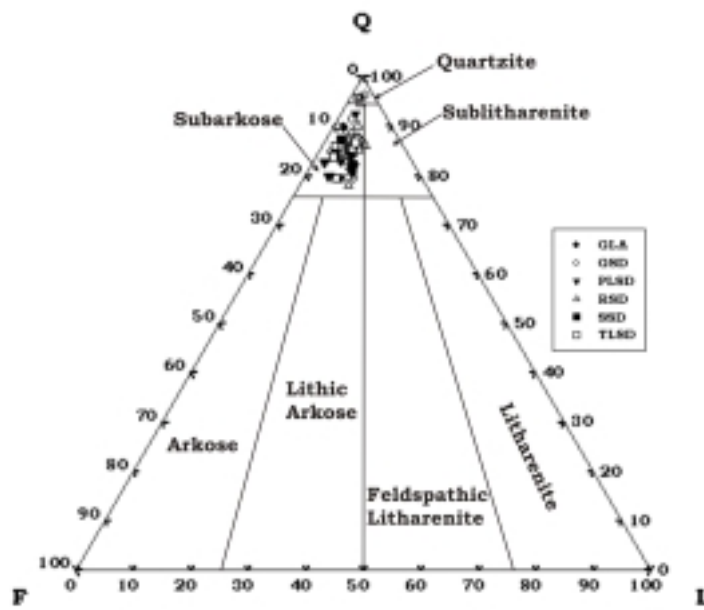


Fig. 6. Q-F-L plots (Folk, 1980) show that the sandstones are mainly quartz arenite-subarkose.

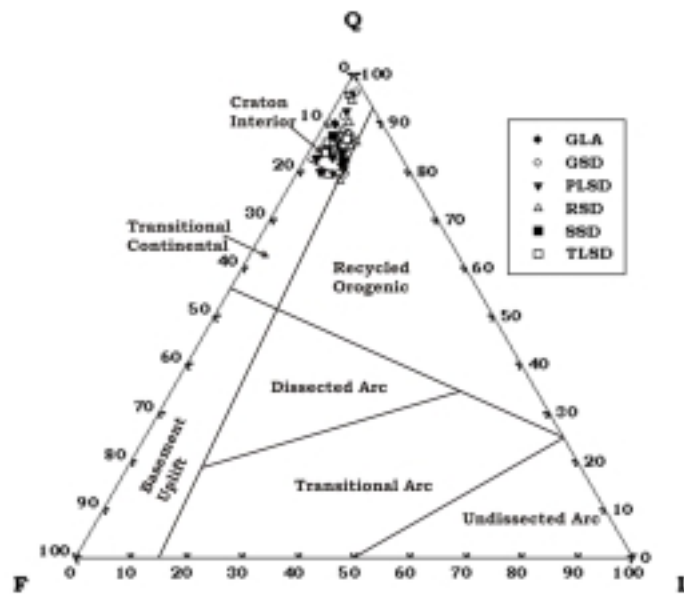


Fig. 7. QFL plots (Dickinson, 1985) show that most of the samples fall in the zone of craton interior and few in the transitional continental zone.

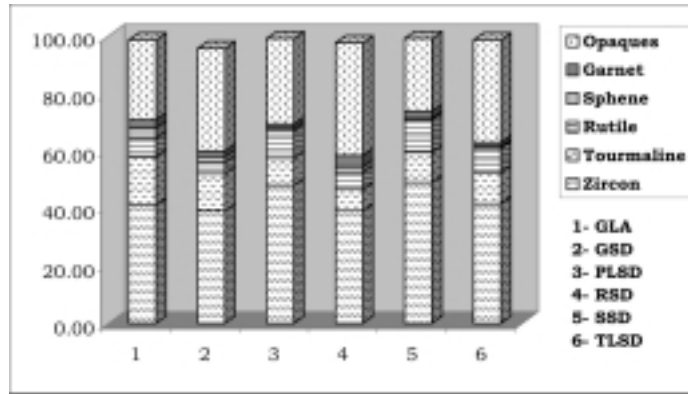


Fig. 8. Bar diagrams showing the percentage distributions of the heavy minerals in different facies.

Table 2. Q-F-L percentage of sandstone samples from different lithofacies with their average.

| Facies | Sample no. | Q% | F% | L% |
|-------------|-------------|-------------|------------|------------|
| GLA | SD 1 | 87.7 | 6.9 | 5.3 |
| | SD 2 | 89.6 | 8.6 | 1.7 |
| | Avg. | 88.6 | 7.7 | 3.5 |
| GSD | SD 3 | 83.0 | 11.3 | 5.6 |
| | SD 4 | 84.6 | 13.1 | 2.2 |
| | SD 5 | 96.1 | 1.5 | 2.2 |
| | SD 6 | 86.5 | 8.5 | 4.9 |
| | SD 7 | 95.7 | 2.4 | 1.7 |
| | SD 8 | 87.3 | 7.2 | 5.4 |
| | SD 9 | 83.7 | 10.7 | 5.5 |
| | SD 10 | 79.4 | 11.8 | 8.6 |
| | SD 11 | 84.1 | 9.5 | 6.2 |
| | SD 12 | 82.0 | 10.4 | 7.5 |
| | SD 13 | 79.6 | 12.8 | 7.5 |
| | SD 14 | 91.3 | 6.2 | 2.4 |
| | SD 15 | 87.4 | 6.8 | 5.7 |
| | SD 16 | 86.9 | 8.5 | 4.4 |
| SD 17 | 87.4 | 7.3 | 5.2 | |
| Avg. | 86.4 | 8.5 | 5.0 | |
| PLSD | SD 18 | 92.4 | 5.1 | 2.4 |
| | SD 19 | 82.6 | 15.3 | 1.9 |
| | SD 20 | 95.7 | 2.8 | 1.3 |
| | SD 21 | 82.8 | 12.4 | 4.6 |
| | SD 22 | 79.8 | 16.0 | 4.1 |
| | SD 23 | 86.1 | 7.9 | 5.9 |
| | SD 24 | 83.6 | 10.2 | 6.0 |
| | SD 25 | 80.3 | 11.6 | 7.9 |
| Avg. | 85.4 | 10.2 | 4.3 | |
| RSD | SD 26 | 78.0 | 13.5 | 8.4 |
| | SD 27 | 84.4 | 11.7 | 3.8 |
| | SD 28 | 88.5 | 7.9 | 3.5 |
| | SD 29 | 85.7 | 9.8 | 4.3 |
| | SD 30 | 95.6 | 2.9 | 1.3 |
| | SD 31 | 87.2 | 8.6 | 4.0 |
| | SD 32 | 87.1 | 8.2 | 4.6 |
| | SD 33 | 85.3 | 7.9 | 6.6 |
| | SD 34 | 94.6 | 3.1 | 2.2 |
| | SD 35 | 90.0 | 5.9 | 3.9 |
| | SD 36 | 85.8 | 8.9 | 5.1 |
| | SD 37 | 89.9 | 9.4 | 0.5 |
| | SD 38 | 81.8 | 11.3 | 6.8 |
| | SD 39 | 86.1 | 6.6 | 7.2 |
| Avg. | 87.2 | 8.3 | 4.5 | |
| SSD | SD 40 | 87.2 | 10.2 | 2.4 |
| | SD 41 | 79.4 | 14.6 | 5.8 |
| | SD 42 | 84.0 | 12.6 | 3.2 |
| | SD 43 | 85.2 | 9.87 | 4.8 |
| | SD 44 | 84.1 | 12.7 | 3.0 |
| | SD 45 | 82.2 | 10.7 | 7.0 |
| | SD 46 | 84.8 | 9.8 | 5.3 |
| Avg. | 83.9 | 11.5 | 4.5 | |
| TLSD | SD 47 | 86.0 | 11.9 | 2.0 |
| | SD 48 | 85.4 | 9.2 | 5.3 |
| | SD 49 | 83.8 | 13.2 | 2.9 |
| | SD 50 | 79.4 | 14.9 | 5.6 |
| | SD 51 | 86.6 | 8.0 | 5.2 |
| Avg. | 84.2 | 11.4 | 4.2 | |

Table 3. Heavy mineral percentage of different litho facies showing non-opaque heavy mineral (HNOP) and opaque heavy mineral (HOP).

| Heavy Minerals | GLA | GSD | PLSD | RSD | SSD | TLSD | |
|----------------|------------|------|------|------|------|------|------|
| HNOP | Zircon | 41.2 | 39.4 | 48.0 | 39.2 | 49.0 | 41.8 |
| | Tourmaline | 16.8 | 12.7 | 9.6 | 7.8 | 10.5 | 10.7 |
| | Rutile | 6.7 | 4.0 | 9.5 | 5.7 | 11.5 | 8.3 |
| | Sphene | 3.3 | 2.1 | 0.8 | 1.8 | 0.5 | 0.8 |
| | Garnet | 2.9 | 1.7 | 1.6 | 3.9 | 2.4 | 1.3 |
| HOP | | 27.6 | 35.9 | 29.6 | 39.4 | 25.1 | 35.9 |

Table 4. Geochemical composition of Kolhan shale in percentage

and rutile grains among the transparent, non-micaceous, detrital heavy minerals (Hubert, 1962). The variation of ZTR indices of the six lithofacies is shown in Fig. 9.

Geochemical Analysis

Bandopadhyaya and Sengupta, (2004) have analysed a few sandstone, shale, calcareous shale and limestone samples of the Kolhan Group. The Kolhan shale are composed of 63.0-68.4 % SiO₂, 14.8-18.0 % Al₂O₃, 3.1-6.2 % K₂O, 0.03-0.5% Na₂O, 0.2-0.4 % CaO, 0.2-2.2 % MgO, 0.1-0.4 % P₂O₅, 0.5-0.7 % TiO₂, 0.07-0.1 % MnO, and 3.8-15.4 % Fe₂O₃ (Table 4). Kolhan shale is characterized by high values of SiO₂, K₂O, Fe₂O₃ and low values of CaO, TiO₂, Na₂O, Al₂O₃, MgO as compared with the average Proterozoic shale (APS). On comparing with the results of Bandopadhyaya and Sengupta, (2004), Kolhan shale shows more or less the same values for SiO₂, Al₂O₃, Fe₂O₃, MnO, MgO content.

Source Rock Composition

Geochemical composition of sedimentary rocks has been successfully used to decipher the composition of source rocks (Naqvi et al., 1998). It has been observed that the ratio of Ti and Al can effectively be used as an index of provenance, since they behave as immobile phases because of their low solubility and similar behavior during weathering (McLennan et al., 1979). Al₂O₃/TiO₂ ratio characteristically ranges from 3 to 11 for mafic rocks, 11 to 21 for intermediate rocks and 21 to 70 for felsic rocks (Sugitani et al., 1996; Hayashi et al., 1997). Al₂O₃/TiO₂ ratios of the Kolhan shales vary from 21.3 to 38.2, suggesting predominance of felsic rock in the provenance. Bivariate plot between Al₂O₃ and TiO₂ is widely used as provenance indicator for many sedimentary terrains (McLennan et al., 1979; Schieber, 1992; Schieber et al., 1992) which discriminate the source rocks into three categories based on relative

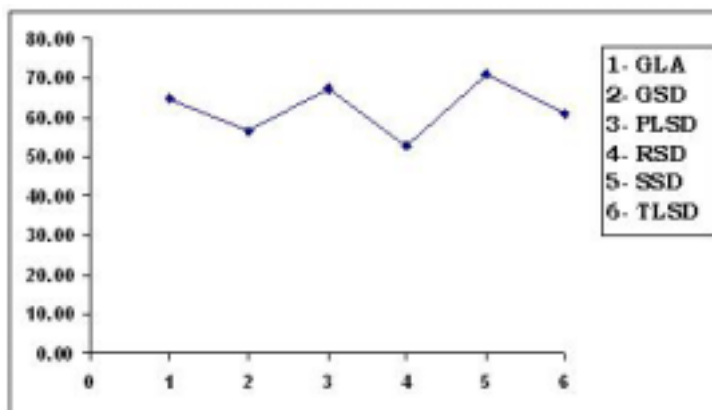


Fig. 9. Plots of ZTR index (zircon-tourmaline-rutile index) of six lithofacies.

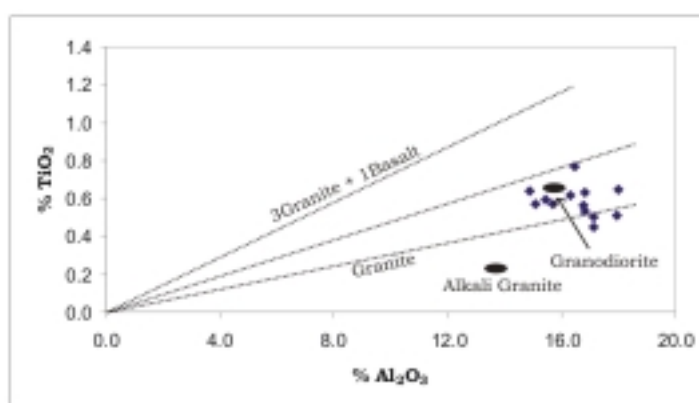


Fig. 10. Bivariate plot between Al_2O_3 and TiO_2 indicating the source rock to be granitic composition.

contribution of granitic and basaltic provenances. Most of the Kolhan shales of the Al_2O_3 vs. TiO_2 plot suggest predominantly the granitic (felsic) field (Fig. 10).

Tectonic setting

The K_2O vs. Na_2O (Crook, 1974), $\text{K}_2\text{O}/\text{Na}_2\text{O}$ vs. SiO_2 plot (Roser and Korsch, 1986) and $\text{CaO}-\text{K}_2\text{O}-\text{Na}_2\text{O}$ ternary plot (Bhatia, 1983) have been used successfully to determine the tectonic setting of shales. The $\text{K}_2\text{O}/\text{Na}_2\text{O}$ ratio varies distinctly for different tectonic environment with respect to the SiO_2 content. Roser and Korsch, 1986 demonstrated three different tectonic setting of sedimentary basin (i.e. active continental margin, passive margin or intracratonic and island arc) based on bivariate plot between SiO_2 and $\text{K}_2\text{O}/\text{Na}_2\text{O}$. The data points for the Kolhan shales plot in the passive margin/intracratonic set up (Fig. 11). In this category of tectonic setting, sediments are deposited in plate interior away from plate margin and the sediments are derived from stable continental areas (Roser and Korsch, 1986). The K_2O vs. Na_2O plots of Kolhan shale fall in quartz rich field of Crook, (1974) suggesting that these lithounits were deposited in plate interior either at stable continental margin or in the intracratonic basin (Fig. 12).

High $\text{SiO}_2/\text{Al}_2\text{O}_3$ and $\text{K}_2\text{O}/\text{Na}_2\text{O}$ ratio of these shales suggest their derivation from a granite dominated upper continental crust (McLennan et al., 1993). In the present case, such type of source terrain (Singhbhum Granite) is exposed in the east of the Kolhan basin. In the $\text{CaO}-\text{K}_2\text{O}-\text{Na}_2\text{O}$ ternary plot, (Bhatia, 1983) the studied shale samples plot in passive margin field (Fig. 13).

Paleoweathering Environment

The rate of chemical weathering of source rock and the erosion rate of weathering profile are controlled by the prevailing climate as well as source rock composition and tectonics. Warm humid climate and stable tectonic setting favor intense chemical weathering. A useful way to assess the paleoweathering and tectonic history of the rock is the Chemical Index of Alteration (CIA) = $\{ \text{Al}_2\text{O}_3 / (\text{Al}_2\text{O}_3 + \text{CaO} + \text{Na}_2\text{O}) \} \times 100$, proposed by Nesbitt and Young (1982) to monitor the progressive alteration of plagioclase and K-feldspar to clay minerals. CIA value increases with increasing weathering intensity, reaching 100 when all Ca, Na and K have been leached out from weathering residue. The CIA value for the Kolhan shale vary from 70.7 to 80.3, (average 75.2) indicating that the source rock underwent moderate to high degree of

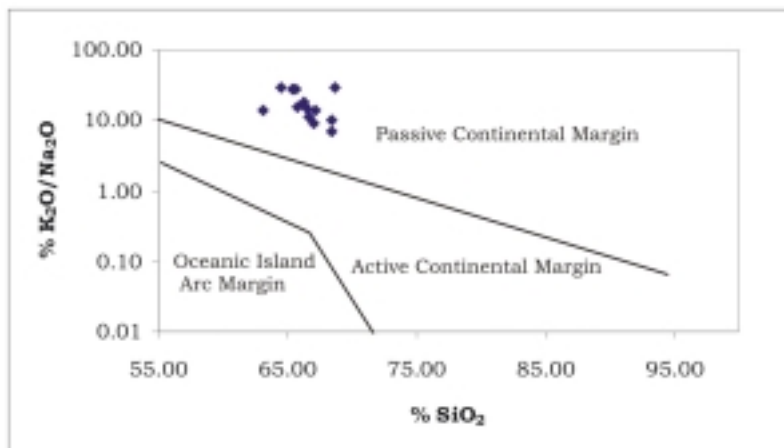


Fig. 11. Tectonic discrimination diagram for the Kolhan shale indicating the passive margin setting.

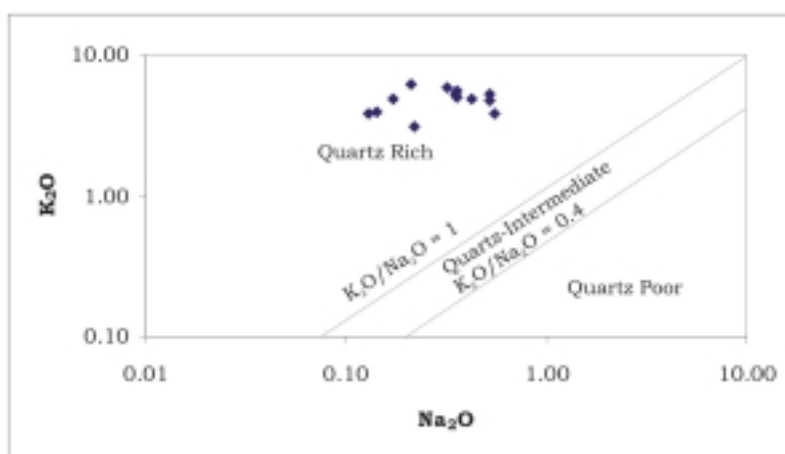


Fig.12. K₂O-Na₂O diagram (Crook, 1974) classifying Kolhan shale as quartz rich type.

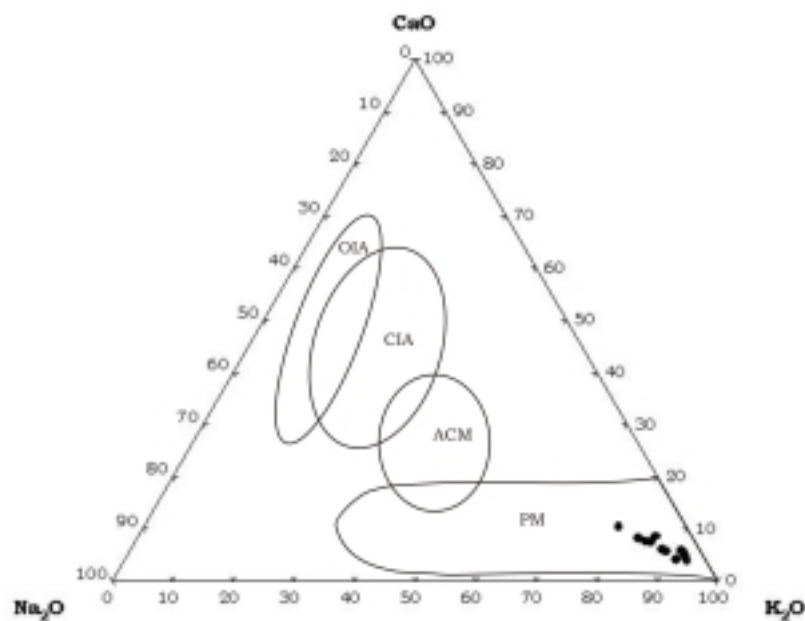


Fig.13. CaO-K₂O-Na₂O triangular diagram (Bhatia, 1983) showing Kolhan shale in the passive margin (PM) field; and also shown fields of different tectonic settings. CAN Active Continental Margin, OIA-Oceanic Island Arc, CIA-Continental Island Arc.

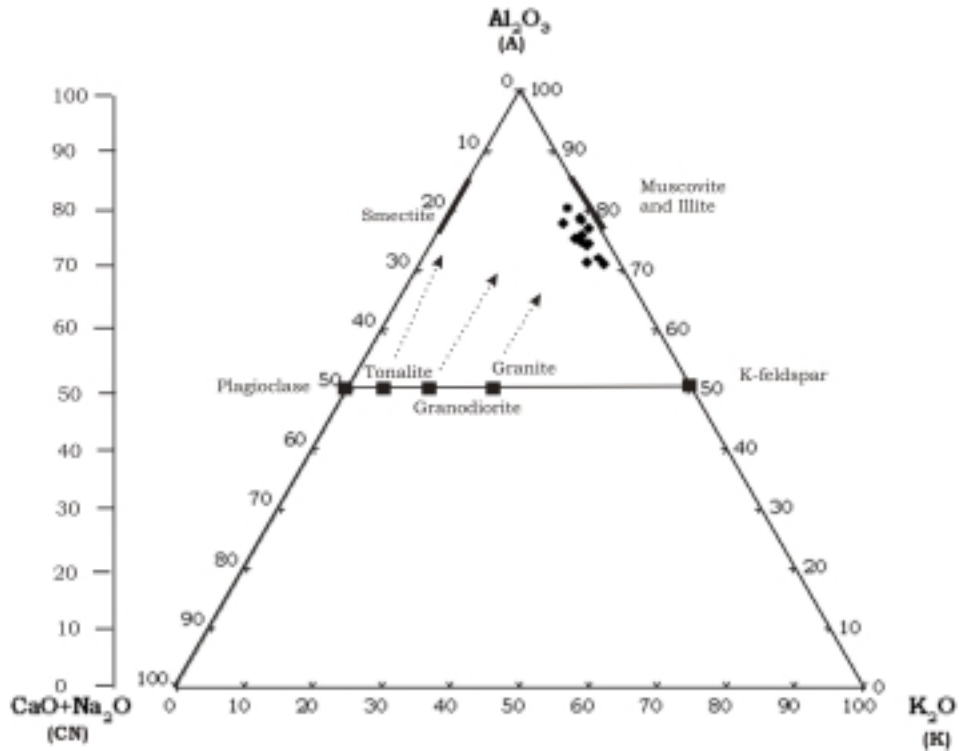


Fig.14. A-CN-K compositional space showing weathering trends for the Kolhan shale. The best fit line parallel to the A-CN join indicates the source to be granite to granitoid. CIA values have been represented in the vertical line to the left of the A-CN-K compositional space.

chemical weathering in humid tropical condition. The weathering history of igneous rocks and the source for various clastic sedimentary sequences have been evaluated by using the A-CN-K ($A=Al_2O_3$; $CN=CaO+Na_2O$; $K=K_2O$) triangular diagram (Nesbitt and Young, 1982). In A-CN-K plot, the compositional trends of various rocks during initial stage of weathering would be almost parallel to A-CN line from their respective fresh unweathered points. These pathways of weathering for mafic and felsic igneous rocks are confirmed by weathering profile and thermodynamics/kinetic calculation (Nesbitt and Young, 1984a). The pathways are parallel to A-CN line because in the initial stage of weathering Na and Ca are removed from plagioclase and as the degree of weathering increases, K-feldspar are destroyed releasing K in preference to Al. During this process the residual bulk composition is enriched with Al_2O_3 . All the samples of Kolhan shale plot parallel and close to the Al_2O_3 - K_2O (Fig. 14) boundary implying that their source area had undergone extensive weathering and produced shaly sedimentation.

CONCLUSIONS

Petrography and heavy mineral analysis (high ZTR indices) suggests the Kolhan sandstone to be mineralogically matured quartz-arenite to sub arkose type deposited in a humid tropical climatic condition.

The tectonic setting of the depositional basin was either passive margin or intracratonic in nature. Hence it clearly indicates Kolhan Group of rocks received detritus from the Singhbhum Granite. This elucidation from sandstone petrography is well supported by the geochemical data which also helps in unraveling the paleoweathering history, and composition and tectonic setting of the provenance. The major element concentration Al_2O_3/TiO_2 ratio of the shale suggests predominantly granitic composition of the source rock. The bivariate plot of K_2O/Na_2O vs. SiO_2 and ternary plot of CaO - K_2O - Na_2O suggest intracratonic nature of the depositional basin. Moderate to high degree of chemical weathering of the source rock is envisaged from the range of CIA values and the A-CN-K compositional trend of the shale samples. Integrated correlation of the petrographic and chemical data of Kolhan sediments from the Chaibasa-Noamundi basin suggest the basin to be an intracratonic basin, where moderate to high degree of chemical weathering prevailed in a humid tropical climate.

Acknowledgements: Authors are highly grateful to Department of Geology and Geophysics and IIT Kharagpur for providing necessary facilities and financial support to carry out the present investigation. Thanks are due to the officers of the XRF laboratory, NML, Jamshedpur for analyzing the samples for geochemical study.

References

- Bandopadhyay, P.C. and Sengupta, S. (2004). Paleoproterozoic supracrustal Kolhan Group in Singhbhum craton, India and the Indo-African Supercontinent, *Gondwana Res.*, 7(4), 1228-1235.
- Basu, A., Young, S. W., Suttner, L. J., James, W. C. and Mack, G. H. (1975). Re-evaluation of the use of undulatory extinction and polycrystallinity in detrital quartz for provenance interpretation. *J. Sed. petrol.*, 45, 873-882.
- Basu, A. (1985). Reading provenance from detrital quartz. In: G. G. Zuffa (Ed.) *Provenance of Arenites. Dordrecht D. Reidal*, 231-247.
- Bhatia, M. R. (1983). Plate tectonics and geochemical composition of sandstones. *J. Geol.*, 91, 611-627.
- Bhattacharya, A.K. and Chatterjee, B.K. (1964). Petrology of Precambrian Kolhan formation of Jhinkpani, Singhbhum district, Bihar. *Geologische Rundschau*, 53, 758-779.
- Chatterjee, B.K. and Bhattacharya, A.K. (1969). Tectonics and sedimentation in a Precambrian shallow epicontinental basin. *Jour. Sed. Petrol.*, 39(4), 1566-1572.
- Condie, K.C. (1967). Geochemistry of early Precambrian greywacke from Wyoming. *Geochemical and Cosmochemical Acta*, 31, 2135-2149.
- Condie, K.C. (1993). Chemical composition and evolution of the upper continental crust: contrasting results from surface samples and shales. *Chem. Geol.*, 104, 145-166.
- Crook, K.A.W. (1974). Lithogenesis and geotectonics: the significance of compositional variations flysch arenites (greywakes). In: Dott, R.H. and Shaver, R.H. (Eds.), *Modern and Ancient Geosynclinal Sedimentation. Soc. Econ. Paleo. Min. Spl. Publ.*, 19, 304-310.
- Dickinson, W.R. (1970). Interpreting detrital modes of graywacke and arkose. *J. Sediment. Petro.*, 40, 695-707.
- Dickinson, W. R. (1985). Interpreting provenance relation from detrital modes of sandstones. In: G. G. Zuffa (Ed.) *Provenance of Arenites. Dordrecht D. Reidal*, 333-363.
- Dunn, J.A. (1940). The stratigraphy of North Singhbhum. *Mem. Geol. Surv. Ind.*, 63(3), 303-369.
- Fedo, C.M., Nesbitt, H.W. and Young, G.M. (1995). Unrevealing the effects of potassium metasomatism in sedimentary rocks and palaeosols, with implications for palaeoweathering conditions and provenance. *Geology*, 23, 921-924.
- Folk, R.L. (1980). *Petrology of Sedimentary Rock*. Hemphill Publ. Co., Austin, Texas, 184p.
- Hayashi, K., Fujisawa, H., Holland, H.D. and Ohmoto, H. (1997). Geochemistry of 1.9 Ga sedimentary rocks from northeastern Labrador, Canada. *Geochimica Cosmochimica Acta*, 61, 4115-4137.
- Hubert, J. F. (1962). A Zircon-Tourmaline-Rutile maturity index and the interdependence of the composition of heavy mineral assemblages with the gross composition and texture of sandstones. *Jour. Sed. Petro.*, 32, 440-450.
- Mahadevan, T. M. (2002). *Geology of Bihar and Jharkhand*. DST Publication, Geol. Soc. India, Bangalore, 563p.
- McLennan, S.M., Fryer, B.J., Fryer, B.J. and Young, G.M. (1979). The geochemistry of the carbonate-rich Espanola Formation (Huronian) with emphasis on the rare earth elements. *Canadian Jour. of Earth Sciences*, 16, 230-239.
- McLennan, S.M. and Taylor, S.R. (1980). Rare earth elements in sedimentary rocks, granites and uranium deposits of the Pine Creek geosyncline. In: Ferguson, J. and Coleby, A.B. (Eds.), *Uranium in the Pine Creek geosyncline, IAEA, Vienna*, p. 175-190.
- McLennan, S.M., Hemming, S., Mcdaniel, D.K. and Hanson, G.N. (1993). Geochemical approaches to sedimentation, provenance and tectonics. In: Johnsson, M J. and Basu, A. (Eds.), *Processes controlling the composition of clastics sediments. Geol. soc. Amer. Spec.*, paper No 284 pp.21-40.
- Mukhopadhyay, D. (2001). The Archean nucleus of Singhbhum: the present state of knowledge. *Gond. Res.*, 4, 307-318.
- Mukhopadhyay, J., Ghosh, G., Nandi, A.K. and Chaudhuri, A.K. (2006). Depositional setting of the Kolhan Group: its implications for the development of a Meso to Neoproterozoic deep-water basin on the South Indian Craton. *South African Jour. of Geol.*, 183-192.
- Naqvi, S.M., Sawkar, R.H., Subba Rao, D.V, Govil, P.K. and Gnaneshwar Rao, T., (1998). Geology and geochemistry and tectonic setting of Archaean greywackes from Karnataka nucleus, India. *Precambrian Res.*, 39, 193-216.
- Nesbitt, H.W. and Young, G. M. (1982). Early Proterozoic climates and plate motions inferred from major elements of lutites. *Nature*, 299, 715-717.
- Nesbitt, H.W. and Young, G.M. (1984a). Prediction of some weathering trends of plutonic and volcanic rocks based on thermodynamics and kinetic consideration. *Geochim. Cosmo. Acta*, 48, 1523-1534
- Potter, P.E. (1978). Significance and origin of big rivers. *J. Geol.*, 86, 13-33.
- Ray, S. and Bose, M.K. (1959). Fold patterns in the Kolhan Formation: *46th Indian Sci. Congr.Proc.* pt.3, p.202.
- Ray, S. and Bose, M.K. (1964). Unique fold pattern in shallow basin. *Rept. 22nd Session, Int. Geol. Cong.*, 4, 163-170.
- Roser, B. P. and Korsch, R. J. (1986). Determination of tectonic setting of sandstone- mudstone suites

- using SiO_2 content and $\text{K}_2\text{O}/\text{Na}_2\text{O}$ ratio. *J. Geol.*, 94, 635–650.
- Saha, A.K. (1948a). A study of limestone near Chaibasa. *Geol. Min. Met. Soc. India, Quart. Jour.*, 20, 49-58.
- Saha, A.K. (1948b). The Kolhan Series-Iron–Ore Series boundary to the west and southwest of Chaibasa, Bihar. *Sci. and Culture*, 14, 77-79.
- Saha, A. K. (1994). Crustal evolution of Singhbhum-North Orissa, Eastern India, *Memoir Geol. Soc. India*, 27, 338 p.
- Saha, A.K., Ray, S.L., and Sarkar, S.N. (1988). Early history of the Earth. Evidence from Eastern Indian Shield. In: D. Mukhopadhyay (Ed.). *Precambrian of the Eastern Indian Shield. Memoir Geological Society of India*, 8, 13-38.
- Schieber, J., (1992). A combined petrographical-geochemical provenance study of the Newland formation, Mid- Proterozoic of Montana. *Geol. Magazine*, 129, 223–237.
- Schieber, U.M., Erikson, P.G., Vander Neut, M. and Snyman, C.P. (1992). Sedimentary petrography of the early Proterozoic Pretoria Group, Transvaal Sequence, South Africa : Implication for tectonic setting. *Sedimentary Geology*, 80, 89-103.
- Sugitani, K., Horiuchi, Y., Adachi M. and Sugisaki, R. (1996). Anomalously low $\text{Al}_2\text{O}_3/\text{TiO}_2$ values for Archean cherts from the Pilbara Block, Western Australia-possible evidence for extensive chemical weathering on the early earth. *Precambrian Res.*, 80, 49–76.

Mapping Seasonal Suspended Sediment Dynamics and Tidal Propagation in Coastal Waters of the Bay of Bengal using Oceansat- I Ocean Colour Monitor Data

B. VEERANARAYANA¹, P.N. SRIDHAR¹, I.V. RAMANA¹, RUPERT. LEACH², K.S.N REDDY³
and M.VENKATESWARA RAO^{3*}

¹National Remote Sensing Agency, Dept. of Space, Oceanography Div., Hyderabad

²Halliburton Engineering Services, Edinburgh, UK, ³Dept. of Geology, Andhra University

*E-mail: venki_mopada@yahoo.co.in

Abstract: The Suspended Sediment Concentrations (SSC) have been mapped along the entire coast of Bay of Bengal (BOB) during 2002-2003 (Pre and Post SW monsoon at low and high tide levels), using high-resolution ocean colour data acquired by Oceansat-1 onboard the Indian Remote Sensing Satellite (IRS-P4-OCM). The SSC distribution in the coastal waters of BOB are highly controlled by diverse forces that include littoral currents, tidal currents, fluvial currents, geostrophic current, coastal circulation and wind stress. The regional SSC distribution pattern along the coast shows seasonal gradient trend from south to north which following the corresponding monsoon and inter monsoon circulations. However, there are also localized variations in the regional SSC distribution occur at selected river mouths, bays and tidal inlets. These variations are mainly controlled by tidal energy, resuspension, shallow bathymetry, coastal and fluvial currents. The regions from south to north have shown to gradually increase in SSC due to the correlation with the micro tidal regime in the south and macro tidal ranges in the northern part of the BOB. The coastal sediment dynamics also show a strong influence on the open ocean. A clear understanding of the pathways of source material and their final destination (probably a sink) as well has been acquired from this study.

Key words: Suspended Sediment Concentration, Bay of Bengal, Ocean Colour, Coastal and Tidal currents.

INTRODUCTION

The enormous amounts of sediment discharged by major rivers such as Ganges- Brahmaputra, Brahmani-Baitarani, Mahanadi, Godavari-Krishna, Pennar and Cauvery flow eastwards into the Bay of Bengal (BOB). The dispersal system of Suspended Sediment Concentrations (SSC) over the coastal waters of BOB areas are characterized by substantial temporal and spatial variability. The sediments are driven by these rivers have many implications, such as transport effects on the bio-geochemical cycle of the coastal areas (Mishra, 2004). Transport of minerals, pollutants and organic matter have an effect on biological productivity of the coastal areas and play a major role in the coastal water quality, turbidity, harbour siltation, estuarine sedimentation, tidal inlet bypass, coral and mangrove health (Ramesh et al, 1995). Thus, the constancy and transport of sediments are essential to the prediction and analysis of environmental quality and marine hazards such as seabed scouring, the siltation of harbours and formation of artificial lakes. This impacts the way the coastline is protected. Therefore, it can be agreed that the dispersal of SSC has huge national and global significance. Remote sensing studies of suspended sediments have been made using the fact that suspended sediments increase the radiance emergent

from surface waters in the visible and near-infrared region of the electromagnetic spectrum (Ritchie and Schiebe, 2000). The main advantage of Ocean Colour Monitor (OCM) data is its extensive spatial and temporal coverage enables us to study basin scale processes.

This paper recommends a review of available information on sediment dynamics in this coastline and an analysis is made of the retrieved suspended sediment concentrations from the OCM data. This study is an interdisciplinary investigation on hydrodynamical conditions as well as on tidal propagation. The sedimentological response has been carried out in order to understand sediment transport processes in the nearshore zone and to estimate the flux and pathways of suspended sediment dynamics.

MATERIALS AND METHODS

Suspended sediment concentrations (SSC) have been mapped along the entire coast of India using satellite images from IRS-P4 Ocean Colour Monitor. The study of suspended Sediment dynamics and flux changes over a large spatial scales by conventional means has its own limitations. The onboard Oceansat-I (IRS-P4) Ocean Colour Monitor data (OCM) has a high spectral range (402-885 nm) and eight spectral bands with 360X250 m ground resolution enabling us to

mapping the suspended coastal sediments. Two sets of satellite images (path/rows of passes 10/13 & 10/14) cover the entire east coast of India, one during the Pre-SW monsoon and the other during the post-SW monsoon period that have been processed by using ERDAS 8.4 software. In addition, the SSC maps are corrected for geometric accuracies using ground control points from base maps. The corresponding tide tables were taken from Indian Tide tables. The SSC have been retrieved using the Tassan algorithm (1994) shown below and validated with insitu data.

From the water leaving radiances, the SSC has been computed using the optical algorithm with OCBM (Optical Back Scattered Model) mentioned below by,

Tassan algorithm (1994):

Total suspended Sediment (TSS) = $\exp [1.83 + 1.26 \cdot \text{Log}(X_s)]$

Where $X_s = [(R_{rs555} + R_{rs670}) \cdot (R_{rs488} / R_{rs555})^{-0.5}]$.

Where, R_{rs} is the Remote sensing reflectance in the corresponding channel.

Improvement in the accuracy of estimation of suspended sediment concentration in coastal waters is observed using the exponential law (AOD) and iteration technique adopted by following an Optical Closure Backscatter Model (OCBM) rather than Black pixel

assumption ($R_{rs}=0$ @ NIR) as the coefficients for obtaining initial estimation. By using the OCBM model, the Water leaving radiance (W_{ln}) contribution in near infra red channels can be computed with appropriate coefficients as water leaving reflectance at 555nm, 488nm and 443nm (Fig. 3). The river discharge and tidal data has been collected from literature and tide tables. Also, wind vectors from Quicksat scatterometer and TOPEX altimeter data for geostrophic currents have been incorporated into this study.

RESULTS AND DISCUSSION

The SSC have been mapped for the entire western boundary of the Bay of Bengal, East coast of India using OCM data. The data has been gathered before and after the SW monsoon period and in order to prepare the study of regional and seasonal SSC distributions at different tide levels. The seasonal SSC distribution patterns shift along the entire coastal waters of BOB, as shown in figure 1 during SW, NE and summer monsoon (pre SW monsoon) periods. The SSC distribution demonstrates the seasonal gradients from south to north of the coastline following a general circulation pattern that corresponds to monsoon or inter-monsoon circulations. The coastal sediment pattern during SW monsoon (Jun-Sept) shows net transport flow is northward, and the

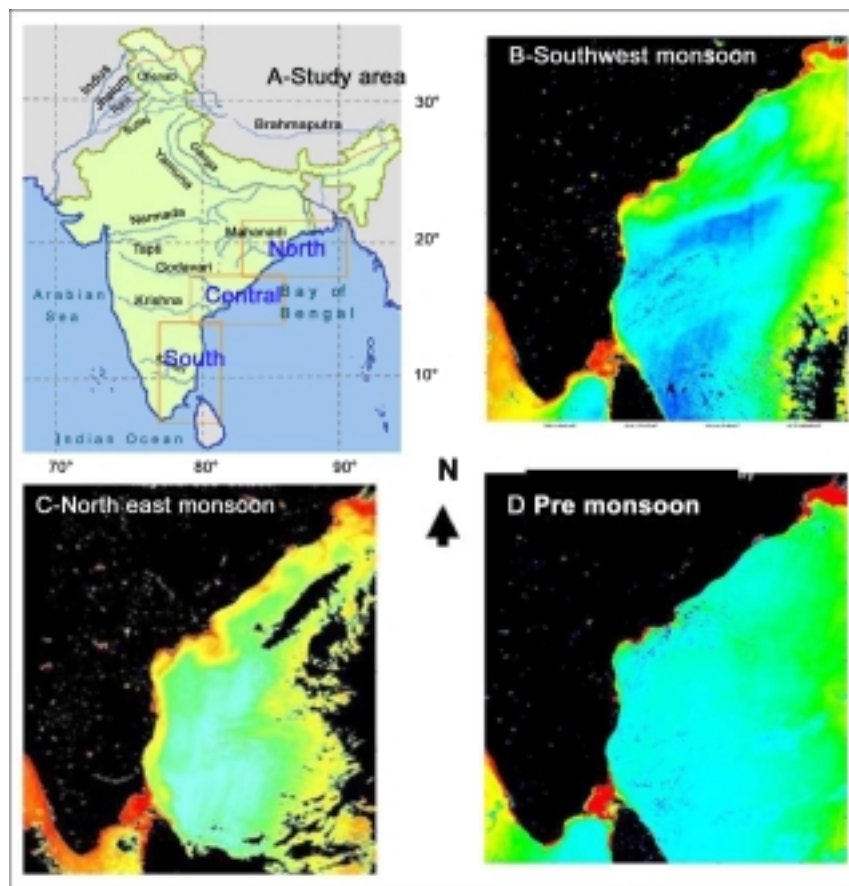


Fig.1. Seasonal suspended sediment distribution pattern along the entire East Coast of India.

NE monsoon (Oct-Jan) flows south while during the summer monsoon (Feb-May) the trend is also towards the north. Therefore, the net transport is towards north along the entire coastline for the above seasonal monsoon due to high river discharge during SW monsoon period. There is a SSC pattern that tends to oscillate clockwise or anti clockwise depending on the monsoon. The cyclonic storms are more frequent along the northern coast of the BOB during the NE monsoon than southern region. As the result, the river discharges sediment extended into outer offshore regions and recycled for a longer timeframe in marine conditions. The SSC distributions at different tidal levels during monsoon and post monsoon periods have been analysed. It is apparent that the regional SSC show a seasonal gradient from north to south that corresponds to monsoon and inter monsoon circulations. However, there are localized variations in the SSC distribution at selected river mouths, bays and tidal inlets that are controlled by tidal and fluvial currents (Quanzhou Gao et al. 2003). For ease of analysis, the entire east coast of India has been divided into three zones are 1) north, 2) central and 3) south.

Northern Zone

This area has enormous levels of sediment discharged into the BOB due to the large rivers of Ganges –Brahmputra, Brahmani, Mahanadi and Vamsadara. This is the reason why higher SSC are found through out the year in this Northern region. This region varies between meso to high meso tidelevels (2 to >4 m) from south of Vamsadara to north of the Ganges. The SSC is highly dependent on tides, coastal currents and shallow bathymetry that cause the resuspension process. The turbidity levels are higher during flooding due to low concentrations of SSC (20-150 mg/l) and a higher areal spread than the ebb tide (40-200 mg/l). The ebb tidal currents are far stronger (1 to >1.5 m/s) in this zone, though flood waters flush vast distances back into the estuary. The SSC variation in pre and post monsoon is shown in Table 1. These currents, driven by density wind allow enhanced sediment resuspension to occur further offshore than normal (Fig. 2.a-d and e-f). In the northern part, almost all SSC is dominated by tides and currents that turn into a southerly direction and have a distinct circular motion. Meanwhile in the south of

Mahanadi cyclones frequently discharge huge amounts of sediment resulting in transportation to the north. As a result, the western Gahirmatha coast appears to be emerging as an ebb delta and acting as a sink. Unfortunately these deltaic regions are vulnerable from even a small scale rise in sealevel or tidal variations that could be disastrous in many ways to this stretch of coastline. Morphologically speaking, these areas are very dynamic due to the complexity of the sediment processes. Based on satellite studies it can be seen that a number of islands and shoals have been appeared in this region. This confirms the depositional and the transport of riverine sediment is restricted to an area from land. The 20 m isobaths are first to develop slowly forming into shoal patches that subsequently merge into small islands. There is no significant change in the offshore region beyond 100m isobaths (Barua et al.1994).

Central Zone

This zone receives sediments from the major rivers of the Krishna and Godavari. The micro tide in this region ranges from 0.5 to 2 m and the concentration of sediment has been highly reworked by the mechanism of waves and currents. According to the Chandramohan et al. (2001), the annual discharge of sediment supply from the Godavari river is about 38.83×10^9 kg from a northerly littoral drift in the order of $56.6 \times 10^4 \text{m}^3/\text{yr}$. Headland and beach erosion contribute to sedimentation of lagoons and the siltation of harbours while sand spits and marshy land supplement the sink by overloading of the littoral drift coming from the south (Mahadevan and Prasada Rao, 1958). This diminishes of riverine sediment supply leading to a corresponding sea level rise causes land erosion (Day et al. 1995). Complex spit formation from the Godavari inlets showed changing wave conditions identified from high-resolution satellite data in recent studies (Fig. 2. h-k and l-m). This particular delta front from the Krishna inlets seems to be affected rather more than the others due to the cyclones emanating from the Bay of Bengal. Unlike the other deltas on the east coast, this delta bulges into the sea and protrudes conspicuously into the Bay of Bengal with four inlets. The fluvial actions appear to be more dominant over marine processes like waves and currents. One reason is due to elongated spits almost

Table 1. SSC (mg/l) variation during pre and post monsoon at different tide levels of the zones along the entire coast of BOB.

| | | Ganges-Mahanadi Northern Zone | Godavari-Krishna Central Zone | Cauvery- Palk Bay Southern Zone |
|------------|-------------|----------------------------------|----------------------------------|------------------------------------|
| 17 Mar. 02 | Spring tide | 30-200 mg/l | 20-80 mg/l | 20-50 mg/l |
| 28 Nov. 02 | | 30-120 | 20-50 | 20-40 |
| 21 Mar. 02 | Neap tide | 20-150 | 30-60 | 10-35 |
| 30 Nov. 02 | | 40-80 | 20-40 | 10-40 |

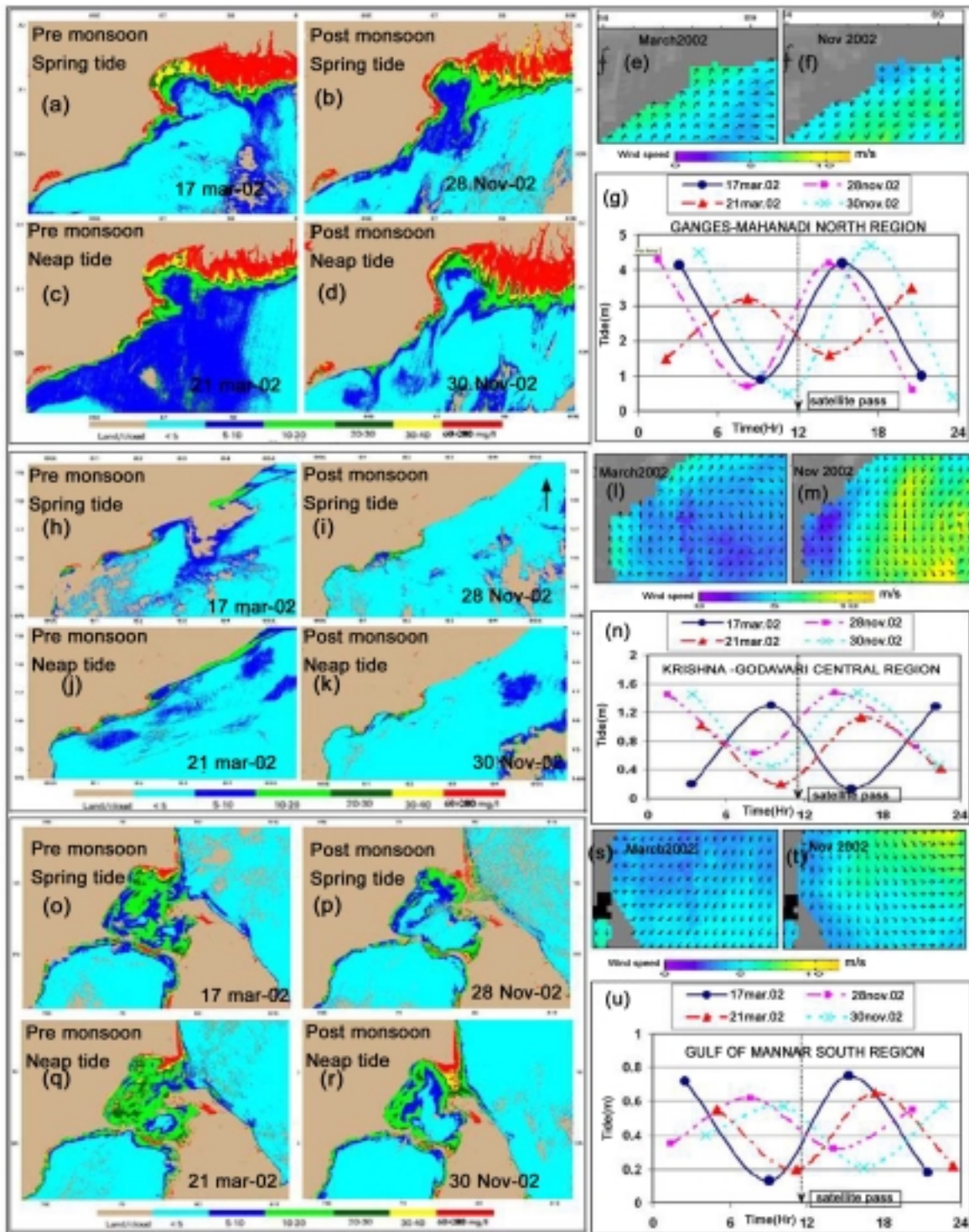


Fig.2. Pre and post monsoon variation of SSC at different tide positions in the above zones along the entire BOB, North zone (a-d), Central zone (h-k) and Southern zone (o-r). Wind vectors and Tidal graphs for North zone (e-f, g), central zone (l-m, n) and southern zone (s-t, u).

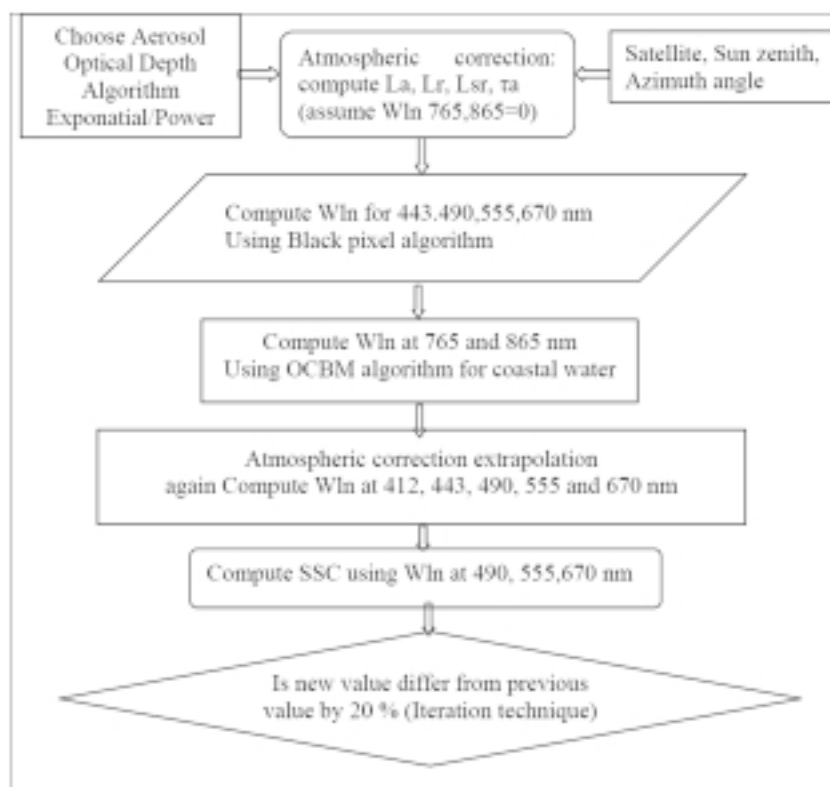


Fig. 3. The flowchart for retrieval suspended sediment concentrations using OCM data.

touching the coast at its distal end. This acts as a quiet water lagoon environment which continues the sediment filling process. By and large, the shallow Nizampattanam bay appears to be a favorable location for deposition of sediments (30-60 mg/l). The bay is sheltered from open wave attacks by the southward extension of the delta itself. The sediment load, which is recycled by wave action in the bay, settles down rapidly. The shelf break off the Krishna inlets confluence dramatically reduces the seaward advancement off the delta towards the shoreline. Subsequently, the delta has grown on the other side resulting in the Nagarjuna canyon progradation. The bathymetry in the shelf runs parallel to the east coast converging on the inlets of Krishna. In the southern Pulicat region, the inlet dynamics have resulted from the pre and post construction of the port. This explains why the inlet dynamics act in a bi-directional long shore transportation system. This results in reduced surface run off causing shoal and coastline orientation where is accretion on the up drift side while erosion is on the down drift side of the inlet (Fig. 2.l-m).

Southern Zone

The encroachment of the sea onto the land has been observed near inlets, particularly along the coast of the Cauvery river delta near Poompohar. This can be explained by the reduction in sediment supply which

also results in silting of the river mouth and depletion in supply to littoral system. Consequently, erosion has been increased significantly in this area (Chandramohan et al. 2001). The sediment contributions from the Vishali and Vaigai rivers have been sourced from various parts of the Tamilnadu coast and have been transported littorally in a southerly direction by entering the Pak bay region (Mallik, 1983). It is a micro tidal region (0.2-1.5 m) showing high SSC variations even though no river discharge. This has been attributed to the influx from the nearshore shallow bathymetry, resuspension and high energy levels resulting from coastal currents and long period waves. The sedimentary process is dominated by longshore sediment transport and resuspension from the high wind stress that varies between 10-40 mg/l. This area is occupied by sand banks, shoals, sand spits and islands that act as a sink and has been a common feature on all the time shows in the SSC (Fig. 2. o-r and s-t). This has led to low wave action within the bay and has also acted as a buffer from the southerly waves originating from the cyclonic storms during the NE monsoon period. This has caused extensive erosion which can be seen in the Nagapattinam-Poompohar region. It receives minimal river discharge during southeast monsoon and the high SSC is restricted to the shallow coastal waters off the Gulf of Mannar. Significantly, the coastal circulation and the biogenic process play a major role in SSC dynamics through out the year. As shown in (Fig.

2.o-r) during the neap tide in the gulf, high SSC prevails.

CONCLUSIONS

This study has been an interdisciplinary investigation that has considered hydrodynamical conditions as well as sedimentological and morphological responses in order that sediment transport processes along a nearshore zone in the BOB

can be further understood. The main factors controlling SSC along these coastal waters are the period of river discharge, availability of fine grained lithogenic sediment and the processes of resuspension by tidal energy and coastal current forces.

Acknowledgements: Authors are highly indebted to the knowledge and advice from the Director of NRSA and also would like to thank the Head, Oceanography Division, NRSA, Dept.of Space, Hyderabad, India.

References

- Barua, D. K., Kuehl, S. A., Miller, R.L. and Moore, W.S. (1994). Suspended sediment distribution and residual transport in the coastal ocean off the Ganges–Brahmaputra River mouth. *Marine Geology*, 120, 41–61.
- Chandramohan, P., Jena, B.K. and Sanil Kumar, V. (2001). Littoral drift sources and sinks along the Indian coast. *Curr. Sci.*, 81 (3), 292-296.
- Day, J. W., Pont, D., Hensel, P.F. and Ibenz. C. (1995). Impacts of sea level rise on deltas of the Gulf of Mexico and Meditarrian; The important of pulsing events to sustainability. *Estuaries*, 18, 638-647.
- Mahadevan, C. and Prasada Rao, R. (1958). Causes of the growth of sand spit north of Godavari confluence. *Andhrauniversity, Mem.of Oceanography*, 2, 69-74.
- Mallik, T.K. (1983). Littoral transport in northern Tamilnadu coast. *Indian Journal of marine sciences*, 12, 203-208.
- Mishra, A.K. (2004). Retrieval of suspended sediment concentration in the estuarine waters using IRS-1C WiFS data, *International Journal of Applied Earth Observation and Geoinformation*, 6, Issue 2, 83-95.
- Quanzhou Gao, Zhen Tao, Meiqi Xie, Kunyan Cui and Feng Zeng (2003). Effects of hydrological processes on the chemical composition of riverine suspended sediment in the Zhujiang River, China, *Hydrol. Process*, 17, 2365–2373.
- Ramesh, R., Purvaja, G. R. and Subramanian, V. (1995). Carbon and Phosphorus Transport by the Major Indian Rivers, *Journal of Biogeography*, 22, No. 2/3, *Terrestrial Ecosystem Interactions with Global Change*, 1, 409-415.
- Ritchie, J.C. and Schiebe, F.R. (2000). Remote Sensing in Hydrology and Water Management, Water Quality, In: G.A. Schultz and E.T. Engman (eds.) Springer-Verlag, Berlin, Germany, 287-303, 351-352.
- Tassan, S. (1994). Local algorithm using SeaWiFS data for retrieval of phytoplankton pigment, suspended sediments and yellow substances in coastal waters. *Applied Optics* 12, 2369–2378.